European Commission

JRC SCIENTIFIC AND POLICY REPORTS

Choice of steel material for bridge bearings to avoid brittle fracture

Background documents in support to the implementation, harmonization and further development of the Eurocodes

M. Feldmann, B. Eichler, G. Sedlacek,
W. Dahl, P. Langenberg, C. Butz,
H. Leendertz, G. Hanswille

Editors: A. Pinto, A. Athanasopoulou and
H. Amorim-Varum

2012

Report EUR 25390 EN

Joint Research Centre

European Commission
Joint Research Centre
Institute for the Protection and Security of the Citizen

Contact information
Artur Pinto
Address: Joint Research Centre, Via Enrico Fermi 2749, TP 480, 21027 Ispra (VA), Italy
E-mail: artur.pinto@jrc.ec.europa.eu
Tel.: +39 0332 78 9294
Fax: +39 0332 78 9049

http://ipsc.jrc.ec.europa.eu/
http://www.jrc.ec.europa.eu/

JRC72676

EUR 25390 EN

ISBN 978-92-79-25439-0

ISSN 1831-9424

doi:10.2788/33897

Luxembourg: Publications Office of the European Union, 2012

Printed in Italy

Choice of steel material for bridge bearings to avoid brittle fracture

**M. Feldmann, B. Eichler, G. Sedlacek, W. Dahl, P. Langenberg, C. Butz,
H. Leendertz, G. Hanswille**

Background documents in support to the implementation, harmonization and further development of the Eurocodes

Joint Report

Prepared in cooperation of experts from
CEN / TC 250, CEN / TC 167 and from metallurgy

Editors: A. Pinto, A. Athanasopoulou and H. Amorim-Varum

The European Convention for Constructional Steelwork (ECCS) is the federation of the National Associations of Steelwork industries and covers a worldwide network of Industrial Companies, Universities and Research Institutes.

http://www.steelconstruct.com/

Contact information
Address: Mies-van-der-Rohe-Straße 1, D-52074 Aachen
E-mail: sed@stb.rwth-aachen.de
Tel.: +49 241 80 25177
Fax: +49 241 80 22140
http://www.stb.rwth-aachen.de

ECC
CECM
E K

In the memory of Professor Dr.-Ing. Gerhard Sedlacek;

With his high scientific and technical skills, Professor Sedlacek he has been a guide and an example to all of us. He was an innovator, a bright and young-minded person. Professor Sedlacek was a real European in spirit and action and his work for the Eurocodes has left a lasting legacy. He has given full support to the Joint Research Centre for the activities concerning the implementation, harmonization and further development of the Eurocodes and he has enthusiastically defended the involvement of the JRC in the Eurocodes activities from the very beginning. Professor Sedlacek will always be remembered.

Joint Research Centre – Eurocodes Team

Foreword

The **construction sector** is of strategic importance to the EU as it delivers the buildings and infrastructure needed by the rest of the economy and society. It represents more than **10% of EU GDP and more than 50% of fixed capital formation**. It is the largest single economic activity and the biggest industrial employer in Europe. The sector employs directly almost 20 million people. In addition, construction is a key element for the implementation of the **Single Market** and other construction relevant EU Policies, e.g.: **Environment and Energy**.

In line with the EU's strategy for smart, sustainable and inclusive growth (EU2020), **Standardization** will play an important part in supporting the strategy. The **EN Eurocodes** are a set of **European standards** which provide common rules for the design of construction works, to check their strength and stability against live and extreme loads such as earthquakes and fire.

With the publication of all the 58 Eurocodes parts in 2007, the implementation of the Eurocodes is extending to all European countries and there are firm steps towards their adoption internationally. The Commission Recommendation of 11 December 2003 stresses the importance of **training in the use of the Eurocodes**, especially in engineering schools and as part of continuous professional development courses for engineers and technicians, noting that they should be promoted both at national and international level.

In light of the Recommendation, DG JRC is collaborating with DG ENTR and CEN/TC250 "Structural Eurocodes" and is publishing the Report Series '**Support to the implementation, harmonization and further development of the Eurocodes**' as JRC Scientific and Technical Reports. This Report Series include, at present, the following types of reports:

1. Policy support documents – Resulting from the work of the JRC and cooperation with partners and stakeholders on 'Support to the implementation, promotion and further development of the Eurocodes and other standards for the building sector.

2. Technical documents – Facilitating the implementation and use of the Eurocodes and containing information and practical examples (Worked Examples) on the use of the Eurocodes and covering the design of structures or their parts (e.g. the technical reports containing the practical examples presented in the workshops on the Eurocodes with worked examples organized by the JRC).

3. Pre-normative documents – Resulting from the works of the CEN/TC250 Working Groups and containing background information and/or first draft of proposed normative parts. These documents can be then converted to CEN technical specifications.

4. Background documents – Providing approved background information on current Eurocode part. The publication of the document is at the request of the relevant CEN/TC250 Sub-Committee.

5. Scientific/Technical information documents – Containing additional, non-contradictory information on current Eurocodes parts which may facilitate implementation and use, preliminary results from pre-normative work and other studies, which may be used in future revisions and further development of the standards. The authors are various stakeholders involved in Eurocodes process and the publication of these documents is authorized by the relevant CEN/TC250 Sub-Committee or Working Group.

Editorial work for this Report Series is **assured by the JRC** together with partners and stakeholders, when appropriate. The publication of the reports type 3, 4 and 5 is made after approval for publication from the CEN/TC250 Co-ordination Group.

The publication of these reports by the JRC serves the purpose of implementation, further harmonization and development of the Eurocodes, However, it is noted that neither the Commission nor CEN are obliged to follow or endorse any recommendation or result included in these reports in the European legislation or standardization processes.

This report is part of the so-called Scientific/Technical information documents (Type 5 above). It is a joint JRC-ECCS report and it part of a series of documents in support to the implementation and further evolution of Eurocode 3.

The editors and authors have sought to present useful and consistent information in this report. However, **users of information contained in this report must satisfy themselves of its suitability for the purpose for which they intend to use it**.

The report is available to download from the “Eurocodes: Building the future” website (http://eurocodes.jrc.ec.europa.eu).

Ispra, June 2012

Artur Pinto and Adamantia Athanasopoulou

European Laboratory for Structural Assessment (ELSA)

Institute for the Protection and Security of the Citizen (IPSC)

Joint Research Centre (JRC) – European Commission

Humberto Amorim-Varum

Departamento de Engenharia Civil

Universidade de Aveiro

(Former Seconded National Expert at the Joint Research Centre)

Acknowledgement

(1) This JRC-Scientific and Technical Report has been prepared in cooperation with the producers of transition joints and bearings for civil engineering works, in particular with the member companies of VHFL, that also sponsored the works.

(2) The draft has been discussed with experts from WG8 of CEN/TC 167, from CEN/TC 250 and other invited experts to achieve consistency across different fields of application of steel. The works of Dr. B. Kühn and Dr. M. Lukic from ECCS-TC6 have been most valuable.

(3) The financial support of the works and the valuable contributions from the cooperation and discussion are gratefully acknowledged.

(4) Particular thanks are to the Joint Research Centre for the editorial works.

Aachen, March 2011

Prof. Dr.-Ing. G. Sedlacek

Director of ECCS-Research

Introduction

(1) This JRC-Scientific and Technical Report deals with the choice of steel material for the production of bearings to avoid brittle fracture of the steel components of these bearings under low temperature conditions.

(2) This report has been initiated by the "VHFL-Vereinigung der Hersteller von Fahrbahnübergangen und Lagern für Bauwerke " (Association of producers of transition joints and bearings for civil engineering works).

(3) The objective was to prepare a tool on the basis of the procedure in EN 1993-1-10 – Choice of material to avoid brittle fracture - for normal steel fabrication, that allows to select the suitable steels for the various components of bearings such, that the regulatory requirements for safety under low temperatures are met.

(4) As this JRC-Report is connected with the product standards for bearings, in particular EN 1337, it has been prepared in cooperation of experts from CEN/TC 250, CEN/TC 167 and invited metallurgists.

(5) The purpose of the JRC-Report is to serve as an information and guidance and also to be used for the further development of EN 1337 and EN 1993.

Executive summary

(1) Due to a significant decrease of toughness properties of structural steel with decreasing temperatures there is a risk that structural steel components may under low temperatures be susceptible to brittle fracture.

(2) EN 1993-1-10 provides a method to avoid such brittle fracture by an appropriate choice of steel grade.

(3) The background of this method is a fracture mechanics safety assessment for a particular accidental scenario that includes extremely low temperatures, the presence of crack-like flaws at critical Hot-Spots, that have grown by fatigue effects, the presence of nominal stresses σ_{Ed}, and of material properties as specified in EN 10025.

(4) The purpose of this report is to adapt the method in EN 1993-1-10 used for normal steel structures to the specific case of steel components of structural bearings that are produced according to EN 1337 and are subject to specific design, fabrication and installation methods.

(5) In this adaptation the specific shapes of components generally machined from plates and the particular loading and verification models for the design of the components have been taken into account, so that eventually selection tables as in EN 1993-1-10 could be established.

(6) In case a Finite-Element analysis is applied in the design of the components of bearings the appropriate method to determine the reference stress σ_{Ed} is a Hot-Spot-stress σ_{HS} as defined by Dong.

(7) For usual dimensions of bearings a simplified procedure is offered that refers to nominal values of $\sigma_{bend,d}$ as the surface stress from the linear bending theory.

(8) A worked example illustrates the use of the simplified procedure.

Ispra, September 2011

J.A. Calgaro, U. Kuhlmann, G. Sedlacek, CEN/TC250

H. Leendertz, CEN/TC 167

A. Pinto, JRC

Table of contents

List of symbols

Capital

$A(T_{Ed})$	Accidental action $A(T_{Ed})$ which is defined as an extreme value of low temperature with a mean return period of 50 years.
D	Width of the sliding plate
E_{cm}	Mean value of the Young's modulus of concrete
E_d	Accidental combination of actions
G, G_k,	The magnitudes of dead loads
H	Force acting in horizontal direction
H_d [kN]	Design force acting in horizontal direction
J_C	Material toughness expressed in terms of J-Integral
KV	Charpy-V-notch impact energy [Joule] determined at a certain temperature T_{KV} contributing to a KV-T-curve.
K_1	Stress intensity factor in mode 1-opening
K_2	Stress intensity factor in mode 2-opening
K	Stress intensity factor
$K^*_{appl,d}$	Design value of the stress intensity factor
K_{appl}	Stress intensity factor determined from a linear elastic fracture mechanics analysis
K_{eff}	Effective stress intensity factor considering that the main stresses are not perpendicular to the crack path
K_{Ic}	Fracture toughness determined from fracture mechanics small scale specimens
$\overline{K}$, $\overline{K}_{eff}$	Normalized distribution of stress-intensity factors for a specific geometry and loading
Q, Q_k, Q_{ki}	The magnitudes of variable loads
S275	Steel grade for structural steel with minimum yield strength 275 N/mm^2
T_{md}	Lowest environmental temperature
$T_{27J,nom}$	Nominal transition temperature corresponding to 27 J acc. to e.g. EN 10025
T_{mrd}	Extreme value of low temperature
T_{min}	Minimum temperature value
$T_{min,d}$	Minimum design temperature value
T	Temperature [°C]
T_{27J}	Test temperature [°C] for notch-impact Charpy-V-tests (CNV-tests) to achieve an impact energy of 27J.
T_{Ed}	Reference temperature [°C] of steel structures for choice of steel material

to avoid brittle fracture according to EN 1993-1-10.

T_{Ed} is the minimum temperature of air T_{mv} [°C] (corresponding to a 50 years return period) minus temperature loss by radiation (-5K), when the standardized conditions for the design size of crack at the hot-spot of notched structural components, for neglecting cold-forming effects and strain rate effects and for the reliability of results all specified in EN 1993-1-10 are adopted.

For other conditions, e.g. with additional cold-forming, T_{Ed} can be modified by temperature shifts, e.g. by ΔT_{cf} [K].

T_{Rd}	Temperature [°C] at which a safe level of fracture toughness can be relied upon under the conditions being evaluated.
V	Force acting in vertical direction

Regular

a	Crack size
a_0	Initial crack size
a_d	Design crack size
a_W	Weld throat size
b	Geometric value
b_{eff}	Critical crack length
c	Crack width
c_0	Initial crack width
d	Geometric value
f_{cd}	Design value of the concrete strength
$f_{y,nom}$	Nominal value of yield strength
f_y	Yield strength of material as specified in EN 10025
$h_{d,max}$	Maximum horizontal force on lateral supports
k_{Dong}	Correlation coefficient between the Dong-Hot-Spot-stress σ_{HS} and the stress σ_{bend} approximately determined by the bending theory
k_{R6}	Factor to consider the interaction between brittle behaviour and local yielding
m	Mean value
r	Geometric value
s	Coordinate along the theoretical crack path
t	element thickness
t_1, t_2, t_3	Geometric dimension
t_{Walz}	Thickness of the parent plate

Greek symbols

Δa, Δc	Crack growth increment from fatigue loading
$\overline{\Delta T_R}$	Temperature shift [K] between the mean value of b_i and the design fractile m+3.03 σ of the distribution of b_i, that represents the design value for measured input values.
ΔT_{cf}	Temperature shift [K] in the notch impact energy-temperature diagram due to cold-forming (cf), also designated as ΔT_{DCF}.
ΔT_{DCF}	See ΔT_{cf}
ΔT_{27J}	Temperature shift due to the inhomogeneity of material toughness in through-thickness direction.
$\Delta T_{\dot{\varepsilon}}$	Temperature shift from high strain-rates
$\Delta T_{\varepsilon cf}$	Temperature shift from cold-forming effects
ΔT_r	Temperature shift due to radiation loss of the structural component
ΔT_σ	Temperature shift caused by $K^*_{appl,d}$
ΔT_R	Additive safety element [K] in the limit state equation with T_{Ed} (action) and T_{Rd} (resistance), that is determined from the evaluation of large scale fracture mechanics tests and yields the required reliability of the design equation that is underlying Table 2.1 in EN 1993-1-10.
$\dot{\varepsilon}$	Strain rate from dynamic actions
$\dot{\varepsilon}_0$	Reference value of the strain rate
ε_{cf}	Degree of cold forming in %
ν	Poisson ratio
ρ	Correction factor to consider the interaction between stresses from external loads and local residual stresses, that are reduced partially by local plastic deformations.
σ	Stress
σ_1	First principal stress
$\sigma_{bend,d}$	The ultimate stress determined in a simplified way according to the elastic bending theory in the critical cross section perpendicular to the neutral axis for action effects from loads factored with γ.
σ_{Ed}	Nominal stress on service level applied from external forces to the structural component, in an accidental design situation according to EN 1993-1-10. The leading action is the temperature T_{Ed} acting on a structural component with a standardized severe notch situation and the design value of crack at the hot spot of the notch. The external forces are from accompanying actions (permanent loads and frequent values of variable loads without partial factors). σ_{Ed} does not include residual stresses.

Residual stresses are included in the procedure of EN 1993-1-10 by two means:

1. Local residual stresses from welding are included in the evaluation procedure of fracture mechanical large scale tests.
2. Global residual stresses from restraints to the weld shrinkage of the component are taken into account by a supplementary nominal stress σ_S = 100 MPa.

$\frac{\sigma_{Ed}}{f_y}$	Utilisation rate from external stresses. EN 1993-1-10 gives in its Table 2.1 information for admissible plate thickness for various steel grades, temperatures T_{Ed} and for the utilisation rates: 0.25, 0.50 and 0.75.
σ_{gy}	Stress to the gross section that causes yielding of the net section.
σ_{HS}	Hot-Spot stress or structural stress
σ_{max}	Maximum stress
σ_N	Nominal stress
σ_P	Primary stress resulting from the accompanying external actions
σ_S	Residual stresses from restraints to the weld shrinkage of the component.
σ_{tot}	$\sigma_{tot} = \sigma_P + \sigma_S$
$\psi_{1.1}$	Combination factor for frequent loads with a return period of – 1 month
$\psi_{2,i}$	Combination factor for „quasi-permanent“ loads

1 Objective

(1) The design rules for steel-structures apply in general to the upper shelf domain of the toughness-temperature diagram, where the steel material exhibits ductile behaviour. To consider the reduction of toughness in the transition range of the toughness-temperature diagram, steels should comply with a procedure for the choice of material to avoid brittle fracture. This procedure is based on a fracture mechanics safety-assessment for a scenario of hypothetical crack-distribution and loading at the time of lowest possible temperature of the structure.

(2) EN 1993-1-10 [2] gives a table for the choice of material which applies for the usual types of dimensions and details of structural steel components and includes the following parameters:

- the lowest possible temperature of the structure T_{Ed},
- the structural detail at the critical spot which is contained in the detail classes in EN 1993-1-9-Fatigue.

  The sketches illustrating the detail classes in EN 1993-1-9 are “cut-outs” from structural steel components, which include the “hot spots” at which fatigue cracks can be expected and are also used for the definition of “nominal stresses”, to which the fatigue resistance of the detail refers.

  For the choice of material the same “hot spot” and the same definition of nominal stresses σ_{Ed} as in EN 1993-1-9 is used, however stresses are not related to “fatigue loads”, but to “frequent loads” according to EN 1990 – Basis of structural design. In the table in EN 1993-1-10 nominal stresses from frequent loads are classified as portion of the yield strength (0.25 f_y, 0.50 f_y, 0.75 f_y).
- the plate thickness (product thickness) at the “hot-spot”.

(3) Bearings for bridges consist of small structural steel components usually produced by machining, the sizes of which frequently do not comply with the geometrical assumptions made for applying the bending theory for steel structures, the loading of which may be dependent on the deformation conditions of interfacing parts and the quality control during fabrication is subject to specific requirements (EN 1337).

(4) Therefore the prerequisites for the use of EN 1993-1-9 and EN 1993-1-10 do in general not apply, so that these standards are not useable for the choice of material for bearings without further information.

(5) This report therefore addresses the choice of steel material for bearings of bridges and gives for details specific to bearings the information for a “safe-sided” choice taking reference to the lowest material temperature T_{Ed}, the type of detail, the stress level σ_{Ed} and the relevant material thickness at the hot spot.

(6) For deriving of the tables in this report the same fracture mechanics procedure is used as in EN 1993-1-10 however with some modifications of the procedure which comprise:

1. The magnitude and the shape of the hypothetical design crack, because fatigue effects as considered in EN 1993-1-10 are not relevant.
2. Definition of “nominal stress” σ_{Ed} for the “hot-spot” which cannot be easily determined in the conventional way by force divided by area as specified in EN 1993-1-9. For the definition of “nominal stresses” σ_{Ed} two methods are used:

i. method for assessing structural components with Finite Elements.

ii. simplified method using the assessment with assumption of the “bending theory”.

(7) The report is structured into the following sections:

1. Fracture mechanics assessment as used in EN 1993-1-10 to avoid brittle fracture.
2. Bearings for bridges, types of bearings and specification, standard components of bearings referred to in the assessment.
3. Modifications of the fracture mechanics assessment as used in EN 1993-1-10 for the specific purposes of bridge bearings.
4. Numerical studies and results.
5. Proposal for a standardisation when using Finite Elements.
6. Proposal for referring to ultimate stress assessments according to the bending theory.
7. Worked example.

2 Fracture mechanics safety assessment to avoid brittle fracture as used in EN 1993-1-10

2.1 General

(1) The procedure for choosing the steel to avoid brittle fracture in EN 1993-1-10 [2] is explained in the JRC-Scientific and Technical Report [3] related to this standard.

(2) In the following an abridged version is given to make the modifications for bridge bearings understandable.

2.2 Basics of the fracture mechanics procedure

(1) The design equation with fracture mechanics properties (here stress intensity factors K) reads

$$K^*_{appl,d} \leq K_{mat,d} \qquad \textbf{(2-1)}$$

where

$K^*_{appl,d}$ is the design value of action effect at the tip of the hypothetical crack which is assumed to be located at the most severe notch of the structure component.

Local plastic zones at the crack tip are taken into account by the correction value k_{R6} according to the simplified Failure Assessment Diagram (FAD). The value $K^*_{appl,d}$ therefore reads

$$K^*_{appl,d} = K_{appl} / (k_{R6} - \rho) \qquad \textbf{(2-2)}$$

where

K_{appl} is determined from a linear elastic fracture mechanics analysis

k_{R6} is a factor to consider the interaction between brittle behaviour and local yielding, see [2]

ρ is a correction factor to consider the interaction between stresses from external loads and local residual stresses, that are reduced partially by local plastic deformations.

(2) The fracture mechanics resistance is defined by $K_{Mat,d}$. That “toughness property” can be determined experimentally. Another option is a numerical determination on the basis of correlations to “toughness properties” specified in the material standards or given in the material certificates. The “toughness properties” in the material standards are given by minimum requirements for Charpy-V-impact energies at a certain testing temperature.

(3) To standardize the fracture mechanics assessment procedure and to adapt it to the toughness properties T_{27J} specified in the product standards, the design equation based on stress-intensity factors has been transformed to a design equation based on temperatures

$T_{Ed} \geq T_{Rd}$ **(2-3)**

(4) The temperature term T_{Ed} contains actions from the temperature of the structural component, influences from the stress-level and strain-rate, the shape and dimensions of the structural component and the size of the hypothetical crack-like flaw.

$$T_{Ed} = T_{md} + \Delta T_r + \Delta T_\sigma + \Delta T_R + \Delta T_{\dot{\varepsilon}} + \Delta T_{\varepsilon cf} \quad \textbf{(2-4)}$$

where

T_{md} is the lowest environmental temperature

ΔT_r is the radiation loss of the structural component: ΔT_r = -5 K

ΔT_R is an additive safety element in terms of a temperature shift

ΔT_σ is the temperature shift caused by $K^*_{appl,d}$, i.e. by the influence of stress level, geometry of the detail and crack configuration:

$$\Delta T_\sigma = -52 \cdot \ln\left[\frac{(K^*_{appl,d} - 20) \cdot \left(\frac{b_{eff}}{25}\right)^{1/4} - 10}{70}\right] \leq 120°C$$

$\Delta T_{\dot{\varepsilon}}$ is the temperature shift from high strain-rates where:

$$\Delta T_{\dot{\varepsilon}} = -\frac{1440 - f_y(t)}{550}\left(\ln\frac{\dot{\varepsilon}}{\dot{\varepsilon}_0}\right)^{1,5}$$

$f_y(t)$ is the yield strength depending on plate thickness t

$\dot{\varepsilon}$ is the strain rate from dynamic actions

$\dot{\varepsilon}_0$ = 0.0001 s^{-1} is the reference value to define static actions

$\Delta T_{\varepsilon cf}$ is the temperature shift from cold-forming effects:

$\Delta T_{\varepsilon cf} = 0$ for $\varepsilon_{cf} \leq$ 2%

$\Delta T_{\varepsilon cf} = -3 \times \varepsilon_{cf}$ for $\varepsilon_{cf} >$ 2%

where ε_{cf} is the degree of cold forming (plastic strain) in %

(5) The resistance side includes the material toughness expressed by

$$T_{Rd} = (T_{27J} - 18) + \Delta T_{27J} \quad \textbf{(2-5)}$$

where

T_{27J} is the testing temperature, for which the Charpy-V-notch impact energy attains 27 Joule

ΔT_{27J} is the temperature shift due to the inhomogeneity of material toughness in through-thickness direction. It should be used where the hypothetical crack penetrates into the inner core area of the product . The inner core area for plates is defined as the inner third of the plate thickness.

2.3 Design situation

(1) For developing EN 1993-1-10 for the choice of material to avoid brittle fracture an accidental design situation (case A_1 - A_2 - A_3 in Figure 2-1) has been assumed that includes the following conditions:

- The assessment is carried out in the region of elastic fracture mechanics (K_{Ic}-region) in the lower part of the toughness-temperature diagram.
- The structural component has a crack at the critical hot spot and the crack has reached a critical size (the crack is understood as an initial crack from production overlooked at production control which has increased by fatigue effects during service).
- The temperature of the structural component has obtained a minimum value T_{min}, at which the value of material toughness has reached its minimum value J_C (point A_1 in Figure 2-1). The temperature T_{Ed} on the action side may be further reduced by the temperature shifts from the influence of cold-forming or impact loads.
- The magnitudes of variable loads Q and of the temperature of the structural component are statistically independent on each other. Therefore the accidental combination of action includes $T_{min,d}$ as the dominant action, which is combined with accompanying frequent loads $G_K + \psi_1 Q_K$ which produce the stress-level from external loads (point A_2 in Figure 2-1).
- Because of the lower level of the frequent loads the stresses in this accidental combination of actions $\sigma_{Ed} = \sigma (G_K + \psi_1 Q_K)$ are in general in the elastic range (point A_3 in Figure 2-1).

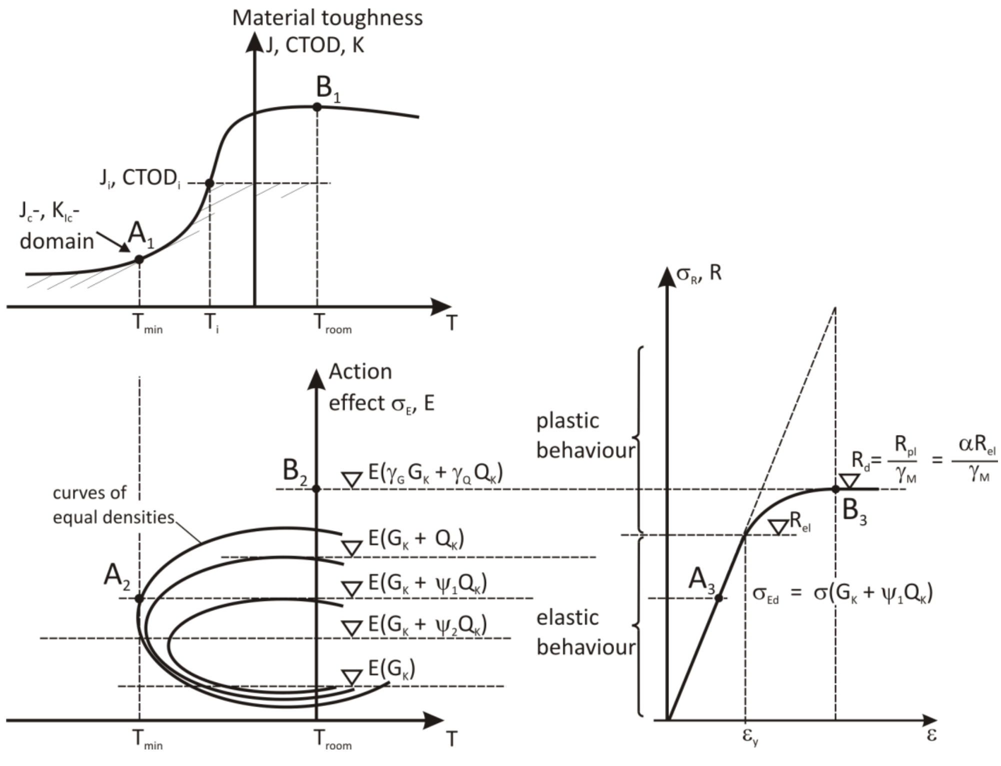

Figure 2-1: Design situations for the choice of material to avoid brittle fracture according to EN 1993-1-10

(2) The accidental combination of actions, which is fully described by

$$E_d = E \{A [T_{Ed}] \text{"+"} \Sigma G_k \text{"+"} \psi_{1,1} Q_{k1} \text{"+"} \Sigma\psi_{2,i} Q_{ki}\} \quad \textbf{(2-6)}$$

is justified by the fact, that a series of adverse influences (low temperature simultaneously with a hypothetical crack overlooked at the most severe location of the structural component) are all combined together.

(3) The accidental action $A(T_{Ed})$ is defined as an extreme value of low temperature with a mean return period of 50 years, e.g. for Germany T_{mrd} = -30 °C including radiation loss.

(4) The accompanying actions are stresses from permanent and variable loads. Because of the limited duration of the accidental extreme temperature the accompanying actions will not take their extreme values but the "frequent values" due the probability of occurrence.

(5) From the accompanying external actions the nominal values are determined using the following load-combination

$$\sigma_P = \sigma \{\Sigma G_k \text{"+"} \psi_{1,1} Q_{k1} \text{"+"} \Sigma\psi_{2,i} Q_{ki}\} \quad \textbf{(2-7)}$$

where

$\psi_{1,1}$ is the combination factor for frequent loads with a return period of – 1 month

$\psi_{2,i}$ is the combination factor for „quasi-permanent“ loads

(6) In addition to these "primary" nominal stresses σ_P also "secondary stresses" σ_S from residual stresses and unforeseen restraints from the assembly of the structure have been taken into account in preparing the table for the choice of material in EN 1993-1-10, so that

$$\sigma_{tot} = \sigma_P + \sigma_S \quad \textbf{(2-8)}$$

where

σ_P is the nominal stress from the external loads, see above

σ_S is the residual stress defined as "global". In preparing the table in EN 1993-1-10 a lump value σ_S = 100 N/mm² has been used. "Local" residual stresses, which occur in the welded area at the hot spot and may be reduced by local cracking need not to be specified as they are considered already in the model uncertainty when the numerical assessment procedure was calibrated to the results of fracture mechanics tests undertaken with large-size welded test-specimens.

(7) The values in the table of EN 1993-1-10 refer to the stress-level $\sigma_{Ed} = \sigma_P$ only, so that for using the table σ_S needs not to be further considered.

(8) Where σ_{Ed} is a compression stress, the structural component should be assessed for the lowest class of tension stress $\sigma_{Ed} = 0.25\, f_y$.

2.4 Assumptions for the structural detail and the magnitude of hypothetical crack

(1) EN 1993-1-10 has been initially developed for the choice of material for steel bridges; therefore the assumptions for the choice of a reference detail and the position and magnitude of the hypothetical cracks were mainly influenced by typical bridge structures.

(2) The reference detail with geometrical parameters chosen for EN 1993-1-10 is a plate in tension with a welded longitudinal attachment as given in Figure 2-2. This detail is typical for bridge structures; because of the geometrical notch effect it represents an enhanced risk for starting brittle fracture. This detail is also included in the detail-classes in EN 1993-1-9 [5]. For determining $K^{*}_{appl,d}$ particular ranges of dimensions (e.g. length of stiffener in relation to plate thickness and plate width, angle and size a of fillet weld) were assumed that are representative for the use in bridges.

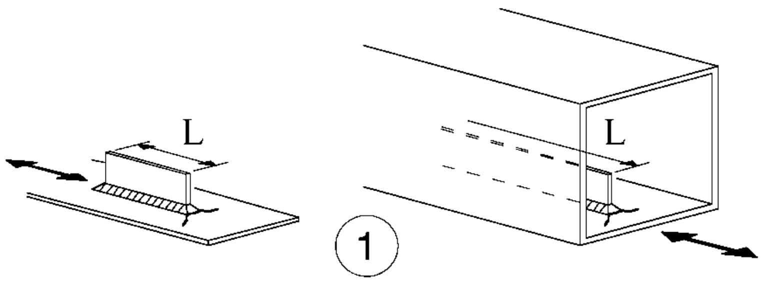

Figure 2-2: Reference structural detail for calculating $K^{*}_{appl,d}$ for the choice of material in EN 1993-1-10

(3) Other detail classes as specified in EN 1993-1-9 are covered by this reference detail and the assessment method applied for it, so that EN 1993-1-10 is safe sided for all fatigue details in EN 1993-1-9. In case of structural details that cannot be classified to EN 1993-1-9 the table for choice of material in EN 1993-1-10 is not applicable.

(4) The assumption for a crack-like flaw is a semi elliptical surface crack at the position of the largest stress-concentration at the end of the longitudinal stiffener. Figure 2-3 shows the cross-section of a rectangular plate with a semi-elliptical crack. The ratio of the crack depth a to the crack-width c has been determined for this reference detail with a/c = 0.4.

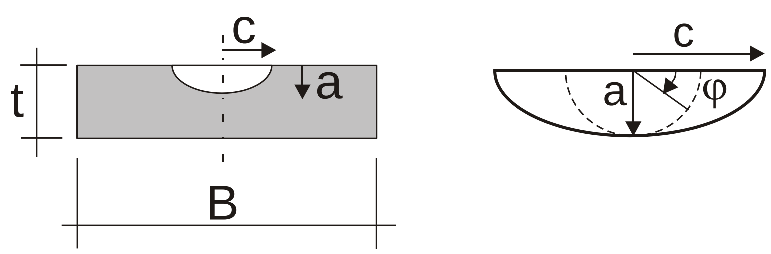

Figure 2-3: Assumption of a semi-elliptical surface crack in a plate with rectangular cross-section

(5) The magnitude of the design values a_d and c_d is determined from two components:

- the initial crack size with the crack depth a_0 and the crack width c_0 is determined in dependence of the product thickness (plate thickness) according to Figure 2-4. This magnitude is considered to be detectable in inspections during production see Figure 2-7 with the usual testing methods used in steel construction.

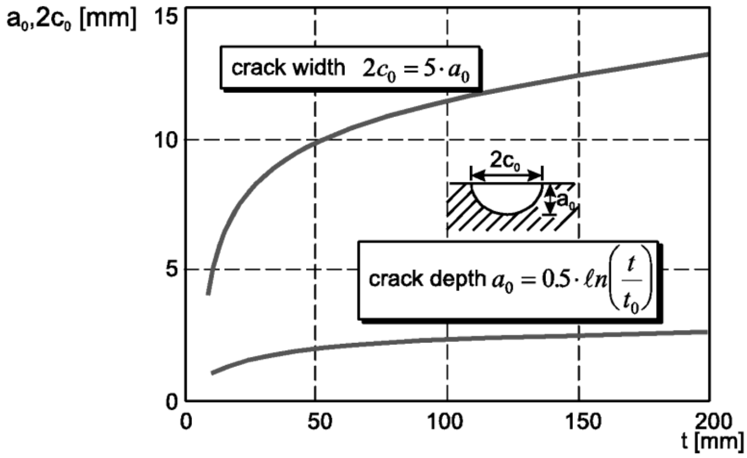

Figure 2-4: **Magnitude of the initial crack from fabrication overlooked in inspections**

- the crack growth Δa, Δc from fatigue in service.

(6) The design values a_d and c_d including crack growth from fatigue in service are functions of the fatigue loading.

(7) For the fatigue loading the detail class $\Delta\sigma_c$ is relevant which gives a maximum total fatigue load of $\Delta\sigma_C^3 \times 2 \cdot 10^6$ for the full design life.

(8) As for steel structures susceptible to fatigue as bridges inspections are required in certain intervals. The crack growth $\Delta a = a_d - a_0$ and $\Delta c = c_d - c_0$ is determined from a portion of the full fatigue load only, for which a quarter (1/4) has been selected. The crack growth was therefore determined for the fatigue load $\Delta\sigma_C^3 \times 500.000$.

(9) The crack growth Δa at the weld toe of the longitudinal attachment with the geometry in Figure 2-2 was determined using the crack-propagation formulas by Paris. As a result the design value $a_d(t)$ dependant on the plate thickness t was obtained, see Figure 2-5.

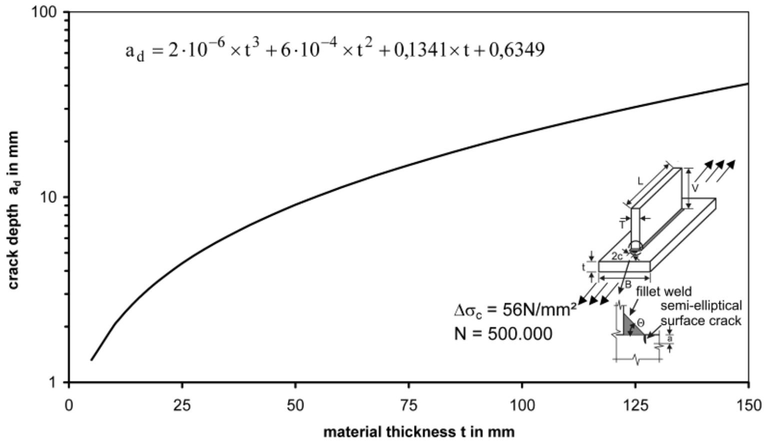

Figure 2-5: **Design values of crack depth $a_d = a_0 + \Delta a$**

(10) The stress intensity-factor for this crack depth a_d is the value $K_{appl,d}$, Figure 2-6.

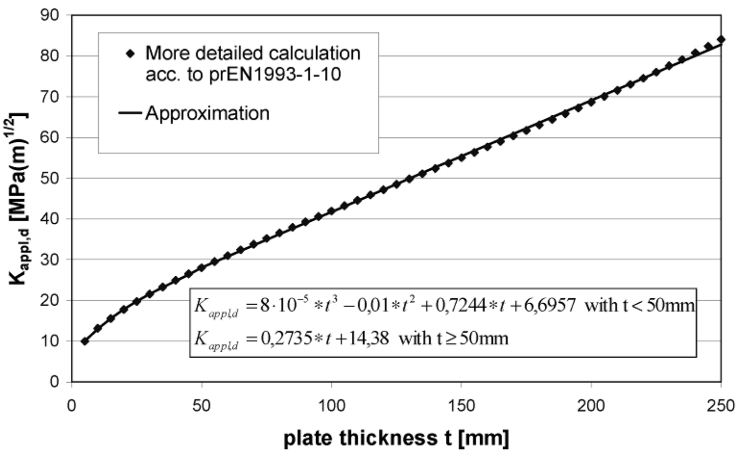

Figure 2-6: Stress intensity factor $K_{appl,d}$ calculated for the design crack depth a_d in figure 2-5

(11) The interpretation of the initial crack size a_0/c_0 as a flaw "overlooked in the production control" is justified by the fact, that the magnitudes of a_0/c_0 are detectable during crack-inspections. Figure 2-7 gives the functions $2c_0$ of the initial crack and $2c_d$ of the design crack in relation to the limits for detectability by visual inspection, colour penetration test, ultrasonic inspection and magnetic particle inspection.

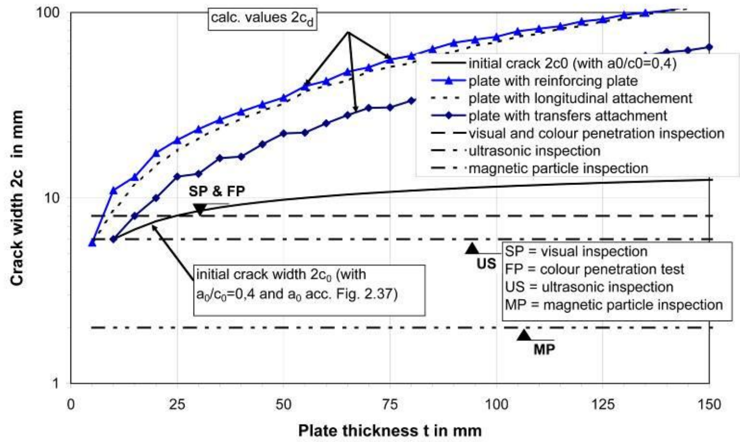

Figure 2-7: Assumptions for initial values and design values of crack size and detectability by testing methods

(12) Hence the initial crack assumed is detectable by production control and can be assumed to be accidentally overlooked.

2.5 Table 2.1 of EN 1993-1-10

(1) Table 2.1 in EN 1993-1-10 gives the results of the fracture mechanics safety assessments, see Figure 2-8. It is applicable for all details listed in EN 1993-1-9.

Figure 2-8: **Table 2.1 in EN 1993-1-10, here with an extension to cover a larger temperature range TEd [4]**

Reference temperature T_{Ed} [°C] — $\sigma_{Ed} = 0{,}75\ f_y(t)$

Steel grade	Sub-grade	Charpy energy CVN at T [°C]	J_{min}	10	0	-10	-20	-30	-40	-50	-60	-70	-80	-90	-100	-110	-120
S235	JR	+20	27	62	51	43	36	30	25	21	18	16	14	12	11	10	9
	J0	0	27	89	74	62	51	43	36	30	25	21	18	16	14	12	11
	J2	-20	27	126	106	89	74	62	51	43	36	30	25	21	18	16	14
S275	JR	+20	27	54	45	37	31	26	22	18	15	13	11	10	9	8	7
	J0	0	27	78	65	54	45	37	31	26	22	18	15	13	11	10	9
	J2	-20	27	112	94	78	65	54	45	37	31	26	22	18	15	13	11
	M, N	-20	40	132	111	93	77	64	53	44	37	31	25	21	18	15	13
	ML, NL	-50	27	185	158	134	112	94	78	65	54	45	37	31	26	22	18
S355	JR	+20	27	43	35	29	24	20	16	14	11	10	8	7	6	5	5
	J0	0	27	63	52	43	35	29	24	20	16	14	11	10	8	7	6
	J2	-20	27	92	76	63	52	43	35	29	24	20	16	14	11	10	8
	K2,M,N	-20	40	109	91	75	62	51	42	35	28	23	19	16	13	11	9
	ML, NL	-50	27	155	131	110	92	76	63	52	43	35	29	24	20	16	14
S420	M, N	-20	40	95	79	65	53	44	36	29	24	19	16	13	11	9	7
	ML, NL	-50	27	137	115	96	80	66	54	44	36	29	24	20	16	13	11
S460	Q	-20	30	77	63	52	42	34	28	23	18	15	12	10	8	7	6
	M, N	-20	40	88	73	60	49	40	32	26	21	17	14	12	9	8	6
	QL	-40	30	112	93	77	63	52	42	34	28	23	18	15	12	10	8
	ML, NL	-50	27	128	107	89	73	60	49	40	33	27	22	18	14	12	10
	QL1	-60	30	157	133	112	93	77	63	52	42	34	28	23	18	15	12
S690	Q	0	40	39	31	25	20	16	13	10	8	6	5	3	2	-	-
	Q	-20	30	52	42	34	27	21	17	13	11	8	7	5	4	2	1
	QL	-20	40	60	48	39	31	25	20	16	13	10	8	6	5	3	2
	QL	-40	30	78	64	52	42	34	27	21	17	13	11	8	7	5	4
	QL1	-40	40	89	73	60	48	39	31	25	20	16	13	10	8	6	5
	QL1	-60	30	113	94	78	64	52	42	34	27	21	17	13	11	8	7

Reference temperature T_{Ed} [°C] — $\sigma_{Ed} = 0{,}50\ f_y(t)$

Steel grade	Sub-grade	Charpy energy CVN at T [°C]	J_{min}	10	0	-10	-20	-30	-40	-50	-60	-70	-80	-90	-100	-110	-120
S235	JR	+20	27	90	77	65	55	47	41	35	31	27	24	21	19	18	16
	J0	0	27	125	106	90	77	65	55	47	41	35	31	27	24	21	19
	J2	-20	27	169	146	125	106	90	77	65	55	47	41	35	31	27	24
S275	JR	+20	27	81	69	58	49	42	36	31	27	24	21	18	17	15	14
	J0	0	27	113	96	81	69	58	49	42	36	31	27	24	21	18	17
	J2	-20	27	156	133	113	96	81	69	58	49	42	36	31	27	24	21
	M, N	-20	40	179	154	132	112	95	81	68	58	49	42	36	31	27	23
	ML, NL	-50	27	199	199	181	156	133	113	96	81	69	58	49	42	36	31
S355	JR	+20	27	68	57	48	40	34	29	25	21	18	16	14	13	11	10
	J0	0	27	96	80	68	57	48	40	34	29	25	21	18	16	14	13
	J2	-20	27	133	113	96	80	68	57	48	40	34	29	25	21	18	16
	K2,M,N	-20	40	155	132	112	95	80	67	56	47	40	34	28	24	21	18
	ML, NL	-50	27	199	181	156	133	113	96	80	68	57	48	40	34	29	25
S420	M, N	-20	40	139	118	99	83	70	58	49	41	34	29	24	20	17	15
	ML, NL	-50	27	190	164	140	119	100	84	71	59	49	41	34	29	24	21
S460	Q	-20	30	116	98	82	68	57	47	39	33	27	23	19	16	14	12
	M, N	-20	40	130	110	93	78	65	54	45	37	31	26	22	18	16	14
	QL	-40	30	160	137	116	98	82	68	57	47	39	33	27	23	19	16
	ML, NL	-50	27	180	155	132	111	94	78	65	54	45	38	31	26	22	19
	QL1	-60	30	199	186	160	137	116	98	82	68	57	47	39	33	27	23
S690	Q	0	40	65	54	44	36	30	24	20	16	13	11	9	8	6	5
	Q	-20	30	84	69	57	47	38	31	26	21	17	14	12	10	8	7
	QL	-20	40	95	79	65	54	44	36	30	24	20	16	13	11	9	8
	QL	-40	30	120	100	84	69	57	47	38	31	26	21	17	14	12	10
	QL1	-40	40	135	114	95	79	65	54	44	36	30	24	20	16	13	11
	QL1	-60	30	166	142	120	100	84	69	57	47	38	31	26	21	17	14

Reference temperature T_{Ed} [°C] — $\sigma_{Ed} = 0{,}25\ f_y(t)$

Steel grade	Sub-grade	Charpy energy CVN at T [°C]	J_{min}	10	0	-10	-20	-30	-40	-50	-60	-70	-80	-90	-100	-110	-120
S235	JR	+20	27	134	116	101	88	77	67	59	53	47	42	39	35	33	31
	J0	0	27	176	154	134	116	101	88	77	67	59	53	47	42	39	35
	J2	-20	27	199	199	176	154	134	116	101	88	77	67	59	53	47	42
S275	JR	+20	27	126	109	95	82	71	62	55	49	43	39	35	32	30	28
	J0	0	27	167	145	126	109	95	82	71	62	55	49	43	39	35	32
	J2	-20	27	199	191	167	145	126	109	95	82	71	62	55	49	43	39
	M, N	-20	40	199	199	189	165	144	125	108	94	81	71	62	55	48	43
	ML, NL	-50	27	229	202	199	199	191	167	145	126	109	95	82	71	62	55
S355	JR	+20	27	112	97	83	72	62	54	47	42	37	33	30	27	25	23
	J0	0	27	150	130	112	97	83	72	62	54	47	42	37	33	30	27
	J2	-20	27	198	173	150	130	112	97	83	72	62	54	47	42	37	33
	K2,M,N	-20	40	199	197	172	149	129	111	96	83	71	62	54	47	41	37
	ML, NL	-50	27	210	199	199	198	173	150	130	112	97	83	72	62	54	47
S420	M, N	-20	40	199	183	159	138	118	102	87	75	64	55	48	42	37	33
	ML, NL	-50	27	199	199	199	185	160	139	119	103	88	75	65	56	48	42
S460	Q	-20	30	183	159	137	118	101	86	74	63	54	47	41	36	31	28
	M, N	-20	40	199	176	152	131	113	96	82	71	61	52	45	39	34	30
	QL	-40	30	199	199	183	159	137	118	101	86	74	63	54	47	41	36
	ML, NL	-50	27	199	199	199	177	153	132	114	97	83	71	61	53	45	39
	QL1	-60	30	222	199	199	199	183	159	137	118	101	86	74	63	54	47
S690	Q	0	40	120	102	87	73	62	52	44	38	32	28	24	21	18	16
	Q	-20	30	147	126	107	91	77	65	55	46	39	34	29	25	22	19
	QL	-20	40	164	141	120	102	87	73	62	52	44	38	32	28	24	21
	QL	-40	30	197	171	147	126	107	91	77	65	55	46	39	34	29	25
	QL1	-40	40	199	189	164	141	120	102	87	73	62	52	44	38	32	28
	QL1	-60	30	199	199	197	171	147	126	107	91	77	65	55	46	39	34

reference temperature

for hot-finished sections T_{Ed}

for cold-formed sections: $T^*_{Ed} = T_{Ed} + \Delta T_{cf}$

Note: *The values in this table are for some parameters slightly different to those given in Table 2.1 of EN 1993-1-10. In a future revision of Table 2.1 of EN 1993-1-10 the values of Figure 2-8 could be adopted.*

3 Structural bearings for bridges, types, product specification and selection of standard components for fracture mechanics assessments

3.1 Types of bearings and product specifications

(1) Bearings for bridges are elements allowing rotation between two members of a structure and transmitting the loads defined in the relevant requirements as well as preventing displacements (fixed bearings) allowing displacements in only one direction (guided bearings) or in all directions of a plane (free bearings) as required.

(2) The functional principles corresponding to the action effects they are built for may be taken from Figure 3-1.

Functional principle	**Sliding**	**Rolling**	**Deforming**
Action effect required			
Translational movement	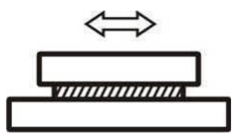	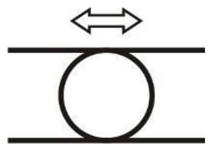	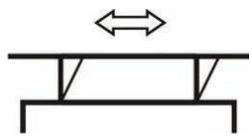
Rotational angle	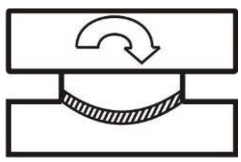	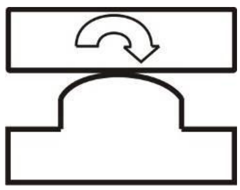	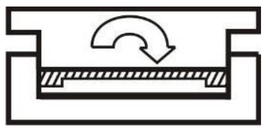

Figure 3-1: Functional principles in response to action effects required for bearings of bridges [7]

(3) The tasks of bearings are:

- to transmit from the 6 spatial action effects in terms of forces and moments, which are possible at the connection between the bridge superstructure and the substructure (primary loads on the bearings), without or with limited relative movements and
- to make relative movements between the bridge superstructure and the substructure in the sense of the other action effects (translational movements, rotations) possible at the supports. These relative movements may be responded by resistances of the bearings (secondary loads from the bearings), which are classified as follows:
  - resistances to movements from moveable bearings (from rolling, sliding and from mechanical guidances)
  - resistances to deformations (elastomeric bearings, pot bearings for rotation)

(4) Bearings for bridges are specified in EN 1337 – structural bearings, the structure of which may be taken from Figure 3-2 [7].

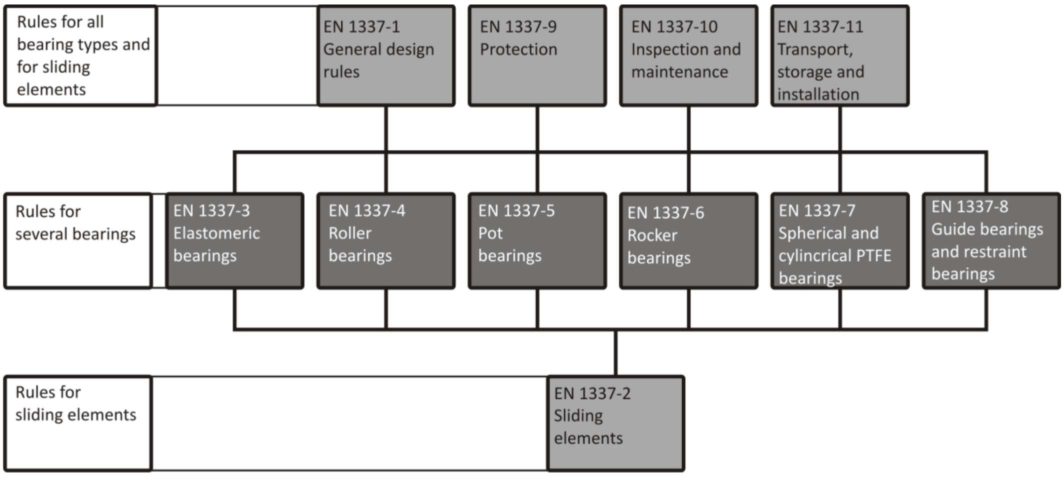

Figure 3-2: **Structure of EN 1337-Structural bearings**

(5) Table 3-1 gives an example for the relationship between the various parts of EN 1337 to the parts of former DIN 4114 (German standard) the contents of which has been fully or partially withdrawn. Such comparison may be made for any other National Standard.

Table 3-1: **Survey on EN 1337 and relation to DIN 4141**

Standard	Title	Status and remarks
DIN EN 1337-1, Februay 2001	General design rule	Standard in force, no product standard, replaces partly DIN V 4141 – 1, -2, -3
DIN EN 1337-2, July 2004	Sliding elements	Standard in force, no product standard
DIN EN 1337-3, July 2005 Product standard	Elastomeric bearing	Standard in force, replaces DIN 4141-14-14/A1, -140/A1, partly -15, -140, -150
DIN EN 1337-4, April 2004 Product standard	Roller bearings	Standard in force, does not replace any DIN-standard
DIN EN 1337-5, July 2005 Product standard	Pot bearings	Standard in force, does not replace any DIN-standard
DIN EN 1337-6, June 2004 Product standard	Rocker bearings	Standard in force, does not replace any DIN-standard

Table 3-1: continued

Standard	Title	Status and remarks
DIN EN 1337-7, August 2003 Product standard	Spherical and cylindrical PTFE bearings	Standard in force, does not replace any DIN-standard
DIN 1337-8, January 2008 Product standard	Guided bearings and restraint bearings	Standard in force, replaces DIN 4141-13
DIN EN 1337-9, April 1998	Protection	Standard in force, no product standard, replaces partly DIN V 4141-1
DIN EN 1337-10, November 2003	Inspection and maintenance	Standard in force replaces partly DIN V 4141-1
DIN EN 1337-11, April 1998	Transport storage and installation	Standard in force replaces DIN 4141-4

(6) EN 1337 deals exclusively with the construction products “bearings”. EN 1337 does not deal with the installation and supplementary equipments of bearings as “anchor plates” and with other requirements which were contained e.g. in Germany in “Allgemeine Bauaufsichliche Zulassungen” (General technical Approvals) and “Lager-Richtzeichungen” (Guidance drawings for bearings) before EN 1337 got into force, see Figure 9-4. As these requirements also control the quality of the bearings with respect to durability and safety of use, they are now summarized in the “Allgemeine Bauaufsichtliche Zulassungen” of the Deutsche Institut für Bautechnik (DIBt) in addition to EN 1337, e.g.

- Z-16.7-444 “Ausstattung von RWSH-Brückenlagern mit CE-Kennzeichung“ (Equipment of RWSH bridge-bearings with CE-marking) or
- Z-16.4-436 or ETA-06/0131 „Maurer MSM®-Kalottenlager“ (Maurer MSM®-spherical and cylindrical PTFE-bearings). The bearing can be installed with the supplementary equipment specified in this Technical Approvals directly into the bridge structure without further additions.

This example should be used to check the situation in other regulatory environments.

(7) The choice of material for the supplementary equipment, e.g. anchoring parts, fasteners, fill plates, wedge plates and additional plates, the material of which should comply with the EN-Standards and be suitable for the purpose and welding, should be according to EN 1993 – Part 2 [9].

(8) The effective temperature of the bearings for determining the application field in accordance with EN 1337 [7] is the minimum and maximum air-temperature.

(9) The aim of this report is the choice of material for steel components of bearings, which complements the rules for choice in EN 1993 – Part 2.

3.2 Selection of standard components of bearings for facture mechanics assessments

(1) From the list of type of bearings according to Figure 3-1 two reference types (Type A and Type B) are selected, see Figure 3-3.

(2) The difference between type A and type B is the detailing of the sliding plate and of the welded lateral guiderail.

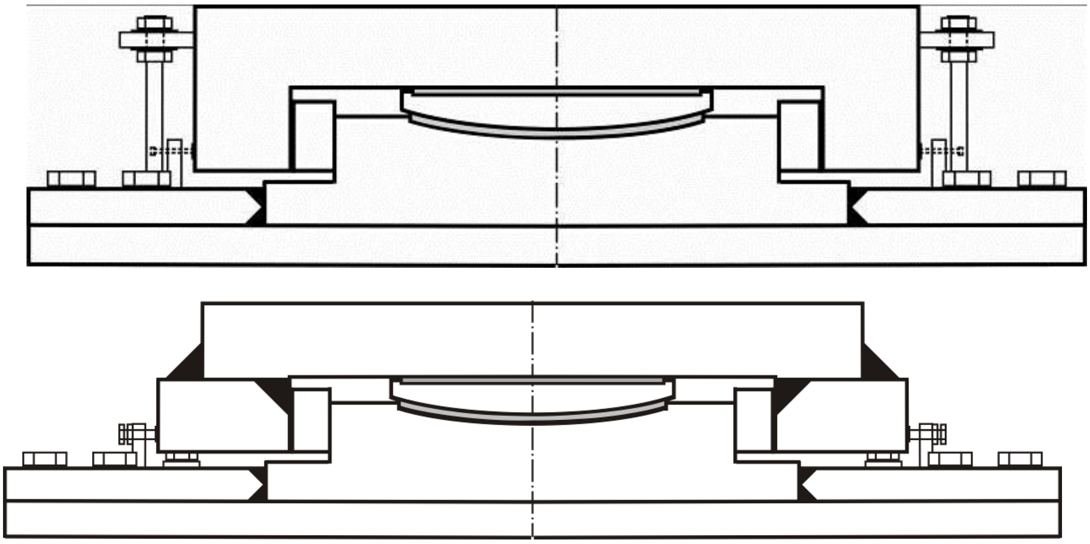

Figure 3-3: Reference type of bearings, Type A (above) and Type B (below)

(3) The investigations comprise all components of the bridge bearing, that comply with the product standard EN 1337-Structural bearings [7] and also the “anchor plate”.

(4) The components of the bearings and their details may be taken from Table 3-2.

(5) The choice of the reference types of bearings according to Figure 3-3 and of the Standard details according to Table 3-2 has been agreed with CEN/TC 167.

(6) Table 3-2 also gives the hot-spots, for which the fracture mechanics assessments are carried out.

Table 3-2: Standard details for bearing components to be investigated

Nr.	Steel component	Geometry Type A	Geometry Type B	Symmetry
1	*Top component* *(Sliding plate and lateral guiderail)* 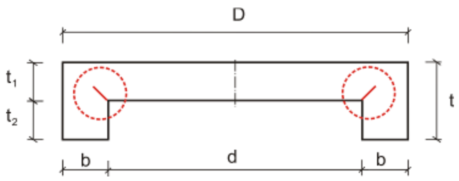	t: 55 – 315 mm t_1: 20 – 215 mm t_2: 25 – 100 mm *D: 500 – 1800 mm* *d: 355 - 1385 mm* *b: 50 - 505 mm*		Rotational symmetry
2A	*Top component* *(sliding plate and lateral guiderail)* 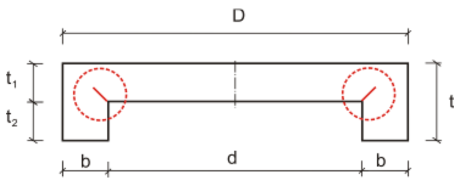	t: 55 – 315 mm t_1: 20 – 215 mm t_2: 25 – 100 mm *D: 500 – 1800 mm* *d: 355 - 1385 mm* *b: 50 - 500 mm*		Axial symmetry
2B	*Top component* *(sliding plate and lateral guiderail)* 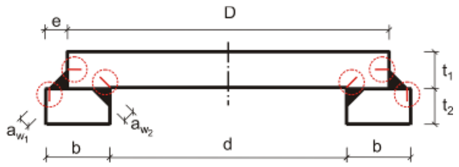		t_1: 55 – 285 mm t_2: 55 – 170 mm a_w: 12 - 42 mm *(K oder Y-weld)* *D: 440 – 2580 mm* *b: 55 - 570 mm*	Axial symmetry
3	*Bottom component* 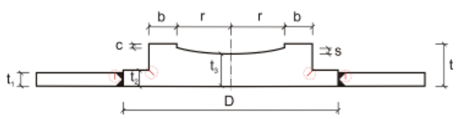	t: 55 – 255 mm t_1: 20 – 55 mm t_2: 20 – 60 mm t_3: 35 – 150 mm *D: 330 – 1800 mm* *b: 40-100 mm* *r: 135-590 mm*	t: 55 – 255 mm t_1: 20 – 55 mm t_2: 20 – 60 mm t_3: 35 – 150 mm *D: 330 – 1800 mm* *b: 40-100 mm* *r: 135-590 mm*	Axial symmetry
4	*Anchor plate* 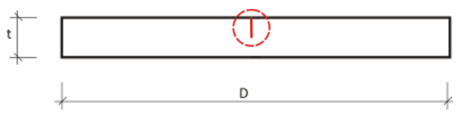	t: ≥ 55 mm *D: 440-3300 mm*	t: ≥ 55 mm *D: 440-3300 mm*	Axial symmetry
5	*Bearing for horizontal forces without rotation and capacity for vertical forces* 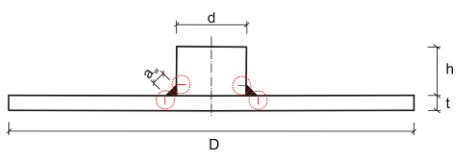	t: 30 – 150 mm d: 55 – 300 mm a_w: 5 – 25 mm *D: 440 - 3300 mm*	t: 30 – 150 mm d: 55 – 300 mm a_w: 5 – 25 mm *D: 440 - 3300 mm*	Rotational symmetry

4 Modification of the fracture mechanics safety assessment

4.1 General

(1) The fracture mechanics safety assessment as used in EN 1993-1-10 had to be adapted to the particularities of steel components for bearings in the following respect:

1. Definition of structural parameters that are typical for steel bearings
2. Definition of “nominal stresses” σ_{Ed} in compliance with the geometry and the loading of the steel components.

4.2 Definition of structural parameters typical for bearings

4.2.1 Model for fracture mechanics assessments

(1) The structural steel components of bearings are either rotationally-symmetric (e.g. for spherical bearings with restraints for all axes) or prismatic (e.g. for cylindrical bearings with unidirectional movable sliding).

(2) For simplifying the calculations for both the rotationally-symmetric and prismatic type of bearings a strip is selected, that in the case of rotationally-symmetric design represents a sector and in the case of prismatic design represents a parallel section transverse to the generator.

In compliance with this simplified model the assumption for the size of the initial crack is that of a continuous notch along the full perimeter of the component for rotationally-symmetric components and as linearly distributed along the length of the generator for axisymmetric components. Such a crack distribution can be interpreted as resulting from an accidental defect imposed during machining or welding.

4.2.2 Shape and magnitude of the design crack

(1) In the strips (either sectors or sections) used as fracture mechanics models the crack depth is constant along the width of the strips and also straight-lined.

It is located at the spot of high stress-concentration, where - in case of fatigue - fatigue cracks could be expected. The crack depth corresponds to the initial crack size in EN 1993-1-10, see Figure 2-4. As bearings considered in this report are not subject to fatigue, the design value of the initial crack depth a_d corresponds to the value of the crack a_0

$$a_d = a_0 = \frac{1}{2} \cdot \ln\left(1 + \frac{t}{t_0}\right) \qquad \text{for} \qquad t < 15\ \text{mm} \qquad \textbf{(4-1)}$$

$$a_d = a_0 = \frac{1}{2} \cdot \ln\left(\frac{t}{t_0}\right) \qquad \text{for} \qquad t \geq 15\ \text{mm} \qquad \textbf{(4-2)}$$

where t_0 = 1 mm.

(2) For the detectability of such cracks during production control see Figure 2-7.

4.2.3 Assumption for residual stresses

(1) EN 1993-1-10 provides two types of residual stresses:

1. Residual stresses in the local region around the welds at the hot spot from weld shrinkage which enhance the stresses in the welds and are reduced where cracks occur (primary residual stresses).
2. Far distance effect of weld shrinkage due to restraints resulting from the boundary conditions of the structural component (secondary residual stresses). These residual stresses are superimposed to the stresses from external loads and are not affected by local cracking at the hot spot.

(2) For the reference types A and B of bearings (see Figure 3-3) the occurrence of significant secondary stresses is improbable. For reference type B (welded alternative to type A) there may be large weld thicknesses (e.g. a_w = 42 mm) which will cause large primary residual stresses.

(3) In EN 1993-1-10 it is assumed that the primary residual stresses are covered by the calibration of the fracture mechanics assessment procedure to the results of fracture mechanics tests with typical large scale welded test specimens that include those primary stresses. For secondary residual stresses an assumption of σ_S = 100 MPa has been made.

(4) For the steel components of bearings it is assumed that primary residual stresses that may be larger than those assumed in EN 1993-1-10 and other unidentified effects from restraints both for type A and type B bearings will be covered by the use of a secondary residual stress of σ_S = 100 MPa.

4.2.4 Critical crack length b_{eff}

(1) The term ΔT_σ (see 2.2 (4)) contains a function

$$f(b_{eff}) = \left(\frac{25}{b_{eff}}\right)^{1/4} \qquad \textbf{(4-3)}$$

which takes into account the effect of the length of cracks on the probability of temperature shift and which has been derived from the “weakest-link-model”. The term b_{eff} refers to the length of the critical crack front. [6] contains information what values b_{eff} should be used depending of the type of crack. For this case of strip-models (sectorial and sectional) with continuous crack fronts the information in [6] are not usable.

(2) Figure 4-1 shows the influence of the length of the crack front b_{eff} on the function f (b_{eff})

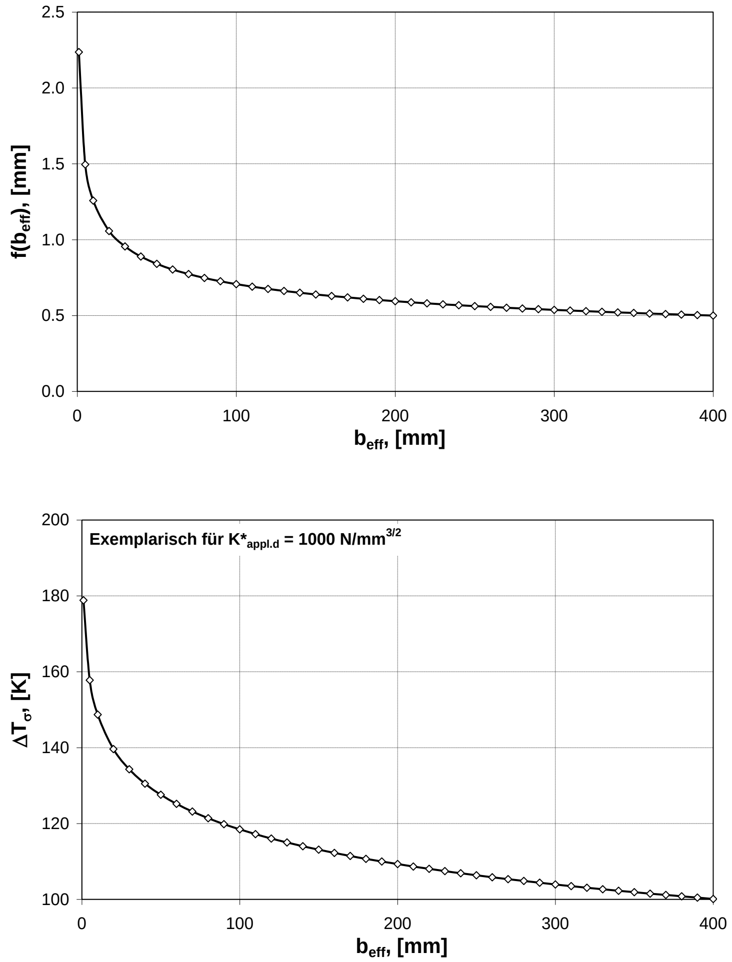

Figure 4-1: Influence of the length of crack front on the temperature term ΔT_{σ}

(3) It is evident from Figure 4-1 that a progressing effective length of crack front reduces the function $f(b_{eff})$. In the limit state equation for brittle fracture a small value of b_{eff} is advantageous, as the temperature T_{Ed} on the action side, which includes ΔT_{σ}, is increased, see Figure 4-1.

(4) In order to take account of the scale effect by $f(b_{eff})$ for bearings the term

$$f(b_{eff}) = \left(\frac{25}{b_{eff}}\right)^{1/4} \quad \textbf{(4-4)}$$

is substituted by

$$f(b_{eff}) = \left(\frac{25}{t}\right)^{1/4} \quad \textbf{(4-5)}$$

where t is the steel product (e.g. plate-) thickness at the hot spot. This assumption corresponds to the procedure to consider the reduction of fatigue resistance for thick plates in EN 1993-1-9.

(5) As a consequence of

$$f(b_{eff}) = \left(\frac{25}{t}\right)^{1/4}$$

the temperature T_{Ed} ($\geq T_{Rd}$) is the more reduced the thicker the plate thickness is.

4.2.5 Determination of the stress limit σ_{gy}

(1) The stress limit σ_{gy} is the stress to the gross section that causes yielding of the net section. This value is needed to determine the correction function k_{R6} from the CEGB-R6-diagram. For the standard case of a straight surface crack, see Figure 4-2, σ_{gy} may be determined according to [6] from

$$\sigma_{gy}(t) = f_y(t) \cdot \left(1 - \frac{a}{t}\right) \tag{4-6}$$

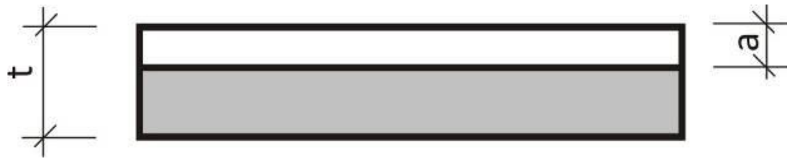

Figure 4-2: Definition of net section yielding

4.2.6 Inhomogenity of toughness in through-thickness direction

(1) Steel components of bearings may be produced from thicker plates by machining. The thickness of the plates may be in the order of magnitude of the thickness of the machined steel component, so that the steel properties of the plate apply. The thickness of the plate may however be greater, so that the position of the steel component in through thickness direction controls whether the properties of the thick plate according to the certificate (position of test sample close to the surface) apply or not.

(2) In case the position of the steel component is outside the position of the test sample for the certificate for the thick plate, particular material tests from the inner part from which the steel component is produced should be considered.

(3) In the fracture mechanics assessment procedure to avoid brittle fracture a "normal" reduction of material toughness in through-thickness direction is taken into account by the term

$$\Delta T_{27J} = 12{,}9 \cdot \tanh\left(2{,}1 \cdot \ln(t) - 7{,}5\right) + 12{,}8 \tag{4-7}$$

This case applies where the thickness of plate to be machined is in the order of the magnitude of the thickness of the steel component.

By the term ΔT_{27J} the temperature T_{Rd} on the resistance side is increased with unfavourable effects.

(4) For the assessment of steel components of bearings the term ΔT_{27J} is generally used to model a certain "normal inhomogeneity", even if the hypothetical crack would not enter into the core part of the material (inner third of material thickness).

(5) A condition for "normal inhomogeneity" for larger thickness of material is, that the steel-properties of the inner parts of thick plates do not "significantly" deviate from the properties at the spot where the sample is taken. Such significant deviations may e.g. be caused by insufficient rolling technology in the steel mill.

(6) As long as EN 10025 does not provide options for specifications of the inner part of thick products, additional tests should be agreed for the material delivery.

4.2.7 Strain rate effects, cold forming

(1) Temperature shifts from high strain-rates or from high degrees of cold-forming are not relevant for bearings and therefore are ignored.

4.3 Definition of the nominal values σ_{Ed} from the geometry and loading of steel components of bearings

4.3.1 General

(1) In the fracture mechanics assessment of structural steel components according to EN 1993-1-10 there is the underlying thought, that according to Figure 4-3 a fracture mechanics test specimen could be cut out of the structural steel component which contains all relevant geometrical and metallurgical parameters as shape, crack configuration and local residual stresses from welding and is loaded at the edges by uniformly distributed nominal stresses σ_{tot} from external loads and from residual stresses from long distanced restraints.

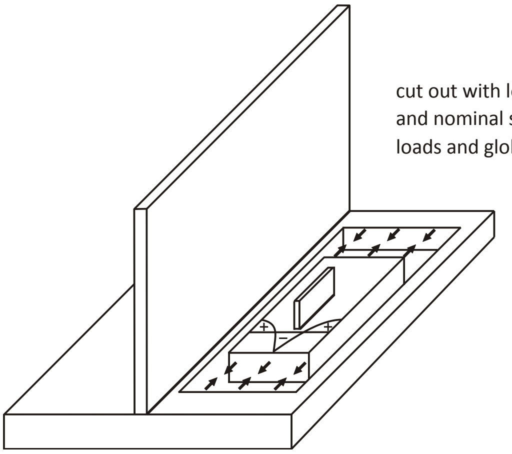

Figure 4-3: Fracture mechanics test specimen cut-out from the structural component

(2) This fracture mechanics test specimen is taken as the fracture mechanics model for which the assessment can be carried out experimentally or numerically.

(3) The stress σ_{Ed} from external loads will be determined using the bending theory for structural components and results from

$$\sigma_{Ed} = \frac{N_{Ed}}{A} + \frac{M_{Ed}}{W} \quad \textbf{(4-8)}$$

Where the stresses are not uniform in through thickness direction the maximum stress σ_{Ed} at the surface is taken as uniform stress on the safe side.

(4) For bearings the geometry of steel components is more compact than that of normal steel structures; therefore the components have already the size and characteristics of fracture mechanics models; they can be reduced in size only by taking advantage of symmetrical effects.

(5) Table 4-1 gives a survey on the fracture mechanics models for the component numbers in Table 3-2 as well as on the load assumptions and boundary conditions for deformations, on which the calculations have been based. These load assumptions and

boundary conditions in Table 4-1 are not realistic in any case, they have however been selected as reference situations suitable for a standardized procedure.

(6) The standardized procedure cannot presume for all cases that the stresses σ_{Ed} can be determined according to the bending theory, see 4.3.1(3); to cover all cases the standard procedure is based more generally on Finite Element calculations in the first instance, on which a simplification with using the bending theory in the second instance is based.

(7) Therefore a relationship must be established between the nominal stress σ_{Ed} used for the choice of material to avoid brittle fracture and the results of Finite Element calculations.

(8) This relationship can be determined as follows:

1. For the models, loading conditions and crack configurations in Table 4-1 the stress intensity-factors $K_{appl,d}$ are calculated along the crack path for unit loading and varying geometrical parameters.
2. For the same situations, crack configurations, unit loading and geometries the distributions of main stresses σ_1 are determined, also along the crack path, and from the distribution of σ_1 the "hot spot-stress" σ_{HS} at the point of crack initiation is derived using the method of Dong.
3. By relating the distribution and the magnitude of the stress intensity factor $K_{appl,d}$ to the hot-spot-stresses σ_{HS} the distribution of the "normalized" stress-intensity factors $\overline{K}$ for the hot-spot stress σ_{HS} = 1 N/mm² is obtained.
4. It can be assumed that this distribution of normalized stress intensity factor $\overline{K}$ is not sensitive to variations of the loading and the boundary condition of the fracture mechanics model. It is therefore applicable to hot-spot-stresses σ_{HS}, which have been determined more realistically with the proper geometry, loading and boundary conditions. Hence the realistic fracture mechanics action effect is

$$K_{appl,d} = \overline{K} \cdot \sigma_{HS} \qquad \textbf{(4-9)}$$

where

$\overline{K}$ is the "normalized" distribution of stress-intensity factors for the geometry and loading according to Table 4-1

σ_{HS} is the hot-spot stress according to Dong determined for realistic geometrical and loading conditions

5. By this procedure the hot-spot stress σ_{HS} according to Dong determined for realistic geometrical conditions and loading receives the status of the "nominal stress" σ_{Ed} according to EN 1993-1-10, so that $\sigma_{Ed} = \sigma_{HS}$.

(9) With this procedure the producer of bearings has the possibility to carry out Finite Element calculations of the steel components of bearings for realistic conditions and to make the choice of material using the normalised value $\overline{K}$ and the reference stress σ_{Ed}.

(10) As it can be shown that steel components of bearings with usual dimensions and made of steel grade S355J2 are not much limited in size by fracture mechanics assessments to avoid brittle fracture, also a simplified procedure is presented at the end of the report that has been derived from the procedure with hot-spot stresses σ_{HS}. This simplified procedure helps to decide on the basis of the results of simplified ultimate limit state

checks using the bending theory whether the usual dimensions are sufficient. This simplified procedure allows to avoid more complex Finite Element calculations.

Table 4-1: **Fracture mechanics models with 2 dimension with assumptions for loading and boundary conditions**

No.	Component	No.	Component
1, 2A	1 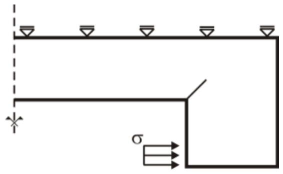 2 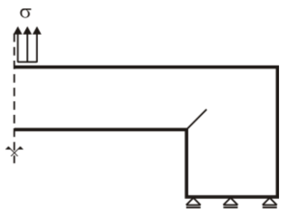	**3**	1 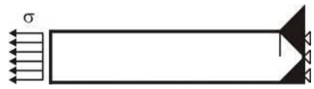 2 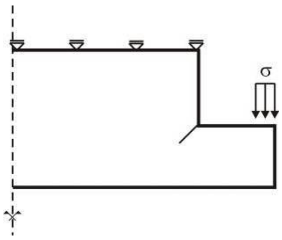
2B	1 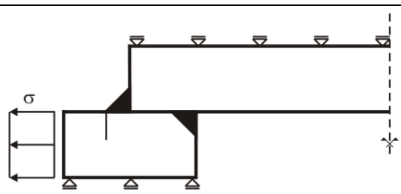 2 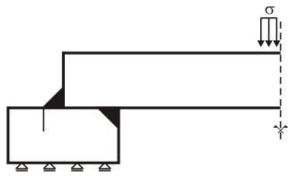 3 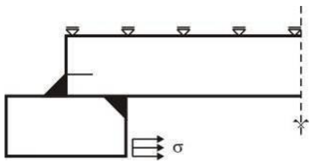 4 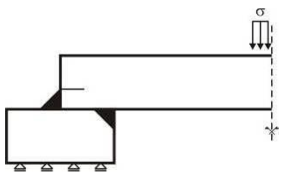 5 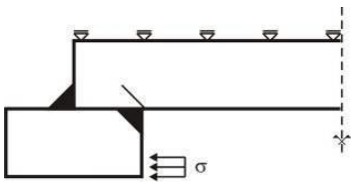 6 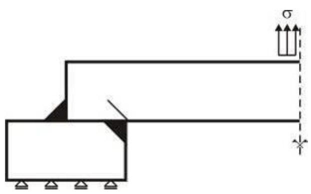	**4**	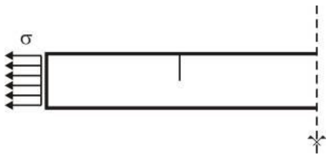
		5	1 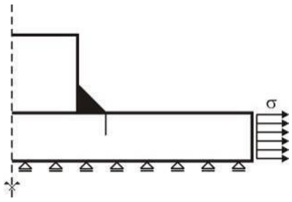 2 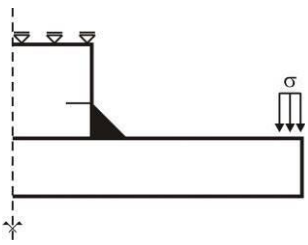

4.3.2 Determination of the reference stress $\sigma_{Ed} = \sigma_{HS}$ according to Dong

(1) For determining the reference stress σ_{Ed} (nominal stress) = σ_{HS} the Hot-Spot-stress method with modifications according to Dong [13], [14] is used.

(2) The standard Hot-Spot-stress method according to IIW-document [10] yields a certain "structural stress" at the Hot-Spot, which can be determined either experimentally or numerically via stress-values at defined "reference points" in the actual elastic stress distribution by extrapolation from these stress values to the "Hot-Spot", see Figure 4-4.

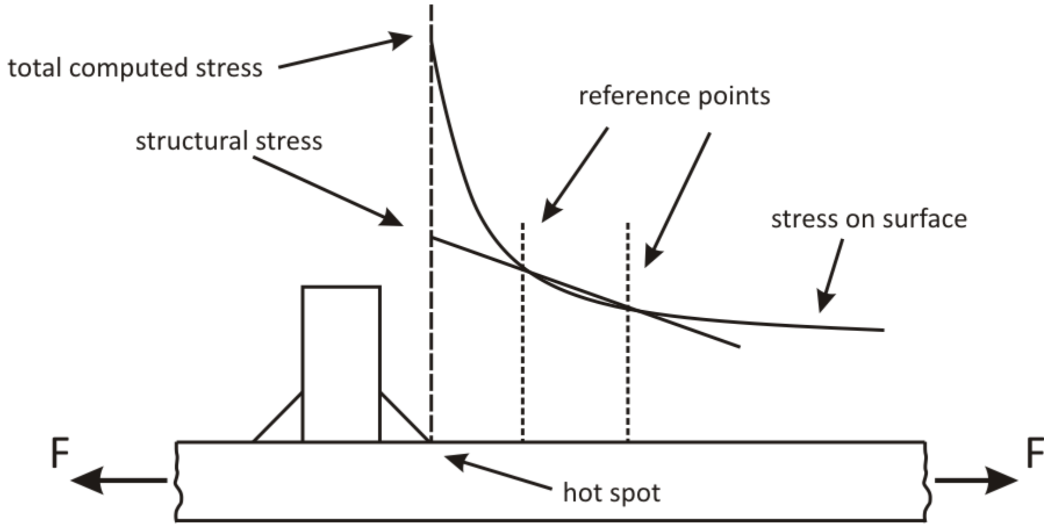

Figure 4-4: Definition of the "structural stress" according to IIW-document [10]

(3) The IIW-document gives recommendations for two types of structural stresses (type "a" with extrapolation on the flat surface of the plate element and type "b" with extrapolation at the cut side (at the edge of the plate element), see Figure 4-5.

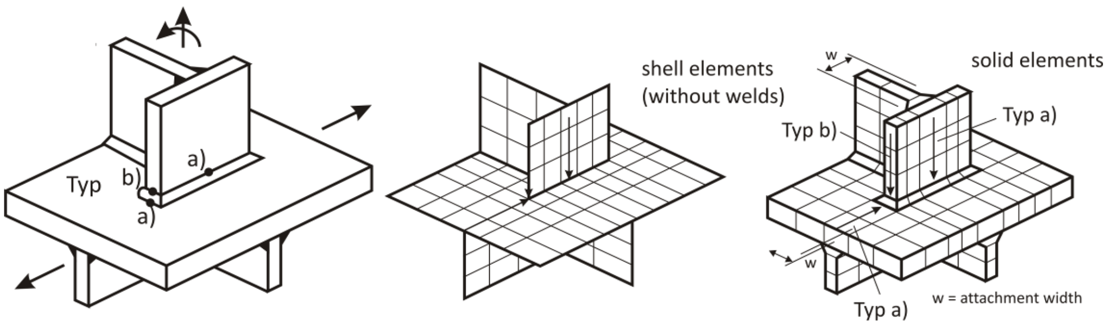

Figure 4-5: Types of structural stress (type "a" and type "b") according to IIW-document [10]

(4) The conditions for the selection of reference points and for the extrapolation function may be taken from Table 4-2.

Table 4-2: Determination of the Hot-Spot-stress σ_{HS} (structural stress) according to IIW-document [10]

Hot-Spot	relative fine mesh (as shown or finer)	relative coarse mesh (fixed element sizes)
type „a“	a) 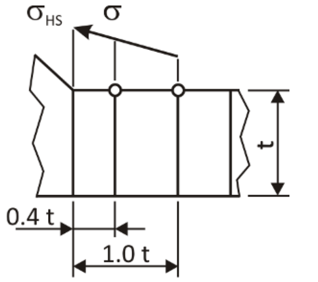 $\sigma_{HS} = 1{,}67 \cdot \sigma_{0{,}4 \cdot t} - 0{,}67 \cdot \sigma_{1{,}0 \cdot t}$ at sharp changes of direction of the applied force or for thick-walled structures. $\sigma_{HS} = 2{,}52 \cdot \sigma_{0{,}4 \cdot t} - 2{,}24 \cdot \sigma_{0{,}9 \cdot t} + 0{,}72 \cdot \sigma_{1{,}4 \cdot t}$	b) 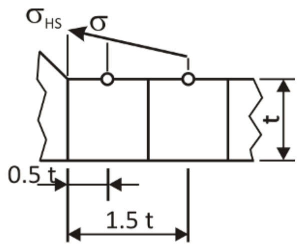 $\sigma_{HS} = 1{,}50 \cdot \sigma_{0{,}5 \cdot t} - 0{,}50 \cdot \sigma_{1{,}5 \cdot t}$
type „b“	c) 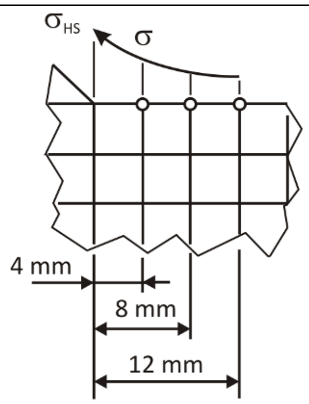 $\sigma_{HS} = 3 \cdot \sigma_{4mm} - 3 \cdot \sigma_{8mm} + \sigma_{12mm}$	d) 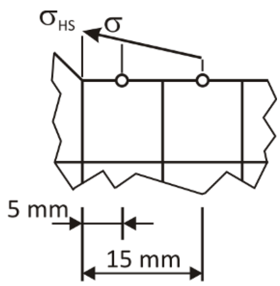 $\sigma_{HS} = 1{,}50 \cdot \sigma_{0{,}5 \cdot t} - 0{,}50 \cdot \sigma_{1{,}5 \cdot t}$

(5) The modified “structural stress” method according to Dong yields the “structural stress” σ_{HS} by linearization of the actual elastic stress distribution along the linear crack-path.

(6) There are three assumptions for the linearization that may be used for steel components of bearings, see Figure 4-6.

case a) Inner linearization for single sided fillet welds for full depth

case b) Inner linearization for single sided fillet welds for specified depth

case c) Inner linearization for double-sided fillet welds

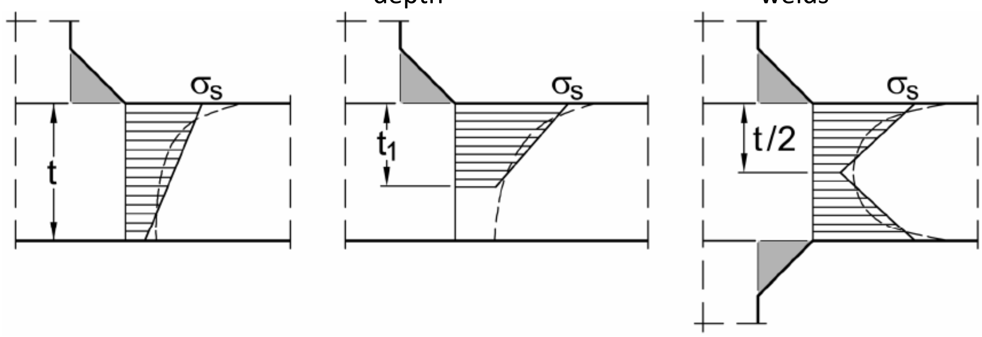

Figure 4-6: Definition of the “structural stress” according to Dong

(7) The advantages of this method in relation to the standard method for determining the Hot-Spot-stresses are the following:

1. The structural stress σ_{HS} determined in this way is from a single, linearization path and clear and unmistakable

2. It is taken into account that the structural stress σ_{HS} is not only controlled by small cracks at the Hot-Spot, but also by larger cracks that have progressed into the thickness of the product. Therefore σ_{HS} represents a certain equivalent for the "total stress" perpendicular to the crack. This "total stress" is approximated by the linearization.

3. The method also has been calibrated to the results of fatigue tests with various geometries of detail.

4. The determination of the structural stress from FE-calculations is relatively insensitive on the Finite-element-net- chosen. The conditions to be applied for fine nets given in Table 4-2 are taken into account.

5. The method is specified for use for pressure vessels and pipelines in the ASME-standard [12].

(8) For the different cases of linearization in Figure 4-6 the following applies:

- case a): monotonous reduction of the actual elastic stress distribution (dotted line) across the section; the "inner" linearization comprises the full cross-section. This results in general in the stresses as determined from the bending theory.

- case b): monotonous reduction of the actual elastic stress distribution (dotted line) in thick or wide cross-section or plates; the "inner" linearization is then recommended to cover only a part of the thick cross-section with a depth $t_1 < t$. It applies e.g. for cracks starting from a notch at the surface. For bearings the depth t_1 was determined at that point, where the actual elastic stress is reduced to 10 % of its maximum value.

- case c): non-monotonous reduction of the actual elastic stress distribution across the depth of the cross-section, e.g. for thick plates with welded attachments at either sides.

  This leads to a bilinear inner linearization.

For welded connections on both sides of the plate and for symmetrical stress distribution the linearization is recommended to be applied over half the plate thickness ($t_1 = t/2$). This gives a supplementary definition of structural stress used by Dong which is applicable for monotonous reduction of stress only.

4.3.3 Example for the determination of structural stress according to Dong

(1) As an example for the determination of the structural stress according to Dong the detail 2A from Figure 4-1 is chosen, for which the dimensions according to Figure 4-7 are applied.

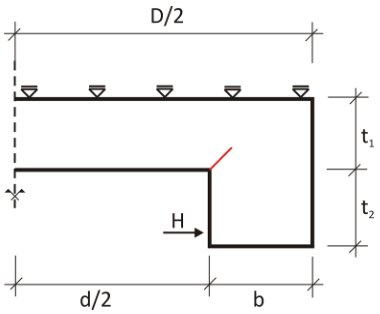

H	=	*10*	*N*
D	=	*1800*	*mm*
B	=	*50*	*mm*
t_1	=	*95*	*mm*
t_2	=	*100*	*mm*

Figure 4-7: **Example of detail 2A from Figure 4-1 for the calculation of structural stress according to Dong**

(2) The calculation was performed with the software ABAQUS with 8-nodal plate-elements with an average size of 1 x 1 mm.

(3) In the first step the standard Hot-Spot methods according to the IIW-document were used to determine the main stress-distributions approximately perpendicular do the potential crack path and to extrapolate with a non-linear extrapolation rule in horizontal and in vertical direction, see Figure 4-8. The results are σ_{HS} = 2,38 N/mm² for the horizontal path and σ_{HS} = 3,65 N/mm² for the vertical path.

(4) An estimation of magnitude of surface stress by the bending theory for the selected crack path would produce σ_{HS} = 2,4 N/mm².

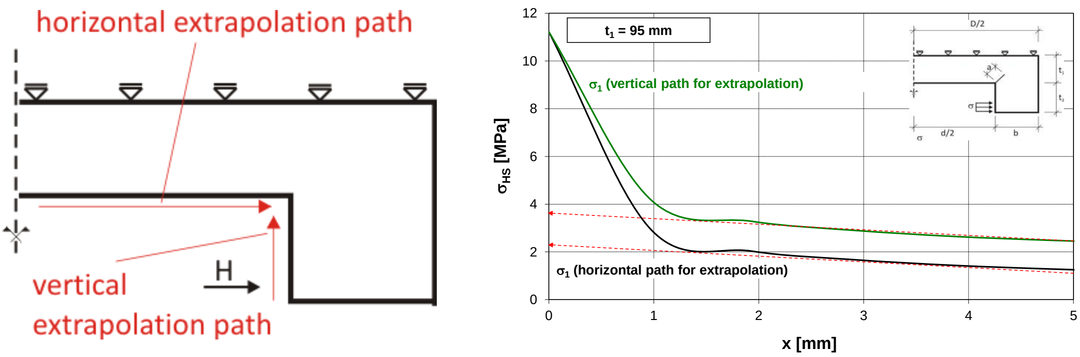

Figure 4-8: **Determination of Hot-Spot-stresses with the conventional Hot-Spot-stress method with extrapolation at the surfaces**

(5) The method of Dong requires an "inner" linearization of the actual stress along the hypothetical crack path (45°), see Figure 4-9. The "inner" linearization is performed automatically be the FE-software ABAQUS. The distribution of main stresses along the hypothetical crack path attains a maximum σ_{max} for s → 0 at the "geometrical singularity" and is reduced monotonously for s > 0.

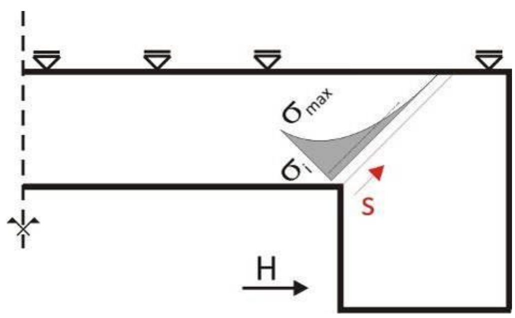

Figure 4-9: **Determination of Hot-Spot-stresses by "inner" linearization according to Dong**

(6) It is evident, that the magnitudes of the Hot-Spot-stresses are dependent on the length s used for the linearization. This length s is limited by the threshold value σ_i, under which stresses are ignored.

(7) In Figure 4-10 the Hot-Spot-stresses are plotted versus the linearization length and the related threshold stress σ_i:

For σ_I > 1.0 N/mm² the value σ_{HS} is σ_{HS} = 4,05 N/mm², for σ_1 = 0,5 N/mm² the value σ_{HS} is σ_{HS} = 3,33 N/mm².

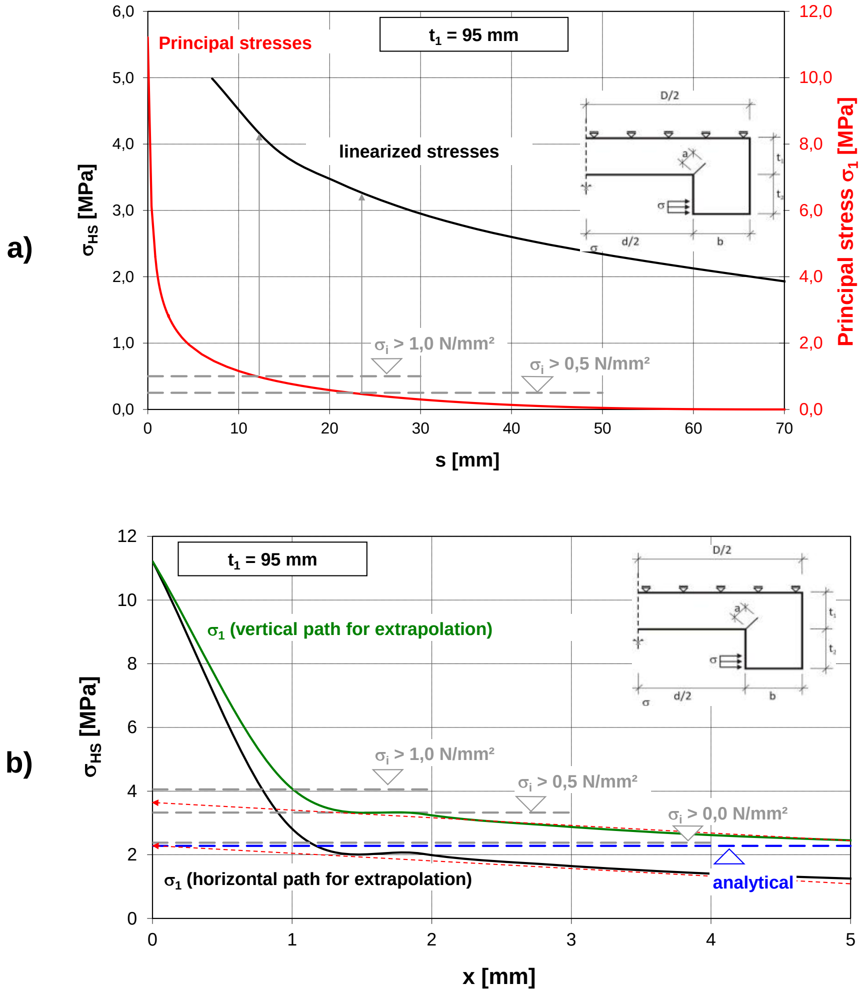

Figure 4-10: **Determination of the Hot-Spot-stress by the "inner" linearization according to Dong (a) and comparison with conventional Hot-Spot-stresses obtained by surface extrapolation (b) according to Figure 4-8**

(8) Figure 4-10 and Table 4-3 also show a comparison of results obtained with the conventional surface extrapolation method.

Table 4-3: **Comparison of Hot-Spot-stresses for the detail 2A**

	bending theory	**Hot-Spot-method**				
		extrapolation		**inner linearization**		
		horizontal	vertical	σ_i > 0,0 MPa	σ_i > 0,5 MPa	σ_i > 1,0 MPa
σ_{HS} [MPa]	2,4	2,38	3,65	1,92	3,33	4,05

(9) The comparison of results shows that the surface extrapolation gives only for the vertical extrapolation path representative values for fracture mechanics assessments. The “inner” linearization according to Dong gives only representative results for the threshold value $\sigma_i > 1{,}0$ N/mm² .

(10) From various such comparisons the conclusion has been drawn that for the method of Dong the threshold value should be fixed with the relative value

$\sigma_I = 0.10\ \sigma_{max}$, see Figure 4-11.

(11) The results of “inner” linearization with this threshold value $\sigma_I = 0.10\ \sigma_{max}$ and of the extrapolation with the vertical surface extrapolation are given in Figure 4-11 as a function of the product thickness t.

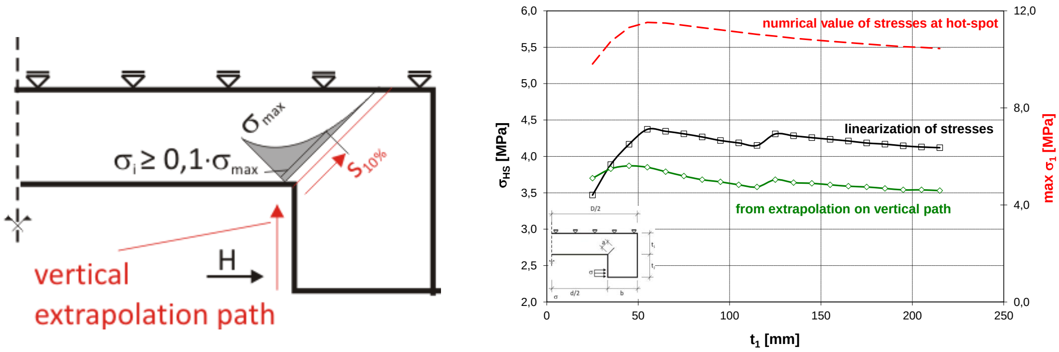

Figure 4-11: Hot-Spot-stresses from “inner” linearization according to Dong for the threshold value $\sigma I \geq 0.10\ \sigma_{max}$, (10 % criterion) and comparison with the results of surface extrapolation

(12) The dependency of the Hot-Spot stresses from the product thickness is affine for all methods.

(13) In the following report therefore the method of inner linearization according to Dong is applied.

(14) In this application the following steps were carried out:

1. Determination of the potential crack path to fix the linearization-path
2. Determination of main stress along the linearization path and derivation of the tensile stress-component perpendicular to the crack path
3. Determination of the length of linearization from the distribution of the maximum tensile stresses (10 % criterion)
4. Performance of the linearization
5. Derivation of the Hot-Spot-stress σ_{HS}.

Note: When preparing the meshing for Finite-Element-calculations it is necessary to provide a suitable radius at the point of “singularity”. Unless other data are available, a radius of 1 mm should be applied.

5 Numerical investigations and results

5.1 General

(1) For the models given in Table 3-2 and Table 4-1 the numerical investigations were performed with the FE-Software ABAQUS, Version 6.8, to obtain

- the Hot-spot-stresses according to section 4.3 of this report
- the stress intensity factor K,

as no catalogues of solutions were available for these details.

(2) The calculations were carried out with a linear elastic material law.

(3) The calculations gave the distributions the stress intensity factors K at the crack front.

(4) Out-puts of the calculations were the K-values for the crack-opening modes K_1 and K_2, see Figure 5-1.

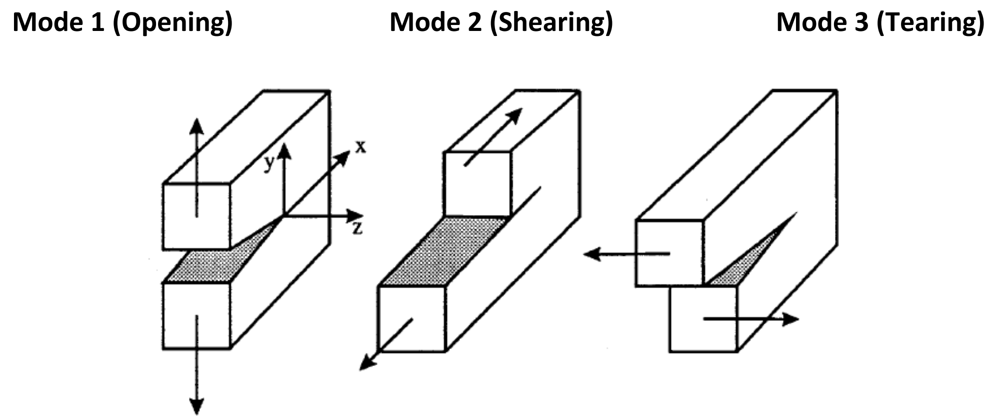

Figure 5-1: Crack opening modes

(5) The assessment method assumes that the main stresses are actions for crack opening mode 1.

(6) In order to cover the fact that the main stresses may possibly not be perpendicular to the crack-path, an effective K_{eff} is determined

$$K_{eff} = \sqrt{K_1^2 + K_1 K_2 + K_2^2} \quad \textbf{(5-1)}$$

(7) The fracture mechanics assessment is carried out with the maximum stress-intensity factor

$$K = \max(K_1, K_{eff}) \quad \textbf{(5-2)}$$

(8) For simplicity reasons the investigations are performed with a unit line load resulting from σ = 1 N/mm for a section with a length of 10 mm (load introduction). Due to linear relationship a different scaling of stresses, strains or stress intensity factors is easily possible.

(9) As a rule two calculations are carried out, one with the maximum, one with the minimum dimensions, that shall clarify, what gives the maximum influence on the risk of brittle fracture. In this report therefore fracture mechanics assessments were performed for the upper bounds and the lower bounds of the geometry of the bearings.

(10) Calculation models were produced using symmetries to reduce the expenditure for modelling and calculation.

(11) The modelling was made with two dimensional plate elements (8 nodal elements). In particular for the modelling of the crack tip a very fine meshing was necessary.

(12) In addition the determination of the stress intensity factor at the crack tip requires a particular meshing of this region with special-collapsed crack tip elements, that take account of the stress singularity at that spot, see Figure 5-2 for the example of the geometry of the detail 1 according to Table 4-1.

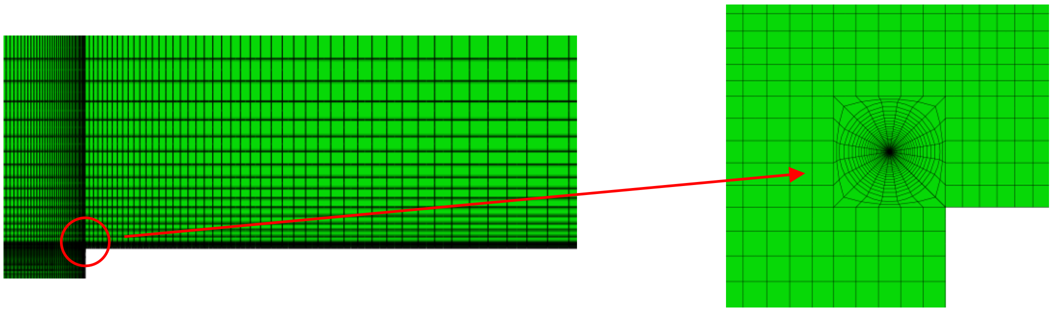

Figure 5-2: Spider web mesh configuration at the crack tip with collapsed finite elements for detail 1 in Table 4-1

5.2 Component No 1 – Rotationally-symmetric top component, type A (sliding plate and lateral guiderail)

5.2.1 Geometry, load assumptions and boundary conditions

(1) The geometry of the top component is given in Figure 5-3.

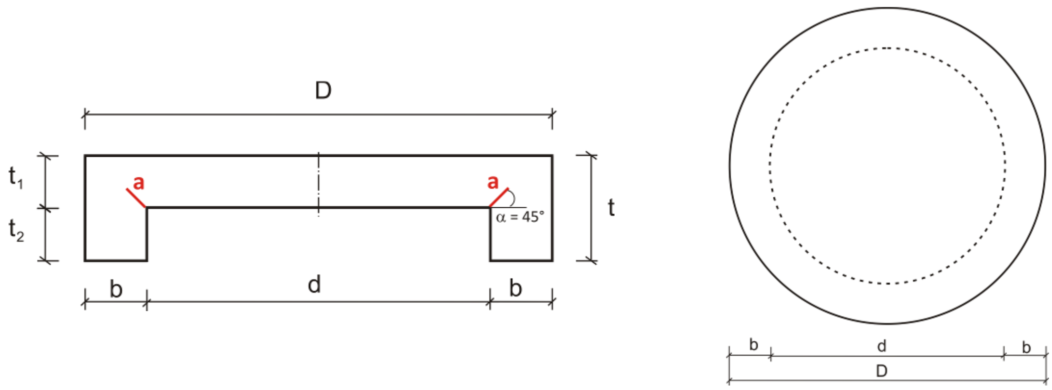

Figure 5-3: Detail No 1 – Top component of type A (sliding plate and guiderail)

(2) The numerical values of dimensions may be taken from Table 5-1.

Table 5-1: Dimensions for detail 1

t [mm]	t_1 [mm]	t_2 [mm]	D [mm]	d [mm]	b [mm]
55 – 315	20 – 215	25 – 100	500 – 1800	355 – 1385	50 - 500

(3) The loading should be independent of individual situations with realistic loading conditions. Therefore standard loading cases have been chosen that lead to representative fracture mechanics loading, see variants 1-1 and 1-2 in Figure 5-4.

(4) Both variants for loading lead to tension stresses in the re-entrant corner at the connection between the sliding plate and the guiderail.

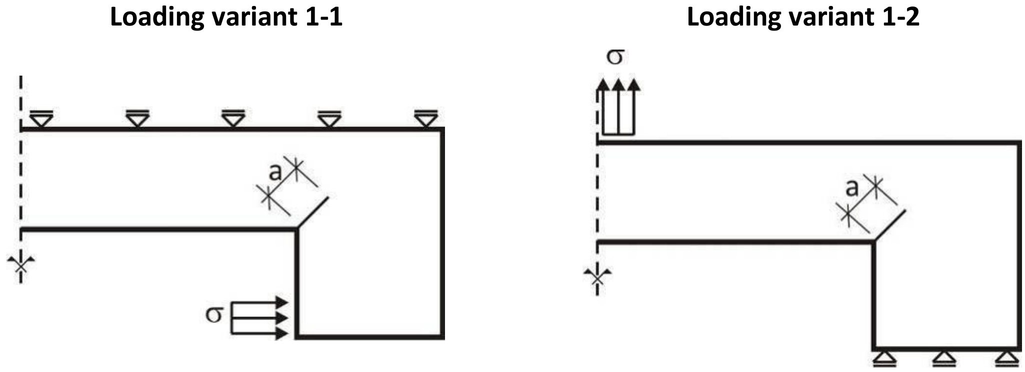

Figure 5-4: Variants for loading for detail 1: Variant 1 with horizontal loading (left), variant 2 with vertical loading (right)

(5) The calculations were performed for two geometrical configurations at the lower and upper bounds of dimensions as recommended by the producers of bearings, see Table 5-2. Besides the plate-thickness t_1 also the width b of the guide-rail has proved to be relevant for the variation of the stress intensity factors. The diameter D of the sliding plate was kept maximum, to produce the maximum bending moment in particular for loading variant 2 at the re-entrant corner.

Table 5-2: **Upper and lower bounds of the geometrical dimension for detail 1**

Upper bounds		Lower bounds	
t_1 [mm]	20 - 215	t_1 [mm]	20 - 215
t_2 [mm]	100	t_2 [mm]	100
D [mm]	1800	D [mm]	1800
d [mm]	970	d [mm]	1700
b [mm]	415	b [mm]	50

(6) The crack orientation for both loading variants was 45°, so that the maximum stress-intensity factor was achieved. Vertical or horizontal crack-configurations with equal crack depths have a small influence on the stress intensity factor and prove to be less critical than the crack configurations with 45°.

(7) The value of the initial crack size a_0 is determined in dependence of the plate thickness t and rises with increasing plate thickness.

(8) Figure 5-5 gives a section of the FE-model as well as the deformations with crack-opening.

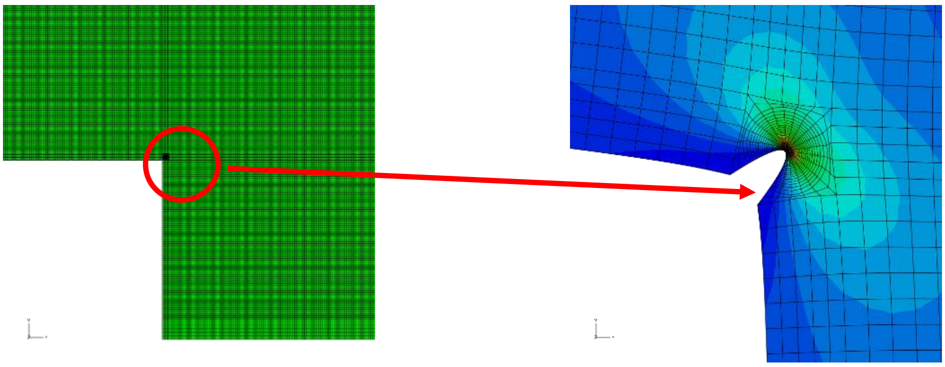

Figure 5-5: Section of the FE-model (left) and part with crack opening (right)

5.2.2 Hot-Spot-stresses

(1) For the loading variant 1-1 Figure 5-6 (left) shows the Hot-Spot-stresses for the upper bounds of the geometrical dimensions according to Table 5-2 and Figure 5-6 (right) gives the values for the lower bounds.

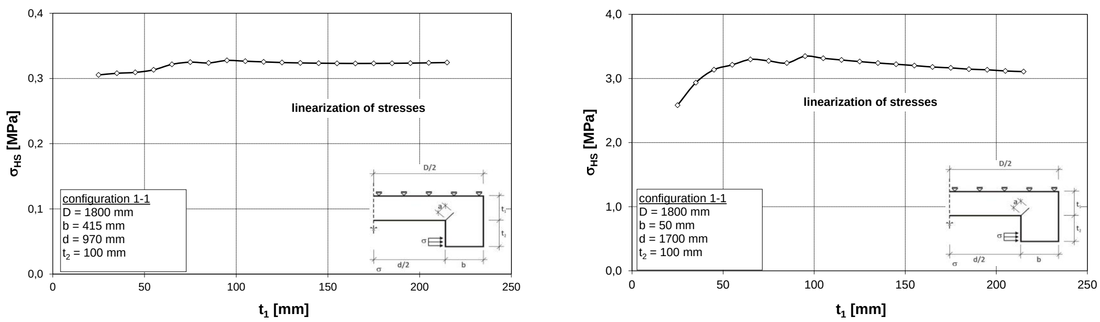

Figure 5-6: Hot-Spot-stresses obtained with "inner" linearization according to Dong for geometric upper bounds (left) and lower bounds (right) for loading variant 1-1

(2) The influence of the product thickness t_1 is small; for the geometric lower bound there is a maximum at t_1 = 95 mm.

(3) For the loading variant 1-2 Figure 5-7 gives the Hot-Spot-stresses in dependence of the product thickness t_1 for the geometric upper bounds (left) and lower bounds (right).

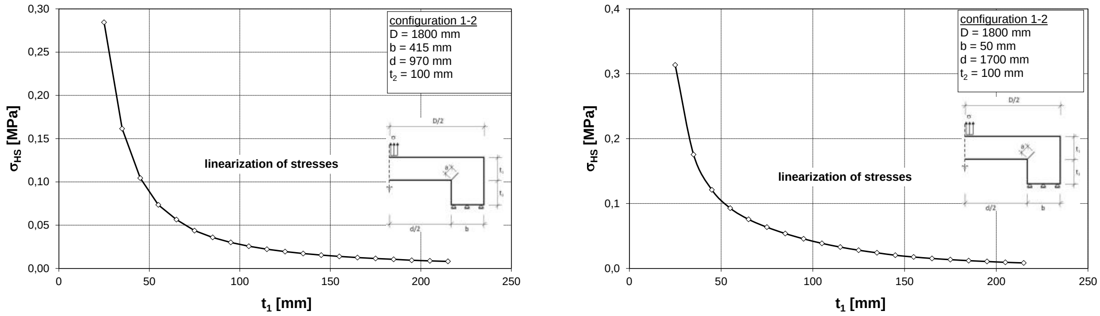

Figure 5-7: **Hot-Spot-stresses obtained with “inner” linearization according to Dong for geometric upper bounds (left) and lower bounds (right) for loading variant 1-2**

(4) The dependency on t_1 is significant; the dependency on the geometric upper bound and lower bound is smaller (slightly higher values for lower bounds)

5.2.3 Stress intensity factors

(1) For the loading variant 1-1 Figure 5-8 (left) shows the dependency of the stress intensity factors on the plate thickness t_1 in the range of 25 mm to 215 mm for the upper bounds of the geometrical dimensions. The function of the K_1 values versus t_1 is rather constant with some slight decrease with increasing t_1. The effect of modus 2 is negligible.

(2) After normalization the K-values by relating them to the unit Hot-Spot-stress $\sigma_{HS} = 1$ N/mm² the normalized values $\overline{K}$ are almost constant for increasing plate-thickness t_1, see Figure 5-8.

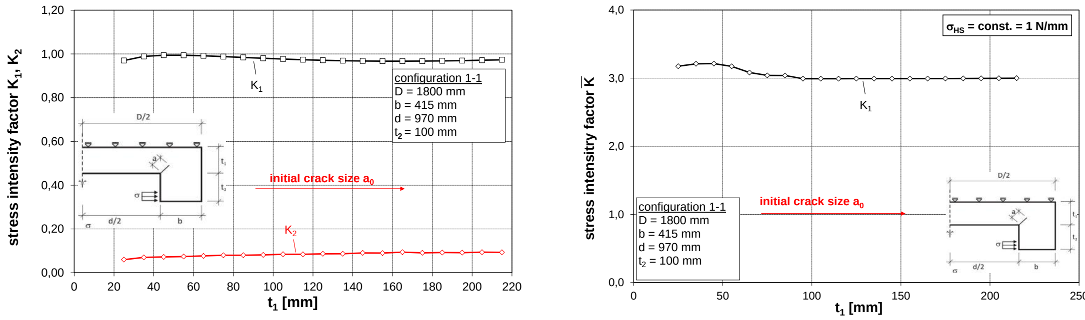

Figure 5-8: **K-values (left) and normalized $\overline{K}$-values (right) related to σ_{HS} = 1 N/mm² for the geometric upper bounds for loading variant 1-1**

(3) The results for the lower bounds of geometric dimensions are given in Figure 5-9.

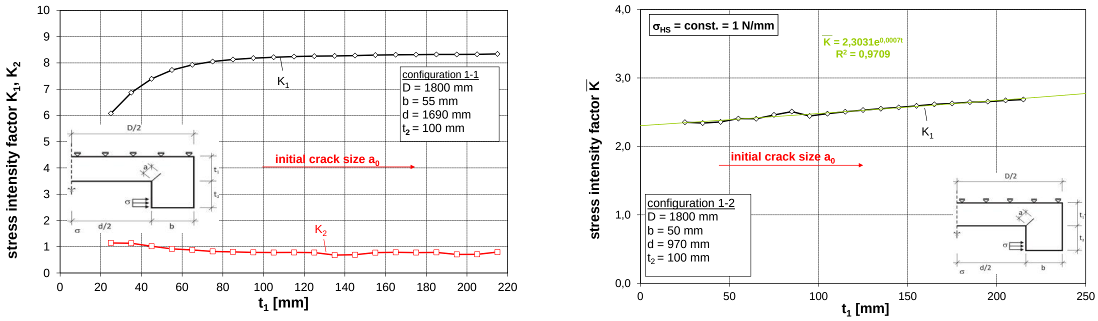

Figure 5-9: **K-values (left) and normalized $\overline{K}$-values (right) related to σ_{HS} = 1 N/mm² for the geometric lower bounds for loading variant 1-1**

(4) Whereas in Figure 5-9 (left) the K-values decrease for t < 100 mm, the normalized $\overline{K}$-values related to σ_{HS} = 1 N/mm² (Figure 5-9, right) are linear and can be approximated by

$$\overline{K} = 2{,}3021 e^{0{,}0007 t_1} \quad \textbf{(5-3)}$$

(5) For loading variant 1-2 Figure 5-10 gives the dependency of the K-values on the product thickness t_1 for the geometrical upper bounds of the dimensions.

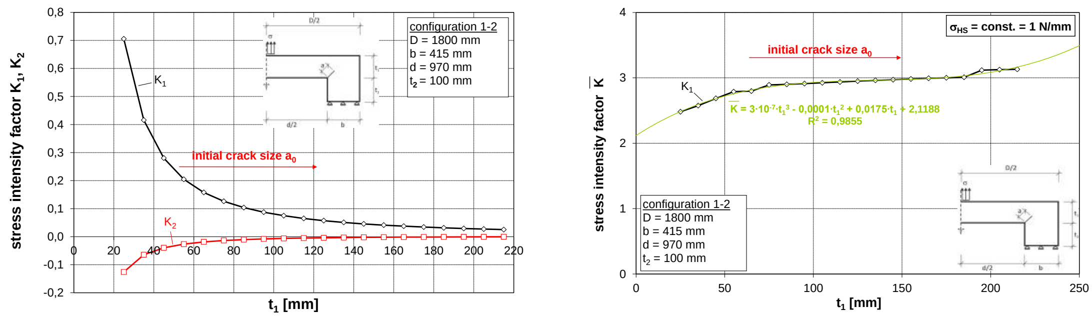

Figure 5-10: K-values (left) and normalized $\overline{K}$-values (right) related to σ_{HS} = 1 N/mm² for the geometric upper bounds of dimensions for loading variant 1-2

(6) After normalising the K-values by relating them to σ_{HS} = 1 N/mm² the normalized $\overline{K}$-values can be approximated by the polynomial

$$\overline{K} = 3{,}0779 \cdot 10^{-7} t_1^3 - 1{,}2514 \cdot 10^{-4} t_1^2 + 1{,}7547 \cdot 10^{-2} t_1 + 2{,}1188 \quad \textbf{(5-4)}$$

(7) In Figure 5-11 similar values $\overline{K}$ are shown for the lower bounds of the geometrical dimensions.

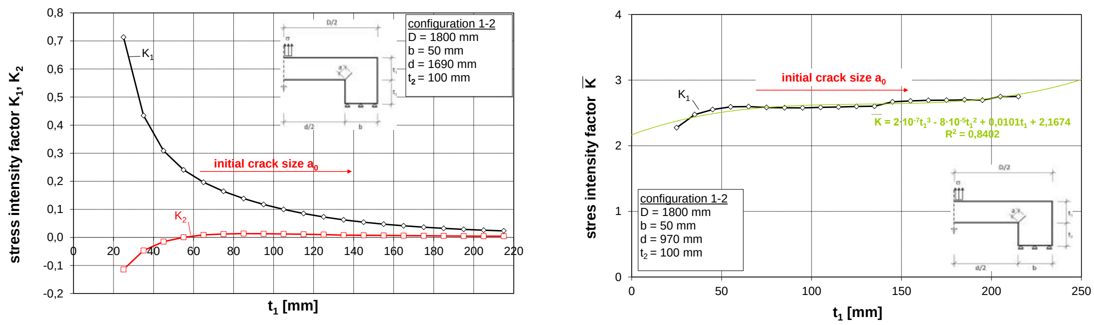

Figure 5-11: K-values (left) and normalized $\overline{K}$-values (right) related to σ_{HS} = 1 N/mm² for the geometric lower bounds of dimensions for loading variant 1-2

(8) After normalizing the K-values by relating them to σ_{HS} = 1 N/mm² the normalized $\overline{K}$-values can be approximated by the polynomial

$$\overline{K} = 1{,}9297 \cdot 10^{-7} t_1^3 - 7{,}5274 \cdot 10^{-5} t_1^2 + 1{,}0121 \cdot 10^{-2} t_1 + 2{,}1674 \quad \textbf{(5-5)}$$

5.2.4 Assessments to avoid brittle fracture

(1) The fracture mechanics assessment was performed for steel S355J2 for

- varying product thicknesses t_1,
- varying utilisation rates $\frac{\sigma_{Ed}}{f_y} = \frac{\sigma_{HS}}{f_y}$ and
- temperatures T_{Ed} of the components

(2) For the loading variant 1-1 Table 5-5 gives the numerical values for the assessments $T_{Ed} = T_{Rd}$ for σ_{Ed}/f_y = 0,75 and T_{Ed} = -50°C, which all lead to a maximum thickness greater than the limit 250 mm assumed for the production.

(3) For the loading variant 1-2 similar calculations, listed in Table 5-6 give small restrictions of the product thickness for σ_{Ed}/f_y = 0,75 and T_{Ed} = -50°C.

(4) From the calculations in Table 5-5 and Table 5-6 the limits of product thickness for loading variant 1-1 are given in Table 5-3 and that for loading variant 1-2 are given in Table 5-4.

(5) The relevant values for standardising the assessment procedure may be taken from Table 5-4.

Table 5-3: Limits of plate thickness t_1 [mm] for the top component of bearing (loading variant 1-1)

Steel grade acc. to EN 10025	σ_{Ed}	0°C	-10°C	-20°C	-30°C	-40°C	-50°C
S355J2	$0{,}25 \cdot f_y$	250*)	250*)	250*)	250*)	250*)	250*)
S355J2	$0{,}50 \cdot f_y$	250*)	250*)	250*)	250*)	250*)	250*)
S355J2	$0{,}75 \cdot f_y$	250*)	250*)	250*)	250*)	250*)	250*)

*) *Assumption of a technical manufacturing limit (in theory element thicknesses with t ≥ 250 mm would be acceptable)*

Table 5-4: Limits of plate thickness t_1 [mm] for the top component of bearing (loading variant 1-2)

Steel grade acc. to EN 10025	σ_{Ed}	0°C	-10°C	-20°C	-30°C	-40°C	-50°C
S355J2	$0{,}25 \cdot f_y$	250*)	250*)	250*)	250*)	250*)	250*)
S355J2	$0{,}50 \cdot f_y$	250*)	250*)	250*)	250*)	250*)	250*)
S355J2	$0{,}75 \cdot f_y$	250*)	250*)	250*)	250*)	250*)	235

*) *Assumption of a technical manufacturing limit (in theory element thicknesses with t ≥ 250 mm would be acceptable)*

Table 5-5: **Fracture mechanics assessments for loading variant 1-1 for component No. 1 (Rotationally-symmetric top component (Sliding plate and guiderail))**

Assessment for $\sigma_{Ed} = 0,75 \cdot f_y$ and T = -50 °C

Nr	σ_P N/mm²	K_1 $N/mm^{3/2}$	σ_{Ed}/f_y [-]	σ_P N/mm²	σ_S N/mm²	a_0 mm	t_1 mm	$K_{1,P}$ $N/mm^{3/2}$	$K_{1,S}$ $N/mm^{3/2}$	$K_{1,ges}$ $N/mm^{3/2}$	$K_{1,ges}$ $MPam^{1/2}$	$f_{y,nom}$ N/mm²	$f_y(t)$ N/mm²	σ_{gy} N/mm²	L_r -	ψ -	ρ_1 -	ρ -	k_{R6} -	$K_{appl,d}$ $N/mm^{3/2}$	$K_{appl,d}$ $MPam^{1/2}$	b_{eff} mm		ΔT_σ °C	$K_{V,nom}$ J	T_{KV} °C	T_{27J} °C	ΔT_{27J} °C	ΔT_R °C	T_{md} °C	ΔT_r °C	ΔT_ε °C	ΔT_{DCF} °C	T_{Ed} °C	T_{Rd} °C	$T_{Ed} \geq T_{Rd}$
1	1,0	3,17	0,75	266,3	100	1,61	25	845	317	1163	36,8	355	349	326	0,82	0,31	0,04	0,04	0,87	1407	44,5	25	14,49	81,9	27	-20	-20	5	7	-45	-5	0	0	**39**	**-33**	no risk
2	1,0	3,21	0,75	266,3	100	1,78	35	855	321	1176	37,2	355	346	329	0,81	0,30	0,04	0,04	0,87	1421	44,9	35	17,13	73,2	27	-20	-20	12	7	-45	-5	0	0	**30**	**-26**	no risk
3	1,0	3,21	0,75	266,3	100	1,90	45	856	321	1177	37,2	355	344	329	0,81	0,30	0,04	0,04	0,87	1422	45,0	45	18,93	68,0	27	-20	-20	19	7	-45	-5	0	0	**25**	**-19**	no risk
4	1,0	3,17	0,75	266,3	100	2,00	55	845	317	1162	36,7	355	341	329	0,81	0,30	0,04	0,04	0,87	1405	44,4	55	19,74	65,8	27	-20	-20	22	7	-45	-5	0	0	**23**	**-16**	no risk
5	1,0	3,08	0,75	266,3	100	2,09	65	821	308	1129	35,7	355	339	328	0,81	0,30	0,04	0,04	0,87	1365	43,2	65	19,41	66,7	27	-20	-20	24	7	-45	-5	0	0	**24**	**-14**	no risk
6	1,0	3,04	0,75	266,3	100	2,16	75	809	304	1113	35,2	355	336	327	0,82	0,31	0,04	0,04	0,87	1347	42,6	75	19,73	65,9	27	-20	-20	25	7	-45	-5	0	0	**23**	**-13**	no risk
7	1,0	3,04	0,75	266,3	100	2,22	85	809	304	1113	35,2	355	334	325	0,82	0,31	0,04	0,04	0,87	1347	42,6	85	20,68	63,4	27	-20	-20	25	7	-45	-5	0	0	**20**	**-13**	no risk
8	1,0	2,99	0,75	266,3	100	2,28	95	796	299	1095	34,6	355	331	323	0,82	0,31	0,04	0,04	0,86	1327	42,0	95	20,66	63,4	27	-20	-20	25	7	-45	-5	0	0	**20**	**-13**	no risk
9	1,0	2,99	0,75	266,3	100	2,33	105	796	299	1096	34,6	355	329	321	0,83	0,31	0,04	0,04	0,86	1328	42,0	105	21,49	61,4	27	-20	-20	25	7	-45	-5	0	0	**18**	**-13**	no risk
10	1,0	2,99	0,75	266,3	100	2,37	115	796	299	1096	34,6	355	326	320	0,83	0,31	0,04	0,04	0,86	1329	42,0	115	22,26	59,6	27	-20	-20	26	7	-45	-5	0	0	**17**	**-12**	no risk
11	1,0	2,99	0,75	266,3	100	2,41	125	797	299	1096	34,7	355	324	317	0,84	0,31	0,04	0,04	0,86	1331	42,1	125	23,02	57,8	27	-20	-20	26	7	-45	-5	0	0	**15**	**-12**	no risk
12	1,0	2,99	0,75	266,3	100	2,45	135	797	299	1096	34,7	355	321	315	0,84	0,32	0,04	0,04	0,86	1332	42,1	135	23,71	56,3	27	-20	-20	26	7	-45	-5	0	0	**13**	**-12**	no risk
13	1,0	2,99	0,75	266,3	100	2,49	145	797	299	1096	34,7	355	319	313	0,85	0,32	0,04	0,03	0,86	1333	42,1	145	24,37	54,9	27	-20	-20	26	7	-45	-5	0	0	**12**	**-12**	no risk
14	1,0	2,99	0,75	266,3	100	2,52	155	797	299	1096	34,7	355	316	311	0,86	0,32	0,04	0,03	0,86	1334	42,2	155	25,01	53,5	27	-20	-20	26	7	-45	-5	0	0	**11**	**-12**	no risk
15	1,0	2,99	0,75	266,3	100	2,55	165	797	299	1096	34,7	355	314	309	0,86	0,32	0,04	0,03	0,85	1336	42,2	165	25,64	52,2	27	-20	-20	26	7	-45	-5	0	0	**9**	**-12**	no risk
16	1,0	2,99	0,75	266,3	100	2,58	175	797	299	1097	34,7	355	311	307	0,87	0,33	0,04	0,03	0,85	1337	42,3	175	26,24	51,0	27	-20	-20	26	7	-45	-5	0	0	**8**	**-12**	no risk
17	1,0	3,00	0,75	266,3	100	2,61	185	798	300	1097	34,7	355	309	304	0,87	0,33	0,04	0,03	0,85	1339	42,3	185	26,85	49,8	27	-20	-20	26	7	-45	-5	0	0	**7**	**-12**	no risk
18	1,0	3,00	0,75	266,3	100	2,64	195	798	300	1097	34,7	355	306	302	0,88	0,33	0,04	0,03	0,85	1341	42,4	195	27,43	48,7	27	-20	-20	26	7	-45	-5	0	0	**6**	**-12**	no risk
19	1,0	3,00	0,75	266,3	100	2,66	205	798	300	1098	34,7	355	304	300	0,89	0,33	0,04	0,03	0,85	1343	42,5	205	28,00	47,7	27	-20	-20	26	7	-45	-5	0	0	**5**	**-12**	no risk
20	1,0	3,00	0,75	266,3	100	2,69	215	799	300	1098	34,7	355	301	297	0,89	0,34	0,05	0,03	0,85	1344	42,5	215	28,56	46,6	27	-20	-20	26	7	-45	-5	0	0	**4**	**-12**	no risk
21	1,0	3,00	0,75	266,3	100	2,71	225	799	300	1098	34,7	355	299	295	0,90	0,34	0,05	0,03	0,84	1346	42,6	225	29,07	45,7	27	-20	-20	26	7	-45	-5	0	0	**3**	**-12**	no risk
22	1,0	3,00	0,75	266,3	100	2,73	235	799	300	1098	34,7	355	296	293	0,91	0,34	0,05	0,03	0,84	1347	42,6	235	29,57	44,8	27	-20	-20	26	7	-45	-5	0	0	**2**	**-12**	no risk
23	1,0	3,00	0,75	266,3	100	2,75	245	799	300	1098	34,7	355	294	290	0,92	0,34	0,05	0,02	0,84	1348	42,6	245	30,06	44,0	27	-20	-20	26	7	-45	-5	0	0	**1**	**-12**	no risk
23	1,0	3,00	0,75	266,3	100	2,76	250	799	300	1098	34,7	355	293	289	0,92	0,35	0,05	0,02	0,84	1349	42,7	250	30,30	43,6	27	-20	-20	26	7	-45	-5	0	0	**1**	**-12**	no risk

Table 5-6: Fracture mechanics assessments for loading variant 1-2 for component No. 1 (Rotationally-symmetric top component (Sliding plate and guiderail))

Assessment for $\sigma_{Ed} = 0,75 \cdot f_y$ and T = -40 °C

Nr	σ_P N/mm²	K_1 N/mm$^{3/2}$	σ_{Ed}/f_y [-]	σ_P N/mm²	σ_S N/mm²	a_0 mm	t_1 mm	$K_{1,P}$ N/mm$^{3/2}$	$K_{1,S}$ N/mm$^{3/2}$	$K_{1,ges}$ N/mm$^{3/2}$	$K_{1,ges}$ MPam$^{1/2}$	$f_{y,nom}$ N/mm²	$f_y(t)$ N/mm²	σ_{gy} N/mm²	L_r -	ψ -	ρ_1 -	ρ -	k_{R6} -	$K_{appl,d}$ N/mm$^{3/2}$	$K_{appl,d}$ MPam$^{1/2}$	b_{eff} mm	ΔT_σ °C	$K_{V,nom}$ J	T_{KV} °C	T_{27J} °C	ΔT_{27J} °C	ΔT_R °C	T_{md} °C	ΔT_r °C	ΔT_ε °C	ΔT_{DCF} °C	T_{Ed} °C	T_{Rd} °C	$T_{Ed} \geq T_{Rd}$
1	1,0	2,481	0,75	266,3	100	1,61	25	661	248	909	28,7	355	349	326	0,82	0,31	0,04	0,04	0,87	1099	34,8	25	120,0	27	-20	-20	5	7	-35	-5	0	0	87	-33	no risk
2	1,0	2,575	0,75	266,3	100	1,78	35	686	257	943	29,8	355	346	329	0,81	0,30	0,04	0,04	0,87	1140	36,0	35	116,5	27	-20	-20	12	7	-35	-5	0	0	83	-26	no risk
3	1,0	2,685	0,75	266,3	100	1,90	45	715	269	983	31,1	355	344	329	0,81	0,30	0,04	0,04	0,87	1188	37,6	45	99,3	27	-20	-20	19	7	-35	-5	0	0	66	-19	no risk
4	1,0	2,788	0,75	266,3	100	2,00	55	742	279	1021	32,3	355	341	329	0,81	0,30	0,04	0,04	0,87	1234	39,0	55	86,8	27	-20	-20	22	7	-35	-5	0	0	54	-16	no risk
5	1,0	2,797	0,75	266,3	100	2,09	65	745	280	1025	32,4	355	339	328	0,81	0,30	0,04	0,04	0,87	1239	39,2	65	82,4	27	-20	-20	24	7	-35	-5	0	0	49	-14	no risk
6	1,0	2,891	0,75	266,3	100	2,16	75	770	289	1059	33,5	355	336	327	0,82	0,31	0,04	0,04	0,87	1281	40,5	75	73,6	27	-20	-20	25	7	-35	-5	0	0	41	-13	no risk
7	1,0	2,900	0,75	266,3	100	2,22	85	772	290	1062	33,6	355	334	325	0,82	0,31	0,04	0,04	0,87	1286	40,7	85	70,5	27	-20	-20	25	7	-35	-5	0	0	37	-13	no risk
8	1,0	2,912	0,75	266,3	100	2,28	95	775	291	1066	33,7	355	331	323	0,82	0,31	0,04	0,04	0,86	1292	40,8	95	67,5	27	-20	-20	25	7	-35	-5	0	0	35	-13	no risk
9	1,0	2,924	0,75	266,3	100	2,33	105	779	292	1071	33,9	355	329	321	0,83	0,31	0,04	0,04	0,86	1298	41,1	105	64,8	27	-20	-20	25	7	-35	-5	0	0	32	-13	no risk
10	1,0	2,936	0,75	266,3	100	2,37	115	782	294	1075	34,0	355	326	320	0,83	0,31	0,04	0,04	0,86	1305	41,3	115	62,3	27	-20	-20	26	7	-35	-5	0	0	29	-12	no risk
11	1,0	2,950	0,75	266,3	100	2,41	125	786	295	1081	34,2	355	324	317	0,84	0,31	0,04	0,04	0,86	1312	41,5	125	59,9	27	-20	-20	26	7	-35	-5	0	0	27	-12	no risk
12	1,0	2,961	0,75	266,3	100	2,45	135	788	296	1085	34,3	355	321	315	0,84	0,32	0,04	0,04	0,86	1318	41,7	135	57,8	27	-20	-20	26	7	-35	-5	0	0	25	-12	no risk
13	1,0	2,971	0,75	266,3	100	2,49	145	791	297	1088	34,4	355	319	313	0,85	0,32	0,04	0,03	0,86	1323	41,9	145	55,9	27	-20	-20	26	7	-35	-5	0	0	23	-12	no risk
14	1,0	2,982	0,75	266,3	100	2,52	155	794	298	1092	34,5	355	316	311	0,86	0,32	0,04	0,03	0,86	1329	42,0	155	54,0	27	-20	-20	26	7	-35	-5	0	0	21	-12	no risk
15	1,0	2,992	0,75	266,3	100	2,55	165	797	299	1096	34,7	355	314	309	0,86	0,32	0,04	0,03	0,85	1335	42,2	165	52,3	27	-20	-20	26	7	-35	-5	0	0	19	-12	no risk
16	1,0	3,001	0,75	266,3	100	2,58	175	799	300	1099	34,8	355	311	307	0,87	0,33	0,04	0,03	0,85	1340	42,4	175	50,7	27	-20	-20	26	7	-35	-5	0	0	18	-12	no risk
17	1,0	3,009	0,75	266,3	100	2,61	185	801	301	1102	34,8	355	309	304	0,87	0,33	0,04	0,03	0,85	1345	42,5	185	49,2	27	-20	-20	26	7	-35	-5	0	0	16	-12	no risk
18	1,0	3,117	0,75	266,3	100	2,64	195	830	312	1142	36,1	355	306	302	0,88	0,33	0,04	0,03	0,85	1395	44,1	195	43,6	27	-20	-20	26	7	-35	-5	0	0	11	-12	no risk
19	1,0	3,125	0,75	266,3	100	2,66	205	832	313	1145	36,2	355	304	300	0,89	0,33	0,04	0,03	0,85	1400	44,3	205	42,3	27	-20	-20	26	7	-35	-5	0	0	9	-12	no risk
20	1,0	3,130	0,75	266,3	100	2,69	215	833	313	1147	36,3	355	301	297	0,89	0,34	0,05	0,03	0,85	1403	44,4	215	41,1	27	-20	-20	26	7	-35	-5	0	0	8	-12	no risk
21	1,0	3,238	0,75	266,3	100	2,71	225	862	324	1186	37,5	355	299	295	0,90	0,34	0,05	0,03	0,84	1453	45,9	225	36,2	27	-20	-20	26	7	-35	-5	0	0	3	-12	no risk
22	1,0	3,326	0,75	266,3	100	2,73	235	886	333	1218	38,5	355	296	293	0,91	0,34	0,05	0,03	0,84	1494	47,2	235	32,2	27	-20	-20	26	7	-35	-5	0	0	-1	-12	no risk
23	1,0	3,433	0,75	266,3	100	2,75	245	914	343	1257	39,8	355	294	290	0,92	0,34	0,05	0,02	0,84	1543	48,8	245	27,9	27	-20	-20	26	7	-35	-5	0	0	-5	-12	no risk
24	1,0	3,494	0,75	266,3	100	2,76	250	930	349	1280	40,5	355	293	289	0,92	0,35	0,05	0,02	0,84	1571	49,7	250	25,6	27	-20	-20	26	7	-35	-5	0	0	-7	-12	no risk

Assessment for $\sigma_{Ed} = 0,75 \cdot f_y$ and T = -50 °C

Nr	σ_P N/mm²	K_1 N/mm$^{3/2}$	σ_{Ed}/f_y [-]	σ_P N/mm²	σ_S N/mm²	a_0 mm	t_1 mm	$K_{1,P}$ N/mm$^{3/2}$	$K_{1,S}$ N/mm$^{3/2}$	$K_{1,ges}$ N/mm$^{3/2}$	$K_{1,ges}$ MPam$^{1/2}$	$f_{y,nom}$ N/mm²	$f_y(t)$ N/mm²	σ_{gy} N/mm²	L_r -	ψ -	ρ_1 -	ρ -	k_{R6} -	$K_{appl,d}$ N/mm$^{3/2}$	$K_{appl,d}$ MPam$^{1/2}$	b_{eff} mm	ΔT_σ °C	$K_{V,nom}$ J	T_{KV} °C	T_{27J} °C	ΔT_{27J} °C	ΔT_R °C	T_{md} °C	ΔT_r °C	ΔT_ε °C	ΔT_{DCF} °C	T_{Ed} °C	T_{Rd} °C	$T_{Ed} \geq T_{Rd}$
1	1,0	2,481	0,75	266,3	100	1,61	25	661	248	909	28,7	355	349	326	0,82	0,31	0,04	0,04	0,87	1099	34,8	25	120,0	27	-20	-20	5	7	-45	-5	0	0	77	-33	no risk
2	1,0	2,575	0,75	266,3	100	1,78	35	686	257	943	29,8	355	346	329	0,81	0,30	0,04	0,04	0,87	1140	36,0	35	116,5	27	-20	-20	12	7	-45	-5	0	0	73	-26	no risk
3	1,0	2,685	0,75	266,3	100	1,90	45	715	269	983	31,1	355	344	329	0,81	0,30	0,04	0,04	0,87	1188	37,6	45	99,3	27	-20	-20	19	7	-45	-5	0	0	56	-19	no risk
4	1,0	2,788	0,75	266,3	100	2,00	55	742	279	1021	32,3	355	341	329	0,81	0,30	0,04	0,04	0,87	1234	39,0	55	86,8	27	-20	-20	22	7	-45	-5	0	0	44	-16	no risk
5	1,0	2,797	0,75	266,3	100	2,09	65	745	280	1025	32,4	355	339	328	0,81	0,30	0,04	0,04	0,87	1239	39,2	65	82,4	27	-20	-20	24	7	-45	-5	0	0	39	-14	no risk
6	1,0	2,891	0,75	266,3	100	2,16	75	770	289	1059	33,5	355	336	327	0,82	0,31	0,04	0,04	0,87	1281	40,5	75	73,6	27	-20	-20	25	7	-45	-5	0	0	31	-13	no risk
7	1,0	2,900	0,75	266,3	100	2,22	85	772	290	1062	33,6	355	334	325	0,82	0,31	0,04	0,04	0,87	1286	40,7	85	70,5	27	-20	-20	25	7	-45	-5	0	0	27	-13	no risk
8	1,0	2,912	0,75	266,3	100	2,28	95	775	291	1066	33,7	355	331	323	0,82	0,31	0,04	0,04	0,86	1292	40,8	95	67,5	27	-20	-20	25	7	-45	-5	0	0	25	-13	no risk
9	1,0	2,924	0,75	266,3	100	2,33	105	779	292	1071	33,9	355	329	321	0,83	0,31	0,04	0,04	0,86	1298	41,1	105	64,8	27	-20	-20	25	7	-45	-5	0	0	22	-13	no risk
10	1,0	2,936	0,75	266,3	100	2,37	115	782	294	1075	34,0	355	326	320	0,83	0,31	0,04	0,04	0,86	1305	41,3	115	62,3	27	-20	-20	26	7	-45	-5	0	0	19	-12	no risk
11	1,0	2,950	0,75	266,3	100	2,41	125	786	295	1081	34,2	355	324	317	0,84	0,31	0,04	0,04	0,86	1312	41,5	125	59,9	27	-20	-20	26	7	-45	-5	0	0	17	-12	no risk
12	1,0	2,961	0,75	266,3	100	2,45	135	788	296	1085	34,3	355	321	315	0,84	0,32	0,04	0,04	0,86	1318	41,7	135	57,8	27	-20	-20	26	7	-45	-5	0	0	15	-12	no risk
13	1,0	2,971	0,75	266,3	100	2,49	145	791	297	1088	34,4	355	319	313	0,85	0,32	0,04	0,03	0,86	1323	41,9	145	55,9	27	-20	-20	26	7	-45	-5	0	0	13	-12	no risk
14	1,0	2,982	0,75	266,3	100	2,52	155	794	298	1092	34,5	355	316	311	0,86	0,32	0,04	0,03	0,86	1329	42,0	155	54,0	27	-20	-20	26	7	-45	-5	0	0	11	-12	no risk
15	1,0	2,992	0,75	266,3	100	2,55	165	797	299	1096	34,7	355	314	309	0,86	0,32	0,04	0,03	0,85	1335	42,2	165	52,3	27	-20	-20	26	7	-45	-5	0	0	9	-12	no risk
16	1,0	3,001	0,75	266,3	100	2,58	175	799	300	1099	34,8	355	311	307	0,87	0,33	0,04	0,03	0,85	1340	42,4	175	50,7	27	-20	-20	26	7	-45	-5	0	0	8	-12	no risk
17	1,0	3,009	0,75	266,3	100	2,61	185	801	301	1102	34,8	355	309	304	0,87	0,33	0,04	0,03	0,85	1345	42,5	185	49,2	27	-20	-20	26	7	-45	-5	0	0	6	-12	no risk
18	1,0	3,117	0,75	266,3	100	2,64	195	830	312	1142	36,1	355	306	302	0,88	0,33	0,04	0,03	0,85	1395	44,1	195	43,6	27	-20	-20	26	7	-45	-5	0	0	1	-12	no risk
19	1,0	3,125	0,75	266,3	100	2,66	205	832	313	1145	36,2	355	304	300	0,89	0,33	0,04	0,03	0,85	1400	44,3	205	42,3	27	-20	-20	26	7	-45	-5	0	0	-1	-12	no risk
20	1,0	3,130	0,75	266,3	100	2,69	215	833	313	1147	36,3	355	301	297	0,89	0,34	0,05	0,03	0,85	1403	44,4	215	41,1	27	-20	-20	26	7	-45	-5	0	0	-2	-12	no risk
21	1,0	3,238	0,75	266,3	100	2,71	225	862	324	1186	37,5	355	299	295	0,90	0,34	0,05	0,03	0,84	1453	45,9	225	36,2	27	-20	-20	26	7	-45	-5	0	0	-7	-12	no risk
22	1,0	3,326	0,75	266,3	100	2,73	235	886	333	1218	38,5	355	296	293	0,91	0,34	0,05	0,03	0,84	1494	47,2	235	32,2	27	-20	-20	26	7	-45	-5	0	0	-11	-12	no risk
23	1,0	3,377	0,75	266,3	100	2,74	240	899	338	1237	39,1	355	295	292	0,91	0,34	0,05	0,03	0,84	1517	48,0	240	30,1	27	-20	-20	26	7	-45	-5	0	0	-13	-12	risk
24	1,0	3,494	0,75	266,3	100	2,76	250	930	349	1280	40,5	355	293	289	0,92	0,35	0,05	0,02	0,84	1571	49,7	250	25,6	27	-20	-20	26	7	-45	-5	0	0	-17	-12	risk

5.3 Component No. 2A – Axisymmetric top component (sliding plate and guiderail)

5.3.1 Geometry, load and assumption and boundary condition

(1) Component No. 2A is the axis-symmetrical variant of the rotationally-symmetric component No. 1, see 5.2.1. The geometry, loading variants and boundary conditions for the strip are identical with those in section 5.2.1 and may be taken from Figure 5-3, Table 5-1, Figure 5-4 and Table 5-2.

5.3.2 Hot-Spot-stresses

(1) The results corresponding to Figure 5-6 are given in Figure 5-12.

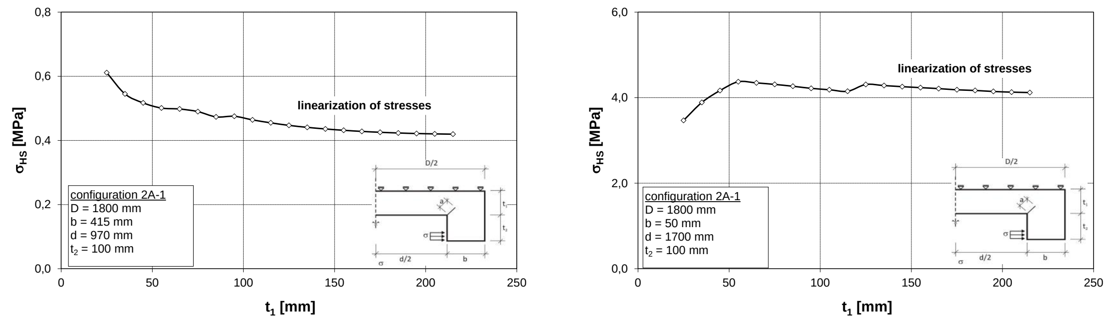

Figure 5-12: Hot-Spot-stresses obtained with "inner" linearization according to Dong for geometrical upper bounds (left) and lower bounds (right) for loading variant 2A-1

(2) The results corresponding to Figure 5-7 and Figure 5-13.

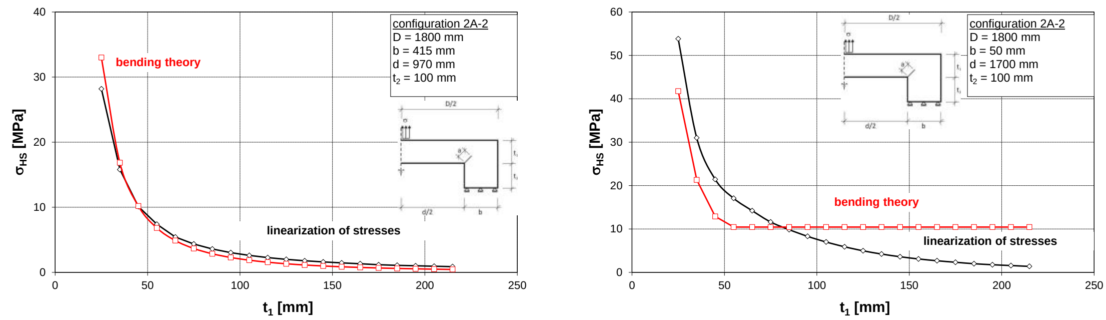

Figure 5-13: Hot-Spot-stresses obtained with "inner" linearization according to Dong for geometrical upper bounds (left) and lower bounds (right) for loading variant 2A-2

(3) For comparison reasons in Figure 5-13 also the surface stresses determined with the bending theory are given using the resistance in the direction of the crack. The calculation leads for t_1 > 50 mm to a constant stress, because of the lower bound b = 50 mm. The comparison also confirms the practicality of the Hot-Spot-stress to consider the stiffness distributions on the distribution of reference stress.

5.3.3 Stress intensity factors

(1) Results corresponding to Figure 5-8 for geometrical upper bounds are shown in Figure 5-14 for the loading variant 2A-1.

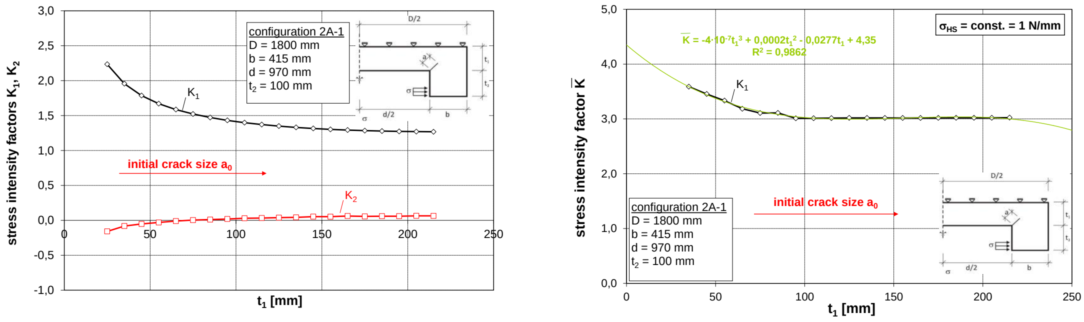

Figure 5-14: **K-values (left) and normalised $\overline{K}$-values (right) related to σ_{HS} = 1 N/mm^2 for the geometric upper bounds for loading variant 2A-1**

(2) The function of the normalised $\overline{K}$-values related to σ_{HS} = 1 N/mm² can be approximated by a polynomial of 3rd degree

$$\overline{K} = 3{,}933 \cdot 10^{-7} t_1^3 + 1{,}8441 \cdot 10^{-4} t_1^2 - 2{,}7747 \cdot 10^{-2} t_1 + 4{,}35 \qquad \textbf{(5-6)}$$

(3) The results corresponding to Figure 5-9 for the geometrical lower bound are given in Figure 5-15.

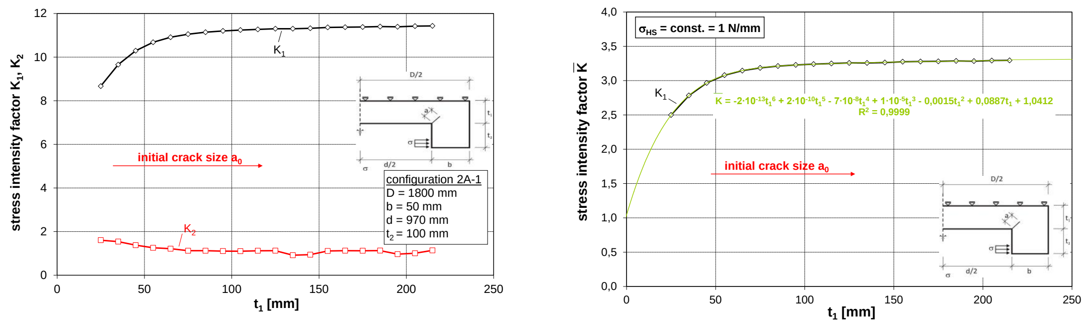

Figure 5-15: **K-values (left) and normalised $\overline{K}$-values (right) related to σ_{HS} = 1 N/mm² for the geometric upper bounds for loading variant 2A-1**

(4) The function of the normalised stress intensity factor $\overline{K}$ in Figure 5-15 (right) can be approximated by a polynomial of 6th degree.

$$\overline{K} = -2{,}1617 \cdot 10^{-13} t_1^6 + 1{,}9489 \cdot 10^{-10} t_1^5 - 7{,}2084 \cdot 10^{-8} t_1^4 + 1{,}4030 \cdot 10^{-5} t_1^3 - 1{,}5232 \cdot 10^{-3} t_1^2 + 8{,}8669 \cdot 10^{-2} t_1 + 1{,}0412 \qquad \textbf{(5-7)}$$

where $\overline{K}$ is an approximation of K_1.

(5) To confirm the insensitivity on other geometric parameters the influence of the width D of the sliding plate keeping the plate thickness t, constant is checked. The result in Figure 5-16 shows that the width D of the sliding plate has no significant influence on the K-values.

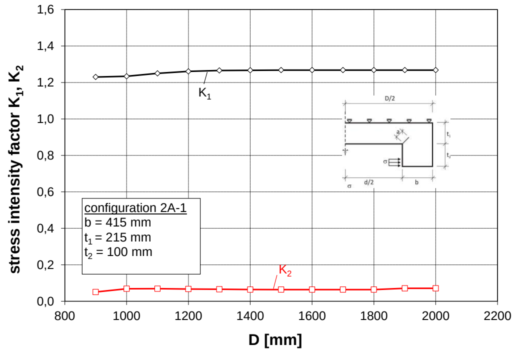

Figure 5-16: **Influence of the width D of the sliding plate with other dimensions kept constant on the K-values for loading variant 2A-1**

(6) For the <u>loading variant 2A-2</u> the results corresponding to Figure 5-10 are given in Figure 5-17.

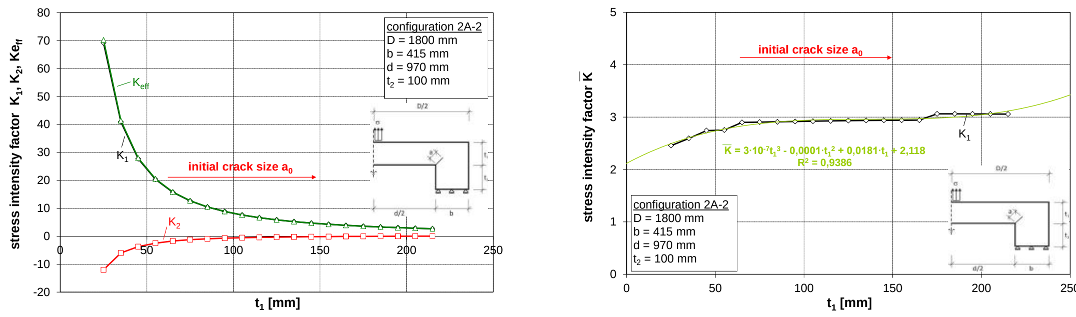

Figure 5-17: **K-values (left) and normalised $\overline{K}$-values (right) related to σ_{HS} = 1 N/mm² for the geometric upper bounds of dimensions for loading variant 2A-2**

(7) The approximation of the distribution of K_1 in Figure 5-17 (right) is possible with a polynomial of 3rd degree:

$$\overline{K} = 3{,}1686 \cdot 10^{-7} \cdot t_1^3 - 1{,}3076 \cdot 10^{-4} \cdot t_1^2 + 1{,}8109 \cdot 10^{-2} \cdot t_1 + 2{,}1180 \qquad \textbf{(5-8)}$$

where $\overline{K}$ denotes the approximation of K_1.

(8) For the lower bound of geometrical dimension the results corresponding to Figure 5-11 are given in Figure 5-18.

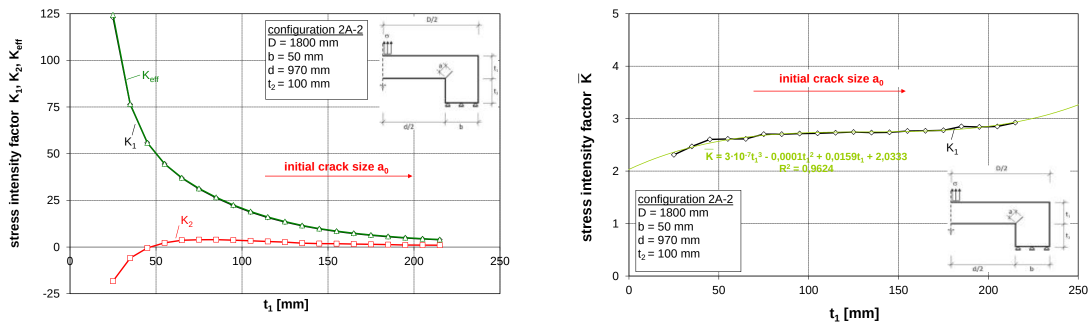

Figure 5-18: **K-values (left) and normalised $\overline{K}$-values (right) related to σ_{HS} = 1 N/mm² for the lower bounds of dimensions for loading variant 2A-2**

(9) The function of $\overline{K}$ in Figure 5-18 is approximated by a polynomial of 3rd degree:

$$\overline{K} = 3{,}0192 \cdot 10^{-7} t_1^3 - 0{,}1949 \cdot 10^{-4} \cdot t_1^2 + 1{,}5920 \cdot 10^{-2} \cdot t_1 + 2{,}0333 \qquad \textbf{(5-9)}$$

where $\overline{K}$ denotes the approximation of K_{eff}.

(10) In contrast to Figure 5-16 the width D of the sliding plate is of significant influence for the loading variant 2A-2 as demonstrated in Figure 5-19.

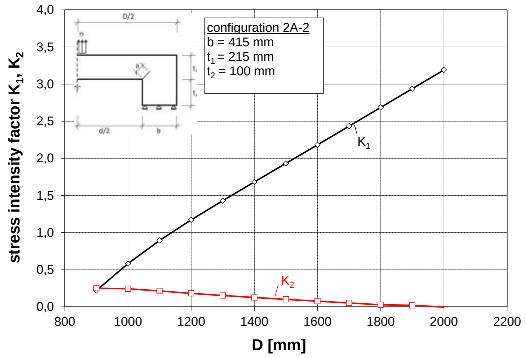

Figure 5-19: **Influence of the width D of the sliding plate with other dimensions kept constant on the K-values for loading variant 2A-2**

5.3.4 Assessments to avoid brittle fracture

(1) The assessments to avoid brittle fracture are carried out as in section 5.2 for the loading variant 2A-1 in Table 5-9 and for loading variant 2A-2 in Table 5-10. The results of the calculations in Table 5-9 and Table 5-10 can be used to identify the maximum product thickness in Table 5-7 for loading variant 2A-1 in Table 5-8 for loading variant 2A-2.

Table 5-7: **Limits of plate thickness t_1 [mm] for the top component of bearing (loading variant 2A-1)**

Steel grade acc. to EN 10025	σ_{Ed}	0°C	-10°C	-20°C	-30°C	-40°C	-50°C
S355J2	0,25 · fy	250*)	250*)	250*)	250*)	250*)	250*)
S355J2	0,50 · fy	250*)	250*)	250*)	250*)	250*)	250*)
S355J2	0,75 · fy	250*)	250*)	250*)	250*)	250*)	250*)

**) Assumption of a technical manufacturing limit (in theory element thicknesses with t ≥ 250 mm would be acceptable)*

Table 5-8: **Limits of plate thickness t_1 [mm] for the top component of bearing (loading variant 2A-2)**

Steel grade acc. to EN 10025	σ_{Ed}	0°C	-10°C	-20°C	-30°C	-40°C	-50°C
S355J2	$0,25 \cdot f_y$	250*)	250*)	250*)	250*)	250*)	250*)
S355J2	$0,50 \cdot f_y$	250*)	250*)	250*)	250*)	250*)	250*)
S355J2	$0,75 \cdot f_y$	250*)	250*)	250*)	250*)	250*)	240

**) Assumption of a technical manufacturing limit (in theory element thicknesses with t ≥ 250 mm would be acceptable)*

Table 5-9: **Fracture mechanics assessments for loading variant 2A-1 for component No. 2A (Axisymmetric top component (sliding plate and guiderail))**

Assessment for $\sigma_{Ed} = 0,75 \cdot f_y$ and T = -50 °C

Nr	σ_P	K_1	σ_{Ed}/f_y	σ_P	σ_S	a_0	t_1	$K_{1,P}$	$K_{1,S}$	$K_{1,ges}$	$K_{1,ges}$	$f_{y,nom}$	$f_y(t)$	σ_{gy}	L_r	ψ	ρ_1	ρ	k_{R6}	$K_{appl,d}$	$K_{appl,d}$	b_{eff}	ΔT_σ	$K_{V,nom}$	T_{KV}	T_{27J}	ΔT_{27J}	ΔT_R	T_{md}	ΔT_r	ΔT_ε	ΔT_{DCF}	T_{Ed}	T_{Rd}	$T_{Ed} \geq T_{Rd}$
	N/mm²	$N/mm^{3/2}$	[-]	N/mm²	N/mm²	mm	mm	$N/mm^{3/2}$	$N/mm^{3/2}$	$N/mm^{3/2}$	$MPam^{1/2}$	N/mm²	N/mm²	N/mm²	-	-	-	-	-	$N/mm^{3/2}$	$MPam^{1/2}$	mm	°C	J	°C	°C	°C	°C	°C	°C	°C	°C	°C	°C	
1	1,0	3,65	0,75	266,3	100	1,61	25	973	365	1339	42,3	355	349	326	0,82	0,31	0,04	0,04	0,87	1619	51,2	25	62,1	27	-20	-20	5	7	-45	-5	0	0	**19**	**-33**	no risk
2	1,0	3,59	0,75	266,3	100	1,78	35	956	359	1314	41,6	355	346	329	0,81	0,30	0,04	0,04	0,87	1589	50,2	35	58,1	27	-20	-20	12	7	-45	-5	0	0	**15**	**-26**	no risk
3	1,0	3,45	0,75	266,3	100	1,90	45	920	345	1265	40,0	355	344	329	0,81	0,30	0,04	0,04	0,87	1529	48,4	45	58,2	27	-20	-20	19	7	-45	-5	0	0	**15**	**-19**	no risk
4	1,0	3,33	0,75	266,3	100	2,00	55	888	333	1221	38,6	355	341	329	0,81	0,30	0,04	0,04	0,87	1476	46,7	55	59,1	27	-20	-20	22	7	-45	-5	0	0	**16**	**-16**	no risk
5	1,0	3,18	0,75	266,3	100	2,09	65	848	318	1166	36,9	355	339	328	0,81	0,30	0,04	0,04	0,87	1410	44,6	65	62,0	27	-20	-20	24	7	-45	-5	0	0	**19**	**-14**	no risk
6	1,0	3,19	0,75	266,3	100	2,16	75	848	319	1167	36,9	355	336	327	0,82	0,31	0,04	0,04	0,87	1412	44,6	75	59,2	27	-20	-20	25	7	-45	-5	0	0	**16**	**-13**	no risk
7	1,0	3,21	0,75	266,3	100	2,22	85	855	321	1176	37,2	355	334	325	0,82	0,31	0,04	0,04	0,87	1424	45,0	85	55,7	27	-20	-20	25	7	-45	-5	0	0	**13**	**-13**	no risk
8	1,0	3,23	0,75	266,3	100	2,28	95	860	323	1183	37,4	355	331	323	0,82	0,31	0,04	0,04	0,86	1433	45,3	95	52,9	27	-20	-20	25	7	-45	-5	0	0	**10**	**-13**	no risk
9	1,0	3,24	0,75	266,3	100	2,33	105	863	324	1187	37,5	355	329	321	0,83	0,31	0,04	0,04	0,86	1439	45,5	105	50,5	27	-20	-20	25	7	-45	-5	0	0	**8**	**-13**	no risk
10	1,0	3,25	0,75	266,3	100	2,37	115	865	325	1190	37,6	355	326	320	0,83	0,31	0,04	0,04	0,86	1444	45,7	115	48,5	27	-20	-20	26	7	-45	-5	0	0	**5**	**-12**	no risk
11	1,0	3,26	0,75	266,3	100	2,41	125	867	326	1193	37,7	355	324	317	0,84	0,31	0,04	0,04	0,86	1449	45,8	125	46,6	27	-20	-20	26	7	-45	-5	0	0	**4**	**-12**	no risk
12	1,0	3,26	0,75	266,3	100	2,45	135	867	326	1193	37,7	355	321	315	0,84	0,32	0,04	0,04	0,86	1450	45,8	135	45,1	27	-20	-20	26	7	-45	-5	0	0	**2**	**-12**	no risk
13	1,0	3,26	0,75	266,3	100	2,49	145	869	326	1195	37,8	355	319	313	0,85	0,32	0,04	0,03	0,86	1454	46,0	145	43,5	27	-20	-20	26	7	-45	-5	0	0	**1**	**-12**	no risk
14	1,0	3,28	0,75	266,3	100	2,52	155	872	328	1200	37,9	355	316	311	0,86	0,32	0,04	0,03	0,86	1460	46,2	155	41,9	27	-20	-20	26	7	-45	-5	0	0	**-1**	**-12**	no risk
15	1,0	3,28	0,75	266,3	100	2,55	165	873	328	1201	38,0	355	314	309	0,86	0,32	0,04	0,03	0,85	1463	46,3	165	40,6	27	-20	-20	26	7	-45	-5	0	0	**-2**	**-12**	no risk
16	1,0	3,28	0,75	266,3	100	2,58	175	874	328	1202	38,0	355	311	307	0,87	0,33	0,04	0,03	0,85	1465	46,3	175	39,4	27	-20	-20	26	7	-45	-5	0	0	**-4**	**-12**	no risk
17	1,0	3,29	0,75	266,3	100	2,61	185	875	329	1204	38,1	355	309	304	0,87	0,33	0,04	0,03	0,85	1469	46,5	185	38,1	27	-20	-20	26	7	-45	-5	0	0	**-5**	**-12**	no risk
18	1,0	3,28	0,75	266,3	100	2,64	195	874	328	1203	38,0	355	306	302	0,88	0,33	0,04	0,03	0,85	1469	46,5	195	37,2	27	-20	-20	26	7	-45	-5	0	0	**-6**	**-12**	no risk
19	1,0	3,29	0,75	266,3	100	2,66	205	877	329	1206	38,1	355	304	300	0,89	0,33	0,04	0,03	0,85	1475	46,6	205	35,9	27	-20	-20	26	7	-45	-5	0	0	**-7**	**-12**	no risk
20	1,0	3,30	0,75	266,3	100	2,69	215	877	330	1207	38,2	355	301	297	0,89	0,34	0,05	0,03	0,85	1477	46,7	215	34,9	27	-20	-20	26	7	-45	-5	0	0	**-8**	**-12**	no risk
21	1,0	3,30	0,75	266,3	100	2,71	225	879	330	1209	38,2	355	299	295	0,90	0,34	0,05	0,03	0,84	1481	46,8	225	33,9	27	-20	-20	26	7	-45	-5	0	0	**-9**	**-12**	no risk
22	1,0	3,30	0,75	266,3	100	2,73	235	879	330	1209	38,2	355	296	293	0,91	0,34	0,05	0,03	0,84	1482	46,9	235	33,1	27	-20	-20	26	7	-45	-5	0	0	**-10**	**-12**	no risk
23	1,0	3,30	0,75	266,3	100	2,75	245	879	330	1209	38,2	355	294	290	0,92	0,34	0,05	0,02	0,84	1484	46,9	245	32,3	27	-20	-20	26	7	-45	-5	0	0	**-11**	**-12**	no risk
23	1,0	3,30	0,75	266,3	100	2,76	250	879	330	1209	38,2	355	293	289	0,92	0,35	0,05	0,02	0,84	1484	46,9	250	31,9	27	-20	-20	26	7	-45	-5	0	0	**-11**	**-12**	no risk

Table 5-10: Fracture mechanics assessments for loading variant 2A-2 for component No. 2A (Axisymmetric top component (sliding plate and guiderail))

Assessment for $\sigma_{Ed} = 0{,}75 \cdot f_y$ and $T = -40$ °C

Nr	σ_P N/mm²	K_1 N/mm$^{3/2}$	σ_{Ed}/f_y [-]	σ_P N/mm²	σ_S N/mm²	a_0 mm	t_1 mm	$K_{1,P}$ N/mm$^{3/2}$	$K_{1,S}$ N/mm$^{3/2}$	$K_{1,ges}$ N/mm$^{3/2}$	$K_{1,ges}$ MPam$^{1/2}$	$f_{y,nom}$ N/mm²	$f_y(t)$ N/mm²	σ_{gy} N/mm²	L_r -	ψ -	ρ_1 -	ρ -	k_{R6} -	$K_{appl,d}$ N/mm$^{3/2}$	$K_{appl,d}$ MPam$^{1/2}$	b_{eff} mm	ΔT_σ °C	$K_{V,nom}$ J	T_{KV} °C	T_{27J} °C	ΔT_{27J} °C	ΔT_R °C	T_{md} °C	ΔT_r °C	ΔT_ε °C	ΔT_{DCF} °C	T_{Ed} °C	T_{Rd} °C	$T_{Ed} \geq T_{Rd}$
1	1,0	2,455	0,75	266,3	100	1,61	25	654	245	899	28,4	355	349	326	0,82	0,31	0,04	0,04	0,87	1088	34,4	25	120,0	27	-20	-20	5	7	-35	-5	0	0	87	-33	no risk
2	1,0	2,592	0,75	266,3	100	1,78	35	690	259	949	30,0	355	346	329	0,81	0,30	0,04	0,04	0,87	1148	36,3	35	114,6	27	-20	-20	12	7	-35	-5	0	0	82	-26	no risk
3	1,0	2,743	0,75	266,3	100	1,90	45	730	274	1004	31,8	355	344	329	0,81	0,30	0,04	0,04	0,87	1214	38,4	45	94,8	27	-20	-20	19	7	-35	-5	0	0	62	-19	no risk
4	1,0	2,752	0,75	266,3	100	2,00	55	733	275	1008	31,9	355	341	329	0,81	0,30	0,04	0,04	0,87	1218	38,5	55	89,3	27	-20	-20	22	7	-35	-5	0	0	56	-16	no risk
5	1,0	2,899	0,75	266,3	100	2,09	65	772	290	1062	33,6	355	339	328	0,81	0,30	0,04	0,04	0,87	1284	40,6	65	76,3	27	-20	-20	24	7	-35	-5	0	0	43	-14	no risk
6	1,0	2,904	0,75	266,3	100	2,16	75	773	290	1063	33,6	355	336	327	0,82	0,31	0,04	0,04	0,87	1286	40,7	75	72,9	27	-20	-20	25	7	-35	-5	0	0	40	-13	no risk
7	1,0	2,909	0,75	266,3	100	2,22	85	775	291	1066	33,7	355	334	325	0,82	0,31	0,04	0,04	0,87	1290	40,8	85	70,0	27	-20	-20	25	7	-35	-5	0	0	37	-13	no risk
8	1,0	2,916	0,75	266,3	100	2,28	95	776	292	1068	33,8	355	331	323	0,82	0,31	0,04	0,04	0,86	1294	40,9	95	67,3	27	-20	-20	25	7	-35	-5	0	0	34	-13	no risk
9	1,0	2,921	0,75	266,3	100	2,33	105	778	292	1070	33,8	355	329	321	0,83	0,31	0,04	0,04	0,86	1297	41,0	105	64,9	27	-20	-20	25	7	-35	-5	0	0	32	-13	no risk
10	1,0	2,926	0,75	266,3	100	2,37	115	779	293	1072	33,9	355	326	320	0,83	0,31	0,04	0,04	0,86	1300	41,1	115	62,8	27	-20	-20	26	7	-35	-5	0	0	30	-12	no risk
11	1,0	2,932	0,75	266,3	100	2,41	125	781	293	1074	34,0	355	324	317	0,84	0,31	0,04	0,04	0,86	1304	41,2	125	60,8	27	-20	-20	26	7	-35	-5	0	0	28	-12	no risk
12	1,0	2,936	0,75	266,3	100	2,45	135	782	294	1075	34,0	355	321	315	0,84	0,32	0,04	0,04	0,86	1306	41,3	135	59,0	27	-20	-20	26	7	-35	-5	0	0	26	-12	no risk
13	1,0	2,938	0,75	266,3	100	2,49	145	782	294	1076	34,0	355	319	313	0,85	0,32	0,04	0,03	0,86	1308	41,4	145	57,5	27	-20	-20	26	7	-35	-5	0	0	24	-12	no risk
14	1,0	2,940	0,75	266,3	100	2,52	155	783	294	1077	34,0	355	316	311	0,86	0,32	0,04	0,03	0,86	1310	41,4	155	56,0	27	-20	-20	26	7	-35	-5	0	0	23	-12	no risk
15	1,0	2,942	0,75	266,3	100	2,55	165	783	294	1077	34,1	355	314	309	0,86	0,32	0,04	0,03	0,85	1313	41,5	165	54,7	27	-20	-20	26	7	-35	-5	0	0	22	-12	no risk
16	1,0	3,061	0,75	266,3	100	2,58	175	815	306	1121	35,5	355	311	307	0,87	0,33	0,04	0,03	0,85	1367	43,2	175	48,1	27	-20	-20	26	7	-35	-5	0	0	15	-12	no risk
17	1,0	3,061	0,75	266,3	100	2,61	185	815	306	1121	35,5	355	309	304	0,87	0,33	0,04	0,03	0,85	1368	43,3	185	47,0	27	-20	-20	26	7	-35	-5	0	0	14	-12	no risk
18	1,0	3,060	0,75	266,3	100	2,64	195	815	306	1121	35,4	355	306	302	0,88	0,33	0,04	0,03	0,85	1369	43,3	195	45,9	27	-20	-20	26	7	-35	-5	0	0	13	-12	no risk
19	1,0	3,058	0,75	266,3	100	2,66	205	814	306	1120	35,4	355	304	300	0,89	0,33	0,04	0,03	0,85	1370	43,3	205	45,0	27	-20	-20	26	7	-35	-5	0	0	12	-12	no risk
20	1,0	3,057	0,75	266,3	100	2,69	215	814	306	1120	35,4	355	301	297	0,89	0,34	0,05	0,03	0,85	1370	43,3	215	44,1	27	-20	-20	26	7	-35	-5	0	0	11	-12	no risk
21	1,0	3,182	0,75	266,3	100	2,71	225	847	318	1165	36,9	355	299	295	0,90	0,34	0,05	0,03	0,84	1428	45,2	225	38,2	27	-20	-20	26	7	-35	-5	0	0	5	-12	no risk
22	1,0	3,265	0,75	266,3	100	2,73	235	869	326	1196	37,8	355	296	293	0,91	0,34	0,05	0,03	0,84	1466	46,4	235	34,3	27	-20	-20	26	7	-35	-5	0	0	1	-12	no risk
23	1,0	3,366	0,75	266,3	100	2,75	245	896	337	1233	39,0	355	294	290	0,92	0,34	0,05	0,02	0,84	1513	47,8	245	30,1	27	-20	-20	26	7	-35	-5	0	0	-3	-12	no risk
24	1,0	3,424	0,75	266,3	100	2,76	250	912	342	1254	39,7	355	293	289	0,92	0,35	0,05	0,02	0,84	1540	48,7	250	27,8	27	-20	-20	26	7	-35	-5	0	0	-5	-12	no risk

Assessment for $\sigma_{Ed} = 0{,}75 \cdot f_y$ and $T = -50$ °C

Nr	σ_P N/mm²	K_1 N/mm$^{3/2}$	σ_{Ed}/f_y [-]	σ_P N/mm²	σ_S N/mm²	a_0 mm	t_1 mm	$K_{1,P}$ N/mm$^{3/2}$	$K_{1,S}$ N/mm$^{3/2}$	$K_{1,ges}$ N/mm$^{3/2}$	$K_{1,ges}$ MPam$^{1/2}$	$f_{y,nom}$ N/mm²	$f_y(t)$ N/mm²	σ_{gy} N/mm²	L_r -	ψ -	ρ_1 -	ρ -	k_{R6} -	$K_{appl,d}$ N/mm$^{3/2}$	$K_{appl,d}$ MPam$^{1/2}$	b_{eff} mm	ΔT_σ °C	$K_{V,nom}$ J	T_{KV} °C	T_{27J} °C	ΔT_{27J} °C	ΔT_R °C	T_{md} °C	ΔT_r °C	ΔT_ε °C	ΔT_{DCF} °C	T_{Ed} °C	T_{Rd} °C	$T_{Ed} \geq T_{Rd}$
1	1,0	2,455	0,75	266,3	100	1,61	25	654	245	899	28,4	355	349	326	0,82	0,31	0,04	0,04	0,87	1088	34,4	25	120,0	27	-20	-20	5	7	-45	-5	0	0	77	-33	no risk
2	1,0	2,592	0,75	266,3	100	1,78	35	690	259	949	30,0	355	346	329	0,81	0,30	0,04	0,04	0,87	1148	36,3	35	114,6	27	-20	-20	12	7	-45	-5	0	0	72	-26	no risk
3	1,0	2,743	0,75	266,3	100	1,90	45	730	274	1004	31,8	355	344	329	0,81	0,30	0,04	0,04	0,87	1214	38,4	45	94,8	27	-20	-20	19	7	-45	-5	0	0	52	-19	no risk
4	1,0	2,752	0,75	266,3	100	2,00	55	733	275	1008	31,9	355	341	329	0,81	0,30	0,04	0,04	0,87	1218	38,5	55	89,3	27	-20	-20	22	7	-45	-5	0	0	46	-16	no risk
5	1,0	2,899	0,75	266,3	100	2,09	65	772	290	1062	33,6	355	339	328	0,81	0,30	0,04	0,04	0,87	1284	40,6	65	76,3	27	-20	-20	24	7	-45	-5	0	0	33	-14	no risk
6	1,0	2,904	0,75	266,3	100	2,16	75	773	290	1063	33,6	355	336	327	0,82	0,31	0,04	0,04	0,87	1286	40,7	75	72,9	27	-20	-20	25	7	-45	-5	0	0	30	-13	no risk
7	1,0	2,909	0,75	266,3	100	2,22	85	775	291	1066	33,7	355	334	325	0,82	0,31	0,04	0,04	0,87	1290	40,8	85	70,0	27	-20	-20	25	7	-45	-5	0	0	27	-13	no risk
8	1,0	2,916	0,75	266,3	100	2,28	95	776	292	1068	33,8	355	331	323	0,82	0,31	0,04	0,04	0,86	1294	40,9	95	67,3	27	-20	-20	25	7	-45	-5	0	0	24	-13	no risk
9	1,0	2,921	0,75	266,3	100	2,33	105	778	292	1070	33,8	355	329	321	0,83	0,31	0,04	0,04	0,86	1297	41,0	105	64,9	27	-20	-20	25	7	-45	-5	0	0	22	-13	no risk
10	1,0	2,926	0,75	266,3	100	2,37	115	779	293	1072	33,9	355	326	320	0,83	0,31	0,04	0,04	0,86	1300	41,1	115	62,8	27	-20	-20	26	7	-45	-5	0	0	20	-12	no risk
11	1,0	2,932	0,75	266,3	100	2,41	125	781	293	1074	34,0	355	324	317	0,84	0,31	0,04	0,04	0,86	1304	41,2	125	60,8	27	-20	-20	26	7	-45	-5	0	0	18	-12	no risk
12	1,0	2,936	0,75	266,3	100	2,45	135	782	294	1075	34,0	355	321	315	0,84	0,32	0,04	0,04	0,86	1306	41,3	135	59,0	27	-20	-20	26	7	-45	-5	0	0	16	-12	no risk
13	1,0	2,938	0,75	266,3	100	2,49	145	782	294	1076	34,0	355	319	313	0,85	0,32	0,04	0,03	0,86	1308	41,4	145	57,5	27	-20	-20	26	7	-45	-5	0	0	14	-12	no risk
14	1,0	2,940	0,75	266,3	100	2,52	155	783	294	1077	34,0	355	316	311	0,86	0,32	0,04	0,03	0,86	1310	41,4	155	56,0	27	-20	-20	26	7	-45	-5	0	0	13	-12	no risk
15	1,0	2,942	0,75	266,3	100	2,55	165	783	294	1077	34,1	355	314	309	0,86	0,32	0,04	0,03	0,85	1313	41,5	165	54,7	27	-20	-20	26	7	-45	-5	0	0	12	-12	no risk
16	1,0	3,061	0,75	266,3	100	2,58	175	815	306	1121	35,5	355	311	307	0,87	0,33	0,04	0,03	0,85	1367	43,2	175	48,1	27	-20	-20	26	7	-45	-5	0	0	5	-12	no risk
17	1,0	3,061	0,75	266,3	100	2,61	185	815	306	1121	35,5	355	309	304	0,87	0,33	0,04	0,03	0,85	1368	43,3	185	47,0	27	-20	-20	26	7	-45	-5	0	0	4	-12	no risk
18	1,0	3,060	0,75	266,3	100	2,64	195	815	306	1121	35,4	355	306	302	0,88	0,33	0,04	0,03	0,85	1369	43,3	195	45,9	27	-20	-20	26	7	-45	-5	0	0	3	-12	no risk
19	1,0	3,058	0,75	266,3	100	2,66	205	814	306	1120	35,4	355	304	300	0,89	0,33	0,04	0,03	0,85	1370	43,3	205	45,0	27	-20	-20	26	7	-45	-5	0	0	2	-12	no risk
20	1,0	3,057	0,75	266,3	100	2,69	215	814	306	1120	35,4	355	301	297	0,89	0,34	0,05	0,03	0,85	1370	43,3	215	44,1	27	-20	-20	26	7	-45	-5	0	0	1	-12	no risk
21	1,0	3,182	0,75	266,3	100	2,71	225	847	318	1165	36,9	355	299	295	0,90	0,34	0,05	0,03	0,84	1428	45,2	225	38,2	27	-20	-20	26	7	-45	-5	0	0	-5	-12	no risk
22	1,0	3,265	0,75	266,3	100	2,73	235	869	326	1196	37,8	355	296	293	0,91	0,34	0,05	0,03	0,84	1466	46,4	235	34,3	27	-20	-20	26	7	-45	-5	0	0	-9	-12	no risk
23	1,0	3,313	0,75	266,3	100	2,74	240	882	331	1213	38,4	355	295	292	0,91	0,34	0,05	0,03	0,84	1489	47,1	240	32,2	27	-20	-20	26	7	-45	-5	0	0	-11	-12	no risk
24	1,0	3,366	0,75	266,3	100	2,75	245	896	337	1233	39,0	355	294	290	0,92	0,34	0,05	0,02	0,84	1513	47,8	245	30,1	27	-20	-20	26	7	-45	-5	0	0	-13	-12	risk

5.4 Component No. 2B – Axisymmetric top component of reference bearing type B (welded variant)

5.4.1 Geometry, load assumptions and boundary conditions

(1) Component No. 2B has the same function as top component No. 2A except that the axisymmetric component is built up by welding according to Figure 5-20.

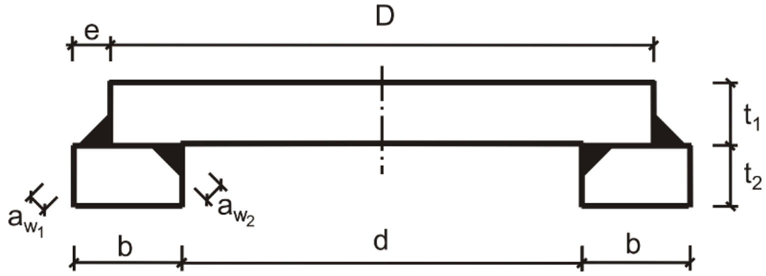

Figure 5-20: Component 2B: top component of reference type B (sliding plate and guiderail)

(2) Table 5-11 gives the numerical values of the dimensions.

Table 5-11: Ranges of geometrical dimensions for detail 2B

t_1 [mm]	t_2 [mm]	D [mm]	b [mm]	a_w [mm]
55 - 285	55 - 170	440 – 2580	55 - 570	12 - 42

(3) In analogy to the investigations in section 5.2 and section 5.3 two loading variants, one with horizontal loading, the other with vertical loading were studied.

(4) The toes of the welds are the potential spots for crack initiation.

(5) For determining the limitation of the plate thickness t_2 the loading variants 2B-1 and 2B-2 were used.

The positions of crack in the guiderails were assumed as given in Figure 5-21. The initial crack depth a0 depends on the thickness t_2. In these regions no significant tensile stresses have to be expected under realistic external loading conditions.

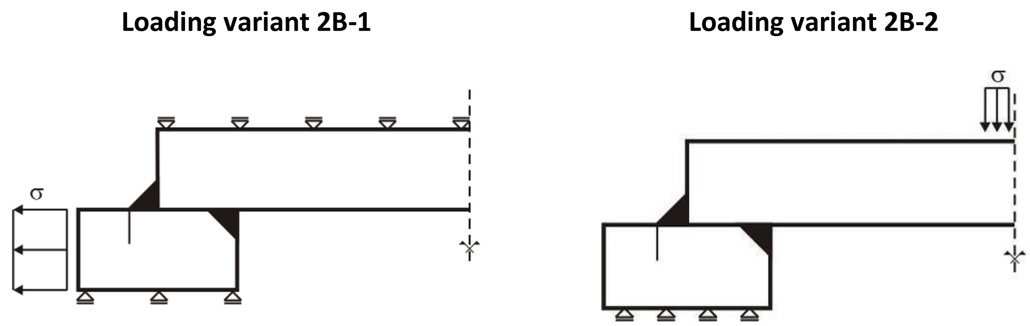

Figure 5-21: Variants for loading for detail 2B: Variant 2B-1 with horizontal loading (left); variant 2B-2 with vertical loading (right)

(6) For determining the limitation of the plate thickness t_1 the models with the loading variants

- 2B-3,
- 2B-4,
- 2B-5,

- 2B-6,

were used. The crack configuration for the loading variants 2B-3 and 2B-4 is rather hypothetical, see Figure 5-22. The initial crack size for these variants depends on the thickness t_1 of the sliding plate. The occurrence of the cracks in Figure 5-22 is also rather hypothetical as no significant stresses have to be expected from realistic external loading conditions.

Loading variant 2B-3 **Loading variant 2B-4**

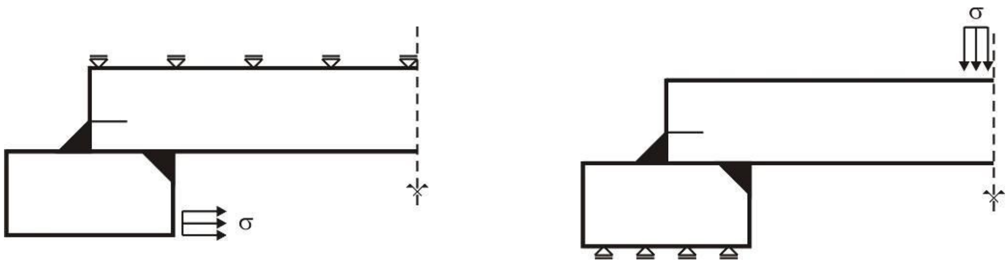

Figure 5-22: Loading variants for detail 2B: Variant 2B-3 with horizontal loading (left) and variant 2B-4 with vertical loading (right)

(7) A further crack configuration is assumed at the re-entrant corner as shown in Figure 5-23. For this crack configuration preliminary studies showed that the crack-orientation with 45 ° was more severe than a vertical orientation. The initial crack length depends on the plate thickness t_1 of the sliding plate. Tensile stresses in this region are realistic.

Loading variant 2B-5 **Loading variant 2B-6**

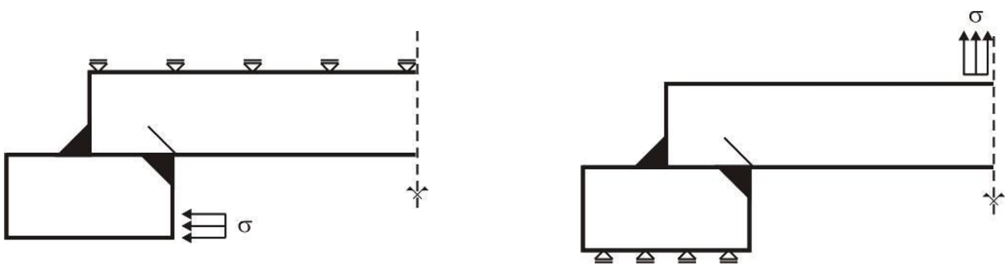

Figure 5-23: Loading variants for detail 2B: Variant 2B-5 with horizontal loading (left) and variant 2B-6 with vertical loading (right)

(8) The calculations were carried out for two different configurations of the dimensions of the bearings in Table 5-12 for the variation of t_2 and in Table 5-13 for the variation of t_1.

The influence of the geometry of the welds on the K-value is only small when thickness is increased. The maximum possible weld thickness of a_w = 42 mm was assumed for the upper bound of the geometrical dimensions. For the lower bound of the geometrical dimensions a throat thickness of a_w = 16 mm was used.

Table 5-12: **Upper and lower bounds of geometrical dimensions for component No. 2B for determining the limit of plate thickness t_2**

Upper bounds		Lower bounds	
t_1 [mm]	285	t_1 [mm]	55
t_2 [mm]	50-200	t_2 [mm]	50 – 200
D [mm]	2580	D [mm]	2580
d [mm]	1980	d [mm]	2525
b [mm]	570	b [mm]	55
a_w [mm]	42	a_w [mm]	16

Table 5-13: **Upper and lower bounds of geometrical dimensions for component No. 2B for determining the limit of plate thickness t_1**

Upper bounds		Lower bounds	
t_1 [mm]	55 – 285	t_1 [mm]	55 – 285
t_2 [mm]	170	t_2 [mm]	170
D [mm]	2580	D [mm]	2580
d [mm]	1980	d [mm]	2525
b [mm]	570	b [mm]	55
a_w [mm]	42	a_w [mm]	16

(9) In Figure 5-24 to Figure 5-26 examples are given for the FE-models used (sections only) together with the associated deformations and crack opening.

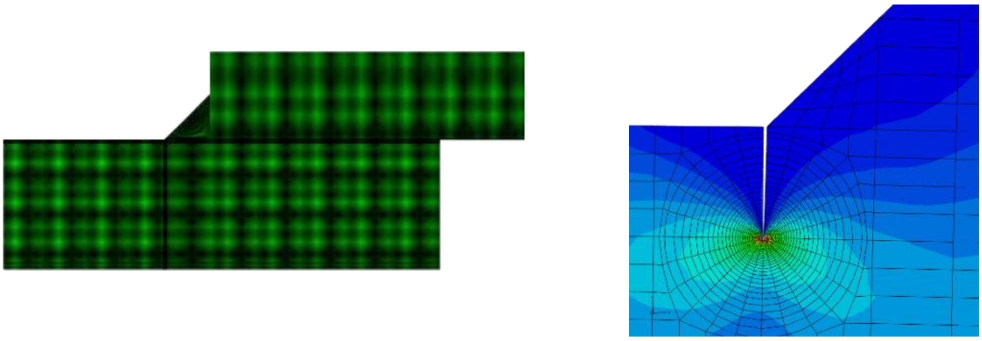

Figure 5-24: **Section from a FE-model (left) and from the plot of deformations including crack-opening (right) for loading variant 2B-1 and 2B-2**

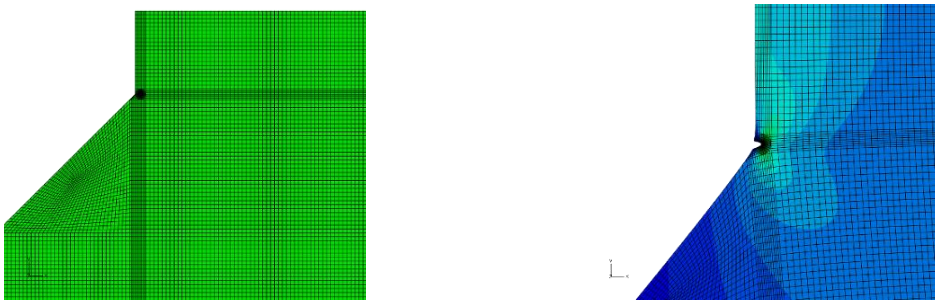

Figure 5-25: **Section from a FE-model (left) and from the plot of deformations including crack-opening (right) for loading variant 2B-3 and 2B-4**

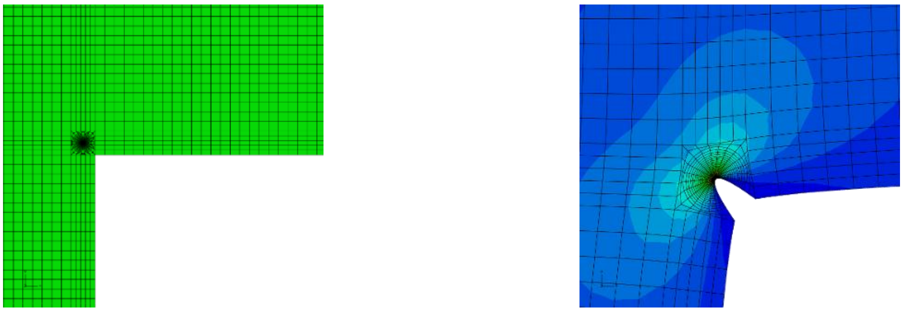

Figure 5-26: **Section from a FE-model (left) and from the plot of deformations including crack-opening (right) for loading variant 2B-5 and 2B-6**

5.4.2 Hot-Spots-stresses

(1) For loading variant 2B-1 the reference stress of the fracture mechanics assessment is identical with the stress loading applied to the FE-model.

(2) For loading variant 2B-2 Figure 5-27 (left) shows the Hot-Spot-stress increasing linearly with increasing thickness t_2 of the guiderail for the upper bound of the geometrical dimensions.

(3) The decreasing effect of thickness t_2 on the Hot-Spot-stresses for the lower bound of geometrical dimensions is given in Figure 5-27 (right). The decrease is also linear.

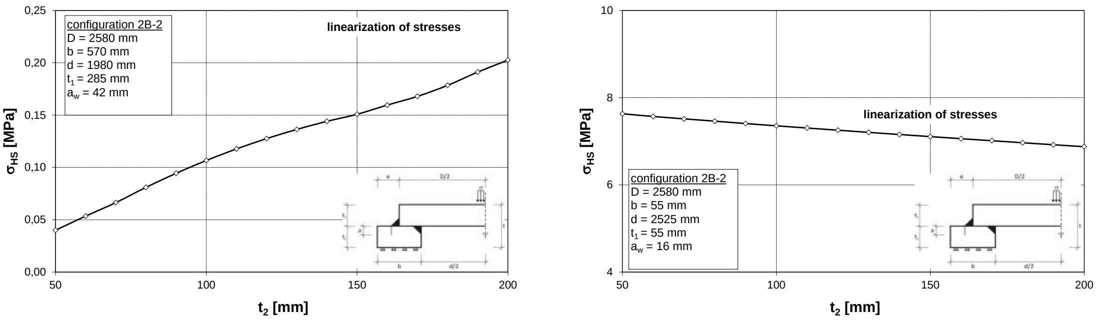

Figure 5-27: **Hot-spot-stresses due to external stress loading (unit stress) for loading variant 2B-2: vertical loading: upper bound of geometrical dimensions (left), lower bound of geometrical dimensions (right)**

(4) Figure 5-28 (left) gives for loading variant 2B-3 the function of Hot-Spot-stresses for the variation of the plate thickness t_1 at the upper bound of geometrical dimensions. The numerical values are rather small and decrease with increasing value of t_1.

(5) Figure 5-28 (right) gives a similar performance for the lower bound of the geometrical dimensions. For t > 160 mm the further distribution can be linearly approximated.

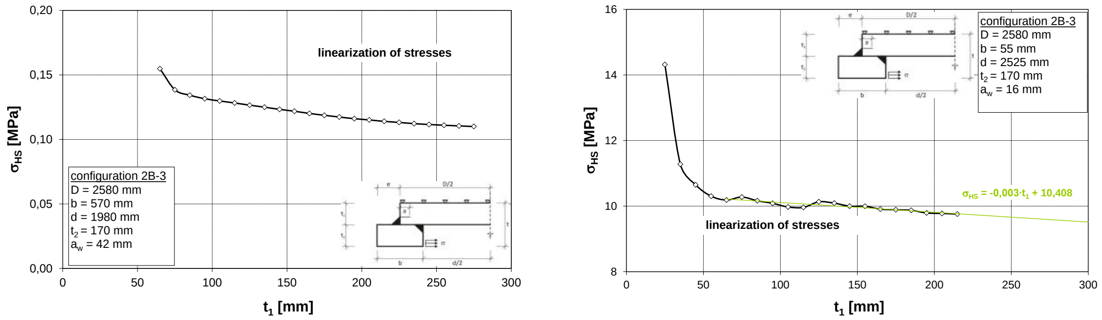

Figure 5-28: **Hot-Spot-stresses due to external stress loading (unit stress) for loading variant 2B-3: horizontal loading; upper bound of geometrical dimensions (left), lower bound of geometrical dimensions (right)**

(6) According to Figure 5-29 (left) the Hot-Spot-stresses for <u>loading variant 2B-4</u> increase with increasing plate thickness t_1 for the upper bound of geometrical dimensions.

(7) Figure 5-29 (right) shows the corresponding distribution of the Hot-Spot-stresses for the lower bound of the geometrical dimensions. In the range 25 mm ≤ t_1 ≤ 55 mm the increase is strong; for t_1 > 55 mm there is an exponential decrease.

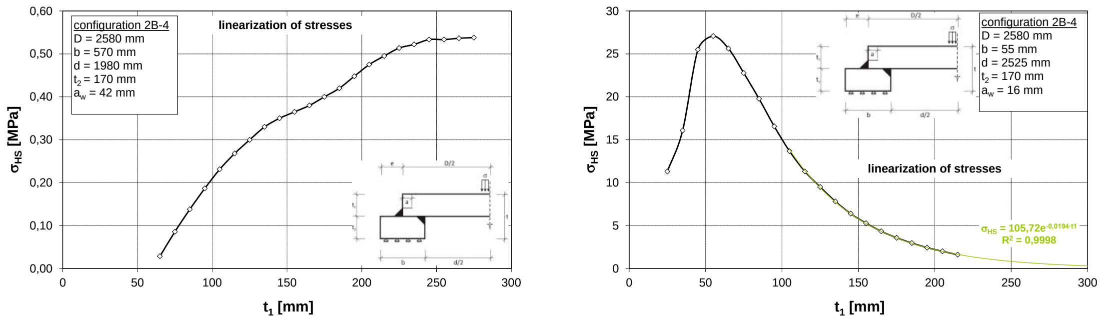

Figure 5-29: **Hot-Spot-stresses due to external unit loading for loading variant 2B-4: vertical loading; upper bound of geometrical dimensions (left), lower bound of geometrical dimensions (right)**

(8) For <u>loading variant 2B-5</u> Figure 5-30 shows the Hot-Spot-stresses for the upper bound of geometrical dimensions .

(9) In Figure 5-30 (right) the Hot-Spot-stresses for the lower bound of geometrical dimensions are shown.

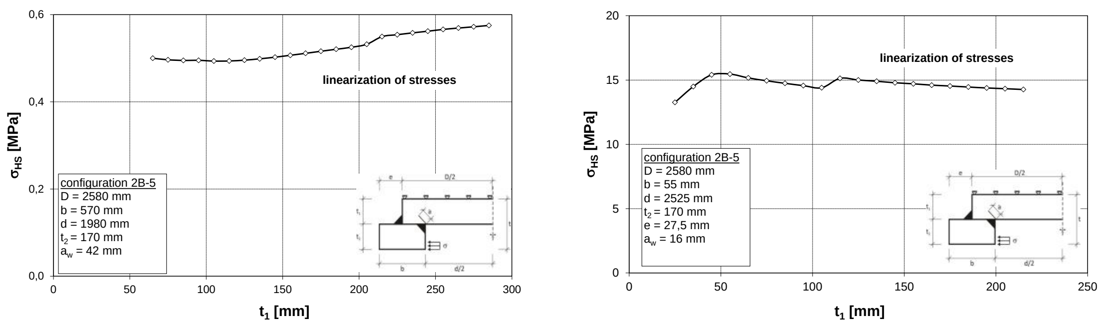

Figure 5-30: **Hot-Spot-stresses due to external unit load for loading variant 2B-5 with horizontal loading: for upper bound of geometrical dimensions (left), lower bound of geometrical dimensions (right)**

(10) Figure 5-31 (left) gives for <u>loading variant 2B-6</u> the monotonously decreasing of the Hot-Spot stress for large plate thicknesses t_1 for the upper bound of the geometrical dimensions.

(11) In Figure 5-31 (right) the decrease of the Hot-Spot-stresses for large plate thicknesses t_1 is shown for the lower bound of the geometric dimension.

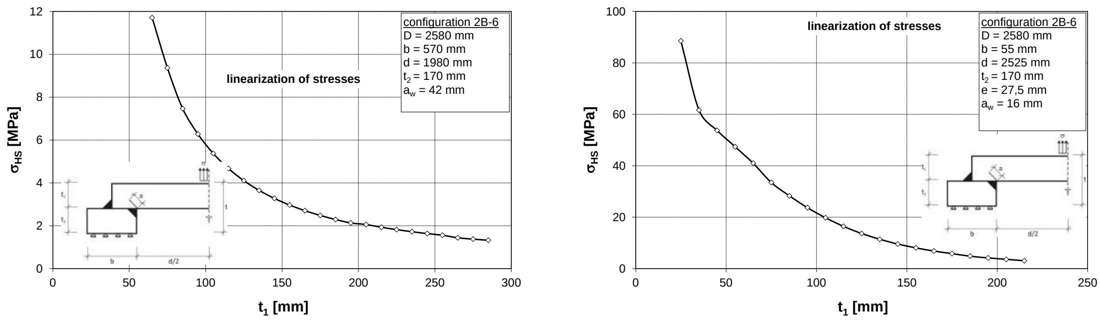

Figure 5-31: **Hot-Spot-stresses due to external unit load for loading variant 2B-6 vertical load: for upper bound of geometrical dimensions (left), lower bound of geometrical dimensions (right)**

5.4.3 Stress intensity factors

(1) For the <u>loading variant 2B-1</u> Figure 5-32 shows the almost linear increase of the K-value with increasing plate thickness t_2 of the guiderail for the upper bound of the geometrical dimensions. The influence of mode 2-stresses is negligible.

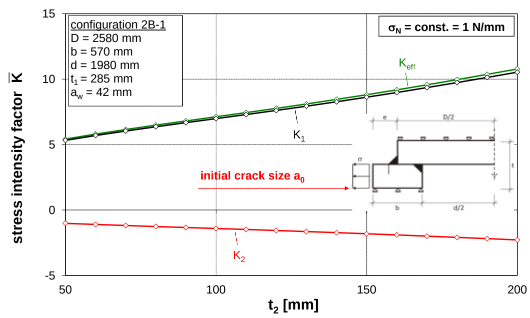

Figure 5-32: **$\overline{\mathrm{K}}$-values for σ_{HS} = 1 N/mm^2 for loading variant 2B-1, horizontal loading for variation of plate thickness t_2; upper bound of geometrical dimensions**

(2) Figure 5-33 shows the distribution of the $\overline{\mathrm{K}}$-values due to σ_{HS} = 1 N/mm^2 for the loading variant 2B-1 for the lower bound of the geometrical dimensions. The $\overline{\mathrm{K}}$-values decrease with increasing thickness t_2 of the guiderail due to the geometry and support conditions chosen. This effects for large t_2-values an increasing influence of mode 2-stresses.

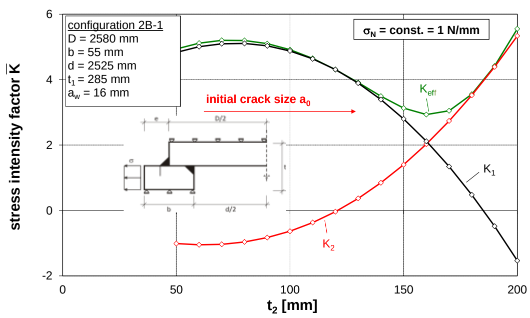

Figure 5-33: **$\overline{\mathrm{K}}$-values for σ_{HS} = 1 N/mm^2 for loading variant 2B-1, horizontal loading; variation of plate thickness t_2; lower bound of geometrical dimensions**

(3) For loading variant 2B-2 the increase of the thickness t_2 of the guiderail effects an increase of the K-values for the upper bound of geometrical dimensions, see Figure 5-34 (left). This is a result of the increase for the initial crack depths a_0 with increasing thickness t_2.

(4) Figure 5-34 (right) shows the function of the effective $\overline{K}$-values related to the Hot-Spot stress σ_{HS} = 1 N/mm^2. The fracture mechanics requirement increases with increasing thickness t_2 of the guiderail.

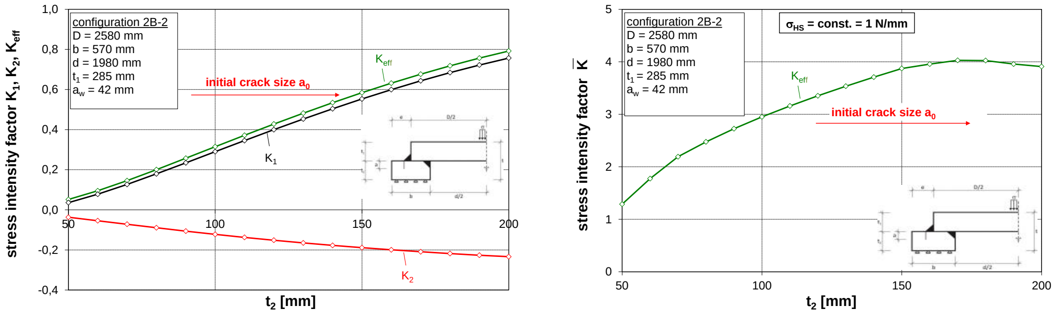

Figure 5-34: **K-values (left) and $\overline{K}$-values related to σ_{HS} = 1 N/mm^2 (right) for the loading variant 2B-2: vertical loading for variation of the plate thickness t_2 and for the upper bound of geometrical dimensions**

(5) For the lower bound of geometrical dimensions and for loading variant 2B-2 the K-values are nearly constant versus the variation of plate thickness t_2, see Figure 5-32 (left). In this case the effective value K_{eff} for taking into account mode 2-stresses is relevant.

(6) The normalized effective $\overline{K}$–values increase slightly with the thickness t_2 of the guiderail as shown in Figure 5-35 (right).

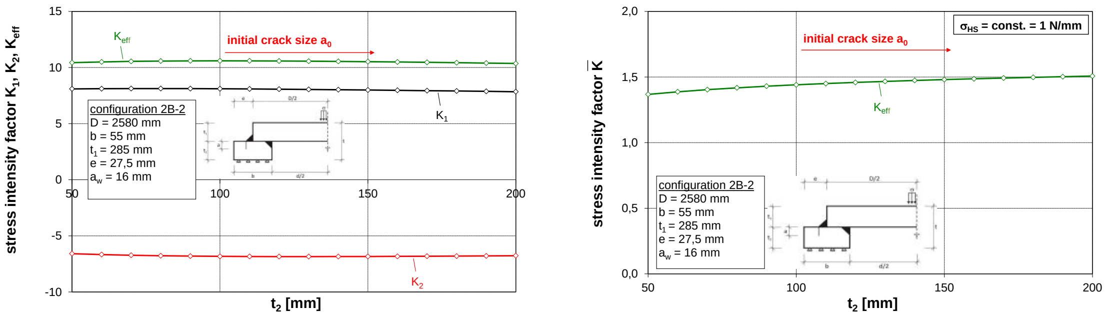

Figure 5-35: **K-values for loading variant 2B-2 - vertical loading for variation of the plate thickness t_2 and lower bound of geometrical dimensions. K-values for unit loading (left), $\overline{K}$-values related to σ_{HS} = 1 N/mm^2 at the Hot-Spot (right)**

(7) For loading variant 2B-3 Figure 5-36 (left) shows the K_1-values for increasing plate thickness t_1 for the upper bound of geometrical dimensions.

(8) For the normalized values $\overline{K}$ related to σ_{HS} = 1 N/mm^2 there is an increasing function for large t_1 according to Figure 5-36 (right).

The function for t > 100 mm can be described by a power function

$$\overline{K} = 3{,}1366 \cdot t_1^{0{,}0071} \quad \textbf{(5-10)}$$

using the effective value K_{eff}, because in this case mode 2-stress cannot be neglected.

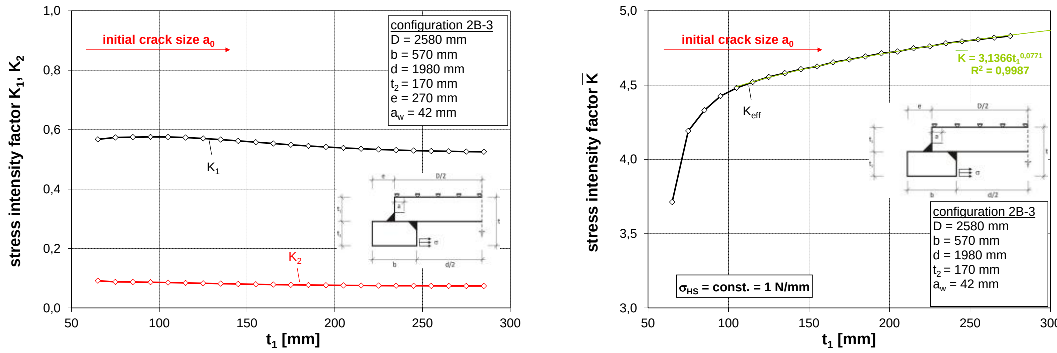

Figure 5-36: **K-values for loading variant 2B-3 - horizontal loading for variation of the plate thickness t1 and upper bound of geometrical dimensions; K-values for unit loading (left), $\overline{K}$-values related to σ_{HS} = 1 N/mm² at the Hot-Spot (right)**

(9) A qualitatively similar performance is shown for the lower bounds of geometrical dimensions in Figure 5-37 (left). The magnitudes of K-values are larger.

(10) The normalised $\overline{K}$-values taking into account mode 2-stresses are increasing with increasing plate thickness t_1, see Figure 5-37 (right).

The function can be described by the power function

$$\overline{K} = 1{,}3661 \cdot t_1^{1{,}1052} \qquad \textbf{(5-11)}$$

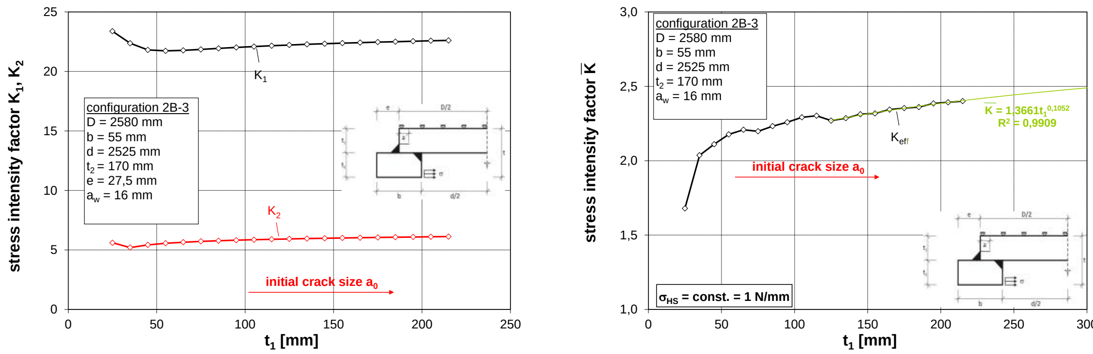

Figure 5-37: **K-values for loading variant 2B-3 - horizontal loading for variation of the plate thickness t_1 and upper bound of geometrical dimensions; K-values for unit loading (left), $\overline{K}$-values related to σ_{HS} = 1 N/mm² at the Hot-Spot (right)**

(11) For loading variant 2B-4 the K-values for the upper bound of the geometrical dimensions are increasing to a maximum value for t_1 = 250 mm and then slightly decrease, see Figure 5-38 (left).

(12) The normalized effective $\overline{K}$-value related to σ_{HS} = 1 N/mm² relevant for the assessment to avoid brittle failure may be taken from Figure 5-38 (right). The maximum is obtained for t_1 = 180 mm, and for t_1 > 180 mm there is a decrease. The function can be described for the range 190 mm ≤ t_1 ≤ 300 mm by a polynomial of 3rd degree:

$$\overline{K} = -5{,}01730 \cdot 10^{-7} \cdot t_1^3 + 4{,}09628 \cdot 10^{-4} \cdot t_1^2 - 1{,}12831 \cdot 10^{-1} \cdot t_1 + 13{,}8884 \qquad \textbf{(5-12)}$$

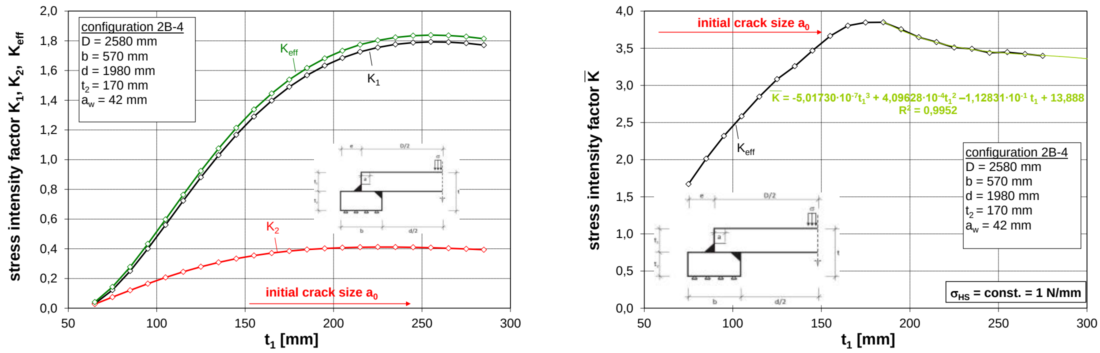

Figure 5-38: **K-values for loading variant 2B-4 - vertical loading for variation of the plate thickness t_1 and upper bound of geometrical dimensions; K-values for unit loading (left), $\overline{K}$-values related to σ_{HS} = 1 N/mm^2 at the Hot-Spot (right)**

(13) For the lower bounds of the geometrical dimensions Figure 5-39 (left) shows a similar behaviour; a steep increase for small thicknesses t_1 and a strong decrease for thicknesses t_1 > 50 mm can be seen.

(14) Figure 5-39 (right) demonstrates an almost constant function of $\overline{K}$-values related to the Hot-Spot stress σ_{HS} = 1 N/mm^2 for $t_1 \geq$ 55 mm with a maximum for t_1 = 35 mm.

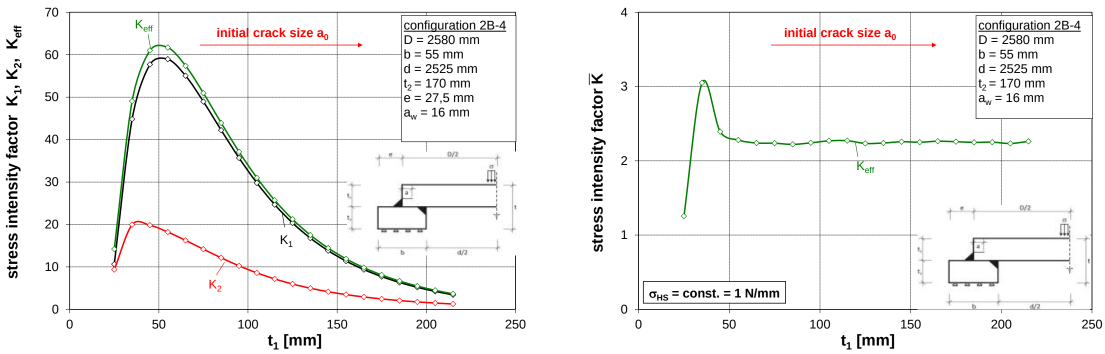

Figure 5-39: **K-values for loading variant 2B-4 – vertical loading for variation of the plate thickness t_1 and upper bound of geometrical dimensions; K-values for unit loading (left), $\overline{K}$-values related to σ_{HS} = 1 N/mm² at the Hot-Spot (right)**

(15) For the loading variant 2B-5 the crack is in the re-entrant corner between the sliding plate and the guiderail. The function of K-values versus the plate thickness t_1 is given for the upper bound of geometrical dimensions in Figure 5-40 (left). The influence of plate thickness t_1 on K for constant external load is small.

(16) Also the influence of the plate thickness t_1 on the normalized value $\overline{K}$ is small as demonstrated in Figure 5-40 (right).

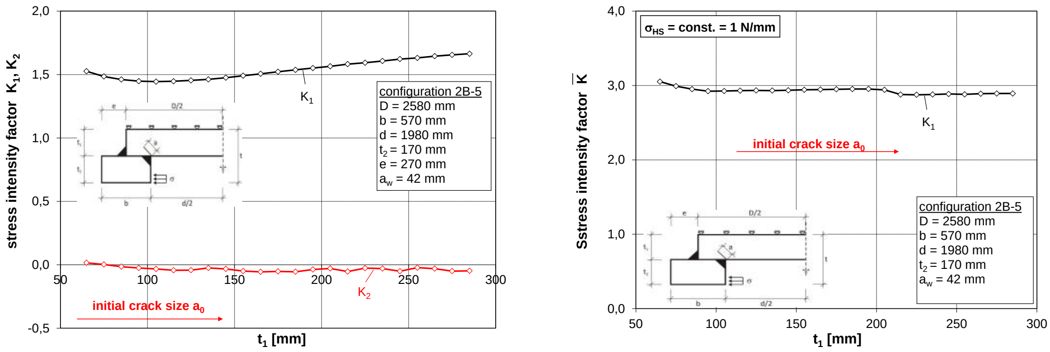

Figure 5-40: **K-values for loading variant 2B-5 - horizontal loading for variation of the plate thickness t_1 and upper bounds of geometrical dimensions; K-values for unit loading (left); $\overline{K}$-values related to σ_{HS} = 1 N/mm^2 at the Hot-Spot (right)**

(17) Figure 5-41 (left) shows the monotonous increase of K-values versus plate thickness t_1 for the loading variant 2B-5 and for the lower bound of geometrical dimensions. In comparison with the value in Figure 5-40 (left) the K-values are larger but do not vary much around a certain level.

(18) The $\overline{K}$-value normalised to σ_{HS} = 1 N/mm^2 gives the function according to Figure 5-41 (right). For t_1 > 215 mm this function can be approximated by $\overline{K} = 2{,}0352e^{0{,}0006t1}$.

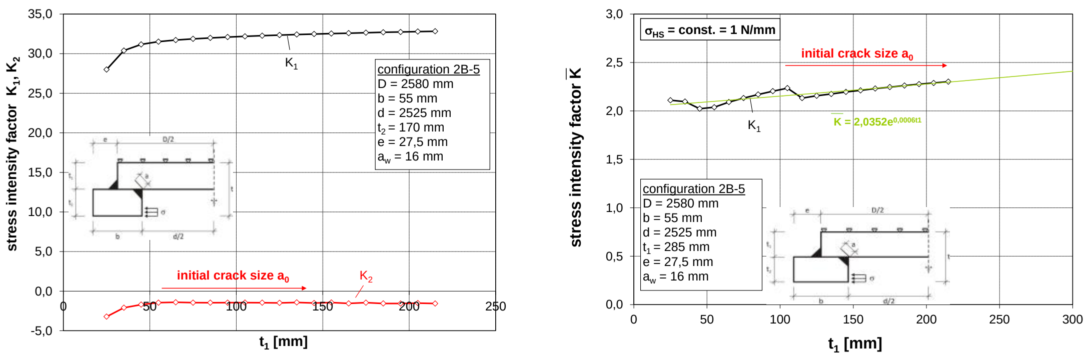

Figure 5-41: **K-values for loading variant 2B-5 - horizontal loading for variation of the plate thickness t_1 and upper bounds of geometrical dimensions; K-values for unit loading (left); $\overline{K}$-values related to σ_{HS} = 1 N/mm^2 at the Hot-Spot (right)**

(19) For loading variant 2B-6 the K-values decrease for large values of t_1, for the upper bound of geometrical dimensions, see Figure 5-42 (left).

(20) The normalised values $\overline{K}$ related to σ_{HS} = 1 N/mm^2 produce however a nearly constant function versus the plate thickness t_1, see Figure 5-42 (right).

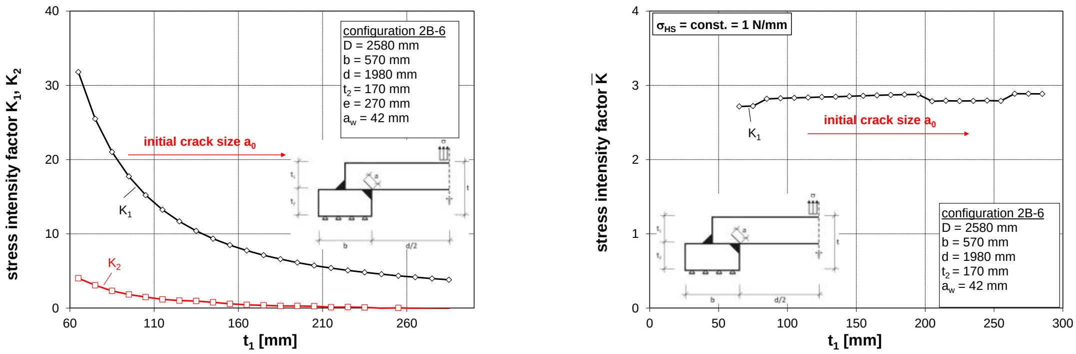

Figure 5-42: **K-values for loading variant 2B-5 - horizontal loading for variation of the plate thickness t_1 and upper bounds for the geometrical dimensions; K-values for unit loading (left); $\overline{K}$-values related to σ_{HS} = 1 N/mm^2 at the Hot-Spot (right)**

(21) Figure 5-43 (left) shows qualitatively a similar behaviour as given in Figure 5-42 (left) for the lower bound of the geometrical dimensions.

(22) The normalized value $\overline{K}$ related to σ_{HS} = 1 N/mm^2 is shown in Figure 5-43 (right) versus the plate thickness t_1. For t_1 > 215 mm the $\overline{K}$-value can be described by a power function

$$\overline{K} = 6{,}8975 \cdot 10^{-9} t_1^3 - 5{,}8020 \cdot 10^{-7} t_1^2 + 1{,}8563 \cdot 10^{-3} t_1 + 2{,}0015 \qquad \textbf{(5-13)}$$

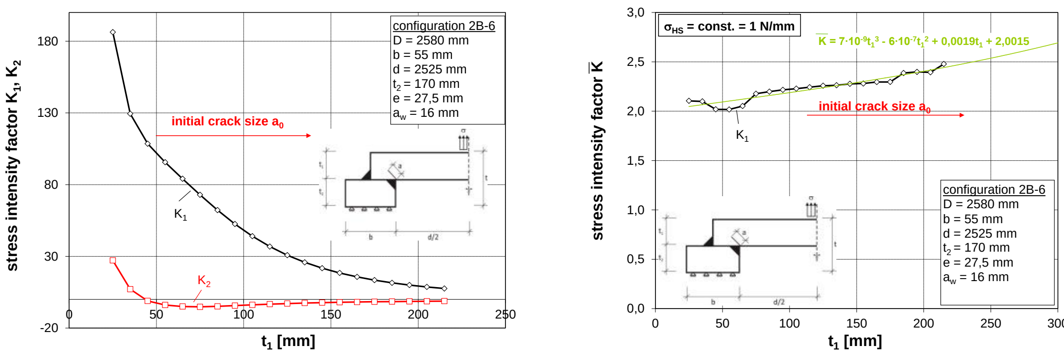

Figure 5-43: **K-values for loading variant 2B-6 - vertical loading for variation of the plate thickness t_1 and lower bounds of the geometrical dimensions; K-values for unit loading (left); $\overline{K}$-values related to σ_{HS} = 1 N/mm^2 at the Hot-Spot (right)**

5.4.4 Assessments to avoid brittle fracture

(1) The assessments to avoid brittle fracture were carried out in Table 5-21 to 5-26 according to the list in Table 5-14.

Table 5-14: Allocation of tabular-calculations to loading variants

Loading variant	Table	Remark
2B-1	Table 5-21	Due to compression maximum stress level $\sigma_{Ed} = 0{,}25 \cdot f_y$*)
2B-2	Table 5-22	Due to compression maximum stress level $\sigma_{Ed} = 0{,}25 \cdot f_y$*)
2B-3	Table 5-23	Due to compression maximum stress level $\sigma_{Ed} = 0{,}25 \cdot f_y$*)
2B-4	Table 5-24	Due to compression maximum stress level $\sigma_{Ed} = 0{,}25 \cdot f_y$*)
2B-5	Table 5-25	
2B-6	Table 5-26	

*) The minimum value of tensile stress for members that are nominally in compression is specified in EN 1993-1-10

(2) The results of the tabular calculations in the Tables 5-21 to 5-26 are presented in Tables 5-15 to 5-20.

Table 5-15: Limits of plate thickness t_2 [mm] for the top component (configuration 2B-1) for compressive stress

Steel grade acc. to EN 10025	σ_{Ed}	0°C	-10°C	-20°C	-30°C	-40°C	-50°C
S355J2	$0{,}25 \cdot f_y$	200*)	200	190	170	150	130

**) Assumption of a technical manufacturing limit (in theory element thicknesses with t ≥ 200 mm would be acceptable)*

Table 5-16: Limits of plate thickness t_2 [mm] for the top component (configuration 2B-2) for compressive stress

Steel grade acc. to EN 10025	σ_{Ed}	0°C	-10°C	-20°C	-30°C	-40°C	-50°C
S355J2	$0{,}25 \cdot f_y$	200*)	200*)	200*)	200*)	200*)	200*)

**) Assumption of a technical manufacturing limit (in theory element thicknesses with t ≥ 200 mm would be acceptable)*

Table 5-17: Limits of plate thickness t_1 [mm] for the top component (configuration 2B-3) for compressive stress

Steel grade acc. to EN 10025	σ_{Ed}	0°C	-10°C	-20°C	-30°C	-40°C	-50°C
S355J2	$0{,}25 \cdot f_y$	300*)	300*)	300*)	300*)	300*)	300*)

*) *Assumption of a technical manufacturing limit (in theory element thicknesses with t ≥ 300 mm would be acceptable)*

Table 5-18: Limits of plate thickness t_1 [mm] for the top component (configuration 2B-4) for compressive stress

Steel grade acc. to EN 10025	σ_{Ed}	0°C	-10°C	-20°C	-30°C	-40°C	-50°C
S355J2	$0{,}25 \cdot f_y$	300*)	300*)	300*)	300*)	300*)	300*)

*) *Assumption of a technical manufacturing limit (in theory element thicknesses with t ≥ 300 mm would be acceptable)*

Table 5-19: Limits of plate thickness t_1 [mm] for the top component (configuration 2B-5)

Steel grade acc. to EN 10025	σ_{Ed}	0°C	-10°C	-20°C	-30°C	-40°C	-50°C
S355J2	$0{,}25 \cdot f_y$	300*)	300*)	300*)	300*)	300*)	300*)
S355J2	$0{,}50 \cdot f_y$	300*)	300*)	300*)	300*)	300*)	300*)
S355J2	$0{,}75 \cdot f_y$	300*)	300*)	300*)	300*)	300*)	300*)

*) *Assumption of a technical manufacturing limit (in theory element thicknesses with t ≥ 300 mm would be acceptable)*

Table 5-20: Limits of plate thickness t_1 [mm] for the top component (configuration 2B-6)

Steel grade acc. to EN 10025	σ_{Ed}	0°C	-10°C	-20°C	-30°C	-40°C	-50°C
S355J2	$0{,}25 \cdot f_y$	300*)	300*)	300*)	300*)	300*)	300*)
S355J2	$0{,}50 \cdot f_y$	300*)	300*)	300*)	300*)	300*)	300*)
S355J2	$0{,}75 \cdot f_y$	300*)	300*)	300*)	300*)	300*)	300*)

*) *Assumption of a technical manufacturing limit (in theory element thicknesses with t ≥ 25x0 mm would be acceptable)*

Table 5-21: **Fracture mechanics assessment for loading variant 2B-1 for component No. 2B (Axisymmetric top component (sliding plate and guide-rail))**

Assessment for $\sigma_{Ed} = 0{,}25 \cdot f_y$ and T = -50 °C

Nr	σ_P	K_1	σ_{Ed}/f_y	σ_P	σ_S	a_0	t_1	$K_{1,P}$	$K_{1,S}$	$K_{1,ges}$	$K_{1,ges}$	$f_{y,nom}$	$f_y(t)$	σ_{gy}	L_r	ψ	ρ_1	ρ	k_{R6}	$K_{appl,d}$	$K_{appl,d}$	b_{eff}	ΔT_σ	$K_{V,nom}$	T_{KV}	T_{27J}	ΔT_{27J}	ΔT_R	T_{md}	ΔT_r	ΔT_ε	ΔT_{DCF}	T_{Ed}	T_{Rd}	$T_{Ed} \geq T_{Rd}$
	N/mm²	$N/mm^{3/2}$	[-]	N/mm²	N/mm²	mm	mm	$N/mm^{3/2}$	$N/mm^{3/2}$	$N/mm^{3/2}$	$MPam^{1/2}$	N/mm²	N/mm²	N/mm²	-	-	-	-	-	$N/mm^{3/2}$	$MPam^{1/2}$	mm	°C	J	°C	°C	°C	°C	°C	°C	°C	°C	°C	°C	
1	1,0	5,323	0,25	88,8	100	1,96	50	472	532	1005	31,8	355	343	329	0,27	0,30	0,04	0,04	0,98	1069	33,8	50	120,0	27	-20	-20	21	7	-45	-5	0	0	**77**	**-17**	no risk
2	1,0	5,694	0,25	88,8	100	2,05	60	505	569	1075	34,0	355	340	328	0,27	0,30	0,04	0,04	0,98	1143	36,2	60	100,6	27	-20	-20	23	7	-45	-5	0	0	**58**	**-15**	no risk
3	1,0	6,036	0,25	88,8	100	2,12	70	536	604	1139	36,0	355	338	327	0,27	0,31	0,04	0,04	0,98	1212	38,3	70	84,8	27	-20	-20	24	7	-45	-5	0	0	**42**	**-14**	no risk
4	1,0	6,360	0,25	88,8	100	2,19	80	564	636	1200	38,0	355	335	326	0,27	0,31	0,04	0,04	0,98	1278	40,4	80	72,7	27	-20	-20	25	7	-45	-5	0	0	**30**	**-13**	no risk
5	1,0	6,673	0,25	88,8	100	2,25	90	592	667	1260	39,8	355	333	324	0,27	0,31	0,04	0,04	0,98	1341	42,4	90	62,9	27	-20	-20	25	7	-45	-5	0	0	**20**	**-13**	no risk
6	1,0	6,982	0,25	88,8	100	2,30	100	620	698	1318	41,7	355	330	322	0,28	0,31	0,04	0,04	0,98	1404	44,4	100	54,6	27	-20	-20	25	7	-45	-5	0	0	**12**	**-13**	no risk
7	1,0	7,293	0,25	88,8	100	2,35	110	647	729	1377	43,5	355	328	321	0,28	0,31	0,04	0,04	0,98	1467	46,4	110	47,3	27	-20	-20	25	7	-45	-5	0	0	**4**	**-13**	no risk
8	1,0	7,609	0,25	88,8	100	2,39	120	675	761	1436	45,4	355	325	319	0,28	0,31	0,04	0,04	0,98	1531	48,4	120	40,6	27	-20	-20	26	7	-45	-5	0	0	**-2**	**-12**	no risk
9	1,0	7,934	0,25	88,8	100	2,43	130	704	793	1498	47,4	355	323	316	0,28	0,32	0,04	0,04	0,98	1597	50,5	130	34,5	27	-20	-20	26	7	-45	-5	0	0	**-9**	**-12**	no risk
10	1,0	8,271	0,25	88,8	100	2,47	140	734	827	1561	49,4	355	320	314	0,28	0,32	0,04	0,04	0,98	1666	52,7	140	28,8	27	-20	-20	26	7	-45	-5	0	0	**-14**	**-12**	risk

Assessment for $\sigma_{Ed} = 0{,}25 \cdot f_y$ and T = -40 °C

Nr	σ_P	K_1	σ_{Ed}/f_y	σ_P	σ_S	a_0	t_1	$K_{1,P}$	$K_{1,S}$	$K_{1,ges}$	$K_{1,ges}$	$f_{y,nom}$	$f_y(t)$	σ_{gy}	L_r	ψ	ρ_1	ρ	k_{R6}	$K_{appl,d}$	$K_{appl,d}$	b_{eff}	ΔT_σ	$K_{V,nom}$	T_{KV}	T_{27J}	ΔT_{27J}	ΔT_R	T_{md}	ΔT_r	ΔT_ε	ΔT_{DCF}	T_{Ed}	T_{Rd}	$T_{Ed} \geq T_{Rd}$
	N/mm²	$N/mm^{3/2}$	[-]	N/mm²	N/mm²	mm	mm	$N/mm^{3/2}$	$N/mm^{3/2}$	$N/mm^{3/2}$	$MPam^{1/2}$	N/mm²	N/mm²	N/mm²	-	-	-	-	-	$N/mm^{3/2}$	$MPam^{1/2}$	mm	°C	J	°C	°C	°C	°C	°C	°C	°C	°C	°C	°C	
1	1,0	5,323	0,25	88,8	100	1,96	50	472	532	1005	31,8	355	343	329	0,27	0,30	0,04	0,04	0,98	1069	33,8	50	120,0	27	-20	-20	21	7	-35	-5	0	0	**87**	**-17**	no risk
2	1,0	5,694	0,25	88,8	100	2,05	60	505	569	1075	34,0	355	340	328	0,27	0,30	0,04	0,04	0,98	1143	36,2	60	100,6	27	-20	-20	23	7	-35	-5	0	0	**68**	**-15**	no risk
3	1,0	6,036	0,25	88,8	100	2,12	70	536	604	1139	36,0	355	338	327	0,27	0,31	0,04	0,04	0,98	1212	38,3	70	84,8	27	-20	-20	24	7	-35	-5	0	0	**52**	**-14**	no risk
4	1,0	6,360	0,25	88,8	100	2,19	80	564	636	1200	38,0	355	335	326	0,27	0,31	0,04	0,04	0,98	1278	40,4	80	72,7	27	-20	-20	25	7	-35	-5	0	0	**40**	**-13**	no risk
5	1,0	6,673	0,25	88,8	100	2,25	90	592	667	1260	39,8	355	333	324	0,27	0,31	0,04	0,04	0,98	1341	42,4	90	62,9	27	-20	-20	25	7	-35	-5	0	0	**30**	**-13**	no risk
6	1,0	6,982	0,25	88,8	100	2,30	100	620	698	1318	41,7	355	330	322	0,28	0,31	0,04	0,04	0,98	1404	44,4	100	54,6	27	-20	-20	25	7	-35	-5	0	0	**22**	**-13**	no risk
7	1,0	7,293	0,25	88,8	100	2,35	110	647	729	1377	43,5	355	328	321	0,28	0,31	0,04	0,04	0,98	1467	46,4	110	47,3	27	-20	-20	25	7	-35	-5	0	0	**14**	**-13**	no risk
8	1,0	7,609	0,25	88,8	100	2,39	120	675	761	1436	45,4	355	325	319	0,28	0,31	0,04	0,04	0,98	1531	48,4	120	40,6	27	-20	-20	26	7	-35	-5	0	0	**8**	**-12**	no risk
9	1,0	7,934	0,25	88,8	100	2,43	130	704	793	1498	47,4	355	323	316	0,28	0,32	0,04	0,04	0,98	1597	50,5	130	34,5	27	-20	-20	26	7	-35	-5	0	0	**1**	**-12**	no risk
10	1,0	8,271	0,25	88,8	100	2,47	140	734	827	1561	49,4	355	320	314	0,28	0,32	0,04	0,04	0,98	1666	52,7	140	28,8	27	-20	-20	26	7	-35	-5	0	0	**-4**	**-12**	no risk
11	1,0	8,619	0,25	88,8	100	2,51	150	765	862	1627	51,4	355	318	312	0,28	0,32	0,04	0,04	0,98	1737	54,9	150	23,4	27	-20	-20	26	7	-35	-5	0	0	**-10**	**-12**	no risk
12	1,0	8,980	0,25	88,8	100	2,54	160	797	898	1695	53,6	355	315	310	0,29	0,32	0,04	0,04	0,98	1810	57,2	160	18,3	27	-20	-20	26	7	-35	-5	0	0	**-15**	**-12**	risk

Assessment for $\sigma_{Ed} = 0{,}25 \cdot f_y$ and T = -30 °C

Nr	σ_P	K_1	σ_{Ed}/f_y	σ_P	σ_S	a_0	t_1	$K_{1,P}$	$K_{1,S}$	$K_{1,ges}$	$K_{1,ges}$	$f_{y,nom}$	$f_y(t)$	σ_{gy}	L_r	ψ	ρ_1	ρ	k_{R6}	$K_{appl,d}$	$K_{appl,d}$	b_{eff}	ΔT_σ	$K_{V,nom}$	T_{KV}	T_{27J}	ΔT_{27J}	ΔT_R	T_{md}	ΔT_r	ΔT_ε	ΔT_{DCF}	T_{Ed}	T_{Rd}	$T_{Ed} \geq T_{Rd}$
	N/mm²	$N/mm^{3/2}$	[-]	N/mm²	N/mm²	mm	mm	$N/mm^{3/2}$	$N/mm^{3/2}$	$N/mm^{3/2}$	$MPam^{1/2}$	N/mm²	N/mm²	N/mm²	-	-	-	-	-	$N/mm^{3/2}$	$MPam^{1/2}$	mm	°C	J	°C	°C	°C	°C	°C	°C	°C	°C	°C	°C	
1	1,0	5,323	0,25	88,8	100	1,96	50	472	532	1005	31,8	355	343	329	0,27	0,30	0,04	0,04	0,98	1069	33,8	50	120,0	27	-20	-20	21	7	-25	-5	0	0	**97**	**-17**	no risk
2	1,0	5,694	0,25	88,8	100	2,05	60	505	569	1075	34,0	355	340	328	0,27	0,30	0,04	0,04	0,98	1143	36,2	60	100,6	27	-20	-20	23	7	-25	-5	0	0	**78**	**-15**	no risk
3	1,0	6,036	0,25	88,8	100	2,12	70	536	604	1139	36,0	355	338	327	0,27	0,31	0,04	0,04	0,98	1212	38,3	70	84,8	27	-20	-20	24	7	-25	-5	0	0	**62**	**-14**	no risk
4	1,0	6,360	0,25	88,8	100	2,19	80	564	636	1200	38,0	355	335	326	0,27	0,31	0,04	0,04	0,98	1278	40,4	80	72,7	27	-20	-20	25	7	-25	-5	0	0	**50**	**-13**	no risk
5	1,0	6,673	0,25	88,8	100	2,25	90	592	667	1260	39,8	355	333	324	0,27	0,31	0,04	0,04	0,98	1341	42,4	90	62,9	27	-20	-20	25	7	-25	-5	0	0	**40**	**-13**	no risk
6	1,0	6,982	0,25	88,8	100	2,30	100	620	698	1318	41,7	355	330	322	0,28	0,31	0,04	0,04	0,98	1404	44,4	100	54,6	27	-20	-20	25	7	-25	-5	0	0	**32**	**-13**	no risk
7	1,0	7,293	0,25	88,8	100	2,35	110	647	729	1377	43,5	355	328	321	0,28	0,31	0,04	0,04	0,98	1467	46,4	110	47,3	27	-20	-20	25	7	-25	-5	0	0	**24**	**-13**	no risk
8	1,0	7,609	0,25	88,8	100	2,39	120	675	761	1436	45,4	355	325	319	0,28	0,31	0,04	0,04	0,98	1531	48,4	120	40,6	27	-20	-20	26	7	-25	-5	0	0	**18**	**-12**	no risk
9	1,0	7,934	0,25	88,8	100	2,43	130	704	793	1498	47,4	355	323	316	0,28	0,32	0,04	0,04	0,98	1597	50,5	130	34,5	27	-20	-20	26	7	-25	-5	0	0	**11**	**-12**	no risk
10	1,0	8,271	0,25	88,8	100	2,47	140	734	827	1561	49,4	355	320	314	0,28	0,32	0,04	0,04	0,98	1666	52,7	140	28,8	27	-20	-20	26	7	-25	-5	0	0	**6**	**-12**	no risk
11	1,0	8,619	0,25	88,8	100	2,51	150	765	862	1627	51,4	355	318	312	0,28	0,32	0,04	0,04	0,98	1737	54,9	150	23,4	27	-20	-20	26	7	-25	-5	0	0	**0**	**-12**	no risk
12	1,0	8,980	0,25	88,8	100	2,54	160	797	898	1695	53,6	355	315	310	0,29	0,32	0,04	0,04	0,98	1810	57,2	160	18,3	27	-20	-20	26	7	-25	-5	0	0	**-5**	**-12**	no risk
13	1,0	9,353	0,25	88,8	100	2,57	170	830	935	1765	55,8	355	313	308	0,29	0,32	0,04	0,04	0,98	1887	59,7	170	13,5	27	-20	-20	26	7	-25	-5	0	0	**-10**	**-12**	no risk
14	1,0	9,736	0,25	88,8	100	2,60	180	864	974	1838	58,1	355	310	306	0,29	0,33	0,04	0,04	0,98	1965	62,1	180	8,9	27	-20	-20	26	7	-25	-5	0	0	**-14**	**-12**	risk

Table 5-21: continued

Assessment for $\sigma_{Ed} = 0,25 \cdot f_y$ and T = -20 °C

Nr	σ_P	K_1	σ_{Ed}/f_y	σ_P	σ_S	a_0	t_1	$K_{1,P}$	$K_{1,S}$	$K_{1,ges}$	$K_{1,ges}$	$f_{y,nom}$	$f_y(t)$	σ_{gy}	L_r	ψ	ρ_1	ρ	k_{R6}	$K_{appl,d}$	$K_{appl,d}$	b_{eff}	ΔT_σ	$K_{V,nom}$	T_{KV}	T_{27J}	ΔT_{27J}	ΔT_R	T_{md}	ΔT_r	ΔT_ε	ΔT_{DCF}	T_{Ed}	T_{Rd}	$T_{Ed} \geq T_{Rd}$
	N/mm²	$N/mm^{3/2}$	[-]	N/mm²	N/mm²	mm	mm	$N/mm^{3/2}$	$N/mm^{3/2}$	$N/mm^{3/2}$	$MPam^{1/2}$	N/mm²	N/mm²	N/mm²	-	-	-	-	-	$N/mm^{3/2}$	$MPam^{1/2}$	mm	°C	J	°C	°C	°C	°C	°C	°C	°C	°C	°C	°C	
1	1,0	5,323	0,25	88,8	100	1,96	50	472	532	1005	31,8	355	343	329	0,27	0,30	0,04	0,04	0,98	1069	33,8	50	120,0	27	-20	-20	21	7	-15	-5	0	0	**107**	**-17**	no risk
2	1,0	5,694	0,25	88,8	100	2,05	60	505	569	1075	34,0	355	340	328	0,27	0,30	0,04	0,04	0,98	1143	36,2	60	100,6	27	-20	-20	23	7	-15	-5	0	0	**88**	**-15**	no risk
3	1,0	6,036	0,25	88,8	100	2,12	70	536	604	1139	36,0	355	338	327	0,27	0,31	0,04	0,04	0,98	1212	38,3	70	84,8	27	-20	-20	24	7	-15	-5	0	0	**72**	**-14**	no risk
4	1,0	6,360	0,25	88,8	100	2,19	80	564	636	1200	38,0	355	335	326	0,27	0,31	0,04	0,04	0,98	1278	40,4	80	72,7	27	-20	-20	25	7	-15	-5	0	0	**60**	**-13**	no risk
5	1,0	6,673	0,25	88,8	100	2,25	90	592	667	1260	39,8	355	333	324	0,27	0,31	0,04	0,04	0,98	1341	42,4	90	62,9	27	-20	-20	25	7	-15	-5	0	0	**50**	**-13**	no risk
6	1,0	6,982	0,25	88,8	100	2,30	100	620	698	1318	41,7	355	330	322	0,28	0,31	0,04	0,04	0,98	1404	44,4	100	54,6	27	-20	-20	25	7	-15	-5	0	0	**42**	**-13**	no risk
7	1,0	7,293	0,25	88,8	100	2,35	110	647	729	1377	43,5	355	328	321	0,28	0,31	0,04	0,04	0,98	1467	46,4	110	47,3	27	-20	-20	25	7	-15	-5	0	0	**34**	**-13**	no risk
8	1,0	7,609	0,25	88,8	100	2,39	120	675	761	1436	45,4	355	325	319	0,28	0,31	0,04	0,04	0,98	1531	48,4	120	40,6	27	-20	-20	26	7	-15	-5	0	0	**28**	**-12**	no risk
9	1,0	7,934	0,25	88,8	100	2,43	130	704	793	1498	47,4	355	323	316	0,28	0,32	0,04	0,04	0,98	1597	50,5	130	34,5	27	-20	-20	26	7	-15	-5	0	0	**21**	**-12**	no risk
10	1,0	8,271	0,25	88,8	100	2,47	140	734	827	1561	49,4	355	320	314	0,28	0,32	0,04	0,04	0,98	1666	52,7	140	28,8	27	-20	-20	26	7	-15	-5	0	0	**16**	**-12**	no risk
11	1,0	8,619	0,25	88,8	100	2,51	150	765	862	1627	51,4	355	318	312	0,28	0,32	0,04	0,04	0,98	1737	54,9	150	23,4	27	-20	-20	26	7	-15	-5	0	0	**10**	**-12**	no risk
12	1,0	8,980	0,25	88,8	100	2,54	160	797	898	1695	53,6	355	315	310	0,29	0,32	0,04	0,04	0,98	1810	57,2	160	18,3	27	-20	-20	26	7	-15	-5	0	0	**5**	**-12**	no risk
13	1,0	9,353	0,25	88,8	100	2,57	170	830	935	1765	55,8	355	313	308	0,29	0,32	0,04	0,04	0,98	1887	59,7	170	13,5	27	-20	-20	26	7	-15	-5	0	0	**0**	**-12**	no risk
14	1,0	9,736	0,25	88,8	100	2,60	180	864	974	1838	58,1	355	310	306	0,29	0,33	0,04	0,04	0,98	1965	62,1	180	8,9	27	-20	-20	26	7	-15	-5	0	0	**-4**	**-12**	no risk
15	1,0	10,130	0,25	88,8	100	2,62	190	899	1013	1912	60,5	355	308	303	0,29	0,33	0,04	0,04	0,98	2046	64,7	190	4,5	27	-20	-20	26	7	-15	-5	0	0	**-8**	**-12**	no risk
16	1,0	10,530	0,25	88,8	100	2,65	200	935	1053	1988	62,9	355	305	301	0,29	0,33	0,04	0,04	0,98	2128	67,3	200	0,4	27	-20	-20	26	7	-15	-5	0	0	**-13**	**-12**	risk

Assessment for $\sigma_{Ed} = 0,25 \cdot f_y$ and T = -10 °C

Nr	σ_P	K_1	σ_{Ed}/f_y	σ_P	σ_S	a_0	t_1	$K_{1,P}$	$K_{1,S}$	$K_{1,ges}$	$K_{1,ges}$	$f_{y,nom}$	$f_y(t)$	σ_{gy}	L_r	ψ	ρ_1	ρ	k_{R6}	$K_{appl,d}$	$K_{appl,d}$	b_{eff}	ΔT_σ	$K_{V,nom}$	T_{KV}	T_{27J}	ΔT_{27J}	ΔT_R	T_{md}	ΔT_r	ΔT_ε	ΔT_{DCF}	T_{Ed}	T_{Rd}	$T_{Ed} \geq T_{Rd}$
	N/mm²	$N/mm^{3/2}$	[-]	N/mm²	N/mm²	mm	mm	$N/mm^{3/2}$	$N/mm^{3/2}$	$N/mm^{3/2}$	$MPam^{1/2}$	N/mm²	N/mm²	N/mm²	-	-	-	-	-	$N/mm^{3/2}$	$MPam^{1/2}$	mm	°C	J	°C	°C	°C	°C	°C	°C	°C	°C	°C	°C	
1	1,0	5,323	0,25	88,8	100	1,96	50	472	532	1005	31,8	355	343	329	0,27	0,30	0,04	0,04	0,98	1069	33,8	50	120,0	27	-20	-20	21	7	-5	-5	0	0	**117**	**-17**	no risk
2	1,0	5,694	0,25	88,8	100	2,05	60	505	569	1075	34,0	355	340	328	0,27	0,30	0,04	0,04	0,98	1143	36,2	60	100,6	27	-20	-20	23	7	-5	-5	0	0	**98**	**-15**	no risk
3	1,0	6,036	0,25	88,8	100	2,12	70	536	604	1139	36,0	355	338	327	0,27	0,31	0,04	0,04	0,98	1212	38,3	70	84,8	27	-20	-20	24	7	-5	-5	0	0	**82**	**-14**	no risk
4	1,0	6,360	0,25	88,8	100	2,19	80	564	636	1200	38,0	355	335	326	0,27	0,31	0,04	0,04	0,98	1278	40,4	80	72,7	27	-20	-20	25	7	-5	-5	0	0	**70**	**-13**	no risk
5	1,0	6,673	0,25	88,8	100	2,25	90	592	667	1260	39,8	355	333	324	0,27	0,31	0,04	0,04	0,98	1341	42,4	90	62,9	27	-20	-20	25	7	-5	-5	0	0	**60**	**-13**	no risk
6	1,0	6,982	0,25	88,8	100	2,30	100	620	698	1318	41,7	355	330	322	0,28	0,31	0,04	0,04	0,98	1404	44,4	100	54,6	27	-20	-20	25	7	-5	-5	0	0	**52**	**-13**	no risk
7	1,0	7,293	0,25	88,8	100	2,35	110	647	729	1377	43,5	355	328	321	0,28	0,31	0,04	0,04	0,98	1467	46,4	110	47,3	27	-20	-20	25	7	-5	-5	0	0	**44**	**-13**	no risk
8	1,0	7,609	0,25	88,8	100	2,39	120	675	761	1436	45,4	355	325	319	0,28	0,31	0,04	0,04	0,98	1531	48,4	120	40,6	27	-20	-20	26	7	-5	-5	0	0	**38**	**-12**	no risk
9	1,0	7,934	0,25	88,8	100	2,43	130	704	793	1498	47,4	355	323	316	0,28	0,32	0,04	0,04	0,98	1597	50,5	130	34,5	27	-20	-20	26	7	-5	-5	0	0	**31**	**-12**	no risk
10	1,0	8,271	0,25	88,8	100	2,47	140	734	827	1561	49,4	355	320	314	0,28	0,32	0,04	0,04	0,98	1666	52,7	140	28,8	27	-20	-20	26	7	-5	-5	0	0	**26**	**-12**	no risk
11	1,0	8,619	0,25	88,8	100	2,51	150	765	862	1627	51,4	355	318	312	0,28	0,32	0,04	0,04	0,98	1737	54,9	150	23,4	27	-20	-20	26	7	-5	-5	0	0	**20**	**-12**	no risk
12	1,0	8,980	0,25	88,8	100	2,54	160	797	898	1695	53,6	355	315	310	0,29	0,32	0,04	0,04	0,98	1810	57,2	160	18,3	27	-20	-20	26	7	-5	-5	0	0	**15**	**-12**	no risk
13	1,0	9,353	0,25	88,8	100	2,57	170	830	935	1765	55,8	355	313	308	0,29	0,32	0,04	0,04	0,98	1887	59,7	170	13,5	27	-20	-20	26	7	-5	-5	0	0	**10**	**-12**	no risk
14	1,0	9,736	0,25	88,8	100	2,60	180	864	974	1838	58,1	355	310	306	0,29	0,33	0,04	0,04	0,98	1965	62,1	180	8,9	27	-20	-20	26	7	-5	-5	0	0	**6**	**-12**	no risk
15	1,0	10,130	0,25	88,8	100	2,62	190	899	1013	1912	60,5	355	308	303	0,29	0,33	0,04	0,04	0,98	2046	64,7	190	4,5	27	-20	-20	26	7	-5	-5	0	0	**2**	**-12**	no risk
16	1,0	10,530	0,25	88,8	100	2,65	200	935	1053	1988	62,9	355	305	301	0,29	0,33	0,04	0,04	0,98	2128	67,3	200	0,4	27	-20	-20	26	7	-5	-5	0	0	**-3**	**-12**	no risk

Table 5-22: **Fracture mechanics assessment for loading variant 2B-2 for component No. 2B (Axisymmetric top component (sliding plate and guide-rail))**

Assessment for $\sigma_{Ed} = 0{,}25 \cdot f_y$ and T = -50 °C

Nr	σ_P	K_1	σ_{Ed}/f_y	σ_P	σ_S	a_0	t_1	$K_{1,P}$	$K_{1,S}$	$K_{1,ges}$	$K_{1,ges}$	$f_{y,nom}$	$f_y(t)$	σ_{gy}	L_r	ψ	ρ_1	ρ	k_{R6}	$K_{appl,d}$	$K_{appl,d}$	b_{eff}	ΔT_σ	$K_{V,nom}$	T_{KV}	T_{27J}	ΔT_{27J}	ΔT_R	T_{md}	ΔT_r	ΔT_ε	ΔT_{DCF}	T_{Ed}	T_{Rd}	$T_{Ed} \geq T_{Rd}$
	N/mm²	$N/mm^{3/2}$	[-]	N/mm²	N/mm²	mm	mm	$N/mm^{3/2}$	$N/mm^{3/2}$	$N/mm^{3/2}$	$MPam^{1/2}$	N/mm²	N/mm²	N/mm²	-	-	-	-	-	$N/mm^{3/2}$	$MPam^{1/2}$	mm	°C	J	°C	°C	°C	°C	°C	°C	°C	°C	°C	°C	
1	1,0	1,37	0,25	88,8	100	1,96	50	121	137	258	8,2	355	343	329	0,27	0,30	0,04	0,04	0,98	275	8,7	50	120,0	27	-20	-20	21	7	-45	-5	0	0	77	-17	no risk
2	1,0	1,77	0,25	88,8	100	2,05	60	157	177	335	10,6	355	340	328	0,27	0,30	0,04	0,04	0,98	356	11,3	60	120,0	27	-20	-20	23	7	-45	-5	0	0	77	-15	no risk
3	1,0	2,19	0,25	88,8	100	2,12	70	195	219	414	13,1	355	338	327	0,27	0,31	0,04	0,04	0,98	440	13,9	70	120,0	27	-20	-20	24	7	-45	-5	0	0	77	-14	no risk
4	1,0	2,48	0,25	88,8	100	2,19	80	220	248	467	14,8	355	335	326	0,27	0,31	0,04	0,04	0,98	497	15,7	80	120,0	27	-20	-20	25	7	-45	-5	0	0	77	-13	no risk
5	1,0	2,72	0,25	88,8	100	2,25	90	242	272	514	16,3	355	333	324	0,27	0,31	0,04	0,04	0,98	548	17,3	90	120,0	27	-20	-20	25	7	-45	-5	0	0	77	-13	no risk
6	1,0	2,95	0,25	88,8	100	2,30	100	262	295	557	17,6	355	330	322	0,28	0,31	0,04	0,04	0,98	593	18,8	100	120,0	27	-20	-20	25	7	-45	-5	0	0	77	-13	no risk
7	1,0	3,16	0,25	88,8	100	2,35	110	280	316	596	18,9	355	328	321	0,28	0,31	0,04	0,04	0,98	635	20,1	110	120,0	27	-20	-20	25	7	-45	-5	0	0	77	-13	no risk
8	1,0	3,35	0,25	88,8	100	2,39	120	298	335	633	20,0	355	325	319	0,28	0,31	0,04	0,04	0,98	675	21,3	120	120,0	27	-20	-20	26	7	-45	-5	0	0	77	-12	no risk
9	1,0	3,53	0,25	88,8	100	2,43	130	314	353	667	21,1	355	323	316	0,28	0,32	0,04	0,04	0,98	712	22,5	130	120,0	27	-20	-20	26	7	-45	-5	0	0	77	-12	no risk
10	1,0	3,71	0,25	88,8	100	2,47	140	329	371	700	22,1	355	320	314	0,28	0,32	0,04	0,04	0,98	747	23,6	140	120,0	27	-20	-20	26	7	-45	-5	0	0	77	-12	no risk
11	1,0	3,87	0,25	88,8	100	2,51	150	344	387	731	23,1	355	318	312	0,28	0,32	0,04	0,04	0,98	780	24,7	150	120,0	27	-20	-20	26	7	-45	-5	0	0	77	-12	no risk
12	1,0	3,96	0,25	88,8	100	2,54	160	351	396	747	23,6	355	315	310	0,29	0,32	0,04	0,04	0,98	798	25,2	160	120,0	27	-20	-20	26	7	-45	-5	0	0	77	-12	no risk
13	1,0	4,03	0,25	88,8	100	2,57	170	357	403	760	24,0	355	313	308	0,29	0,32	0,04	0,04	0,98	812	25,7	170	120,0	27	-20	-20	26	7	-45	-5	0	0	77	-12	no risk
14	1,0	4,02	0,25	88,8	100	2,60	180	357	402	759	24,0	355	310	306	0,29	0,33	0,04	0,04	0,98	812	25,7	180	120,0	27	-20	-20	26	7	-45	-5	0	0	77	-12	no risk
15	1,0	3,96	0,25	88,8	100	2,62	190	351	396	747	23,6	355	308	303	0,29	0,33	0,04	0,04	0,98	799	25,3	190	120,0	27	-20	-20	26	7	-45	-5	0	0	77	-12	no risk
16	1,0	3,91	0,25	88,8	100	2,65	200	347	391	738	23,3	355	305	301	0,29	0,33	0,04	0,04	0,98	790	25,0	200	120,0	27	-20	-20	26	7	-45	-5	0	0	77	-12	no risk

Table 5-23: **Fracture mechanics assessment for loading variant 2B-3 for component No. 2B (Axisymmetric top component (sliding plate and guide-rail))**

Assessment for $\sigma_{Ed} = 0{,}25 \cdot f_y$ and T = -50 °C

Nr	σ_P	K_1	σ_{Ed}/f_y	σ_P	σ_S	a_0	t_1	$K_{1,P}$	$K_{1,S}$	$K_{1,ges}$	$K_{1,ges}$	$f_{y,nom}$	$f_y(t)$	σ_{gy}	L_r	ψ	ρ_1	ρ	k_{R6}	$K_{appl,d}$	$K_{appl,d}$	b_{eff}	ΔT_σ	$K_{V,nom}$	T_{KV}	T_{27J}	ΔT_{27J}	ΔT_R	T_{md}	ΔT_r	ΔT_ε	ΔT_{DCF}	T_{Ed}	T_{Rd}	$T_{Ed} \geq T_{Rd}$
	N/mm²	N/mm^3/2	[-]	N/mm²	N/mm²	mm	mm	N/mm^3/2	N/mm^3/2	N/mm^3/2	MPam^1/2	N/mm²	N/mm²	N/mm²	-	-	-	-	-	N/mm^3/2	MPam^1/2	mm	°C	J	°C	°C	°C	°C	°C	°C	°C	°C	°C	°C	
1	1,0	3,71	0,25	88,8	100	2,09	65	330	371	701	22,2	355	339	328	0,27	0,30	0,04	0,04	0,98	746	23,6	65	120,0	27	-20	-20	24	7	-45	-5	0	0	**77**	**-14**	no risk
2	1,0	4,19	0,25	88,8	100	2,16	75	372	419	791	25,0	355	336	327	0,27	0,31	0,04	0,04	0,98	842	26,6	75	120,0	27	-20	-20	25	7	-45	-5	0	0	**77**	**-13**	no risk
3	1,0	4,33	0,25	88,8	100	2,22	85	384	433	817	25,8	355	334	325	0,27	0,31	0,04	0,04	0,98	870	27,5	85	120,0	27	-20	-20	25	7	-45	-5	0	0	**77**	**-13**	no risk
4	1,0	4,43	0,25	88,8	100	2,28	95	393	443	835	26,4	355	331	323	0,27	0,31	0,04	0,04	0,98	890	28,1	95	120,0	27	-20	-20	25	7	-45	-5	0	0	**77**	**-13**	no risk
5	1,0	4,48	0,25	88,8	100	2,33	105	398	448	846	26,7	355	329	321	0,28	0,31	0,04	0,04	0,98	901	28,5	105	120,0	27	-20	-20	25	7	-45	-5	0	0	**77**	**-13**	no risk
6	1,0	4,52	0,25	88,8	100	2,37	115	401	452	853	27,0	355	326	320	0,28	0,31	0,04	0,04	0,98	909	28,8	115	120,0	27	-20	-20	26	7	-45	-5	0	0	**77**	**-12**	no risk
7	1,0	4,56	0,25	88,8	100	2,41	125	404	456	860	27,2	355	324	317	0,28	0,31	0,04	0,04	0,98	917	29,0	125	120,0	27	-20	-20	26	7	-45	-5	0	0	**77**	**-12**	no risk
8	1,0	4,58	0,25	88,8	100	2,45	135	407	458	865	27,3	355	321	315	0,28	0,32	0,04	0,04	0,98	922	29,2	135	120,0	27	-20	-20	26	7	-45	-5	0	0	**77**	**-12**	no risk
9	1,0	4,61	0,25	88,8	100	2,49	145	409	461	870	27,5	355	319	313	0,28	0,32	0,04	0,04	0,98	928	29,4	145	120,0	27	-20	-20	26	7	-45	-5	0	0	**77**	**-12**	no risk
10	1,0	4,63	0,25	88,8	100	2,52	155	411	463	873	27,6	355	316	311	0,29	0,32	0,04	0,04	0,98	932	29,5	155	120,0	27	-20	-20	26	7	-45	-5	0	0	**77**	**-12**	no risk
11	1,0	4,65	0,25	88,8	100	2,55	165	413	465	878	27,8	355	314	309	0,29	0,32	0,04	0,04	0,98	938	29,7	165	120,0	27	-20	-20	26	7	-45	-5	0	0	**77**	**-12**	no risk
12	1,0	4,67	0,25	88,8	100	2,58	175	415	467	882	27,9	355	311	307	0,29	0,33	0,04	0,04	0,98	943	29,8	175	120,0	27	-20	-20	26	7	-45	-5	0	0	**77**	**-12**	no risk
13	1,0	4,69	0,25	88,8	100	2,61	185	417	469	886	28,0	355	309	304	0,29	0,33	0,04	0,04	0,98	947	30,0	185	120,0	27	-20	-20	26	7	-45	-5	0	0	**77**	**-12**	no risk
14	1,0	4,71	0,25	88,8	100	2,64	195	418	471	890	28,1	355	306	302	0,29	0,33	0,04	0,04	0,98	952	30,1	195	120,0	27	-20	-20	26	7	-45	-5	0	0	**77**	**-12**	no risk
15	1,0	4,73	0,25	88,8	100	2,66	205	419	473	892	28,2	355	304	300	0,30	0,33	0,04	0,04	0,98	955	30,2	205	117,8	27	-20	-20	26	7	-45	-5	0	0	**75**	**-12**	no risk
16	1,0	4,75	0,25	88,8	100	2,69	215	421	475	896	28,3	355	301	297	0,30	0,34	0,05	0,05	0,98	960	30,4	215	114,4	27	-20	-20	26	7	-45	-5	0	0	**71**	**-12**	no risk
17	1,0	4,76	0,25	88,8	100	2,71	225	423	476	899	28,4	355	299	295	0,30	0,34	0,05	0,05	0,98	963	30,5	225	112,0	27	-20	-20	26	7	-45	-5	0	0	**69**	**-12**	no risk
18	1,0	4,78	0,25	88,8	100	2,73	235	424	478	903	28,5	355	296	293	0,30	0,34	0,05	0,05	0,98	968	30,6	235	109,1	27	-20	-20	26	7	-45	-5	0	0	**66**	**-12**	no risk
19	1,0	4,79	0,25	88,8	100	2,75	245	426	479	905	28,6	355	294	290	0,31	0,34	0,05	0,05	0,98	971	30,7	245	106,8	27	-20	-20	26	7	-45	-5	0	0	**64**	**-12**	no risk
20	1,0	4,81	0,25	88,8	100	2,77	255	427	481	907	28,7	355	291	288	0,31	0,35	0,05	0,05	0,98	975	30,8	255	104,7	27	-20	-20	26	7	-45	-5	0	0	**62**	**-12**	no risk
21	1,0	4,82	0,25	88,8	100	2,79	265	428	482	910	28,8	355	289	286	0,31	0,35	0,05	0,05	0,98	978	30,9	265	102,7	27	-20	-20	26	7	-45	-5	0	0	**60**	**-12**	no risk
22	1,0	4,83	0,25	88,8	100	2,81	275	429	483	912	28,8	355	286	283	0,31	0,35	0,05	0,05	0,98	981	31,0	275	100,9	27	-20	-20	26	7	-45	-5	0	0	**58**	**-12**	no risk
23	1,0	4,85	0,25	88,8	100	2,83	285	430	485	915	28,9	355	284	281	0,32	0,36	0,05	0,05	0,98	985	31,2	285	98,6	27	-20	-20	26	7	-45	-5	0	0	**56**	**-12**	no risk
24	1,0	4,86	0,25	88,8	100	2,84	295	432	486	918	29,0	355	281	279	0,32	0,36	0,05	0,05	0,98	989	31,3	295	96,8	27	-20	-20	26	7	-45	-5	0	0	**54**	**-12**	no risk
25	1,0	4,87	0,25	88,8	100	2,85	300	432	487	919	29,1	355	280	277	0,32	0,36	0,05	0,05	0,98	990	31,3	300	95,9	27	-20	-20	26	7	-45	-5	0	0	**53**	**-12**	no risk

Table 5-24: **Fracture mechanics assessment for loading variant 2B-4 for component No. 2B (Axisymmetric top component (sliding plate and guide-rail))**

Assessment for σ_{Ed} = 0,25·f_y and T = -50 °C

Nr	σ_P	K_1	σ_{Ed}/f_y	σ_P	σ_S	a_0	t_1	$K_{1,P}$	$K_{1,S}$	$K_{1,ges}$	$K_{1,ges}$	$f_{y,nom}$	$f_y(t)$	σ_{gy}	L_r	ψ	ρ_1	ρ	k_{R6}	$K_{appl,d}$	$K_{appl,d}$	b_{eff}	ΔT_σ	$K_{V,nom}$	T_{KV}	T_{27J}	ΔT_{27J}	ΔT_R	T_{md}	ΔT_r	ΔT_ε	ΔT_{DCF}	T_{Ed}	T_{Rd}	$T_{Ed} \geq T_{Rd}$
	N/mm²	N/mm$^{3/2}$	[-]	N/mm²	N/mm²	mm	mm	N/mm$^{3/2}$	N/mm$^{3/2}$	N/mm$^{3/2}$	MPam$^{1/2}$	N/mm²	N/mm²	N/mm²	-	-	-	-	-	N/mm$^{3/2}$	MPam$^{1/2}$	mm	°C	J	°C	°C	°C	°C	°C	°C	°C	°C	°C	°C	
1	1,0	2,240	0,25	88,8	100	2,09	65	199	224	423	13,4	355	339	328	0,27	0,30	0,04	0,04	0,98	450	14,2	65	120,0	27	-20	-20	24	7	-45	-5	0	0	77	-14	no risk
2	1,0	2,237	0,25	88,8	100	2,16	75	199	224	422	13,4	355	336	327	0,27	0,31	0,04	0,04	0,98	449	14,2	75	120,0	27	-20	-20	25	7	-45	-5	0	0	77	-13	no risk
3	1,0	2,221	0,25	88,8	100	2,22	85	197	222	419	13,3	355	334	325	0,27	0,31	0,04	0,04	0,98	446	14,1	85	120,0	27	-20	-20	25	7	-45	-5	0	0	77	-13	no risk
4	1,0	2,319	0,25	88,8	100	2,28	95	206	232	438	13,8	355	331	323	0,27	0,31	0,04	0,04	0,98	466	14,7	95	120,0	27	-20	-20	25	7	-45	-5	0	0	77	-13	no risk
5	1,0	2,584	0,25	88,8	100	2,33	105	229	258	488	15,4	355	329	321	0,28	0,31	0,04	0,04	0,98	520	16,4	105	120,0	27	-20	-20	25	7	-45	-5	0	0	77	-13	no risk
6	1,0	2,848	0,25	88,8	100	2,37	115	253	285	537	17,0	355	326	320	0,28	0,31	0,04	0,04	0,98	573	18,1	115	120,0	27	-20	-20	26	7	-45	-5	0	0	77	-12	no risk
7	1,0	3,083	0,25	88,8	100	2,41	125	274	308	582	18,4	355	324	317	0,28	0,31	0,04	0,04	0,98	620	19,6	125	120,0	27	-20	-20	26	7	-45	-5	0	0	77	-12	no risk
8	1,0	3,258	0,25	88,8	100	2,45	135	289	326	615	19,4	355	321	315	0,28	0,32	0,04	0,04	0,98	656	20,7	135	120,0	27	-20	-20	26	7	-45	-5	0	0	77	-12	no risk
9	1,0	3,468	0,25	88,8	100	2,49	145	308	347	655	20,7	355	319	313	0,28	0,32	0,04	0,04	0,98	699	22,1	145	120,0	27	-20	-20	26	7	-45	-5	0	0	77	-12	no risk
10	1,0	3,665	0,25	88,8	100	2,52	155	325	367	692	21,9	355	316	311	0,29	0,32	0,04	0,04	0,98	739	23,4	155	120,0	27	-20	-20	26	7	-45	-5	0	0	77	-12	no risk
11	1,0	3,804	0,25	88,8	100	2,55	165	338	380	718	22,7	355	314	309	0,29	0,32	0,04	0,04	0,98	767	24,3	165	120,0	27	-20	-20	26	7	-45	-5	0	0	77	-12	no risk
12	1,0	3,847	0,25	88,8	100	2,58	175	341	385	726	23,0	355	311	307	0,29	0,33	0,04	0,04	0,98	776	24,5	175	120,0	27	-20	-20	26	7	-45	-5	0	0	77	-12	no risk
13	1,0	3,850	0,25	88,8	100	2,61	185	342	385	727	23,0	355	309	304	0,29	0,33	0,04	0,04	0,98	777	24,6	185	120,0	27	-20	-20	26	7	-45	-5	0	0	77	-12	no risk
14	1,0	3,755	0,25	88,8	100	2,64	195	333	376	709	22,4	355	306	302	0,29	0,33	0,04	0,04	0,98	758	24,0	195	120,0	27	-20	-20	26	7	-45	-5	0	0	77	-12	no risk
15	1,0	3,649	0,25	88,8	100	2,66	205	324	365	689	21,8	355	304	300	0,30	0,33	0,04	0,04	0,98	737	23,3	205	120,0	27	-20	-20	26	7	-45	-5	0	0	77	-12	no risk
16	1,0	3,583	0,25	88,8	100	2,69	215	318	358	676	21,4	355	301	297	0,30	0,34	0,05	0,05	0,98	725	22,9	215	120,0	27	-20	-20	26	7	-45	-5	0	0	77	-12	no risk
17	1,0	3,510	0,25	88,8	100	2,71	225	311	351	662	20,9	355	299	295	0,30	0,34	0,05	0,05	0,98	710	22,5	225	120,0	27	-20	-20	26	7	-45	-5	0	0	77	-12	no risk
18	1,0	3,492	0,25	88,8	100	2,73	235	310	349	659	20,8	355	296	293	0,30	0,34	0,05	0,05	0,98	707	22,4	235	120,0	27	-20	-20	26	7	-45	-5	0	0	77	-12	no risk
19	1,0	3,439	0,25	88,8	100	2,75	245	305	344	649	20,5	355	294	290	0,31	0,34	0,05	0,05	0,98	697	22,0	245	120,0	27	-20	-20	26	7	-45	-5	0	0	77	-12	no risk
20	1,0	3,447	0,25	88,8	100	2,77	255	306	345	651	20,6	355	291	288	0,31	0,35	0,05	0,05	0,98	699	22,1	255	120,0	27	-20	-20	26	7	-45	-5	0	0	77	-12	no risk
21	1,0	3,422	0,25	88,8	100	2,79	265	304	342	646	20,4	355	289	286	0,31	0,35	0,05	0,05	0,98	694	22,0	265	120,0	27	-20	-20	26	7	-45	-5	0	0	77	-12	no risk
22	1,0	3,398	0,25	88,8	100	2,81	275	302	340	641	20,3	355	286	283	0,31	0,35	0,05	0,05	0,98	690	21,8	275	120,0	27	-20	-20	26	7	-45	-5	0	0	77	-12	no risk
23	1,0	3,389	0,25	88,8	100	2,83	285	301	339	640	20,2	355	284	281	0,32	0,36	0,05	0,05	0,98	689	21,8	285	120,0	27	-20	-20	26	7	-45	-5	0	0	77	-12	no risk
24	1,0	3,371	0,25	88,8	100	2,84	295	299	337	636	20,1	355	281	279	0,32	0,36	0,05	0,05	0,98	685	21,7	295	120,0	27	-20	-20	26	7	-45	-5	0	0	77	-12	no risk
25	1,0	3,359	0,25	88,8	100	2,85	300	298	336	634	20,0	355	280	277	0,32	0,36	0,05	0,05	0,98	683	21,6	300	120,0	27	-20	-20	26	7	-45	-5	0	0	77	-12	no risk

Table 5-25: **Fracture mechanics assessment for loading variant 2B-5 for component No. 2B (Axisymmetric top component (sliding plate and guide-rail))**

Assessment for $\sigma_{Ed} = 0{,}75 \cdot f_y$ and T = -50 °C

Nr	σ_P	K_1	σ_{Ed}/f_y	σ_P	σ_S	a_0	t_1	$K_{1,P}$	$K_{1,S}$	$K_{1,ges}$	$K_{1,ges}$	$f_{y,nom}$	$f_y(t)$	σ_{gy}	L_r	ψ	ρ_1	ρ	k_{R6}	$K_{appl,d}$	$K_{appl,d}$	b_{eff}	ΔT_σ	$K_{V,nom}$	T_{KV}	T_{27J}	ΔT_{27J}	ΔT_R	T_{md}	ΔT_r	ΔT_ε	ΔT_{DCF}	T_{Ed}	T_{Rd}	$T_{Ed} \geq T_{Rd}$
	N/mm²	$N/mm^{3/2}$	[-]	N/mm²	N/mm²	mm	mm	$N/mm^{3/2}$	$N/mm^{3/2}$	$N/mm^{3/2}$	$MPam^{1/2}$	N/mm²	N/mm²	N/mm²	-	-	-	-	-	$N/mm^{3/2}$	$MPam^{1/2}$	mm	°C	J	°C	°C	°C	°C	°C	°C	°C	°C	°C	°C	
1	1,0	3,052	0,75	266,3	100	2,09	65	813	305	1118	35,3	355	339	328	0,81	0,30	0,04	0,04	0,87	1352	42,7	65	68,2	27	-20	-20	24	7	-45	-5	0	0	**25**	**-14**	no risk
2	1,0	2,991	0,75	266,3	100	2,16	75	796	299	1096	34,6	355	336	327	0,82	0,31	0,04	0,04	0,87	1325	41,9	75	68,3	27	-20	-20	25	7	-45	-5	0	0	**25**	**-13**	no risk
3	1,0	2,952	0,75	266,3	100	2,22	85	786	295	1081	34,2	355	334	325	0,82	0,31	0,04	0,04	0,87	1308	41,4	85	67,7	27	-20	-20	25	7	-45	-5	0	0	**25**	**-13**	no risk
4	1,0	2,924	0,75	266,3	100	2,28	95	778	292	1071	33,9	355	331	323	0,82	0,31	0,04	0,04	0,86	1297	41,0	95	66,9	27	-20	-20	25	7	-45	-5	0	0	**24**	**-13**	no risk
5	1,0	2,926	0,75	266,3	100	2,33	105	779	293	1072	33,9	355	329	321	0,83	0,31	0,04	0,04	0,86	1299	41,1	105	64,7	27	-20	-20	25	7	-45	-5	0	0	**22**	**-13**	no risk
6	1,0	2,931	0,75	266,3	100	2,37	115	780	293	1073	33,9	355	326	320	0,83	0,31	0,04	0,04	0,86	1302	41,2	115	62,6	27	-20	-20	26	7	-45	-5	0	0	**20**	**-12**	no risk
7	1,0	2,934	0,75	266,3	100	2,41	125	781	293	1075	34,0	355	324	317	0,84	0,31	0,04	0,04	0,86	1305	41,3	125	60,7	27	-20	-20	26	7	-45	-5	0	0	**18**	**-12**	no risk
8	1,0	2,932	0,75	266,3	100	2,45	135	781	293	1074	34,0	355	321	315	0,84	0,32	0,04	0,04	0,86	1305	41,3	135	59,2	27	-20	-20	26	7	-45	-5	0	0	**16**	**-12**	no risk
9	1,0	2,936	0,75	266,3	100	2,49	145	782	294	1075	34,0	355	319	313	0,85	0,32	0,04	0,03	0,86	1308	41,3	145	57,6	27	-20	-20	26	7	-45	-5	0	0	**15**	**-12**	no risk
10	1,0	2,942	0,75	266,3	100	2,52	155	783	294	1078	34,1	355	316	311	0,86	0,32	0,04	0,03	0,86	1312	41,5	155	55,9	27	-20	-20	26	7	-45	-5	0	0	**13**	**-12**	no risk
11	1,0	2,946	0,75	266,3	100	2,55	165	784	295	1079	34,1	355	314	309	0,86	0,32	0,04	0,03	0,85	1314	41,6	165	54,5	27	-20	-20	26	7	-45	-5	0	0	**11**	**-12**	no risk
12	1,0	2,949	0,75	266,3	100	2,58	175	785	295	1080	34,2	355	311	307	0,87	0,33	0,04	0,03	0,85	1317	41,7	175	53,1	27	-20	-20	26	7	-45	-5	0	0	**10**	**-12**	no risk
13	1,0	2,952	0,75	266,3	100	2,61	185	786	295	1081	34,2	355	309	304	0,87	0,33	0,04	0,03	0,85	1320	41,7	185	51,8	27	-20	-20	26	7	-45	-5	0	0	**9**	**-12**	no risk
14	1,0	2,953	0,75	266,3	100	2,64	195	786	295	1082	34,2	355	306	302	0,88	0,33	0,04	0,03	0,85	1321	41,8	195	50,7	27	-20	-20	26	7	-45	-5	0	0	**8**	**-12**	no risk
15	1,0	2,942	0,75	266,3	100	2,66	205	783	294	1077	34,1	355	304	300	0,89	0,33	0,04	0,03	0,85	1317	41,7	205	50,2	27	-20	-20	26	7	-45	-5	0	0	**7**	**-12**	no risk
16	1,0	2,878	0,75	266,3	100	2,69	215	766	288	1054	33,3	355	301	297	0,89	0,34	0,05	0,03	0,85	1290	40,8	215	52,3	27	-20	-20	26	7	-45	-5	0	0	**9**	**-12**	no risk
17	1,0	2,875	0,75	266,3	100	2,71	225	766	288	1053	33,3	355	299	295	0,90	0,34	0,05	0,03	0,84	1290	40,8	225	51,4	27	-20	-20	26	7	-45	-5	0	0	**8**	**-12**	no risk
18	1,0	2,879	0,75	266,3	100	2,73	235	767	288	1054	33,3	355	296	293	0,91	0,34	0,05	0,03	0,84	1293	40,9	235	50,4	27	-20	-20	26	7	-45	-5	0	0	**7**	**-12**	no risk
19	1,0	2,886	0,75	266,3	100	2,75	245	768	289	1057	33,4	355	294	290	0,92	0,34	0,05	0,02	0,84	1297	41,0	245	49,1	27	-20	-20	26	7	-45	-5	0	0	**6**	**-12**	no risk
20	1,0	2,881	0,75	266,3	100	2,77	255	767	288	1055	33,4	355	291	288	0,92	0,35	0,05	0,02	0,84	1296	41,0	255	48,5	27	-20	-20	26	7	-45	-5	0	0	**6**	**-12**	no risk
21	1,0	2,890	0,75	266,3	100	2,79	265	769	289	1058	33,5	355	289	286	0,93	0,35	0,05	0,02	0,84	1302	41,2	265	47,3	27	-20	-20	26	7	-45	-5	0	0	**4**	**-12**	no risk
22	1,0	2,893	0,75	266,3	100	2,81	275	770	289	1059	33,5	355	286	283	0,94	0,35	0,05	0,02	0,83	1304	41,2	275	46,4	27	-20	-20	26	7	-45	-5	0	0	**3**	**-12**	no risk
23	1,0	2,893	0,75	266,3	100	2,83	285	770	289	1059	33,5	355	284	281	0,95	0,36	0,05	0,02	0,83	1305	41,3	285	45,6	27	-20	-20	26	7	-45	-5	0	0	**3**	**-12**	no risk
24	1,0	2,893	0,75	266,3	100	2,84	295	770	289	1059	33,5	355	281	279	0,96	0,36	0,05	0,02	0,83	1307	41,3	295	44,9	27	-20	-20	26	7	-45	-5	0	0	**2**	**-12**	no risk
24	1,0	2,893	0,75	266,3	100	2,85	300	770	289	1059	33,5	355	280	277	0,96	0,36	0,05	0,02	0,83	1307	41,3	300	44,5	27	-20	-20	26	7	-45	-5	0	0	**2**	**-12**	no risk

Table 5-26: **Fracture mechanics assessment for loading variant 2B-6 for component No. 2B (Axisymmetric top component (sliding plate and guide-rail))**

Assessment for $\sigma_{Ed} = 0{,}75 \cdot f_y$ and T = -50 °C

Nr	σ_P	K_1	σ_{Ed}/f_y	σ_P	σ_S	a_0	t_1	$K_{1,P}$	$K_{1,S}$	$K_{1,ges}$	$K_{1,ges}$	$f_{y,nom}$	$f_y(t)$	σ_{gy}	L_r	ψ	ρ_1	ρ	k_{R6}	$K_{appl,d}$	$K_{appl,d}$	b_{eff}	ΔT_σ	$K_{V,nom}$	T_{KV}	T_{27J}	ΔT_{27J}	ΔT_R	T_{md}	ΔT_r	ΔT_ε	ΔT_{DCF}	T_{Ed}	T_{Rd}	$T_{Ed} \geq T_{Rd}$
	N/mm²	$N/mm^{3/2}$	[-]	N/mm²	N/mm²	mm	mm	$N/mm^{3/2}$	$N/mm^{3/2}$	$N/mm^{3/2}$	$MPam^{1/2}$	N/mm²	N/mm²	N/mm²	-	-	-	-	-	$N/mm^{3/2}$	$MPam^{1/2}$	mm	°C	J	°C	°C	°C	°C	°C	°C	°C	°C	°C	°C	
1	1,0	2,716	0,75	266,3	100	2,09	65	723	272	995	31,5	355	339	328	0,81	0,30	0,04	0,04	0,87	1203	38,0	65	88,0	27	-20	-20	24	7	-45	-5	0	0	**45**	**-14**	no risk
2	1,0	2,722	0,75	266,3	100	2,16	75	725	272	997	31,5	355	336	327	0,82	0,31	0,04	0,04	0,87	1206	38,1	75	84,2	27	-20	-20	25	7	-45	-5	0	0	**41**	**-13**	no risk
3	1,0	2,818	0,75	266,3	100	2,22	85	750	282	1032	32,6	355	334	325	0,82	0,31	0,04	0,04	0,87	1249	39,5	85	75,2	27	-20	-20	25	7	-45	-5	0	0	**32**	**-13**	no risk
4	1,0	2,826	0,75	266,3	100	2,28	95	752	283	1035	32,7	355	331	323	0,82	0,31	0,04	0,04	0,86	1254	39,6	95	72,3	27	-20	-20	25	7	-45	-5	0	0	**29**	**-13**	no risk
5	1,0	2,831	0,75	266,3	100	2,33	105	754	283	1037	32,8	355	329	321	0,83	0,31	0,04	0,04	0,86	1257	39,7	105	69,9	27	-20	-20	25	7	-45	-5	0	0	**27**	**-13**	no risk
6	1,0	2,836	0,75	266,3	100	2,37	115	755	284	1039	32,8	355	326	320	0,83	0,31	0,04	0,04	0,86	1260	39,8	115	67,6	27	-20	-20	26	7	-45	-5	0	0	**25**	**-12**	no risk
7	1,0	2,843	0,75	266,3	100	2,41	125	757	284	1041	32,9	355	324	317	0,84	0,31	0,04	0,04	0,86	1264	40,0	125	65,5	27	-20	-20	26	7	-45	-5	0	0	**22**	**-12**	no risk
8	1,0	2,846	0,75	266,3	100	2,45	135	758	285	1042	33,0	355	321	315	0,84	0,32	0,04	0,04	0,86	1266	40,0	135	63,7	27	-20	-20	26	7	-45	-5	0	0	**21**	**-12**	no risk
9	1,0	2,853	0,75	266,3	100	2,49	145	760	285	1045	33,0	355	319	313	0,85	0,32	0,04	0,03	0,86	1271	40,2	145	61,8	27	-20	-20	26	7	-45	-5	0	0	**19**	**-12**	no risk
10	1,0	2,860	0,75	266,3	100	2,52	155	761	286	1047	33,1	355	316	311	0,86	0,32	0,04	0,03	0,86	1275	40,3	155	60,1	27	-20	-20	26	7	-45	-5	0	0	**17**	**-12**	no risk
11	1,0	2,866	0,75	266,3	100	2,55	165	763	287	1050	33,2	355	314	309	0,86	0,32	0,04	0,03	0,85	1279	40,4	165	58,4	27	-20	-20	26	7	-45	-5	0	0	**15**	**-12**	no risk
12	1,0	2,871	0,75	266,3	100	2,58	175	764	287	1051	33,2	355	311	307	0,87	0,33	0,04	0,03	0,85	1282	40,5	175	56,9	27	-20	-20	26	7	-45	-5	0	0	**14**	**-12**	no risk
13	1,0	2,875	0,75	266,3	100	2,61	185	766	288	1053	33,3	355	309	304	0,87	0,33	0,04	0,03	0,85	1285	40,6	185	55,5	27	-20	-20	26	7	-45	-5	0	0	**13**	**-12**	no risk
14	1,0	2,878	0,75	266,3	100	2,64	195	766	288	1054	33,3	355	306	302	0,88	0,33	0,04	0,03	0,85	1288	40,7	195	54,3	27	-20	-20	26	7	-45	-5	0	0	**11**	**-12**	no risk
15	1,0	2,785	0,75	266,3	100	2,66	205	742	279	1020	32,3	355	304	300	0,89	0,33	0,04	0,03	0,85	1247	39,4	205	58,1	27	-20	-20	26	7	-45	-5	0	0	**15**	**-12**	no risk
16	1,0	2,792	0,75	266,3	100	2,69	215	743	279	1023	32,3	355	301	297	0,89	0,34	0,05	0,03	0,85	1252	39,6	215	56,7	27	-20	-20	26	7	-45	-5	0	0	**14**	**-12**	no risk
17	1,0	2,789	0,75	266,3	100	2,71	225	743	279	1021	32,3	355	299	295	0,90	0,34	0,05	0,03	0,84	1251	39,6	225	55,9	27	-20	-20	26	7	-45	-5	0	0	**13**	**-12**	no risk
18	1,0	2,790	0,75	266,3	100	2,73	235	743	279	1022	32,3	355	296	293	0,91	0,34	0,05	0,03	0,84	1253	39,6	235	54,9	27	-20	-20	26	7	-45	-5	0	0	**12**	**-12**	no risk
19	1,0	2,795	0,75	266,3	100	2,75	245	744	280	1024	32,4	355	294	290	0,92	0,34	0,05	0,02	0,84	1257	39,7	245	53,7	27	-20	-20	26	7	-45	-5	0	0	**11**	**-12**	no risk
20	1,0	2,791	0,75	266,3	100	2,77	255	743	279	1022	32,3	355	291	288	0,92	0,35	0,05	0,02	0,84	1256	39,7	255	53,1	27	-20	-20	26	7	-45	-5	0	0	**10**	**-12**	no risk
21	1,0	2,888	0,75	266,3	100	2,79	265	769	289	1058	33,4	355	289	286	0,93	0,35	0,05	0,02	0,84	1301	41,1	265	47,4	27	-20	-20	26	7	-45	-5	0	0	**4**	**-12**	no risk
22	1,0	2,887	0,75	266,3	100	2,81	275	769	289	1057	33,4	355	286	283	0,94	0,35	0,05	0,02	0,83	1302	41,2	275	46,7	27	-20	-20	26	7	-45	-5	0	0	**4**	**-12**	no risk
23	1,0	2,885	0,75	266,3	100	2,83	285	768	288	1057	33,4	355	284	281	0,95	0,36	0,05	0,02	0,83	1302	41,2	285	46,0	27	-20	-20	26	7	-45	-5	0	0	**3**	**-12**	no risk
24	1,0	2,887	0,75	266,3	100	2,84	295	769	289	1057	33,4	355	281	279	0,96	0,36	0,05	0,02	0,83	1304	41,2	295	45,2	27	-20	-20	26	7	-45	-5	0	0	**2**	**-12**	no risk
24	1,0	2,887	0,75	266,3	100	2,85	300	769	289	1057	33,4	355	280	277	0,96	0,36	0,05	0,02	0,83	1305	41,3	300	44,8	27	-20	-20	26	7	-45	-5	0	0	**2**	**-12**	no risk

5.5 Component No. 3 – Axisymmetric bottom component of bearing

5.5.1 Geometry, load assumptions and boundary conditions

(1) Component No. 3 is the axisymmetric bottom component of the bearing, see Figure 5-44.

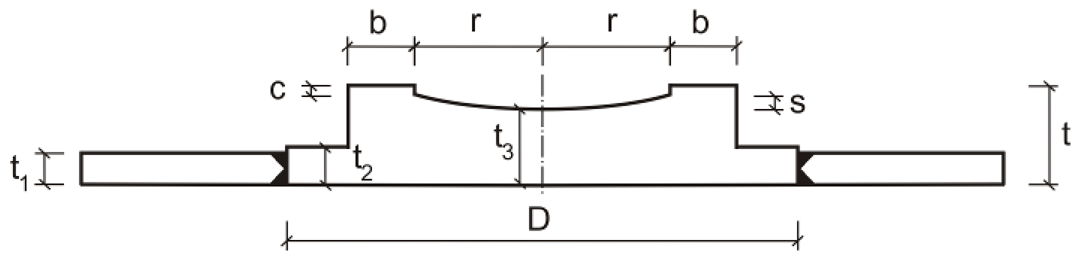

Figure 5-44: Component No. 3 – Axisymmetric bottom component of the bearing

(2) Table 5-27 gives the range of geometrical dimensions for component No. 3.

Table 5-27: Ranges of geometrical dimensions for Detail 3

t_1 [mm]	t_2 [mm]	t_3 [mm]	D [mm]	b [mm]	r [mm]
20 – 55	20 – 60	35 – 150	330 – 1800	40 – 100	135 - 590

(3) The fracture mechanics assessments are carried out for the loading variant 3-1 for a plate welded to the cylindrical part and for the loading variant 3-2 for the cylindrical part itself, see Figure 5-45.

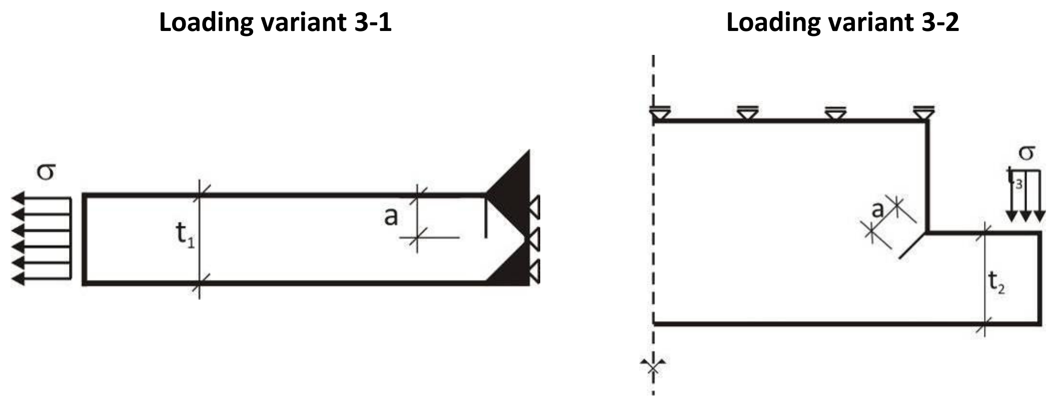

Figure 5-45: Loading variants for component No. 3: Loading variant 3-1: Horizontal loading (left), Loading variant 3-2: Vertical loading (right)

(4) For loading variant 3-1 the welded connection is detailed as a K-weld. The location for a potential crack initiation for this detail is the weld toe according to Figure 5-45 (left); the crack path is perpendicular to the plate surface. The hypothetical loading is horizontal (perpendicular to the crack), so that the external nominal stress load σ_N is equal to the unit loading.

(5) The loading variant 3-2 is applied to the proper bottom component. For simplicity reasons the cylindrical recess is not modelled. The crack will be applied according to Figure 5-45 (right) at the re-entrant corner with an angle of 45°, the depth of which is determined from the plate thickness t_2.

The loading in vertical direction as applied is not very realistic. The bottom component is loaded realistically by a horizontal loading component, which gives only small fracture mechanics requirements. Therefore the hypothetical vertical loading has been chosen, to create conservatively a significant tensile stress for the crack.

(6) The magnitude of the stress intensity factors for loading variant 3-1 depends only on the plate-thickness t_1. Therefore only a single configuration is studied.

For the loading variant 3-2 the investigations are carried out for two bounds of geometrical dimensions, see Table 5-28, taking account of the influence of the width b+r of the cylindrical part. For the upper bound of geometrical dimensions the maximum value b+r = 690 mm was used, for the lower bound the minimum value at the lower bound b+r = 175 mm was chosen. As a consequence of the choice of vertical loading and for achieving the maximum bending moment at the crack-location assumed the width of the bottom component D was fixed with the maximum value D = 1800 mm.

Table 5-28: Upper and lower bounds of the geometrical dimensions for loading variant 3-2

Upper bounds		Lower bounds	
t_2 [mm]	20 - 60	t_2 [mm]	20 - 60
t_3[mm]	150	t_3 [mm]	150
D [mm]	1800	D [mm]	1800
b + r [mm]	690	b + r [mm]	175

(7) Figure 5-46 shows a section of the plot of deformations and the crack opening for the loading variants 3-1 and 3-2 from the FE-model.

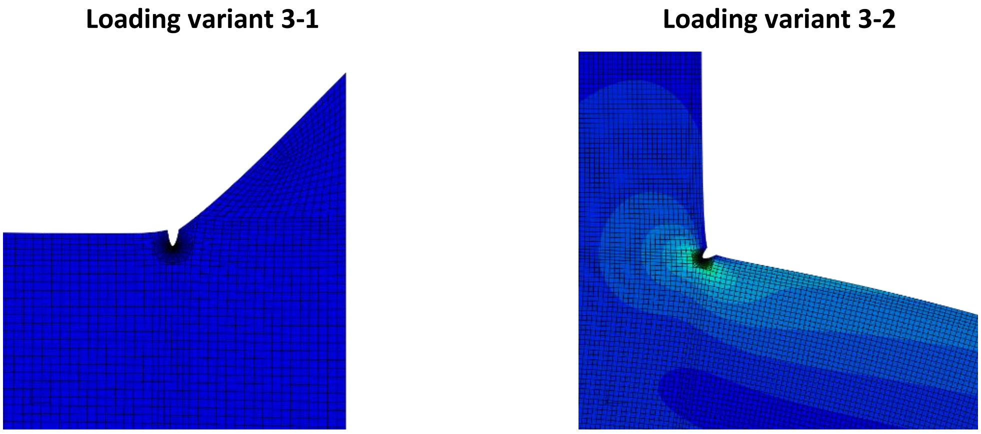

Figure 5-46: Section of plot with deformations and crack opening for loading variant 3-1: welded plate to the bottom component (left) and for loading variant 3-2: cylindrical part of the bottom component (right)

5.5.2 Hot-Spot stresses

(1) The stresses σ_{HS} necessary for the fracture mechanics assessment are calculated for loading variant 3-1 according to the bending theory.

(2) The nominal stress σ_{Ed} is equal to σ_{HS} and corresponds to the external stress loading applied to the FE-model.

(3) In Figure 5-47 (left) the distribution of the Hot-Spot-stresses for the upper bound of geometrical dimensions is shown for loading variant 3-2. There is a decrease of σ_{HS} converging to a small value.

Also the stress distribution as calculated from the bending theory is plotted, which is qualitatively analogous however yields about double the stresses rather than σ_{HS} for small values t_2. The evaluation and the performance of the fracture mechanics assessment therefore is made with the Hot-Spot-stresses.

(4) Figure 5-47 (right) shows the corresponding function of Hot-Spot-stresses for the loading variant 3-2 and the lower bound for geometrical dimensions.

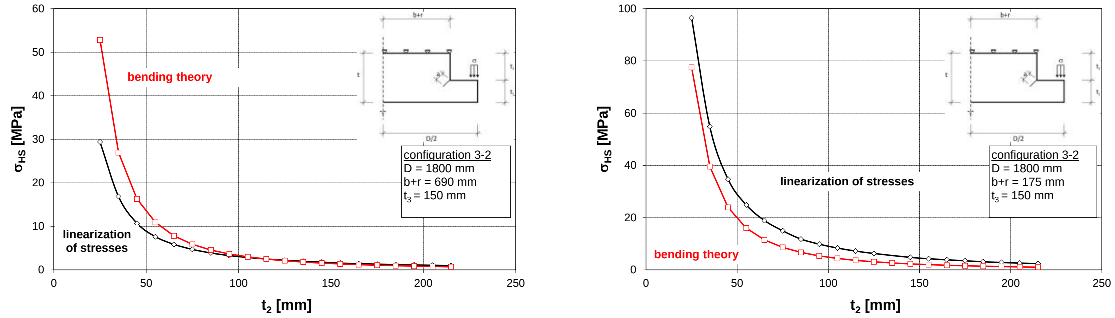

Figure 5-47: **Hot-Spot-stresses due to external unit loading for loading variant 3-2 - vertical loading; for upper bound of geometrical dimensions (left), for lower bound of geometrical dimensions (right)**

5.5.3 Stress-intensity factors

(1) The fracture mechanics investigations for <u>loading variant 3-1</u> were carried out up to a thickness of 200 mm.

(2) The trend from the calculations is that the stress-intensity factors K_1 increase with increasing plate thickness t_1 (and increasing crack depth a_0), see Figure 5-48 (left).

The crack depth for a plate with t = 10 mm is a_0 = 1,151 mm and for the maximum plate thickness (t = 100 mm) a_0 = 2,303 mm.

(3) Figure 5-48 (right) shows the reduction of the stress-intensity factors related to a constant load F_H with increasing plate thickness.

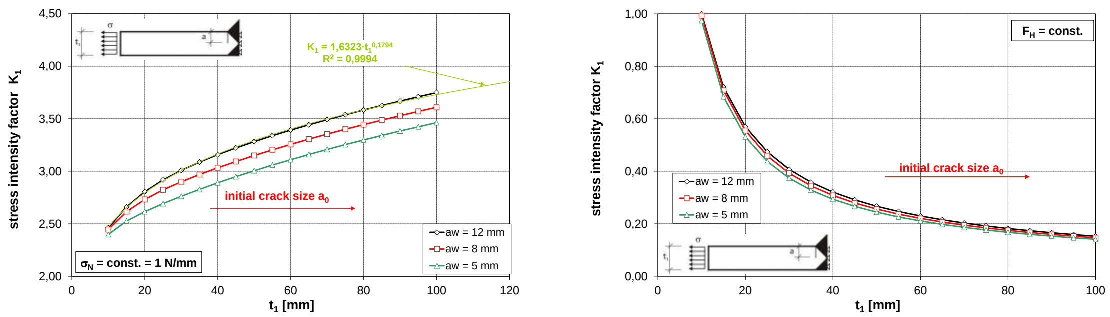

Figure 5-48: **K-values for detail 3-1 caused by an edge loading σ_N (t) = 1 N/mm (left); K-values related to a constant load F_H = const. (right)**

(4) In addition the influence of the throat thickness a_w was checked for three thicknesses a_w. Figure 5-48 (right) makes clear that larger throat thicknesses are more critical, however the influence is rather small. For the fracture mechanics assessments the largest throat thickness was used.

(5) For <u>loading variant 3-2</u> Figure 5-49 (left) shows the functions of the K-values for the upper bound and lower bound of the geometrical dimensions. The K_1-value decreases with increasing plate thickness t_2 and is converging to zero for very large plate-thicknesses.

The smaller the width b+r of the bottom component the larger is the stress-intensity factor.

The influence of mode 2-stresses can be neglected.

(6) The Figure 5-49 (right) gives the function of the normalized $\overline{K}$-values related to σ_{HS} = 1 N/mm² at the Hot-Spot. Apparently the relevant case for the fracture mechanics assessment is the case of lower bound of geometrical dimensions.

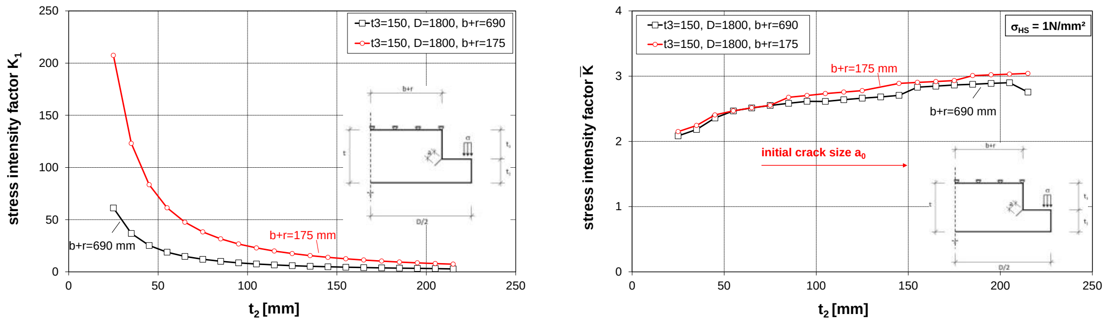

Figure 5-49: **K-values for the loading variant 3-2 with variation of the plate thickness t_2; K-values for the unit-loading (left), $\overline{K}$-values related to σ_{HS}= 1 N/mm² at the Hot-Spot (right)**

(7) Figure 5-50 gives the effects of a variation of the thickness t_3 of the bottom component of the bearing. The K-value is not influenced by t_3. The relevant parameter for variation is the plate thickness t_2 as presented in Figure 5-49.

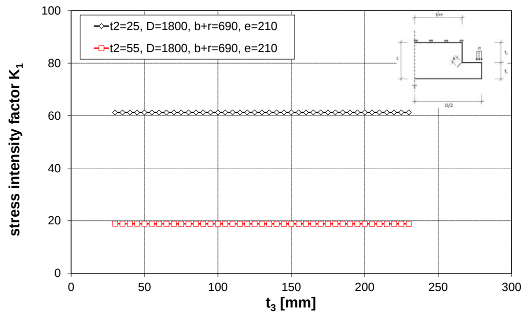

Figure 5-50: **K-values for the loading variant 3-2: variation of the plate thickness t_3; K-values due to unit loading**

5.5.4 Assessments to avoid brittle fracture

(1) The assessments to avoid brittle fracture are carried out for loading variant 3-1 in Table 5-31 and for loading variant 3-2 in Table 5-32.

(2) The results for which examples of the tabular calculations are given in Table 5-31 and Table 5-32 are presented in Table 5-29 and Table 5-30.

Table 5-29: **Limits of plate thickness [mm] for the bottom component of the bearing (loading variant 3-1)**

Steel grade acc. to EN 10025	σ_{Ed}	0°C	-10°C	-20°C	-30°C	-40°C	-50°C
S355J2	$0{,}25 \cdot f_y$	250*)	250*)	250*)	250*)	250*)	250*)
S355J2	$0{,}50 \cdot f_y$	250*)	250*)	250*)	250*)	250*)	250*)
S355J2	$0{,}75 \cdot f_y$	250*)	250*)	250*)	200	140	110

*) *Assumption of a technical manufacturing limit (in theory element thicknesses with t ≥ 250 mm would be acceptable)*

Table 5-30: Limits of plate thickness [mm] for the bottom component of the bearing (loading variant 3-2)

Steel grade acc. to EN 10025	σ_{Ed}	0°C	-10°C	-20°C	-30°C	-40°C	-50°C
S355J2	$0{,}25 \cdot f_y$	200*)	200*)	200*)	200*)	200*)	200*)
S355J2	$0{,}50 \cdot f_y$	200*)	200*)	200*)	200*)	200*)	200*)
S355J2	$0{,}75 \cdot f_y$	200*)	200*)	200*)	200*)	200*)	200*)

*) *Assumption of a technical manufacturing limit (in theory element thicknesses with t ≥ 200 mm would be acceptable)*

Table 5-31: Fracture mechanics assessment for loading variant 3-1 for component No. 3

Assessment for $\sigma_{Ed} = 0{,}75 \cdot f_y$ and T = -30 °C

Nr	σ_P	K_1	σ_{Ed}/f_y	σ_P	σ_S	a_0	t_1	$K_{1,P}$	$K_{1,S}$	$K_{1,ges}$	$K_{1,ges}$	$f_{y,nom}$	$f_y(t)$	σ_{gy}	L_r	ψ	ρ_1	ρ	k_{R6}	$K_{appl,d}$	$K_{appl,d}$	b_{eff}	ΔT_σ	$K_{V,nom}$	T_{KV}	T_{27J}	ΔT_{27J}	ΔT_R	T_{md}	ΔT_r	ΔT_ε	ΔT_{DCF}	T_{Ed}	T_{Rd}	$T_{Ed} \geq T_{Rd}$
	N/mm²	$N/mm^{3/2}$	[-]	N/mm²	N/mm²	mm	mm	$N/mm^{3/2}$	$N/mm^{3/2}$	$N/mm^{3/2}$	$MPam^{1/2}$	N/mm²	N/mm²	N/mm²	-	-	-	-	-	$N/mm^{3/2}$	$MPam^{1/2}$	mm	°C	J	°C	°C	°C	°C	°C	°C	°C	°C	°C	°C	
1	1,0	2,462	0,75	266,3	100	1,15	10	656	246	902	28,5	355	353	312	0,85	0,32	0,04	0,03	0,86	1097	34,7	10	120,0	27	-20	-20	0	7	-25	-5	0	0	97	-38	no risk
2	1,0	2,661	0,75	266,3	100	1,35	15	708	266	975	30,8	355	351	320	0,83	0,31	0,04	0,04	0,86	1182	37,4	15	120,0	27	-20	-20	1	7	-25	-5	0	0	97	-37	no risk
3	1,0	2,805	0,75	266,3	100	1,50	20	747	281	1027	32,5	355	350	324	0,82	0,31	0,04	0,04	0,86	1244	39,3	20	110,9	27	-20	-20	2	7	-25	-5	0	0	88	-36	no risk
4	1,0	2,917	0,75	266,3	100	1,61	25	777	292	1068	33,8	355	349	326	0,82	0,31	0,04	0,04	0,87	1293	40,9	25	96,8	27	-20	-20	5	7	-25	-5	0	0	74	-33	no risk
5	1,0	3,008	0,75	266,3	100	1,70	30	801	301	1102	34,8	355	348	328	0,81	0,31	0,04	0,04	0,87	1332	42,1	30	86,9	27	-20	-20	8	7	-25	-5	0	0	64	-30	no risk
6	1,0	3,087	0,75	266,3	100	1,78	35	822	309	1131	35,8	355	346	329	0,81	0,30	0,04	0,04	0,87	1367	43,2	35	79,2	27	-20	-20	12	7	-25	-5	0	0	56	-26	no risk
7	1,0	3,158	0,75	266,3	100	1,84	40	841	316	1157	36,6	355	345	329	0,81	0,30	0,04	0,04	0,87	1398	44,2	40	72,9	27	-20	-20	16	7	-25	-5	0	0	50	-22	no risk
8	1,0	3,222	0,75	266,3	100	1,90	45	858	322	1180	37,3	355	344	329	0,81	0,30	0,04	0,04	0,87	1426	45,1	45	67,6	27	-20	-20	19	7	-25	-5	0	0	45	-19	no risk
9	1,0	3,282	0,75	266,3	100	1,96	50	874	328	1202	38,0	355	343	329	0,81	0,30	0,04	0,04	0,87	1453	45,9	50	63,0	27	-20	-20	21	7	-25	-5	0	0	40	-17	no risk
10	1,0	3,339	0,75	266,3	100	2,00	55	889	334	1223	38,7	355	341	329	0,81	0,30	0,04	0,04	0,87	1478	46,7	55	58,9	27	-20	-20	22	7	-25	-5	0	0	36	-16	no risk
11	1,0	3,392	0,75	266,3	100	2,05	60	903	339	1242	39,3	355	340	328	0,81	0,30	0,04	0,04	0,87	1502	47,5	60	55,2	27	-20	-20	23	7	-25	-5	0	0	32	-15	no risk
12	1,0	3,442	0,75	266,3	100	2,09	65	916	344	1261	39,9	355	339	328	0,81	0,30	0,04	0,04	0,87	1524	48,2	65	51,9	27	-20	-20	24	7	-25	-5	0	0	29	-14	no risk
13	1,0	3,491	0,75	266,3	100	2,12	70	929	349	1279	40,4	355	338	327	0,81	0,31	0,04	0,04	0,87	1546	48,9	70	48,8	27	-20	-20	24	7	-25	-5	0	0	26	-14	no risk
14	1,0	3,538	0,75	266,3	100	2,16	75	942	354	1296	41,0	355	336	327	0,82	0,31	0,04	0,04	0,87	1568	49,6	75	46,0	27	-20	-20	25	7	-25	-5	0	0	23	-13	no risk
15	1,0	3,583	0,75	266,3	100	2,19	80	954	358	1312	41,5	355	335	326	0,82	0,31	0,04	0,04	0,87	1588	50,2	80	43,3	27	-20	-20	25	7	-25	-5	0	0	20	-13	no risk
16	1,0	3,626	0,75	266,3	100	2,22	85	965	363	1328	42,0	355	334	325	0,82	0,31	0,04	0,04	0,87	1608	50,8	85	40,9	27	-20	-20	25	7	-25	-5	0	0	18	-13	no risk
17	1,0	3,668	0,75	266,3	100	2,25	90	977	367	1343	42,5	355	333	324	0,82	0,31	0,04	0,04	0,86	1627	51,4	90	38,6	27	-20	-20	25	7	-25	-5	0	0	16	-13	no risk
18	1,0	3,709	0,75	266,3	100	2,28	95	988	371	1358	43,0	355	331	323	0,82	0,31	0,04	0,04	0,86	1645	52,0	95	36,5	27	-20	-20	25	7	-25	-5	0	0	13	-13	no risk
19	1,0	3,749	0,75	266,3	100	2,30	100	998	375	1373	43,4	355	330	322	0,83	0,31	0,04	0,04	0,86	1664	52,6	100	34,4	27	-20	-20	25	7	-25	-5	0	0	11	-13	no risk
20	1,0	4,223	0,75	266,3	100	2,65	200	1124	422	1547	48,9	355	305	301	0,88	0,33	0,04	0,03	0,85	1890	59,8	200	10,8	27	-20	-20	26	7	-25	-5	0	0	-12	-12	no risk

Assessment for $\sigma_{Ed} = 0{,}75 \cdot f_y$ and T = -40 °C

Nr	σ_P	K_1	σ_{Ed}/f_y	σ_P	σ_S	a_0	t_1	$K_{1,P}$	$K_{1,S}$	$K_{1,ges}$	$K_{1,ges}$	$f_{y,nom}$	$f_y(t)$	σ_{gy}	L_r	ψ	ρ_1	ρ	k_{R6}	$K_{appl,d}$	$K_{appl,d}$	b_{eff}	ΔT_σ	$K_{V,nom}$	T_{KV}	T_{27J}	ΔT_{27J}	ΔT_R	T_{md}	ΔT_r	ΔT_ε	ΔT_{DCF}	T_{Ed}	T_{Rd}	$T_{Ed} \geq T_{Rd}$
	N/mm²	$N/mm^{3/2}$	[-]	N/mm²	N/mm²	mm	mm	$N/mm^{3/2}$	$N/mm^{3/2}$	$N/mm^{3/2}$	$MPam^{1/2}$	N/mm²	N/mm²	N/mm²	-	-	-	-	-	$N/mm^{3/2}$	$MPam^{1/2}$	mm	°C	J	°C	°C	°C	°C	°C	°C	°C	°C	°C	°C	
1	1,0	2,462	0,75	266,3	100	1,15	10	656	246	902	28,5	355	353	312	0,85	0,32	0,04	0,03	0,86	1097	34,7	10	120,0	27	-20	-20	0	7	-35	-5	0	0	87	-38	no risk
2	1,0	2,661	0,75	266,3	100	1,35	15	708	266	975	30,8	355	351	320	0,83	0,31	0,04	0,04	0,86	1182	37,4	15	120,0	27	-20	-20	1	7	-35	-5	0	0	87	-37	no risk
3	1,0	2,805	0,75	266,3	100	1,50	20	747	281	1027	32,5	355	350	324	0,82	0,31	0,04	0,04	0,86	1244	39,3	20	110,9	27	-20	-20	2	7	-35	-5	0	0	78	-36	no risk
4	1,0	2,917	0,75	266,3	100	1,61	25	777	292	1068	33,8	355	349	326	0,82	0,31	0,04	0,04	0,87	1293	40,9	25	96,8	27	-20	-20	5	7	-35	-5	0	0	64	-33	no risk
5	1,0	3,008	0,75	266,3	100	1,70	30	801	301	1102	34,8	355	348	328	0,81	0,31	0,04	0,04	0,87	1332	42,1	30	86,9	27	-20	-20	8	7	-35	-5	0	0	54	-30	no risk
6	1,0	3,087	0,75	266,3	100	1,78	35	822	309	1131	35,8	355	346	329	0,81	0,30	0,04	0,04	0,87	1367	43,2	35	79,2	27	-20	-20	12	7	-35	-5	0	0	46	-26	no risk
7	1,0	3,158	0,75	266,3	100	1,84	40	841	316	1157	36,6	355	345	329	0,81	0,30	0,04	0,04	0,87	1398	44,2	40	72,9	27	-20	-20	16	7	-35	-5	0	0	40	-22	no risk
8	1,0	3,222	0,75	266,3	100	1,90	45	858	322	1180	37,3	355	344	329	0,81	0,30	0,04	0,04	0,87	1426	45,1	45	67,6	27	-20	-20	19	7	-35	-5	0	0	35	-19	no risk
9	1,0	3,282	0,75	266,3	100	1,96	50	874	328	1202	38,0	355	343	329	0,81	0,30	0,04	0,04	0,87	1453	45,9	50	63,0	27	-20	-20	21	7	-35	-5	0	0	30	-17	no risk
10	1,0	3,339	0,75	266,3	100	2,00	55	889	334	1223	38,7	355	341	329	0,81	0,30	0,04	0,04	0,87	1478	46,7	55	58,9	27	-20	-20	22	7	-35	-5	0	0	26	-16	no risk
11	1,0	3,392	0,75	266,3	100	2,05	60	903	339	1242	39,3	355	340	328	0,81	0,30	0,04	0,04	0,87	1502	47,5	60	55,2	27	-20	-20	23	7	-35	-5	0	0	22	-15	no risk
12	1,0	3,442	0,75	266,3	100	2,09	65	916	344	1261	39,9	355	339	328	0,81	0,30	0,04	0,04	0,87	1524	48,2	65	51,9	27	-20	-20	24	7	-35	-5	0	0	19	-14	no risk
13	1,0	3,491	0,75	266,3	100	2,12	70	929	349	1279	40,4	355	338	327	0,81	0,31	0,04	0,04	0,87	1546	48,9	70	48,8	27	-20	-20	24	7	-35	-5	0	0	16	-14	no risk
14	1,0	3,538	0,75	266,3	100	2,16	75	942	354	1296	41,0	355	336	327	0,82	0,31	0,04	0,04	0,87	1568	49,6	75	46,0	27	-20	-20	25	7	-35	-5	0	0	13	-13	no risk
15	1,0	3,583	0,75	266,3	100	2,19	80	954	358	1312	41,5	355	335	326	0,82	0,31	0,04	0,04	0,87	1588	50,2	80	43,3	27	-20	-20	25	7	-35	-5	0	0	10	-13	no risk
16	1,0	3,626	0,75	266,3	100	2,22	85	965	363	1328	42,0	355	334	325	0,82	0,31	0,04	0,04	0,87	1608	50,8	85	40,9	27	-20	-20	25	7	-35	-5	0	0	8	-13	no risk
17	1,0	3,668	0,75	266,3	100	2,25	90	977	367	1343	42,5	355	333	324	0,82	0,31	0,04	0,04	0,86	1627	51,4	90	38,6	27	-20	-20	25	7	-35	-5	0	0	6	-13	no risk
18	1,0	3,709	0,75	266,3	100	2,28	95	988	371	1358	43,0	355	331	323	0,82	0,31	0,04	0,04	0,86	1645	52,0	95	36,5	27	-20	-20	25	7	-35	-5	0	0	3	-13	no risk
19	1,0	3,749	0,75	266,3	100	2,30	100	998	375	1373	43,4	355	330	322	0,83	0,31	0,04	0,04	0,86	1664	52,6	100	34,4	27	-20	-20	25	7	-35	-5	0	0	1	-13	no risk
20	1,0	3,961	0,75	266,3	100	2,47	140	1055	396	1451	45,9	355	320	314	0,85	0,32	0,04	0,04	0,86	1764	55,8	140	22,9	27	-20	-20	26	7	-35	-5	0	0	-10	-12	no risk

Table 5-31: Continued

Assessment for $\sigma_{Ed} = 0,75 \cdot f_y$ and $T = -50$ °C

Nr	σ_P N/mm²	K_1 N/mm$^{3/2}$	σ_{Ed}/f_y [-]	σ_P N/mm²	σ_S N/mm²	a_0 mm	t_1 mm	$K_{1,P}$ N/mm$^{3/2}$	$K_{1,S}$ N/mm$^{3/2}$	$K_{1,ges}$ N/mm$^{3/2}$	$K_{1,ges}$ MPam$^{1/2}$	$f_{y,nom}$ N/mm²	$f_y(t)$ N/mm²	σ_{gy} N/mm²	L_r -	ψ -	ρ_1 -	ρ -	k_{R6} -	$K_{appl,d}$ N/mm$^{3/2}$	$K_{appl,d}$ MPam$^{1/2}$	b_{eff} mm	ΔT_σ °C	$K_{V,nom}$ J	T_{KV} °C	T_{27J} °C	ΔT_{27J} °C	ΔT_R °C	T_{md} °C	ΔT_r °C	ΔT_ε °C	ΔT_{DCF} °C	T_{Ed} °C	T_{Rd} °C	$T_{Ed} \geq T_{Rd}$
1	1,0	2,462	0,75	266,3	100	1,15	10	656	246	902	28,5	355	353	312	0,85	0,32	0,04	0,03	0,86	1097	34,7	10	120,0	27	-20	-20	0	7	-45	-5	0	0	77	-38	no risk
2	1,0	2,661	0,75	266,3	100	1,35	15	708	266	975	30,8	355	351	320	0,83	0,31	0,04	0,04	0,86	1182	37,4	15	120,0	27	-20	-20	1	7	-45	-5	0	0	77	-37	no risk
3	1,0	2,805	0,75	266,3	100	1,50	20	747	281	1027	32,5	355	350	324	0,82	0,31	0,04	0,04	0,86	1244	39,3	20	110,9	27	-20	-20	2	7	-45	-5	0	0	68	-36	no risk
4	1,0	2,917	0,75	266,3	100	1,61	25	777	292	1068	33,8	355	349	326	0,82	0,31	0,04	0,04	0,87	1293	40,9	25	96,8	27	-20	-20	5	7	-45	-5	0	0	54	-33	no risk
5	1,0	3,008	0,75	266,3	100	1,70	30	801	301	1102	34,8	355	348	328	0,81	0,31	0,04	0,04	0,87	1332	42,1	30	86,9	27	-20	-20	8	7	-45	-5	0	0	44	-30	no risk
6	1,0	3,087	0,75	266,3	100	1,78	35	822	309	1131	35,8	355	346	329	0,81	0,30	0,04	0,04	0,87	1367	43,2	35	79,2	27	-20	-20	12	7	-45	-5	0	0	36	-26	no risk
7	1,0	3,158	0,75	266,3	100	1,84	40	841	316	1157	36,6	355	345	329	0,81	0,30	0,04	0,04	0,87	1398	44,2	40	72,9	27	-20	-20	16	7	-45	-5	0	0	30	-22	no risk
8	1,0	3,222	0,75	266,3	100	1,90	45	858	322	1180	37,3	355	344	329	0,81	0,30	0,04	0,04	0,87	1426	45,1	45	67,6	27	-20	-20	19	7	-45	-5	0	0	25	-19	no risk
9	1,0	3,282	0,75	266,3	100	1,96	50	874	328	1202	38,0	355	343	329	0,81	0,30	0,04	0,04	0,87	1453	45,9	50	63,0	27	-20	-20	21	7	-45	-5	0	0	20	-17	no risk
10	1,0	3,339	0,75	266,3	100	2,00	55	889	334	1223	38,7	355	341	329	0,81	0,30	0,04	0,04	0,87	1478	46,7	55	58,9	27	-20	-20	22	7	-45	-5	0	0	16	-16	no risk
11	1,0	3,392	0,75	266,3	100	2,05	60	903	339	1242	39,3	355	340	328	0,81	0,30	0,04	0,04	0,87	1502	47,5	60	55,2	27	-20	-20	23	7	-45	-5	0	0	12	-15	no risk
12	1,0	3,442	0,75	266,3	100	2,09	65	916	344	1261	39,9	355	339	328	0,81	0,30	0,04	0,04	0,87	1524	48,2	65	51,9	27	-20	-20	24	7	-45	-5	0	0	9	-14	no risk
13	1,0	3,491	0,75	266,3	100	2,12	70	929	349	1279	40,4	355	338	327	0,81	0,31	0,04	0,04	0,87	1546	48,9	70	48,8	27	-20	-20	24	7	-45	-5	0	0	6	-14	no risk
14	1,0	3,538	0,75	266,3	100	2,16	75	942	354	1296	41,0	355	336	327	0,82	0,31	0,04	0,04	0,87	1568	49,6	75	46,0	27	-20	-20	25	7	-45	-5	0	0	3	-13	no risk
15	1,0	3,583	0,75	266,3	100	2,19	80	954	358	1312	41,5	355	335	326	0,82	0,31	0,04	0,04	0,87	1588	50,2	80	43,3	27	-20	-20	25	7	-45	-5	0	0	0	-13	no risk
16	1,0	3,626	0,75	266,3	100	2,22	85	965	363	1328	42,0	355	334	325	0,82	0,31	0,04	0,04	0,87	1608	50,8	85	40,9	27	-20	-20	25	7	-45	-5	0	0	-2	-13	no risk
17	1,0	3,668	0,75	266,3	100	2,25	90	977	367	1343	42,5	355	333	324	0,82	0,31	0,04	0,04	0,86	1627	51,4	90	38,6	27	-20	-20	25	7	-45	-5	0	0	-4	-13	no risk
18	1,0	3,709	0,75	266,3	100	2,28	95	988	371	1358	43,0	355	331	323	0,82	0,31	0,04	0,04	0,86	1645	52,0	95	36,5	27	-20	-20	25	7	-45	-5	0	0	-7	-13	no risk
19	1,0	3,749	0,75	266,3	100	2,30	100	998	375	1373	43,4	355	330	322	0,83	0,31	0,04	0,04	0,86	1664	52,6	100	34,4	27	-20	-20	25	7	-45	-5	0	0	-9	-13	no risk
20	1,0	3,793	0,75	266,3	100	2,35	110	1010	379	1389	43,9	355	328	321	0,83	0,31	0,04	0,04	0,86	1685	53,3	110	31,5	27	-20	-20	25	7	-45	-5	0	0	-11	-13	no risk

Table 5-32: Fracture mechanics assessment for loading variant 3-2 for component No. 3

Assessment for σ_{Ed} = 0,75·f_y and T = -50 °C

Nr	σ_P	K_1	σ_{Ed}/f_y	σ_P	σ_S	a_0	t_1	$K_{1,P}$	$K_{1,S}$	$K_{1,ges}$	$K_{1,ges}$	$f_{y,nom}$	$f_y(t)$	σ_{gy}	L_r	ψ	ρ_1	ρ	k_{R6}	$K_{appl,d}$	$K_{appl,d}$	b_{eff}	ΔT_σ	$K_{V,nom}$	T_{KV}	T_{27J}	ΔT_{27J}	ΔT_R	T_{md}	ΔT_r	ΔT_ε	ΔT_{DCF}	T_{Ed}	T_{Rd}	$T_{Ed} \geq T_{Rd}$
	N/mm²	N/mm$^{3/2}$	[-]	N/mm²	N/mm²	mm	mm	N/mm$^{3/2}$	N/mm$^{3/2}$	N/mm$^{3/2}$	MPam$^{1/2}$	N/mm²	N/mm²	N/mm²	-	-	-	-	-	N/mm$^{3/2}$	MPam$^{1/2}$	mm	°C	J	°C	°C	°C	°C	°C	°C	°C	°C	°C	°C	
1	1,0	2,149	0,75	266,3	100	1,61	25	572	215	787	24,9	355	349	326	0,82	0,31	0,04	0,04	0,87	952	30,1	25	120,0	27	-20	-20	5	7	-45	-5	0	0	**77**	**-33**	no risk
2	1,0	2,244	0,75	266,3	100	1,78	35	598	224	822	26,0	355	346	329	0,81	0,30	0,04	0,04	0,87	994	31,4	35	120,0	27	-20	-20	12	7	-45	-5	0	0	**77**	**-26**	no risk
3	1,0	2,406	0,75	266,3	100	1,90	45	641	241	881	27,9	355	344	329	0,81	0,30	0,04	0,04	0,87	1065	33,7	45	120,0	27	-20	-20	19	7	-45	-5	0	0	**77**	**-19**	no risk
4	1,0	2,468	0,75	266,3	100	2,00	55	657	247	904	28,6	355	341	329	0,81	0,30	0,04	0,04	0,87	1093	34,6	55	114,6	27	-20	-20	22	7	-45	-5	0	0	**72**	**-16**	no risk
5	1,0	2,515	0,75	266,3	100	2,09	65	670	252	921	29,1	355	339	328	0,81	0,30	0,04	0,04	0,87	1114	35,2	65	104,8	27	-20	-20	24	7	-45	-5	0	0	**62**	**-14**	no risk
6	1,0	2,553	0,75	266,3	100	2,16	75	680	255	935	29,6	355	336	327	0,82	0,31	0,04	0,04	0,87	1131	35,8	75	97,4	27	-20	-20	25	7	-45	-5	0	0	**54**	**-13**	no risk
7	1,0	2,676	0,75	266,3	100	2,22	85	712	268	980	31,0	355	334	325	0,82	0,31	0,04	0,04	0,87	1186	37,5	85	84,5	27	-20	-20	25	7	-45	-5	0	0	**42**	**-13**	no risk
8	1,0	2,703	0,75	266,3	100	2,28	95	720	270	990	31,3	355	331	323	0,82	0,31	0,04	0,04	0,86	1199	37,9	95	80,0	27	-20	-20	25	7	-45	-5	0	0	**37**	**-13**	no risk
9	1,0	2,733	0,75	266,3	100	2,33	105	728	273	1001	31,7	355	329	321	0,83	0,31	0,04	0,04	0,86	1213	38,4	105	75,8	27	-20	-20	25	7	-45	-5	0	0	**33**	**-13**	no risk
10	1,0	2,756	0,75	266,3	100	2,37	115	734	276	1009	31,9	355	326	320	0,83	0,31	0,04	0,04	0,86	1224	38,7	115	72,3	27	-20	-20	26	7	-45	-5	0	0	**29**	**-12**	no risk
11	1,0	2,778	0,75	266,3	100	2,41	125	740	278	1018	32,2	355	324	317	0,84	0,31	0,04	0,04	0,86	1235	39,1	125	69,2	27	-20	-20	26	7	-45	-5	0	0	**26**	**-12**	no risk
12	1,0	2,830	0,75	266,3	100	2,45	135	753	283	1036	32,8	355	321	315	0,84	0,32	0,04	0,04	0,86	1259	39,8	135	64,6	27	-20	-20	26	7	-45	-5	0	0	**22**	**-12**	no risk
13	1,0	2,889	0,75	266,3	100	2,49	145	769	289	1058	33,5	355	319	313	0,85	0,32	0,04	0,03	0,86	1287	40,7	145	59,9	27	-20	-20	26	7	-45	-5	0	0	**17**	**-12**	no risk
14	1,0	2,904	0,75	266,3	100	2,52	155	773	290	1064	33,6	355	316	311	0,86	0,32	0,04	0,03	0,86	1295	40,9	155	57,8	27	-20	-20	26	7	-45	-5	0	0	**15**	**-12**	no risk
15	1,0	2,917	0,75	266,3	100	2,55	165	777	292	1069	33,8	355	314	309	0,86	0,32	0,04	0,03	0,85	1302	41,2	165	55,8	27	-20	-20	26	7	-45	-5	0	0	**13**	**-12**	no risk
16	1,0	2,932	0,75	266,3	100	2,58	175	781	293	1074	34,0	355	311	307	0,87	0,33	0,04	0,03	0,85	1310	41,4	175	53,9	27	-20	-20	26	7	-45	-5	0	0	**11**	**-12**	no risk
17	1,0	3,009	0,75	266,3	100	2,61	185	801	301	1102	34,8	355	309	304	0,87	0,33	0,04	0,03	0,85	1345	42,5	185	49,2	27	-20	-20	26	7	-45	-5	0	0	**6**	**-12**	no risk
18	1,0	3,021	0,75	266,3	100	2,64	195	804	302	1106	35,0	355	306	302	0,88	0,33	0,04	0,03	0,85	1352	42,7	195	47,6	27	-20	-20	26	7	-45	-5	0	0	**5**	**-12**	no risk
19	1,0	3,031	0,75	266,3	100	2,66	205	807	303	1110	35,1	355	304	300	0,89	0,33	0,04	0,03	0,85	1358	42,9	205	46,2	27	-20	-20	26	7	-45	-5	0	0	**3**	**-12**	no risk
20	1,0	3,042	0,75	266,3	100	2,69	215	810	304	1114	35,2	355	301	297	0,89	0,34	0,05	0,03	0,85	1363	43,1	215	44,8	27	-20	-20	26	7	-45	-5	0	0	**2**	**-12**	no risk

5.6 Component No. 4 – Axisymmetric anchor plate

5.6.1 Geometry, load assumptions and boundary conditions

(1) The anchor plate is axis-symmetrical, Figure 5-51. It is the basement for the bottom component of the bearing and is usually connected to it by bolting.

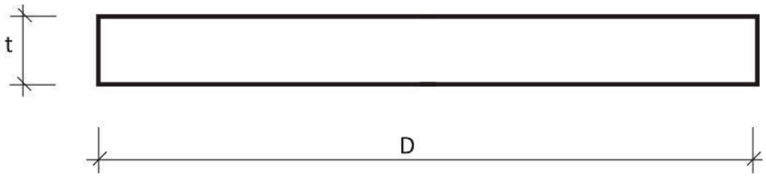

Figure 5-51: Component No. 4. Anchor plate with axial symmetry

(2) Table 5-33 gives the ranges for geometrical dimensions on which the investigations were based.

Table 5-33: Ranges of geometrical dimensions

t [mm]	D [mm]
≥ 55	440 - 3300

(3) The bolt holes are the potential Hot-Spots for the occurrence of crack-like flaws from fabrication. However for the assessment to avoid brittle fracture a more conservative fracture mechanics model according to Figure 5-25 is used, which has a vertical continuous surface crack with the depth a(t) perpendicular to the stresses.

As the anchor plate is mainly stressed by compression from the bearing and by horizontal forces, a stress σ_{Ed} constant over the thickness of the plate is taken as a representative loading.

The crack position on the plate surface has no influence on the magnitude of the K-values and therefore is only controlled by the assumption for σ_{Ed}. The crack depth is dependent on the plate thickness t.

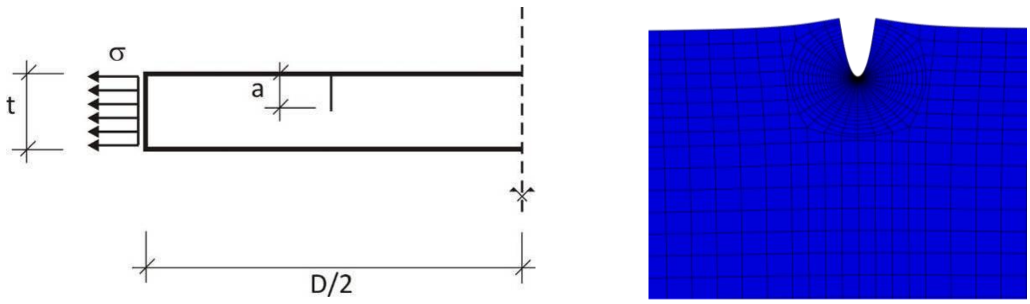

Figure 5-52: Boundary conditions for the FE-model for component No. 4; anchor plate (left) and section from the FE-model with opened crack under tension (right)

5.6.2 Hot-Spot-stresses

(1) The calculation of the stresses σ_{Ed} for component No. 4 are carried out according to the bending theory.

(2) The “nominal” stresses σ_{Ed} are equal to the stresses used as loading in the FE-model.

5.6.3 Stress intensity factors

(1) The ranges of dimensions for the anchor plate include a standard thickness t = 75 mm and a width of 440-3300 mm.

(2) Figure 5-53 (left) shows the results of the fracture mechanics calculations for a unit loading σ = 1 N/mm² constant over the plate thickness.

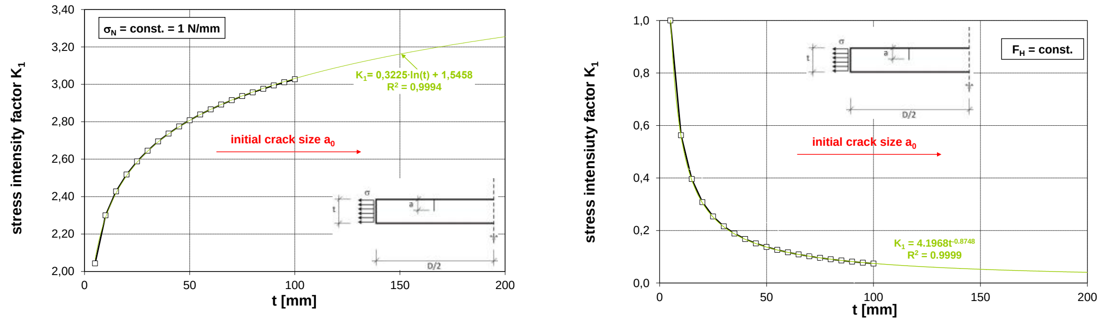

Figure 5-53: K-values for component No. 4 due to the nominal stress $\sigma_N(t)$ = 1 N/mm (left) K-values related to a constant load F_H = const. (right)

(3) As expected, the stress intensity factors increase with increasing plate thickness due to the increasing force and the increasing initial crack depth a_0.

The crack depth would be a_0 = 0,805 mm for the smallest theoretical plate thickness t = 5 mm and a_0 = 2,303 mm for the largest plate thickness (t = 100 mm). The plate width D does not influence the magnitude of the stress intensity factors in the fracture mechanics model selected.

(4) Figure 5-53 (right) shows the K-values related to a constant horizontal load F_H.

5.6.4 Assessments to avoid brittle fracture

(1) The assessments are carried in a tabular way in Table 5-35.

(2) The results are summarized in Table 5-34.

Table 5-34: Limits of plate thickness [mm] for the component “anchor plate”

Steel grade acc. to EN 10025	σ_{Ed}	0°C	-10°C	-20°C	-30°C	-40°C	-50°C
S355J2	$0{,}25 \cdot f_y$	250*)	250*)	250*)	250*)	250*)	250*)
S355J2	$0{,}50 \cdot f_y$	250*)	250*)	250*)	250*)	250*)	250*)
S355J2	$0{,}75 \cdot f_y$	250*)	250*)	250*)	250*)	250*)	250*)

**) Assumption of a technical manufacturing limit (in theory element thicknesses with t ≥ 250 mm would be acceptable)*

Table 5-35: Fracture mechanics assessments for component No. 4

Assessment for $\sigma_{Ed} = 0,75 \cdot f_y$ and T = -50 °C

Nr	σ_P	K_1	σ_{Ed}/f_y	σ_P	σ_S	a_0	t_1	$K_{1,P}$	$K_{1,S}$	$K_{1,ges}$	$K_{1,ges}$	$f_{y,nom}$	$f_y(t)$	σ_{gy}	L_r	ψ	ρ_1	ρ	k_{R6}	$K_{appl,d}$	$K_{appl,d}$	b_{eff}	ΔT_σ	$K_{V,nom}$	T_{KV}	T_{27J}	ΔT_{27J}	ΔT_R	T_{md}	ΔT_r	ΔT_ε	ΔT_{DCF}	T_{Ed}	T_{Rd}	$T_{Ed} \geq T_{Rd}$
	N/mm²	$N/mm^{3/2}$	[-]	N/mm²	N/mm²	mm	mm	$N/mm^{3/2}$	$N/mm^{3/2}$	$N/mm^{3/2}$	$MPam^{1/2}$	N/mm²	N/mm²	N/mm²	-	-	-	-	-	$N/mm^{3/2}$	$MPam^{1/2}$	mm	°C	J	°C	°C	°C	°C	°C	°C	°C	°C	°C	°C	
1	1,0	2,043	0,75	266,3	100	0,80	5	544	204	748	23,7	355	354	297	0,90	0,34	0,05	0,03	0,84	916	29,0	5	120,0	27	-20	-20	0	7	-45	-5	0	0	**77**	**-38**	no risk
2	1,0	2,300	0,75	266,3	100	1,15	10	612	230	842	26,6	355	353	312	0,85	0,32	0,04	0,03	0,86	1025	32,4	10	120,0	27	-20	-20	0	7	-45	-5	0	0	**77**	**-38**	no risk
3	1,0	2,428	0,75	266,3	100	1,35	15	646	243	889	28,1	355	351	320	0,83	0,31	0,04	0,04	0,86	1079	34,1	15	120,0	27	-20	-20	1	7	-45	-5	0	0	**77**	**-37**	no risk
4	1,0	2,518	0,75	266,3	100	1,50	20	670	252	922	29,2	355	350	324	0,82	0,31	0,04	0,04	0,86	1117	35,3	20	120,0	27	-20	-20	2	7	-45	-5	0	0	**77**	**-36**	no risk
5	1,0	2,588	0,75	266,3	100	1,61	25	689	259	948	30,0	355	349	326	0,82	0,31	0,04	0,04	0,87	1147	36,3	25	120,0	27	-20	-20	5	7	-45	-5	0	0	**77**	**-33**	no risk
6	1,0	2,645	0,75	266,3	100	1,70	30	704	265	969	30,6	355	348	328	0,81	0,31	0,04	0,04	0,87	1171	37,0	30	113,9	27	-20	-20	8	7	-45	-5	0	0	**71**	**-30**	no risk
7	1,0	2,695	0,75	266,3	100	1,78	35	718	270	987	31,2	355	346	329	0,81	0,30	0,04	0,04	0,87	1193	37,7	35	105,0	27	-20	-20	12	7	-45	-5	0	0	**62**	**-26**	no risk
8	1,0	2,737	0,75	266,3	100	1,84	40	729	274	1002	31,7	355	345	329	0,81	0,30	0,04	0,04	0,87	1211	38,3	40	98,2	27	-20	-20	16	7	-45	-5	0	0	**55**	**-22**	no risk
9	1,0	2,775	0,75	266,3	100	1,90	45	739	278	1016	32,1	355	344	329	0,81	0,30	0,04	0,04	0,87	1228	38,8	45	92,5	27	-20	-20	19	7	-45	-5	0	0	**49**	**-19**	no risk
10	1,0	2,808	0,75	266,3	100	1,96	50	748	281	1028	32,5	355	343	329	0,81	0,30	0,04	0,04	0,87	1243	39,3	50	87,7	27	-20	-20	21	7	-45	-5	0	0	**45**	**-17**	no risk
11	1,0	2,839	0,75	266,3	100	2,00	55	756	284	1040	32,9	355	341	329	0,81	0,30	0,04	0,04	0,87	1257	39,7	55	83,5	27	-20	-20	22	7	-45	-5	0	0	**41**	**-16**	no risk
12	1,0	2,866	0,75	266,3	100	2,05	60	763	287	1050	33,2	355	340	328	0,81	0,30	0,04	0,04	0,87	1269	40,1	60	79,9	27	-20	-20	23	7	-45	-5	0	0	**37**	**-15**	no risk
13	1,0	2,892	0,75	266,3	100	2,09	65	770	289	1059	33,5	355	339	328	0,81	0,30	0,04	0,04	0,87	1281	40,5	65	76,7	27	-20	-20	24	7	-45	-5	0	0	**34**	**-14**	no risk
14	1,0	2,915	0,75	266,3	100	2,12	70	776	292	1068	33,8	355	338	327	0,81	0,31	0,04	0,04	0,87	1291	40,8	70	73,8	27	-20	-20	24	7	-45	-5	0	0	**31**	**-14**	no risk
15	1,0	2,937	0,75	266,3	100	2,16	75	782	294	1076	34,0	355	336	327	0,82	0,31	0,04	0,04	0,87	1301	41,1	75	71,1	27	-20	-20	25	7	-45	-5	0	0	**28**	**-13**	no risk
16	1,0	2,957	0,75	266,3	100	2,19	80	787	296	1083	34,2	355	335	326	0,82	0,31	0,04	0,04	0,87	1311	41,4	80	68,7	27	-20	-20	25	7	-45	-5	0	0	**26**	**-13**	no risk
17	1,0	2,976	0,75	266,3	100	2,22	85	792	298	1090	34,5	355	334	325	0,82	0,31	0,04	0,04	0,87	1319	41,7	85	66,5	27	-20	-20	25	7	-45	-5	0	0	**23**	**-13**	no risk
18	1,0	2,994	0,75	266,3	100	2,25	90	797	299	1097	34,7	355	333	324	0,82	0,31	0,04	0,04	0,86	1328	42,0	90	64,4	27	-20	-20	25	7	-45	-5	0	0	**21**	**-13**	no risk
19	1,0	3,011	0,75	266,3	100	2,28	95	802	301	1103	34,9	355	331	323	0,82	0,31	0,04	0,04	0,86	1336	42,2	95	62,5	27	-20	-20	25	7	-45	-5	0	0	**19**	**-13**	no risk
20	1,0	3,027	0,75	266,3	100	2,30	100	806	303	1109	35,1	355	330	322	0,83	0,31	0,04	0,04	0,86	1343	42,5	100	60,7	27	-20	-20	25	7	-45	-5	0	0	**18**	**-13**	no risk
21	1,0	3,326	0,75	266,3	100	2,30	250	886	333	1218	38,5	355	293	290	0,92	0,35	0,05	0,02	0,84	1496	47,3	250	31,0	27	-20	-20	26	7	-45	-5	0	0	**-12**	**-12**	no risk

5.7 Component No. 5 – Bearing for horizontal forces without rotation and capacity for vertical forces

5.7.1 Geometry, load assumptions and boundary conditions

(1) A particular investigation was made for bearings for horizontal forces only as sketched in Figure 5-54. This bearing does not provide rotation capacities.

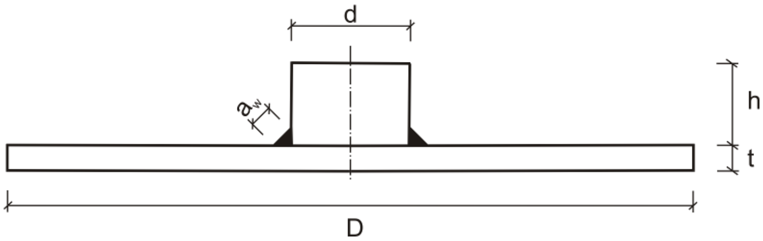

Figure 5-54: Component No. 5. – Bearing for horizontal forces without rotation and capacity for vertical forces

(2) The component consists of a cylindrical pin, which is welded to a plate with the thickness t.

(3) Table 5-36 gives the range of geometrical dimensions for component No. 5. The length of the cylinder does not play an important role in the fracture mechanics checks.

Table 5-36: Ranges of geometrical dimensions for Detail 5

t [mm]	D [mm]	d [mm]	a_w [mm]
30 – 150	440 - 3300	55 – 300	5 - 25

(4) For the fracture mechanics models the hypothetical loading and crack-scenarios according to Figure 5-55 are selected. The boundary conditions were selected such, that the stress intensity factors were high and also the deformation conditions of the bearings did not deviate too much from realistic conditions after installation.

(5) For the loading variant 5-1 the crack occurs at the weld toe at the plate surface; it receives a pure mode 1 stressing.

(6) The loading variant 5-2 considers a crack at the weld toe at the cylinder that is stressed also in bending.

Loading variant 5-1 **Loading variant 5-2**

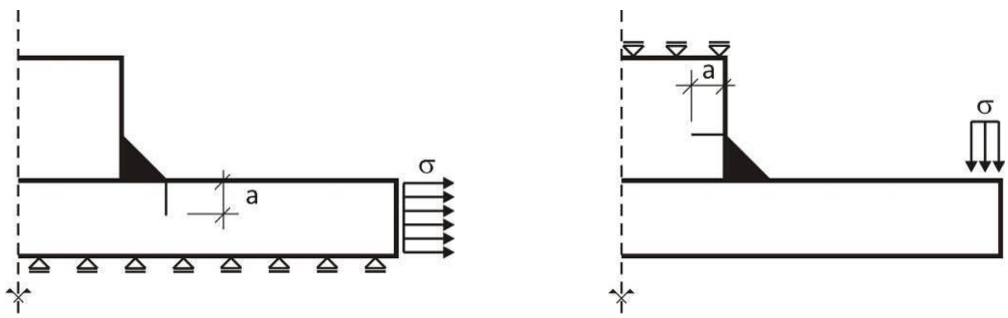

Figure 5-55: Loading variants for component No. 5; loading variant 5-1: horizontal loading (left), loading variant 5-2: vertical loading (right)

(7) For loading variant 5-1 the plate thickness t is of relevant importance. Therefor only a single configuration is investigated.

For the loading variant 5-2 two configurations with different geometrical dimensions are checked: a cylinder with the maximum diameter d = 300 mm and with a minimum diameter d = 55 mm.

The length of the cylinder h as well as the width D of the plate of the bearing were kept constant.

Table 5-37: Upper and lower bounds of the geometrical dimensions used for loading variant 5-2

Upper bounds		Lower bounds	
t [mm]	30-150	t [mm]	30 - 150
D [mm]	3300	D [mm]	3300
d [mm]	300	d [mm]	50
h [mm]	100	h [mm]	100
a_w [mm]	25	a_w [mm]	25

(8) Figure 5-56 shows a section from the FE-models with deformations and crack opening for the loading variants 5-1 and 5-2.

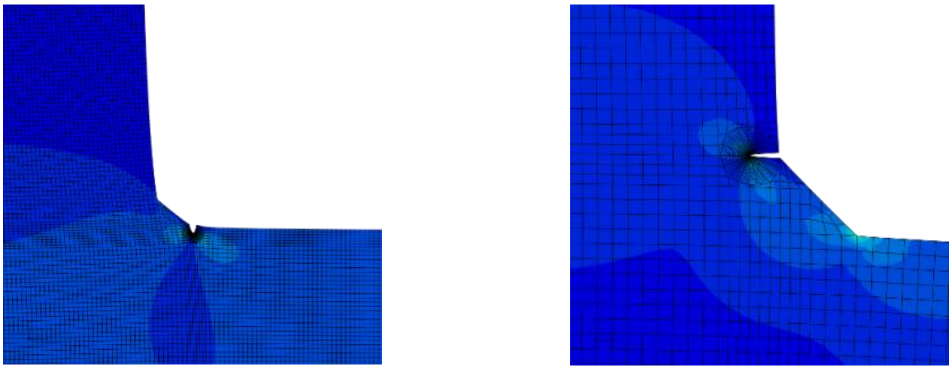

Figure 5-56: Sections from the FE-model with deformations and crack opening: for loading variant 5-1 with horizontal loading (left) and for loading variant 5-2 with vertical loading (right)

5.7.2 Hot-Spot-stresses

(1) The calculation of the reference stresses σ_{HS} necessary for the assessment to avoid brittle fracture is performed for loading variant 5-1 according to the bending theory.

The nominal stress σ_{Ed} are identical with the loading applied in the FE-model.

(2) Figure 5-57 (left) gives for loading variant 5-2 the distribution of the Hot-Spot-stresses versus the plate thickness t for the upper bound of the geometrical dimensions. The Hot-Spot-stresses decrease with increasing plate thickness t.

The Hot-Spot-stresses are larger for smaller plate thicknesses t and for welds with a_w = 5 mm larger than those for welds with a_w = 25 mm.

For larger values of plate thickness t the difference between the Hot-Spot-stresses for a_w = 5 mm and a_w = 25 mm gets smaller.

(3) Figure 5-57 (right) shows an identical behaviour of the Hot-spot-stresses with variation of the plate thickness for the lower bound of the geometrical dimensions. For t > 100 mm the Hot-spot-stress does not vary anymore.

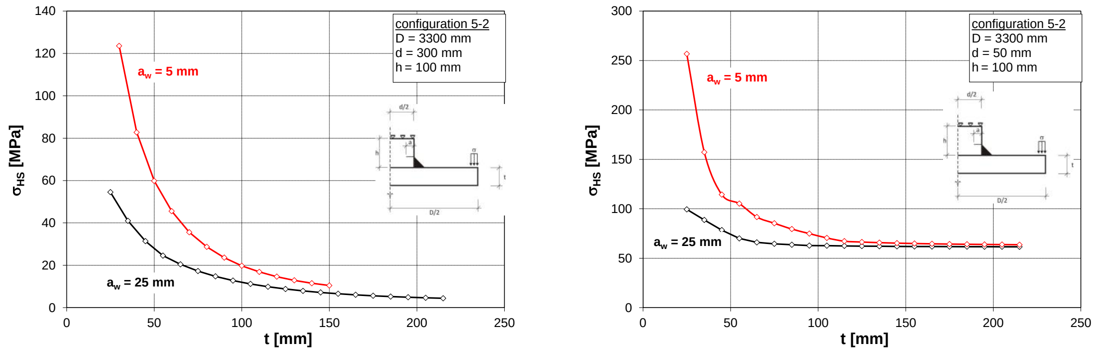

Figure 5-57: **Hot-Spot-stresses due to external unit loading for the loading variant 5-2: for upper bound of geometrical dimensions (left), for lower bound of geometrical dimensions (right)**

5.7.3 Stress intensity factors

(1) Figure 5-58 (left) shows for the <u>loading variant 5-1</u> the increase of the stress intensity factor K_1 when the plate thickness t and hence the crack depth a_0 is increased, all for the unit loading σ_N = 1 N/mm².

(2) The crack depths a_0 are in the range of 1,701 mm to 2,505 mm.

The plate width D, the height h and the diameter d of the cylinder have no significant influence on K_1.

(3) The Figure 5-58 (right) shows the minor influence of the throat thickness a_w on K_1. The calculations were performed with the maximum values a_w.

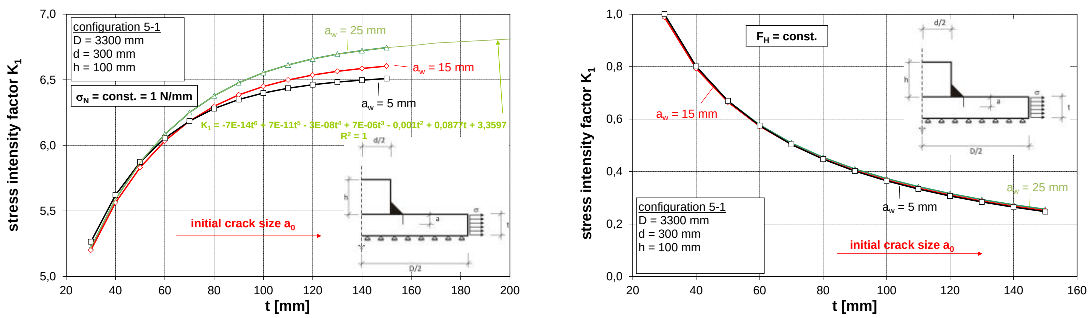

Figure 5-58: **K-values for the loading variant 5-1 for a unit loading σ_N (t) = 1 N/mm (left) and K-values related to a constant horizontal load F_H (right)**

(4) For <u>loading variant 5-2</u> Figure 5-59 (left) indicates the decrease of K with increasing plate thickness for the upper bound of the geometrical dimensions.

The mode 2 stresses lead to effective K_{eff}-values which are a bit larger than the K_1-values due to mode 1 stresses. For small weld sizes a_w the K-values get larger.

(5) Figure 5-59 (right) gives the normalized $\overline{K}$-values, however with the relevant values for large throat thicknesses. The $\overline{K}$-values increase with increasing plate thicknesses t.

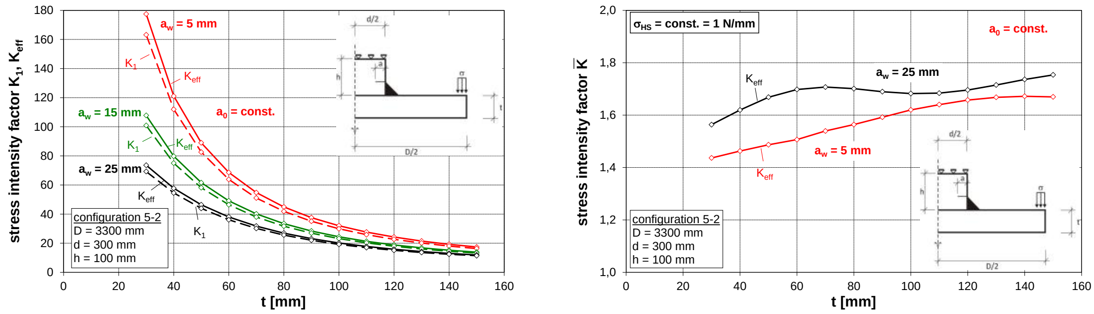

Figure 5-59: **K-values for the loading variant 5-2 for variation of plate thickness t and upper bound of geometrical dimensions. K-values due to unit loading (left), normalized $\overline{K}$-values related to σ_{HS} = 1 N/mm² (right)**

(6) For the lower bound of geometrical dimensions the function of K-values is similar as the one in Figure 5-60 (left). As derived for the upper bound of the geometrical dimensions the K-values get relevant for large weld sizes. The magnitude of K-values for the lower bound is significantly larger.

(7) In Figure 5-60 (right) the $\overline{K}$-values and also $\overline{K}_{eff}$-values normalized for σ_{HS} = 1 N/mm² are given; there is an increase of $\overline{K}$-values with larger t-values.

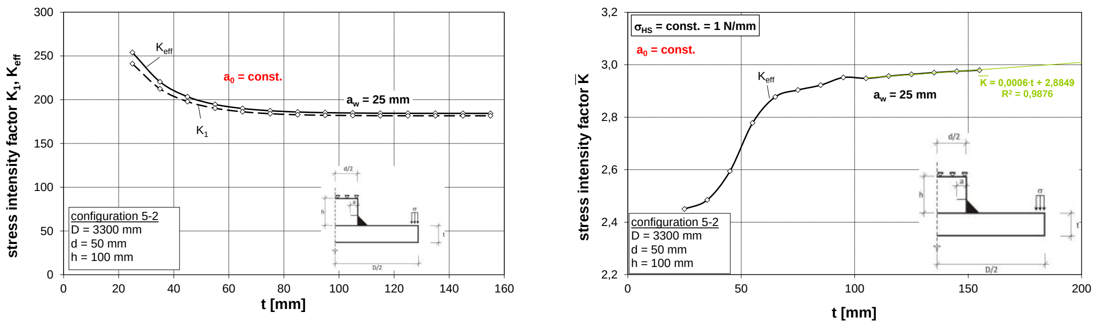

Figure 5-60: **K-values for the loading variant 5-2 for variation of plate thickness t and lower bound of geometrical dimensions. K-values for unit loading (left), normalized $\overline{K}$-values related to σ_{HS} = 1 N/mm² (right)**

5.7.4 Assessments to avoid brittle fracture

(1) The fracture-mechanics assessment are carried out for component No. 5 – Bearing for horizontal forces – for loading variant 5-1 in Table 5-40 and for loading variant 5-2 in Table 5-41.

(2) The results of the calculations are given in Table 5-38 and Table 5-39

Table 5-38: **Limits of plate thickness for the component No. 5 for loading variant 5-1**

Steel grade acc. to EN 10025	σ_{Ed}	0°C	-10°C	-20°C	-30°C	-40°C	-50°C
S355J2	$0{,}25 \cdot f_y$	250*)	250*)	250*)	250*)	250*)	250*)
S355J2	$0{,}50 \cdot f_y$	250*)	250*)	180	110	80	60
S355J2	$0{,}75 \cdot f_y$	120	80	60	40	40	30

*) *Assumption of a technical manufacturing limit (in theory element thicknesses with t ≥ 250 mm would be acceptable)*

Table 5-39: Limits of plate thickness for the component No. 5 for loading variant 5-2

Steel grade acc. to EN 10025	σ_{Ed}	0°C	-10°C	-20°C	-30°C	-40°C	-50°C
S355J2	$0,25 \cdot f_y$	200*)	200*)	200*)	200*)	200*)	200*)
S355J2	$0,50 \cdot f_y$	200*)	200*)	200*)	200*)	200*)	200*)
S355J2	$0,75 \cdot f_y$	200*)	200*)	200*)	200*)	200*)	200*)

**) Assumption of a technical manufacturing limit (in theory element thicknesses with t ≥ 200 mm would be acceptable)*

Table 5-40: Fracture mechanics assessment for the component No. 5 for loading variant 5-1

Assessment for $\sigma_{Ed} = 0{,}75 \cdot f_y$ and $T = 0$ °C

Nr	σ_P	K_1	σ_{Ed}/f_y	σ_P	σ_S	a_0	t_1	$K_{1,P}$	$K_{1,S}$	$K_{1,ges}$	$K_{1,ges}$	$f_{y,nom}$	$f_y(t)$	σ_{gy}	L_r	ψ	ρ_1	ρ	k_{R6}	$K_{appl,d}$	$K_{appl,d}$	b_{eff}	ΔT_σ	$K_{V,nom}$	T_{KV}	T_{27J}	ΔT_{27J}	ΔT_R	T_{md}	ΔT_r	ΔT_ε	ΔT_{DCF}	T_{Ed}	T_{Rd}	$T_{Ed} \geq T_{Rd}$
	N/mm²	$N/mm^{3/2}$	[-]	N/mm²	N/mm²	mm	mm	$N/mm^{3/2}$	$N/mm^{3/2}$	$N/mm^{3/2}$	$MPam^{1/2}$	N/mm²	N/mm²	N/mm²	-	-	-	-	-	$N/mm^{3/2}$	$MPam^{1/2}$	mm	°C	J	°C	°C	°C	°C	°C	°C	°C	°C	°C	°C	
1	1,0	5,220	0,75	266,3	100	1,70	30	1390	522	1912	60,5	355	348	328	0,81	0,31	0,04	0,04	0,87	2312	73,1	30	22,3	27	-20	-20	8	7	5	-5	0	0	29	-30	no risk
2	1,0	5,590	0,75	266,3	100	1,84	40	1488	559	2047	64,7	355	345	329	0,81	0,30	0,04	0,04	0,87	2474	78,2	40	12,1	27	-20	-20	16	7	5	-5	0	0	19	-22	no risk
3	1,0	5,870	0,75	266,3	100	1,96	50	1563	587	2150	68,0	355	343	329	0,81	0,30	0,04	0,04	0,87	2598	82,2	50	4,7	27	-20	-20	21	7	5	-5	0	0	12	-17	no risk
4	1,0	6,084	0,75	266,3	100	2,05	60	1620	608	2228	70,5	355	340	328	0,81	0,30	0,04	0,04	0,87	2694	85,2	60	-0,8	27	-20	-20	23	7	5	-5	0	0	6	-15	no risk
5	1,0	6,250	0,75	266,3	100	2,12	70	1664	625	2289	72,4	355	338	327	0,81	0,31	0,04	0,04	0,87	2768	87,5	70	-5,2	27	-20	-20	24	7	5	-5	0	0	2	-14	no risk
6	1,0	6,378	0,75	266,3	100	2,19	80	1698	638	2336	73,9	355	335	326	0,82	0,31	0,04	0,04	0,87	2827	89,4	80	-8,7	27	-20	-20	25	7	5	-5	0	0	-2	-13	no risk
7	1,0	6,477	0,75	266,3	100	2,25	90	1725	648	2372	75,0	355	333	324	0,82	0,31	0,04	0,04	0,86	2872	90,8	90	-11,6	27	-20	-20	25	7	5	-5	0	0	-5	-13	no risk
8	1,0	6,554	0,75	266,3	100	2,30	100	1745	655	2400	75,9	355	330	322	0,83	0,31	0,04	0,04	0,86	2909	92,0	100	-14,1	27	-20	-20	25	7	5	-5	0	0	-7	-13	no risk
9	1,0	6,613	0,75	266,3	100	2,35	110	1761	661	2422	76,6	355	328	321	0,83	0,31	0,04	0,04	0,86	2937	92,9	110	-16,2	27	-20	-20	25	7	5	-5	0	0	-9	-13	no risk
10	1,0	6,659	0,75	266,3	100	2,39	120	1773	666	2439	77,1	355	325	319	0,84	0,31	0,04	0,04	0,86	2960	93,6	120	-18,0	27	-20	-20	26	7	5	-5	0	0	-11	-12	no risk
11	1,0	6,695	0,75	266,3	100	2,43	130	1783	670	2452	77,5	355	323	316	0,84	0,32	0,04	0,04	0,86	2978	94,2	130	-19,6	27	-20	-20	26	7	5	-5	0	0	-13	-12	risk
12	1,0	6,722	0,75	266,3	100	2,47	140	1790	672	2462	77,9	355	320	314	0,85	0,32	0,04	0,04	0,86	2993	94,6	140	-21,0	27	-20	-20	26	7	5	-5	0	0	-14	-12	risk
13	1,0	6,745	0,75	266,3	100	2,51	150	1796	675	2470	78,1	355	318	312	0,85	0,32	0,04	0,03	0,86	3006	95,0	150	-22,3	27	-20	-20	26	7	5	-5	0	0	-15	-12	risk
20	1,0	6,790	0,75	266,3	100	2,60	180	1808	679	2487	78,6	355	310	306	0,87	0,33	0,04	0,03	0,85	3034	95,9	180	-25,5	27	-20	-20	26	7	5	-5	0	0	-19	-12	risk

Assessment for $\sigma_{Ed} = 0{,}75 \cdot f_y$ and $T = -10$ °C

Nr	σ_P	K_1	σ_{Ed}/f_y	σ_P	σ_S	a_0	t_1	$K_{1,P}$	$K_{1,S}$	$K_{1,ges}$	$K_{1,ges}$	$f_{y,nom}$	$f_y(t)$	σ_{gy}	L_r	ψ	ρ_1	ρ	k_{R6}	$K_{appl,d}$	$K_{appl,d}$	b_{eff}	ΔT_σ	$K_{V,nom}$	T_{KV}	T_{27J}	ΔT_{27J}	ΔT_R	T_{md}	ΔT_r	ΔT_ε	ΔT_{DCF}	T_{Ed}	T_{Rd}	$T_{Ed} \geq T_{Rd}$
	N/mm²	$N/mm^{3/2}$	[-]	N/mm²	N/mm²	mm	mm	$N/mm^{3/2}$	$N/mm^{3/2}$	$N/mm^{3/2}$	$MPam^{1/2}$	N/mm²	N/mm²	N/mm²	-	-	-	-	-	$N/mm^{3/2}$	$MPam^{1/2}$	mm	°C	J	°C	°C	°C	°C	°C	°C	°C	°C	°C	°C	
1	1,0	5,220	0,75	266,3	100	1,70	30	1390	522	1912	60,5	355	348	328	0,81	0,31	0,04	0,04	0,87	2312	73,1	30	22,3	27	-20	-20	8	7	-5	-5	0	0	19	-30	no risk
2	1,0	5,590	0,75	266,3	100	1,84	40	1488	559	2047	64,7	355	345	329	0,81	0,30	0,04	0,04	0,87	2474	78,2	40	12,1	27	-20	-20	16	7	-5	-5	0	0	9	-22	no risk
3	1,0	5,870	0,75	266,3	100	1,96	50	1563	587	2150	68,0	355	343	329	0,81	0,30	0,04	0,04	0,87	2598	82,2	50	4,7	27	-20	-20	21	7	-5	-5	0	0	2	-17	no risk
4	1,0	6,084	0,75	266,3	100	2,05	60	1620	608	2228	70,5	355	340	328	0,81	0,30	0,04	0,04	0,87	2694	85,2	60	-0,8	27	-20	-20	23	7	-5	-5	0	0	-4	-15	no risk
5	1,0	6,250	0,75	266,3	100	2,12	70	1664	625	2289	72,4	355	338	327	0,81	0,31	0,04	0,04	0,87	2768	87,5	70	-5,2	27	-20	-20	24	7	-5	-5	0	0	-8	-14	no risk
6	1,0	6,378	0,75	266,3	100	2,19	80	1698	638	2336	73,9	355	335	326	0,82	0,31	0,04	0,04	0,87	2827	89,4	80	-8,7	27	-20	-20	25	7	-5	-5	0	0	-12	-13	no risk
7	1,0	6,477	0,75	266,3	100	2,25	90	1725	648	2372	75,0	355	333	324	0,82	0,31	0,04	0,04	0,86	2872	90,8	90	-11,6	27	-20	-20	25	7	-5	-5	0	0	-15	-13	risk
8	1,0	6,554	0,75	266,3	100	2,30	100	1745	655	2400	75,9	355	330	322	0,83	0,31	0,04	0,04	0,86	2909	92,0	100	-14,1	27	-20	-20	25	7	-5	-5	0	0	-17	-13	risk
9	1,0	6,613	0,75	266,3	100	2,35	110	1761	661	2422	76,6	355	328	321	0,83	0,31	0,04	0,04	0,86	2937	92,9	110	-16,2	27	-20	-20	25	7	-5	-5	0	0	-19	-13	risk
10	1,0	6,659	0,75	266,3	100	2,39	120	1773	666	2439	77,1	355	325	319	0,84	0,31	0,04	0,04	0,86	2960	93,6	120	-18,0	27	-20	-20	26	7	-5	-5	0	0	-21	-12	risk
11	1,0	6,695	0,75	266,3	100	2,43	130	1783	670	2452	77,5	355	323	316	0,84	0,32	0,04	0,04	0,86	2978	94,2	130	-19,6	27	-20	-20	26	7	-5	-5	0	0	-23	-12	risk
12	1,0	6,722	0,75	266,3	100	2,47	140	1790	672	2462	77,9	355	320	314	0,85	0,32	0,04	0,04	0,86	2993	94,6	140	-21,0	27	-20	-20	26	7	-5	-5	0	0	-24	-12	risk
13	1,0	6,745	0,75	266,3	100	2,51	150	1796	675	2470	78,1	355	318	312	0,85	0,32	0,04	0,03	0,86	3006	95,0	150	-22,3	27	-20	-20	26	7	-5	-5	0	0	-25	-12	risk
20	1,0	6,790	0,75	266,3	100	2,60	180	1808	679	2487	78,6	355	310	306	0,87	0,33	0,04	0,03	0,85	3034	95,9	180	-25,5	27	-20	-20	26	7	-5	-5	0	0	-29	-12	risk

Table 5-40: Continued

Assessment for σ_{Ed} = 0,75·f_y and T = -20 °C

Nr	σ_P	K_1	σ_{Ed}/f_y	σ_P	σ_S	a_0	t_1	$K_{1,P}$	$K_{1,S}$	$K_{1,ges}$	$K_{1,ges}$	$f_{y,nom}$	$f_y(t)$	σ_{gy}	L_r	ψ	ρ_1	ρ	k_{R6}	$K_{appl,d}$	$K_{appl,d}$	b_{eff}	ΔT_σ	$K_{V,nom}$	T_{KV}	T_{27J}	ΔT_{27J}	ΔT_R	T_{md}	ΔT_r	ΔT_ε	ΔT_{DCF}	T_{Ed}	T_{Rd}	$T_{Ed} \geq T_{Rd}$
	N/mm²	N/mm$^{3/2}$	[-]	N/mm²	N/mm²	mm	mm	N/mm$^{3/2}$	N/mm$^{3/2}$	N/mm$^{3/2}$	MPam$^{1/2}$	N/mm²	N/mm²	N/mm²	-	-	-	-	-	N/mm$^{3/2}$	MPam$^{1/2}$	mm	°C	J	°C	°C	°C	°C	°C	°C	°C	°C	°C	°C	
1	1,0	5,220	0,75	266,3	100	1,70	30	1390	522	1912	60,5	355	348	328	0,81	0,31	0,04	0,04	0,87	2312	73,1	30	22,3	27	-20	-20	8	7	-15	-5	0	0	9	-30	no risk
2	1,0	5,590	0,75	266,3	100	1,84	40	1488	559	2047	64,7	355	345	329	0,81	0,30	0,04	0,04	0,87	2474	78,2	40	12,1	27	-20	-20	16	7	-15	-5	0	0	-1	-22	no risk
3	1,0	5,870	0,75	266,3	100	1,96	50	1563	587	2150	68,0	355	343	329	0,81	0,30	0,04	0,04	0,87	2598	82,2	50	4,7	27	-20	-20	21	7	-15	-5	0	0	-8	-17	no risk
4	1,0	6,084	0,75	266,3	100	2,05	60	1620	608	2228	70,5	355	340	328	0,81	0,30	0,04	0,04	0,87	2694	85,2	60	-0,8	27	-20	-20	23	7	-15	-5	0	0	-14	-15	no risk
5	1,0	6,250	0,75	266,3	100	2,12	70	1664	625	2289	72,4	355	338	327	0,81	0,31	0,04	0,04	0,87	2768	87,5	70	-5,2	27	-20	-20	24	7	-15	-5	0	0	-18	-14	risk
6	1,0	6,378	0,75	266,3	100	2,19	80	1698	638	2336	73,9	355	335	326	0,82	0,31	0,04	0,04	0,87	2827	89,4	80	-8,7	27	-20	-20	25	7	-15	-5	0	0	-22	-13	risk
7	1,0	6,477	0,75	266,3	100	2,25	90	1725	648	2372	75,0	355	333	324	0,82	0,31	0,04	0,04	0,86	2872	90,8	90	-11,6	27	-20	-20	25	7	-15	-5	0	0	-25	-13	risk
8	1,0	6,554	0,75	266,3	100	2,30	100	1745	655	2400	75,9	355	330	322	0,83	0,31	0,04	0,04	0,86	2909	92,0	100	-14,1	27	-20	-20	25	7	-15	-5	0	0	-27	-13	risk
9	1,0	6,613	0,75	266,3	100	2,35	110	1761	661	2422	76,6	355	328	321	0,83	0,31	0,04	0,04	0,86	2937	92,9	110	-16,2	27	-20	-20	25	7	-15	-5	0	0	-29	-13	risk
10	1,0	6,659	0,75	266,3	100	2,39	120	1773	666	2439	77,1	355	325	319	0,84	0,31	0,04	0,04	0,86	2960	93,6	120	-18,0	27	-20	-20	26	7	-15	-5	0	0	-31	-12	risk
11	1,0	6,695	0,75	266,3	100	2,43	130	1783	670	2452	77,5	355	323	316	0,84	0,32	0,04	0,04	0,86	2978	94,2	130	-19,6	27	-20	-20	26	7	-15	-5	0	0	-33	-12	risk
12	1,0	6,722	0,75	266,3	100	2,47	140	1790	672	2462	77,9	355	320	314	0,85	0,32	0,04	0,04	0,86	2993	94,6	140	-21,0	27	-20	-20	26	7	-15	-5	0	0	-34	-12	risk
13	1,0	6,745	0,75	266,3	100	2,51	150	1796	675	2470	78,1	355	318	312	0,85	0,32	0,04	0,03	0,86	3006	95,0	150	-22,3	27	-20	-20	26	7	-15	-5	0	0	-35	-12	risk
20	1,0	6,790	0,75	266,3	100	2,60	180	1808	679	2487	78,6	355	310	306	0,87	0,33	0,04	0,03	0,85	3034	95,9	180	-25,5	27	-20	-20	26	7	-15	-5	0	0	-39	-12	risk

Assessment for σ_{Ed} = 0,75·f_y and T = -30 °C

Nr	σ_P	K_1	σ_{Ed}/f_y	σ_P	σ_S	a_0	t_1	$K_{1,P}$	$K_{1,S}$	$K_{1,ges}$	$K_{1,ges}$	$f_{y,nom}$	$f_y(t)$	σ_{gy}	L_r	ψ	ρ_1	ρ	k_{R6}	$K_{appl,d}$	$K_{appl,d}$	b_{eff}	ΔT_σ	$K_{V,nom}$	T_{KV}	T_{27J}	ΔT_{27J}	ΔT_R	T_{md}	ΔT_r	ΔT_ε	ΔT_{DCF}	T_{Ed}	T_{Rd}	$T_{Ed} \geq T_{Rd}$
	N/mm²	N/mm$^{3/2}$	[-]	N/mm²	N/mm²	mm	mm	N/mm$^{3/2}$	N/mm$^{3/2}$	N/mm$^{3/2}$	MPam$^{1/2}$	N/mm²	N/mm²	N/mm²	-	-	-	-	-	N/mm$^{3/2}$	MPam$^{1/2}$	mm	°C	J	°C	°C	°C	°C	°C	°C	°C	°C	°C	°C	
1	1,0	5,220	0,75	266,3	100	1,70	30	1390	522	1912	60,5	355	348	328	0,81	0,31	0,04	0,04	0,87	2312	73,1	30	22,3	27	-20	-20	8	7	-25	-5	0	0	-1	-30	no risk
2	1,0	5,590	0,75	266,3	100	1,84	40	1488	559	2047	64,7	355	345	329	0,81	0,30	0,04	0,04	0,87	2474	78,2	40	12,1	27	-20	-20	16	7	-25	-5	0	0	-11	-22	no risk
3	1,0	5,870	0,75	266,3	100	1,96	50	1563	587	2150	68,0	355	343	329	0,81	0,30	0,04	0,04	0,87	2598	82,2	50	4,7	27	-20	-20	21	7	-25	-5	0	0	-18	-17	risk
4	1,0	6,084	0,75	266,3	100	2,05	60	1620	608	2228	70,5	355	340	328	0,81	0,30	0,04	0,04	0,87	2694	85,2	60	-0,8	27	-20	-20	23	7	-25	-5	0	0	-24	-15	risk
5	1,0	6,250	0,75	266,3	100	2,12	70	1664	625	2289	72,4	355	338	327	0,81	0,31	0,04	0,04	0,87	2768	87,5	70	-5,2	27	-20	-20	24	7	-25	-5	0	0	-28	-14	risk
6	1,0	6,378	0,75	266,3	100	2,19	80	1698	638	2336	73,9	355	335	326	0,82	0,31	0,04	0,04	0,87	2827	89,4	80	-8,7	27	-20	-20	25	7	-25	-5	0	0	-32	-13	risk
7	1,0	6,477	0,75	266,3	100	2,25	90	1725	648	2372	75,0	355	333	324	0,82	0,31	0,04	0,04	0,86	2872	90,8	90	-11,6	27	-20	-20	25	7	-25	-5	0	0	-35	-13	risk
8	1,0	6,554	0,75	266,3	100	2,30	100	1745	655	2400	75,9	355	330	322	0,83	0,31	0,04	0,04	0,86	2909	92,0	100	-14,1	27	-20	-20	25	7	-25	-5	0	0	-37	-13	risk
9	1,0	6,613	0,75	266,3	100	2,35	110	1761	661	2422	76,6	355	328	321	0,83	0,31	0,04	0,04	0,86	2937	92,9	110	-16,2	27	-20	-20	25	7	-25	-5	0	0	-39	-13	risk
10	1,0	6,659	0,75	266,3	100	2,39	120	1773	666	2439	77,1	355	325	319	0,84	0,31	0,04	0,04	0,86	2960	93,6	120	-18,0	27	-20	-20	26	7	-25	-5	0	0	-41	-12	risk
11	1,0	6,695	0,75	266,3	100	2,43	130	1783	670	2452	77,5	355	323	316	0,84	0,32	0,04	0,04	0,86	2978	94,2	130	-19,6	27	-20	-20	26	7	-25	-5	0	0	-43	-12	risk
12	1,0	6,722	0,75	266,3	100	2,47	140	1790	672	2462	77,9	355	320	314	0,85	0,32	0,04	0,04	0,86	2993	94,6	140	-21,0	27	-20	-20	26	7	-25	-5	0	0	-44	-12	risk
13	1,0	6,745	0,75	266,3	100	2,51	150	1796	675	2470	78,1	355	318	312	0,85	0,32	0,04	0,03	0,86	3006	95,0	150	-22,3	27	-20	-20	26	7	-25	-5	0	0	-45	-12	risk
20	1,0	6,860	0,75	266,3	100	2,76	250	1826	686	2512	79,5	355	293	289	0,92	0,35	0,05	0,02	0,84	3086	97,6	250	-31,4	27	-20	-20	26	7	-25	-5	0	0	-54	-12	risk

Table 5-40: Continued

Assessment for $\sigma_{Ed} = 0{,}75 \cdot f_y$ and T = -40 °C

Nr	σ_P	K_1	σ_{Ed}/f_y	σ_P	σ_S	a_0	t_1	$K_{1,P}$	$K_{1,S}$	$K_{1,ges}$	$K_{1,ges}$	$f_{y,nom}$	$f_y(t)$	σ_{gy}	L_r	ψ	ρ_1	ρ	k_{R6}	$K_{appl,d}$	$K_{appl,d}$	b_{eff}	ΔT_σ	$K_{V,nom}$	T_{KV}	T_{27J}	ΔT_{27J}	ΔT_R	T_{md}	ΔT_r	ΔT_ε	ΔT_{DCF}	T_{Ed}	T_{Rd}	$T_{Ed} \geq T_{Rd}$
	N/mm²	$N/mm^{3/2}$	[-]	N/mm²	N/mm²	mm	mm	$N/mm^{3/2}$	$N/mm^{3/2}$	$N/mm^{3/2}$	$MPam^{1/2}$	N/mm²	N/mm²	N/mm²	-	-	-	-	-	$N/mm^{3/2}$	$MPam^{1/2}$	mm	°C	J	°C	°C	°C	°C	°C	°C	°C	°C	°C	°C	
1	1,0	5,220	0,75	266,3	100	1,70	30	1390	522	1912	60,5	355	348	328	0,81	0,31	0,04	0,04	0,87	2312	73,1	30	22,3	27	-20	-20	8	7	-35	-5	0	0	**-11**	**-30**	no risk
2	1,0	5,590	0,75	266,3	100	1,84	40	1488	559	2047	64,7	355	345	329	0,81	0,30	0,04	0,04	0,87	2474	78,2	40	12,1	27	-20	-20	16	7	-35	-5	0	0	**-21**	**-22**	no risk
3	1,0	5,870	0,75	266,3	100	1,96	50	1563	587	2150	68,0	355	343	329	0,81	0,30	0,04	0,04	0,87	2598	82,2	50	4,7	27	-20	-20	21	7	-35	-5	0	0	**-28**	**-17**	risk
4	1,0	6,084	0,75	266,3	100	2,05	60	1620	608	2228	70,5	355	340	328	0,81	0,30	0,04	0,04	0,87	2694	85,2	60	-0,8	27	-20	-20	23	7	-35	-5	0	0	**-34**	**-15**	risk
5	1,0	6,250	0,75	266,3	100	2,12	70	1664	625	2289	72,4	355	338	327	0,81	0,31	0,04	0,04	0,87	2768	87,5	70	-5,2	27	-20	-20	24	7	-35	-5	0	0	**-38**	**-14**	risk
6	1,0	6,378	0,75	266,3	100	2,19	80	1698	638	2336	73,9	355	335	326	0,82	0,31	0,04	0,04	0,87	2827	89,4	80	-8,7	27	-20	-20	25	7	-35	-5	0	0	**-42**	**-13**	risk
7	1,0	6,477	0,75	266,3	100	2,25	90	1725	648	2372	75,0	355	333	324	0,82	0,31	0,04	0,04	0,86	2872	90,8	90	-11,6	27	-20	-20	25	7	-35	-5	0	0	**-45**	**-13**	risk
8	1,0	6,554	0,75	266,3	100	2,30	100	1745	655	2400	75,9	355	330	322	0,83	0,31	0,04	0,04	0,86	2909	92,0	100	-14,1	27	-20	-20	25	7	-35	-5	0	0	**-47**	**-13**	risk
9	1,0	6,613	0,75	266,3	100	2,35	110	1761	661	2422	76,6	355	328	321	0,83	0,31	0,04	0,04	0,86	2937	92,9	110	-16,2	27	-20	-20	25	7	-35	-5	0	0	**-49**	**-13**	risk
10	1,0	6,659	0,75	266,3	100	2,39	120	1773	666	2439	77,1	355	325	319	0,84	0,31	0,04	0,04	0,86	2960	93,6	120	-18,0	27	-20	-20	26	7	-35	-5	0	0	**-51**	**-12**	risk
11	1,0	6,695	0,75	266,3	100	2,43	130	1783	670	2452	77,5	355	323	316	0,84	0,32	0,04	0,04	0,86	2978	94,2	130	-19,6	27	-20	-20	26	7	-35	-5	0	0	**-53**	**-12**	risk
12	1,0	6,722	0,75	266,3	100	2,47	140	1790	672	2462	77,9	355	320	314	0,85	0,32	0,04	0,04	0,86	2993	94,6	140	-21,0	27	-20	-20	26	7	-35	-5	0	0	**-54**	**-12**	risk
13	1,0	6,745	0,75	266,3	100	2,51	150	1796	675	2470	78,1	355	318	312	0,85	0,32	0,04	0,03	0,86	3006	95,0	150	-22,3	27	-20	-20	26	7	-35	-5	0	0	**-55**	**-12**	risk
20	1,0	6,860	0,75	266,3	100	2,76	250	1826	686	2512	79,5	355	293	289	0,92	0,35	0,05	0,02	0,84	3086	97,6	250	-31,4	27	-20	-20	26	7	-35	-5	0	0	**-64**	**-12**	risk

Assessment for $\sigma_{Ed} = 0{,}75 \cdot f_y$ and T = -50 °C

Nr	σ_P	K_1	σ_{Ed}/f_y	σ_P	σ_S	a_0	t_1	$K_{1,P}$	$K_{1,S}$	$K_{1,ges}$	$K_{1,ges}$	$f_{y,nom}$	$f_y(t)$	σ_{gy}	L_r	ψ	ρ_1	ρ	k_{R6}	$K_{appl,d}$	$K_{appl,d}$	b_{eff}	ΔT_σ	$K_{V,nom}$	T_{KV}	T_{27J}	ΔT_{27J}	ΔT_R	T_{md}	ΔT_r	ΔT_ε	ΔT_{DCF}	T_{Ed}	T_{Rd}	$T_{Ed} \geq T_{Rd}$
	N/mm²	$N/mm^{3/2}$	[-]	N/mm²	N/mm²	mm	mm	$N/mm^{3/2}$	$N/mm^{3/2}$	$N/mm^{3/2}$	$MPam^{1/2}$	N/mm²	N/mm²	N/mm²	-	-	-	-	-	$N/mm^{3/2}$	$MPam^{1/2}$	mm	°C	J	°C	°C	°C	°C	°C	°C	°C	°C	°C	°C	
1	1,0	5,220	0,75	266,3	100	1,70	30	1390	522	1912	60,5	355	348	328	0,81	0,31	0,04	0,04	0,87	2312	73,1	30	22,3	27	-20	-20	8	7	-45	-5	0	0	**-21**	**-30**	no risk
2	1,0	5,590	0,75	266,3	100	1,84	40	1488	559	2047	64,7	355	345	329	0,81	0,30	0,04	0,04	0,87	2474	78,2	40	12,1	27	-20	-20	16	7	-45	-5	0	0	**-31**	**-22**	risk
3	1,0	5,870	0,75	266,3	100	1,96	50	1563	587	2150	68,0	355	343	329	0,81	0,30	0,04	0,04	0,87	2598	82,2	50	4,7	27	-20	-20	21	7	-45	-5	0	0	**-38**	**-17**	risk
4	1,0	6,084	0,75	266,3	100	2,05	60	1620	608	2228	70,5	355	340	328	0,81	0,30	0,04	0,04	0,87	2694	85,2	60	-0,8	27	-20	-20	23	7	-45	-5	0	0	**-44**	**-15**	risk
5	1,0	6,250	0,75	266,3	100	2,12	70	1664	625	2289	72,4	355	338	327	0,81	0,31	0,04	0,04	0,87	2768	87,5	70	-5,2	27	-20	-20	24	7	-45	-5	0	0	**-48**	**-14**	risk
6	1,0	6,378	0,75	266,3	100	2,19	80	1698	638	2336	73,9	355	335	326	0,82	0,31	0,04	0,04	0,87	2827	89,4	80	-8,7	27	-20	-20	25	7	-45	-5	0	0	**-52**	**-13**	risk
7	1,0	6,477	0,75	266,3	100	2,25	90	1725	648	2372	75,0	355	333	324	0,82	0,31	0,04	0,04	0,86	2872	90,8	90	-11,6	27	-20	-20	25	7	-45	-5	0	0	**-55**	**-13**	risk
8	1,0	6,554	0,75	266,3	100	2,30	100	1745	655	2400	75,9	355	330	322	0,83	0,31	0,04	0,04	0,86	2909	92,0	100	-14,1	27	-20	-20	25	7	-45	-5	0	0	**-57**	**-13**	risk
9	1,0	6,613	0,75	266,3	100	2,35	110	1761	661	2422	76,6	355	328	321	0,83	0,31	0,04	0,04	0,86	2937	92,9	110	-16,2	27	-20	-20	25	7	-45	-5	0	0	**-59**	**-13**	risk
10	1,0	6,659	0,75	266,3	100	2,39	120	1773	666	2439	77,1	355	325	319	0,84	0,31	0,04	0,04	0,86	2960	93,6	120	-18,0	27	-20	-20	26	7	-45	-5	0	0	**-61**	**-12**	risk
11	1,0	6,695	0,75	266,3	100	2,43	130	1783	670	2452	77,5	355	323	316	0,84	0,32	0,04	0,04	0,86	2978	94,2	130	-19,6	27	-20	-20	26	7	-45	-5	0	0	**-63**	**-12**	risk
12	1,0	6,722	0,75	266,3	100	2,47	140	1790	672	2462	77,9	355	320	314	0,85	0,32	0,04	0,04	0,86	2993	94,6	140	-21,0	27	-20	-20	26	7	-45	-5	0	0	**-64**	**-12**	risk
13	1,0	6,745	0,75	266,3	100	2,51	150	1796	675	2470	78,1	355	318	312	0,85	0,32	0,04	0,03	0,86	3006	95,0	150	-22,3	27	-20	-20	26	7	-45	-5	0	0	**-65**	**-12**	risk
20	1,0	6,860	0,75	266,3	100	2,76	250	1826	686	2512	79,5	355	293	289	0,92	0,35	0,05	0,02	0,84	3086	97,6	250	-31,4	27	-20	-20	26	7	-45	-5	0	0	**-74**	**-12**	risk

Table 5-41: Fracture mechanics assessment for the component No. 5 for loading variant 5-2

Assessment for σ_{Ed} = 0,75·f_y and T = -50 °C

Nr	σ_P	K_1	σ_{Ed}/f_y	σ_P	σ_S	a_0	t_1	$K_{1,P}$	$K_{1,S}$	$K_{1,ges}$	$K_{1,ges}$	$f_{y,nom}$	$f_y(t)$	σ_{gy}	L_r	ψ	ρ_1	ρ	k_{R6}	$K_{appl,d}$	$K_{appl,d}$	b_{eff}	ΔT_σ	$K_{V,nom}$	T_{KV}	T_{27J}	ΔT_{27J}	ΔT_R	T_{md}	ΔT_r	ΔT_ε	ΔT_{DCF}	T_{Ed}	T_{Rd}	$T_{Ed} \geq T_{Rd}$
	N/mm²	$N/mm^{3/2}$	[-]	N/mm²	N/mm²	mm	mm	$N/mm^{3/2}$	$N/mm^{3/2}$	$N/mm^{3/2}$	$MPam^{1/2}$	N/mm²	N/mm²	N/mm²	-	-	-	-	-	$N/mm^{3/2}$	$MPam^{1/2}$	mm	°C	J	°C	°C	°C	°C	°C	°C	°C	°C	°C	°C	
1	1,0	2,450	0,75	266,3	100	2,85	25	652	245	897	28,4	355	349	344	0,77	0,29	0,04	0,04	0,88	1073	33,9	25	120,0	27	-20	-20	5	7	-45	-5	0	0	**77**	**-33**	no risk
2	1,0	2,485	0,75	266,3	100	2,85	35	662	248	910	28,8	355	346	342	0,78	0,29	0,04	0,04	0,88	1090	34,5	35	120,0	27	-20	-20	12	7	-45	-5	0	0	**77**	**-26**	no risk
3	1,0	2,594	0,75	266,3	100	2,85	45	691	259	950	30,0	355	344	339	0,79	0,29	0,04	0,04	0,87	1140	36,1	45	109,0	27	-20	-20	19	7	-45	-5	0	0	**66**	**-19**	no risk
4	1,0	2,778	0,75	266,3	100	2,85	55	740	278	1017	32,2	355	341	337	0,79	0,30	0,04	0,04	0,87	1224	38,7	55	88,5	27	-20	-20	22	7	-45	-5	0	0	**45**	**-16**	no risk
5	1,0	2,878	0,75	266,3	100	2,85	65	766	288	1054	33,3	355	339	334	0,80	0,30	0,04	0,04	0,87	1270	40,2	65	78,0	27	-20	-20	24	7	-45	-5	0	0	**35**	**-14**	no risk
6	1,0	2,904	0,75	266,3	100	2,85	75	773	290	1064	33,6	355	336	332	0,80	0,30	0,04	0,04	0,87	1284	40,6	75	73,2	27	-20	-20	25	7	-45	-5	0	0	**30**	**-13**	no risk
7	1,0	2,922	0,75	266,3	100	2,85	85	778	292	1070	33,8	355	334	329	0,81	0,30	0,04	0,04	0,87	1293	40,9	85	69,5	27	-20	-20	25	7	-45	-5	0	0	**27**	**-13**	no risk
8	1,0	2,952	0,75	266,3	100	2,85	95	786	295	1081	34,2	355	331	327	0,81	0,31	0,04	0,04	0,87	1308	41,3	95	65,6	27	-20	-20	25	7	-45	-5	0	0	**23**	**-13**	no risk
9	1,0	2,948	0,75	266,3	100	2,85	105	785	295	1080	34,1	355	329	324	0,82	0,31	0,04	0,04	0,86	1307	41,3	105	63,7	27	-20	-20	25	7	-45	-5	0	0	**21**	**-13**	no risk
10	1,0	2,957	0,75	266,3	100	2,85	115	787	296	1083	34,2	355	326	322	0,83	0,31	0,04	0,04	0,86	1312	41,5	115	61,4	27	-20	-20	26	7	-45	-5	0	0	**18**	**-12**	no risk
11	1,0	2,964	0,75	266,3	100	2,85	125	789	296	1085	34,3	355	324	319	0,83	0,31	0,04	0,04	0,86	1317	41,6	125	59,3	27	-20	-20	26	7	-45	-5	0	0	**16**	**-12**	no risk
12	1,0	2,970	0,75	266,3	100	2,85	135	791	297	1088	34,4	355	321	317	0,84	0,32	0,04	0,04	0,86	1321	41,8	135	57,5	27	-20	-20	26	7	-45	-5	0	0	**14**	**-12**	no risk
13	1,0	2,975	0,75	266,3	100	2,85	145	792	298	1090	34,5	355	319	314	0,85	0,32	0,04	0,04	0,86	1324	41,9	145	55,7	27	-20	-20	26	7	-45	-5	0	0	**13**	**-12**	no risk
14	1,0	2,979	0,75	266,3	100	2,85	155	793	298	1091	34,5	355	316	312	0,85	0,32	0,04	0,03	0,86	1328	42,0	155	54,2	27	-20	-20	26	7	-45	-5	0	0	**11**	**-12**	no risk
15	1,0	2,984	0,75	266,3	100	2,85	165	794	298	1093	34,6	355	314	310	0,86	0,32	0,04	0,03	0,85	1331	42,1	165	52,7	27	-20	-20	26	7	-45	-5	0	0	**10**	**-12**	no risk
16	1,0	2,990	0,75	266,3	100	2,85	175	796	299	1095	34,6	355	311	307	0,87	0,33	0,04	0,03	0,85	1335	42,2	175	51,2	27	-20	-20	26	7	-45	-5	0	0	**8**	**-12**	no risk
17	1,0	2,996	0,75	266,3	100	2,85	185	798	300	1097	34,7	355	309	305	0,87	0,33	0,04	0,03	0,85	1339	42,3	185	49,8	27	-20	-20	26	7	-45	-5	0	0	**7**	**-12**	no risk
18	1,0	3,002	0,75	266,3	100	2,85	195	799	300	1099	34,8	355	306	302	0,88	0,33	0,04	0,03	0,85	1343	42,5	195	48,5	27	-20	-20	26	7	-45	-5	0	0	**5**	**-12**	no risk
19	1,0	3,008	0,75	266,3	100	2,85	205	801	301	1102	34,8	355	304	300	0,89	0,33	0,04	0,03	0,85	1347	42,6	205	47,2	27	-20	-20	26	7	-45	-5	0	0	**4**	**-12**	no risk

6 Proposal for a standard procedure for the assessment to avoid brittle fracture when using FE-calculations

(1) The relevant locations for the assessments to avoid brittle fracture at the steel components of bearings may be taken from Table 6-1. The locations are those where notch effects due to geometrical detailing and due to welding are present and where tensile stresses occur.

Table 6-1: Critical locations for the assessments to avoid brittle fracture for the steel components of bearings

Comp.	Loading	Hot-Spot Location	Stress type
1 2A	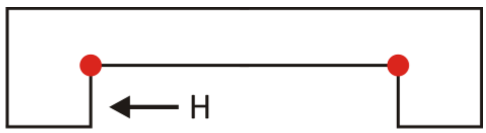	re-entrant corners	tension
2B	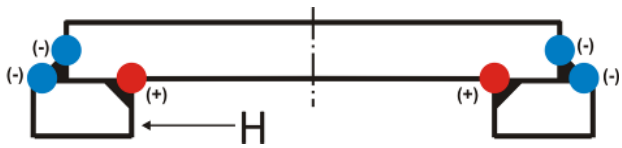	re-entrant corners weld toe top weld toe bottom	tension compress. compress.
3		re-entrant corners weld toe	tension tension
4		surface defects	tension
5	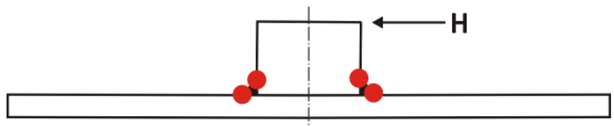	weld toe top weld toe bottom	tension tension

(2) With the assumptions, that initial cracks may occur at these locations with a critical direction of these cracks, see Table 6-2, the relevant reference stresses σ_{Ed} are determined at the surface where cracks initiate for the "frequent load combination", that is supposed to occur when the temperature of the components T_{Ed} gets its minimum value. With these two input values: σ_{Ed} and T_{Ed}, the limit of product thickness is calculated.

(3) The references stresses σ_{Ed} are obtained from hot-spot stresses σ_{HS} from a linear extrapolation of the tensile stresses along the crack path according to the method of Dong. This "inner" extrapolation covers the distribution of the tensile stresses along the crack path between the values σ_{max} (surface) and 0,1 σ_{max} (inner point).

(4) The maximum product thickness t is a function of the reference stress σ_{Ed} and temperature T_{Ed} determined specifically for each of the components, see Table 6-3 to Table 6-10 as associated in Table 6-2.

(5) These tables give the results for the most onerous loading variant used in section 5.

Table 6-2: Locations and directions of cracks as used to determined $\sigma_{Ed} = \sigma_{HS}$

Component	Sketch	Results
1	**Top component – rotationally-symmetric** 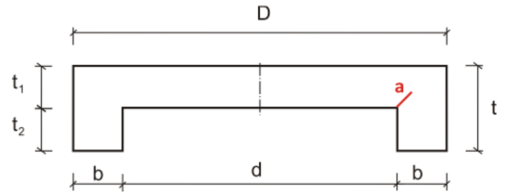	Table 6-3
2A	**Top component – axisymmetric** 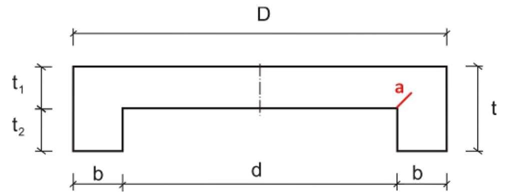	Table 6-4
2B	**Top component – axisymmetric, welded** 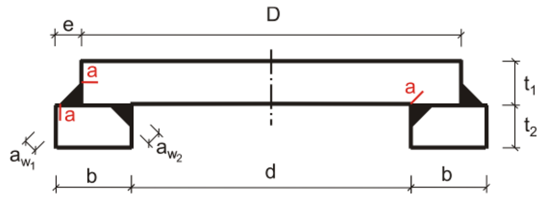	Table 6-5 (element thickness t_1) Table 6-6 (element thickness t_2)
3	**Bottom component** 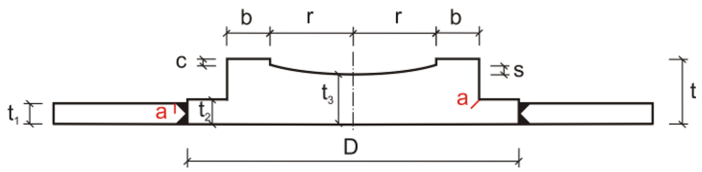	Table 6-7 (element thickness t_1) Table 6-8 (element thickness t_2)
4	**Anchor plate** 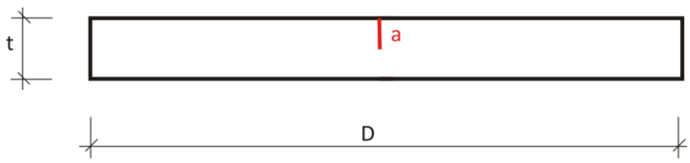	Table 6-9
5	**Bearing for horizontal forces** 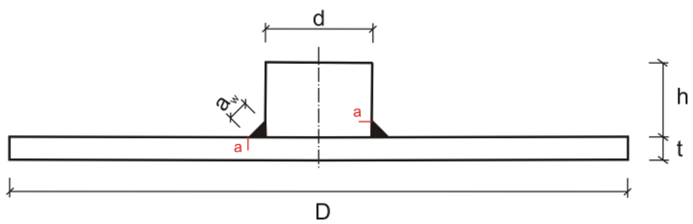	Table 6-10

Table 6-3: **Limits of plate thickness for component No. 1 – Rotationally-symmetric top component of bearing**

Steel grade acc. to EN 10025	σ_{Ed}	0°C	-10°C	-20°C	-30°C	-40°C	-50°C
		[mm]					
S355J2	0,25 · f_y	250*)	250*)	250*)	250*)	250*)	250*)
S355J2	0,50 · f_y	250*)	250*)	250*)	250*)	250*)	250*)
S355J2	0,75 · f_y	250*)	250*)	250*)	250*)	250*)	235

*) *Assumption of a technical manufacturing limit (in theory element thicknesses with t ≥ 250 mm would be acceptable)*

Table 6-4: **Limits of plate thickness for component No. 2A – Axisymmetric top component**

Steel grade acc. to EN 10025	σ_{Ed}	0°C	-10°C	-20°C	-30°C	-40°C	-50°C
		[mm]					
S355J2	0,25 · f_y	250*)	250*)	250*)	250*)	250*)	250*)
S355J2	0,50 · f_y	250*)	250*)	250*)	250*)	250*)	250*)
S355J2	0,75 · f_y	250*)	250*)	250*)	250*)	250*)	240

*) *Assumption of a technical manufacturing limit (in theory element thicknesses with t ≥ 250 mm would be acceptable)*

Table 6-5: **Limits of plate thickness t_1 for component No. 2B - Welded top component of bearing**

Steel grade acc. to EN 10025	σ_{Ed}	0°C	-10°C	-20°C	-30°C	-40°C	-50°C
		[mm]					
S355J2	0,25 · f_y	300*)	300*)	300*)	300*)	300*)	300*)
S355J2	0,50 · f_y	300*)	300*)	300*)	300*)	300*)	300*)
S355J2	0,75 · f_y	300*)	300*)	300*)	300*)	300*)	300*)

*) *Assumption of a technical manufacturing limit (in theory element thicknesses with t ≥ 300 mm would be acceptable)*

Table 6-6: **Limits of plate thickness t_2 for component No. 2B - Welded top component of bearing**

Steel grade acc. to EN 10025	σ_{Ed}	0°C	-10°C	-20°C	-30°C	-40°C	-50°C
		[mm]					
S355J2	0,25 · f_y	200*)	200	190	170	150	130

*) *Assumption of a technical manufacturing limit (in theory element thicknesses with t ≥ 200 mm would be acceptable)*

Table 6-7: Limits of plate thickness t_1 for component No. 3 - Bottom component of bearing

Steel grade acc. to EN 10025	σ_{Ed}	0°C	-10°C	-20°C	-30°C	-40°C	-50°C
		[mm]					
S355J2	$0,25 \cdot f_y$	250*)	250*)	250*)	250*)	250*)	250*)
S355J2	$0,50 \cdot f_y$	250*)	250*)	250*)	250*)	250*)	250*)
S355J2	$0,75 \cdot f_y$	250*)	250*)	250*)	200	140	110

*) *Assumption of a technical manufacturing limit (in theory element thicknesses with t ≥ 250 mm would be acceptable)*

Table 6-8: Limits of plate thickness t_2 for component No. 3 - Bottom component of bearing

Steel grade acc. to EN 10025	σ_{Ed}	0°C	-10°C	-20°C	-30°C	-40°C	-50°C
		[mm]					
S355J2	$0,25 \cdot f_y$	250*)	250*)	250*)	250*)	250*)	250*)
S355J2	$0,50 \cdot f_y$	250*)	250*)	250*)	250*)	250*)	250*)
S355J2	$0,75 \cdot f_y$	250*)	250*)	250*)	200	140	110

*) *Assumption of a technical manufacturing limit (in theory element thicknesses with t ≥ 250 mm would be acceptable)*

Table 6-9: Limits of plate thickness for component No. 4 - Anchor plate

Steel grade acc. to EN 10025	σ_{Ed}	0°C	-10°C	-20°C	-30°C	-40°C	-50°C
		[mm]					
S355J2	$0,25 \cdot f_y$	250*)	250*)	250*)	250*)	250*)	250*)
S355J2	$0,50 \cdot f_y$	250*)	250*)	250*)	250*)	250*)	250*)
S355J2	$0,75 \cdot f_y$	250*)	250*)	250*)	250*)	250*)	250*)

*) *Assumption of a technical manufacturing limit (in theory element thicknesses with t ≥ 250 mm would be acceptable)*

Table 6-10: Limits of plate thickness for component No. 5 – Bearing for horizontal loads

Steel grade acc. to EN 10025	σ_{Ed}	0°C	-10°C	-20°C	-30°C	-40°C	-50°C
		[mm]					
S355J2	$0,25 \cdot f_y$	250*)	250*)	250*)	250*)	250*)	250*)
S355J2	$0,50 \cdot f_y$	250*)	250*)	180	110	80	60
S355J2	$0,75 \cdot f_y$	120	80	60	40	40	30

*) *Assumption of a technical manufacturing limit (in theory element thicknesses with t ≥ 250 mm would be acceptable)*

7 Worked example for the assessment to avoid brittle fracture using FE-calculations

7.1 General

(1) The worked example deals with a top component of a bearing loaded by pressure from a concrete bridge, see Figure 7-1.

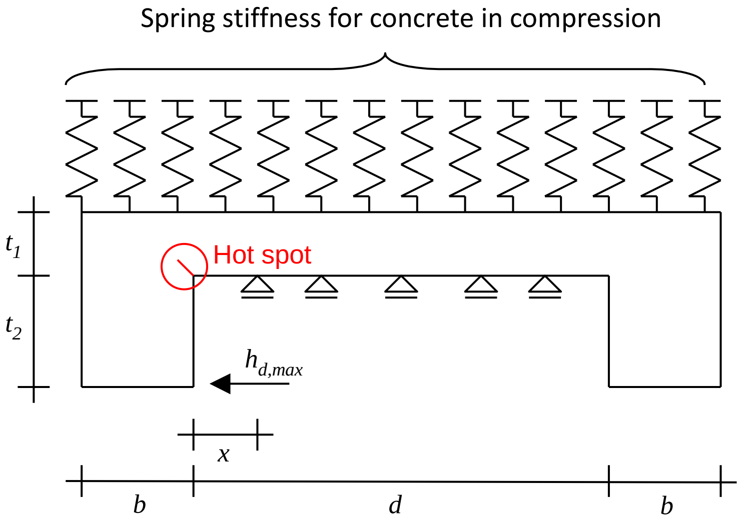

Figure 7-1: Top component of a bearing with elastic contact to the concrete part and horizontal load

(2) This type of component complies with component No. 1 (spherical bearing with RS beyond the rotating part) or component No. 2A (cylindrical bearing with unidirectional sliding part).

(3) For component No. 1 the horizontal forces would be distributed parabolically; for component No. 2A the distribution would be constant.

(4) In this case the assessment is performed for component No. 1 using the properties and loading in Table 7-1.

Table 7-1: Properties and loading for component No. 1

Geometry		
Plate thickness	t_1 [mm]	60
Height of lateral support	t_2 [mm]	65
Thickness of the parent plate	t_{Walz} [mm]	130
Width of lateral support	b [mm]	142,5
Distance between inside of the lateral support and the calotte	x [mm]	50
Inner diameter of top component	d [mm]	543
Loading		
Horizontal force	H_d [kN]	1936
Maximum horizontal force on lateral supports	$h_{d,max}$ [N/mm]	3404
Yield strength	f_y ($t_{steel\ product}$) [N/mm^2]	295

(5) In order to take into account non-linear effects of the elastic contact between concrete and steel the calculation has been carried out using FEM.

(6) For concrete C30/40 was chosen.

(7) The concrete pressure is determined by bi-linear spring-elements, see Figure 7-2, where the limit pressure of $3 \cdot f_{cd}$ has been used.

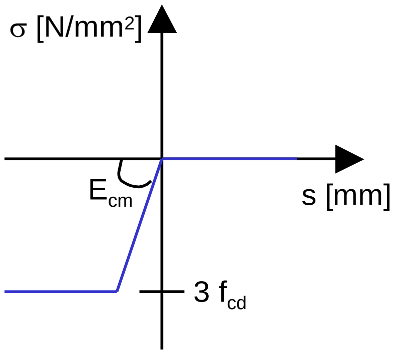

Figure 7-2: Spring-characteristic for the concrete surface

(8) The numerical analysis was carried with the programme ANSYS12. The use of 2-dimensional sections makes the use of 2-dimensional Finite Elements possible:

- Plane 82 for linear elastic material properties for steel, i.e. modulus of elasticity 210.000 N/mm² and Poisson ratio $\nu = 0.3$,
- COMBIN 39 as bilinear spring model for the concrete pressure.

7.2 Determination of the Hot-Spot-stresses

(1) The mechanical model in Figure 7-1 can be simplified for the safety assessment at the potential crack location to the model given in Figure 7-3.

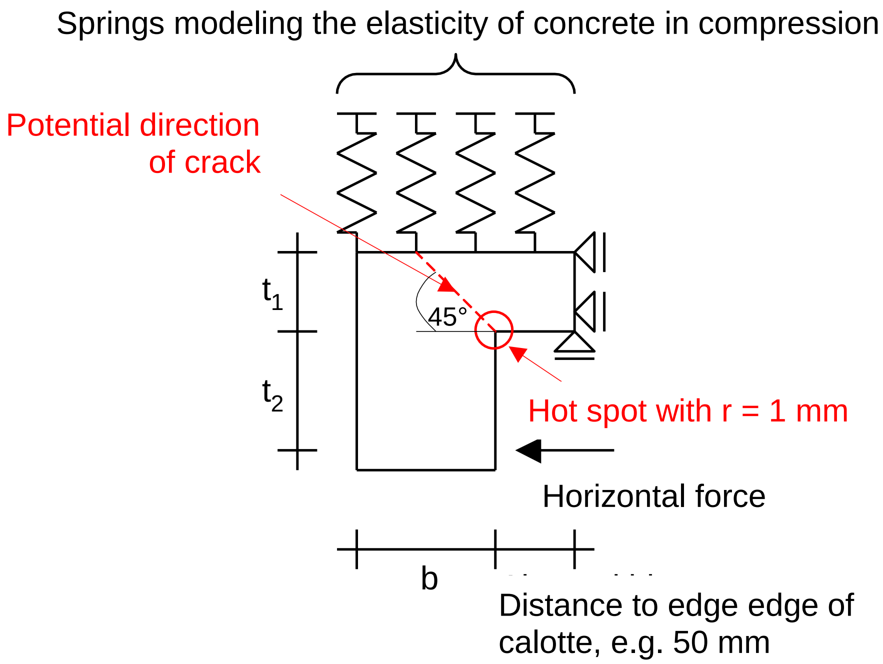

Figure 7-3: Mechanical model for the potential crack detail

(2) The calculations are performed with a Finite-Element-model according to Figure 7-4, where the interface to the concrete is reproduced by bilinear springs.

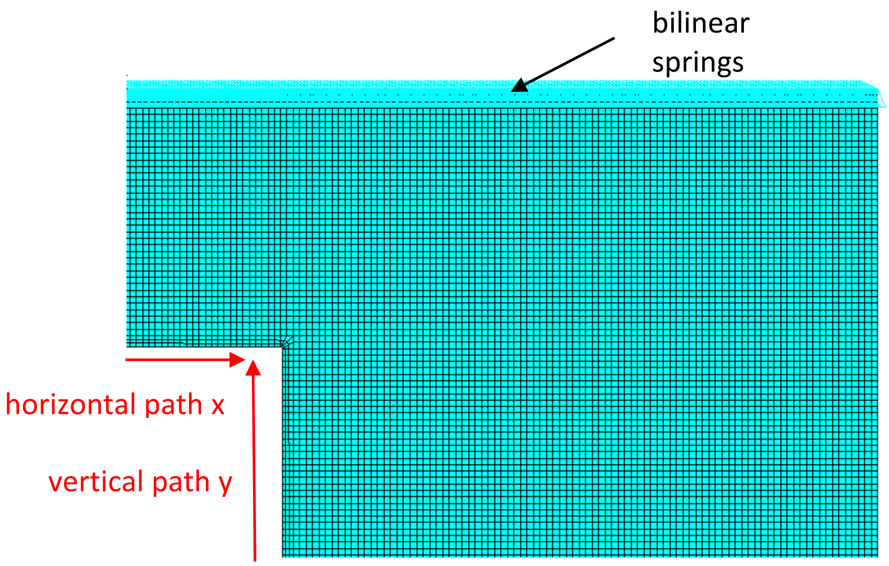

Figure 7-4: **Location and orientation of crack in the FE-mesh**

(3) The radius at the critical detail is 1 mm.

(4) The horizontal force applied is 3404 N/mm.

(5) The mesh-length in the area of crack is 1x1 mm and has been confirmed by convergence-studies.

(6) For the evaluation of the principal stresses, which are nearly orientated perpendicularly to the potential crack direction, the standard hot-spot-stress method with non-linear surface extrapolation along the horizontal and the vertical path in Figure 7-4 is used.

(7) The principal stress σ_{HS} for the horizontal extrapolation gives 106,3 N/mm² and for the vertical extrapolation 127,4 N/mm². For the vertical extrapolation the effect on the principal stress at the lateral supports at the point of the horizontal load application was separated.

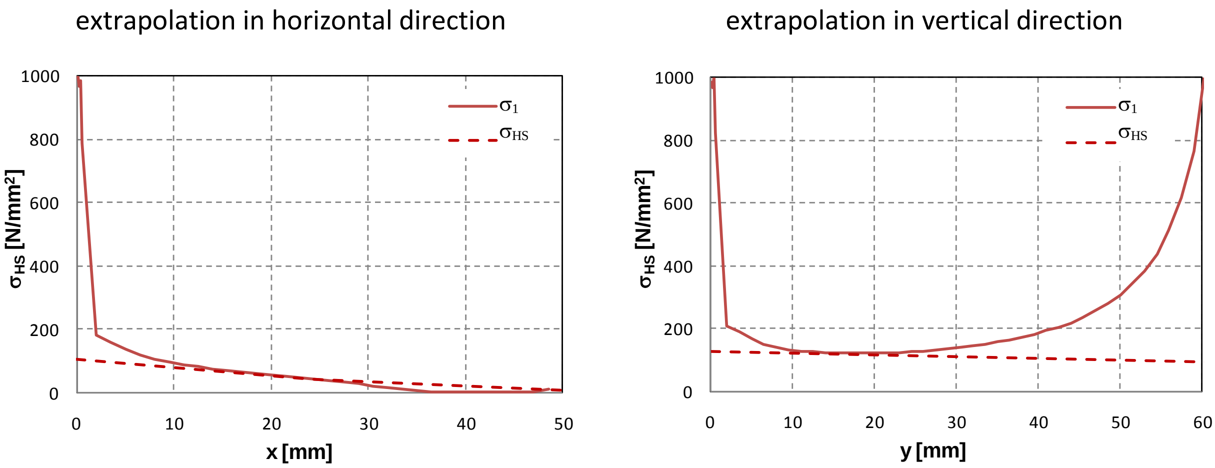

Figure 7-5: **Determination of the principal hot-spot stress σ_{HS} by means of non-linear surface extrapolation**

7.3 Assessment

(1) The assessment is based on

σ_{Ed} = 178 N/mm²

resulting from the static analysis of the bearing and hence

$$\frac{\sigma_{Ed}}{f_y} = \frac{178}{295} = 0,64$$

(2) According to Table 6-3 the dimensions of the steel-component are in the safe-area.

8 Simplified assessment with reference to ultimate limit state verifications

8.1 General

(1) The design of bearings for Ultimate Limit States yields in general the dimensions as given in Table 3-2.

(2) In the following it is assumed that

1. the ultimate limit state assessments are carried out using the elastic bending theory for bars with the stress $\sigma_{bend,d}$ limited by the yield strength,
2. the loading assumptions are compatible with deformations,
3. assessments are carried out for the critical sections perpendicular to the neutral axis (and not in the direction of the probable crack path),
4. assessments are performed with the design values of action effects (from factored loads),
5. notch effects are neglected in using the elastic bending theory for bars.

(3) In order to establish a link between the reference stresses σ_{Ed} defined as Hot-Spot-stresses according to Dong, for which the fracture mechanics assessments yielded the thickness limits in Table 6-3 to Table 6-10, and the stresses $\sigma_{bend,d}$ from the ultimate limit state assessments the following correlations are necessary:

1. Difference between the load-level for “frequent” loads and the load level for ultimate limit state checks,
2. Differences between the Hot-Spot-stress σ_{HS} from the linearization along the crack path and the bending stress $\sigma_{bend,d}$ limited by the yield strength f_y in the adjacent critical section perpendicular to the neutral axis.

8.2 Correlations

(1) To estimate the difference between the load-level for “frequent loads” and for ultimate limit state assessment, the case of canal bridges is adopted, for which

- the “frequent” load is defined by the permanent load (G+W) and
- the design load for ultimate limit states is γ_G(G+W) where γ_G = 1,35.

Hence the “frequent” load is equal to 1/1.35 = 0,75 of the ultimate load.

(2) As the bending stress $\sigma_{bend,d}$ for the critical cross-section perpendicular to the neutral axis according to Figure 4-6a is in general smaller than the Hot-Spot-stress σ_{Ed} along the crack path, it is assumed, that the reference stress σ_{Ed} equal to the Hot-Spot-stress along the crack path can be correlated with the bending stress $\sigma_{bend,d}$ according to the bending theory in the following way:

(3) Using the assumptions (1) and (2) the reference stress σ_{Ed} for the fracture mechanics assessment can be defined by

$$\sigma_{Ed} = 0.75 \cdot k_{Dong} \cdot \sigma_{bend,d} \qquad \textbf{(8-1)}$$

where

σ_{Ed} is determined according to the linear bending theory in the critical section perpendicular to the neutral axis for "frequent" loads

$\sigma_{bend,d}$ is the ultimate stress determined in a simplified way according to the elastic bending theory in the critical cross section perpendicular to the neutral axis for action effects from loads factored with γ.

f_y is the yield strength which limits the ultimate limit state assessment in the critical section perpendicular to the neutral axis

0,75 is the correlation factor between "frequent" load and the design load for ultimate limit states.

k_{Dong} is the correlation coefficient between the Hot-Spot-stress σ_{HS} according to Dong, see Figure 4-11 and the stress σ_{bend} determined according to the elastic bending theory for the critical cross section perpendicular to the neutral axis however with the same load level as for σ_{HS}.

Figure 8-1 gives an example.

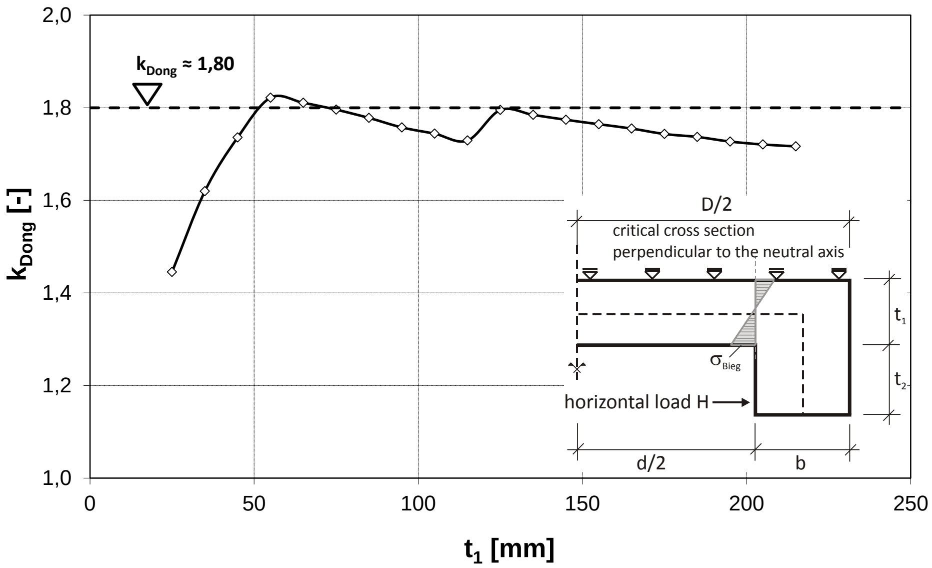

Figure 8-1: Correlation coefficient between the Hot-Spot-stress σ_{HS} according to Dong and stress σ_{bend} according to the bending theory for the critical cross section perpendicular to the neutral axis

8.3 Consequences for the choice of material to avoid brittle fracture

(1) The consequences from the simplifications in 8.1 and 8.2 are demonstrated in Table 8-1. The results are safe-sided.

Table 8-1: **Choice of material for steel components of bearings for the upper and bounds of dimensions for bearing type A and type B and steel S355J2 for T_{Ed} = - 30°C**

No.	Component	Geometry Type A	Geometry Type B	Limits
1	*Top component* *(Sliding plate and lateral guiderail)* 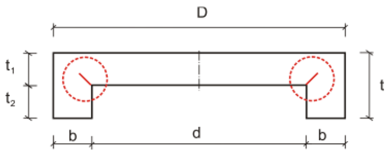	t: 55 – 315 mm t_1: 20 – 215 mm t_2: 25 – 100 mm *D: 500 – 1800 mm* *d: 355 - 1385 mm* *b: 50 - 505 mm*		t = 250 mm
2A	*Top component* *(sliding plate and lateral guiderail)* 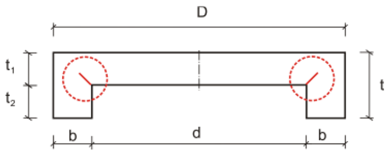	t: 55 – 315 mm t_1: 20 – 215 mm t_2: 25 – 100 mm *D: 500 – 1800 mm* *d: 355 - 1385 mm* *b: 50 - 500 mm*		t = 250 mm
2B	*Top component* *(sliding plate and lateral guiderail)* 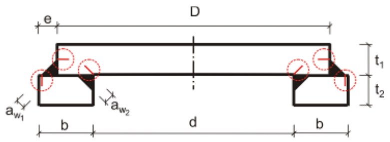		t_1: 55 – 285 mm t_2: 55 – 170 mm a_w: 12 - 42 mm *(K oder Y-Naht)* *D: 440 – 2580 mm* *b: 55 - 570 mm*	t_1 = 300 mm t_2 = 170 mm
3	*Bottom component* 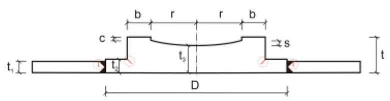	t: 55 – 255 mm t_1: 20 – 55 mm t_2: 20 – 60 mm t_3: 35 – 150 mm *D: 330 – 1800 mm* *b: 40-100 mm* *r: 135-590 mm*	t: 55 – 255 mm t_1: 20 – 55 mm t_2: 20 – 60 mm t_3: 35 – 150 mm *D: 330 – 1800 mm* *b: 40-100 mm* *r: 135-590 mm*	t_1 = 200 mm t_2 = 200 mm
4	*Anchor plate* 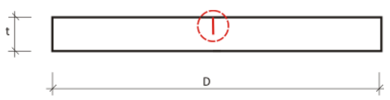	t: ≥ 55 mm *D: 440-3300 mm*	t: ≥ 55 mm *D: 440-3300 mm*	t = 250 mm
5	*Bearing for horizontal forces without rotation and capacity for vertical forces* 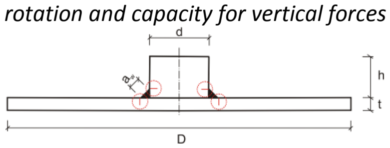	t: 30 – 150 mm d: 55 – 300 mm a_W: 5 – 25 mm *D: 440 - 3300 mm*	t: 30 – 150 mm d: 55 – 300 mm a_W: 5 – 25 mm *D: 440 - 3300 mm*	t = 40 mm

9 Worked examples

9.1 General

(1) The worked examples shall demonstrate with a bridge recently built in Germany the use of the tables 6.2 to 6.10 for the choice of steel material to avoid brittle fracture for bearings.

(2) The railway bridge located in Hamburg, from which the worked example for bearings has been selected, has been designed according EN 1993-2 in connection with the associated German National Annex in force.

(3) The rules in this German National Annex for determining the action effects and movements for bearings, which supplement the rules given in EN 1990 and EN 1337, are given in Annex E for information. Other National Annexes may lead to other requirements for the bearings.

(4) For comparison sake in addition to the demonstration of the use of tables 6.2 to 6.10 section 9.4 also gives a complete fracture mechanics assessment of the bearings selected as worked examples.

9.2 Design situation

(1) The bearing plan used for a railway bridge is given in Figure 9-1.

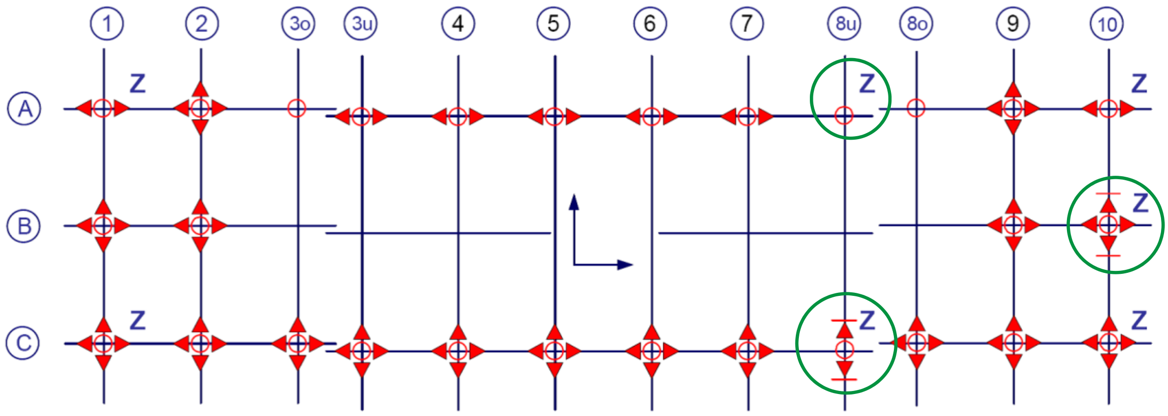

Figure 9-1: Bearing plan for a railway bridge with reference bearings 8u/A, 8u/C and 10/B

(2) At the marked positions the bearings designed as spherical bearings for both compression and tension forces, shall be assessed.

(3) The principle structure of the bearings may be taken from Figure 9-2.

(4) The magnitudes of the compression forces and tension forces in the ultimate limit state for the reference bearings is given in Figure 9-3.

(5) Details of the bearings may be taken from Figure 9-4, Figure 9-5 and Figure 9-6.

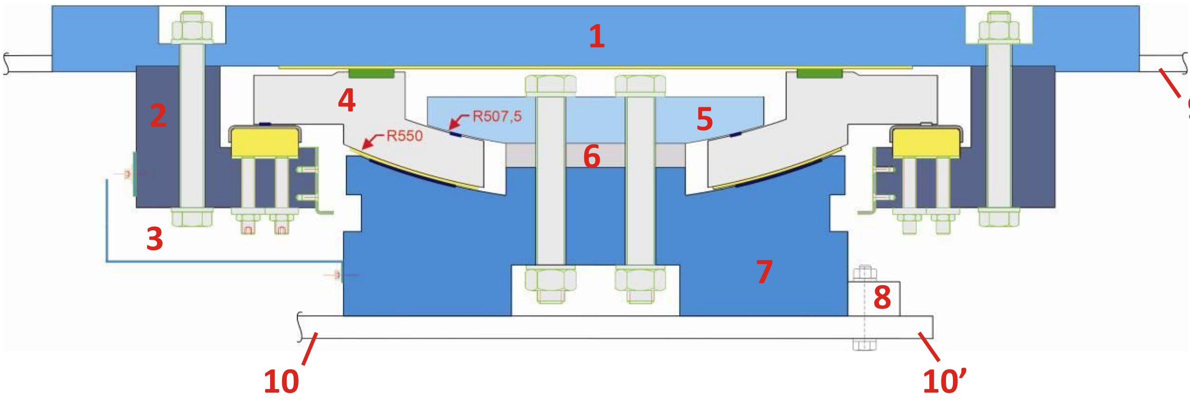

1) Sliding plate
2) Lateral guiderail
3) bolted connection (top component – lateral guiderail)
4) calotte (compression)
5) calotte (tension)
6) fill plate
7) bottom component
8) bolted connection to anchor plate
9) auxiliary attachment for transport
10, 10') anchor plate (welded or bolted)

Figure 9-2: Spherical bearings for both compressive and tensile forces

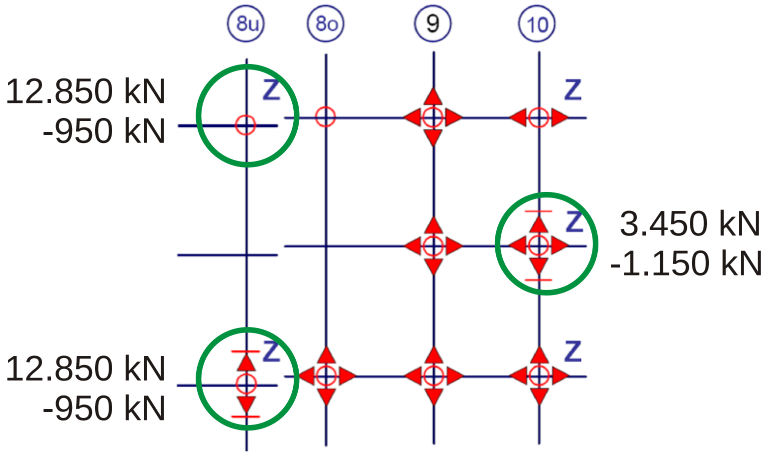

Figure 9-3: Maximum and minimum vertical forces for the reference bearings 8u/A, 8u/C, 10/B

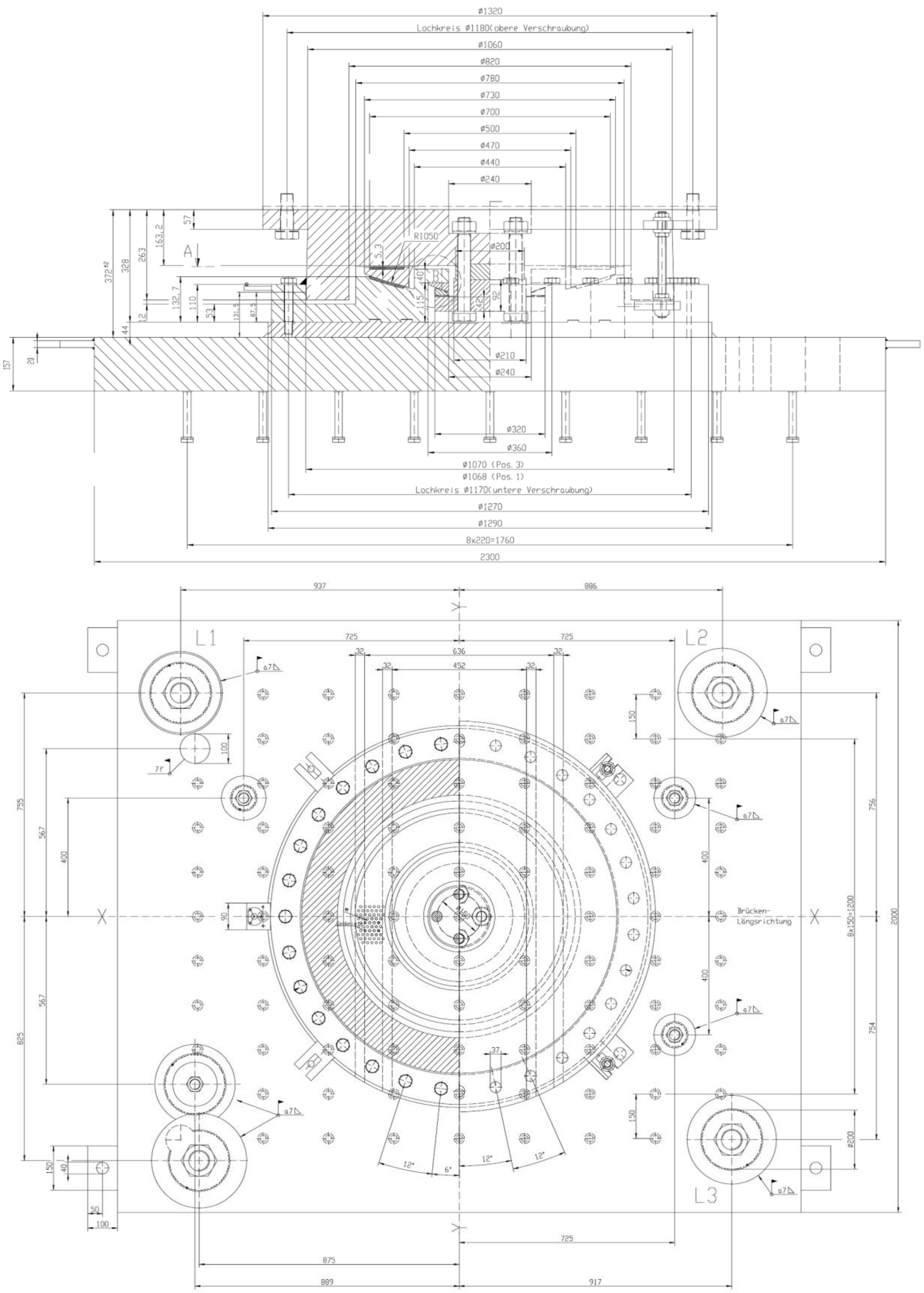

Figure 9-4: **Bearing in axis 8u/A according to Figure 9-1**

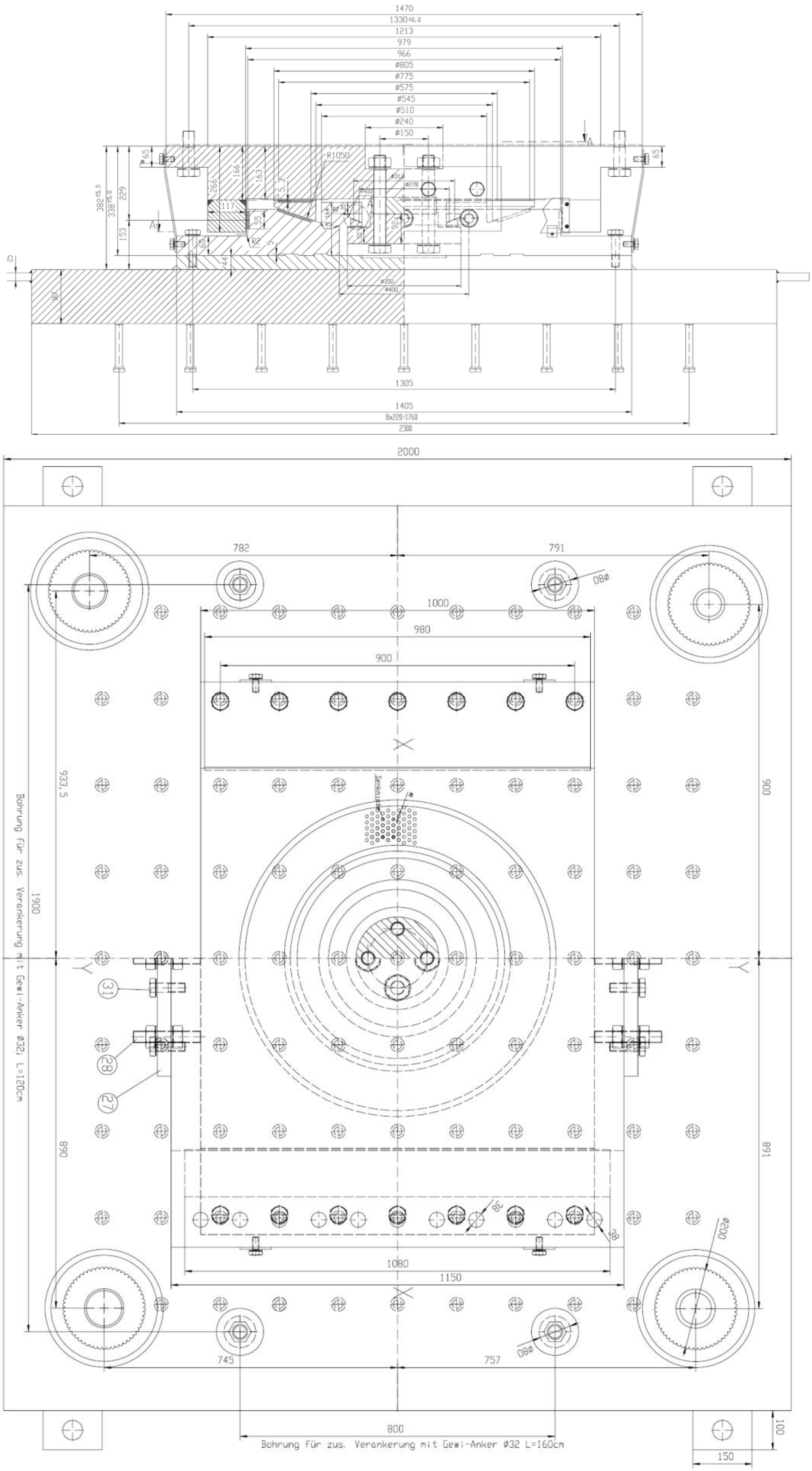

Figure 9-5: **Bearing in axis 8u/C according to Figure 9-1**

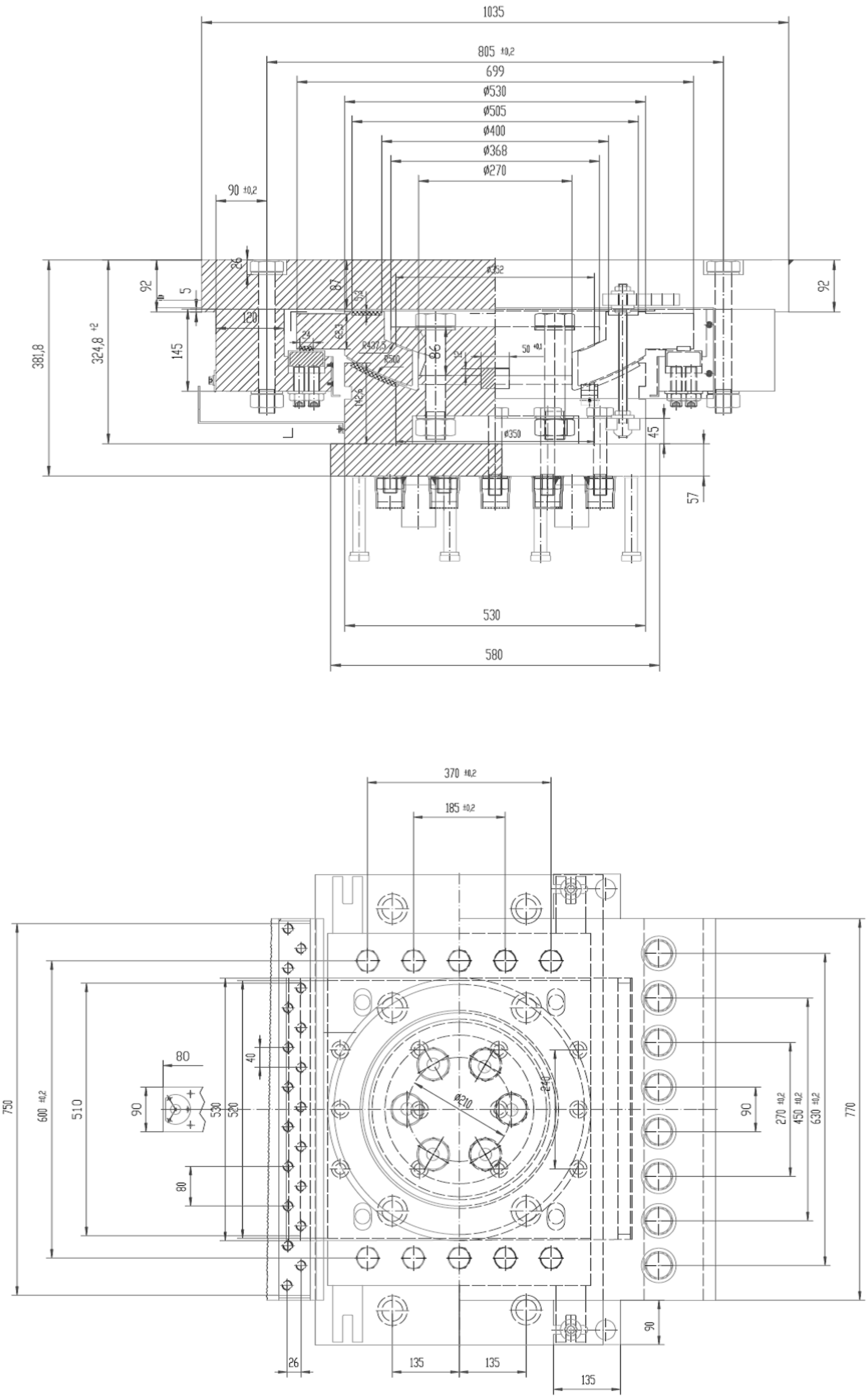

Figure 9-6: Bearing in axis 10/B according to Figure 9-1

9.3 Choice of material for the bearings to avoid brittle fracture

9.3.1 Bearings in axis 8u/A

(1) The shape and the dimensions of the steel components may be taken from Table 9-1.

Table 9-1: Steel components of bearings in axis 8u/A

No.	Steel component	Sketch	Table	Result
1	top component	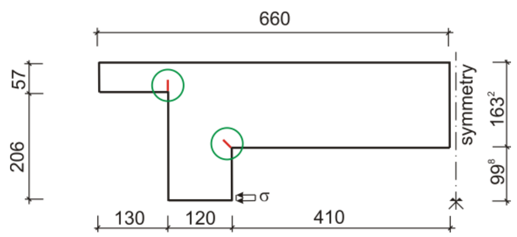 $\sigma_{Ed} = \sigma_{HS} = 86$ N/mm² (= $0{,}24 \cdot f_y$)	6.3 for $\sigma_{Ed}/f_y = 0{,}5$ as safe-sided assumption	fulfilled
2	bottom component	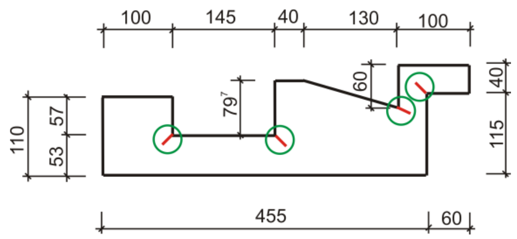 $\sigma_{Ed} = \sigma_{HS} = 212$ N/mm² (= $0{,}60 \cdot f_y$)	6.3 for $\sigma_{Ed}/f_y = 0{,}75$ as safe-sided assumption	fulfilled
3	calotte	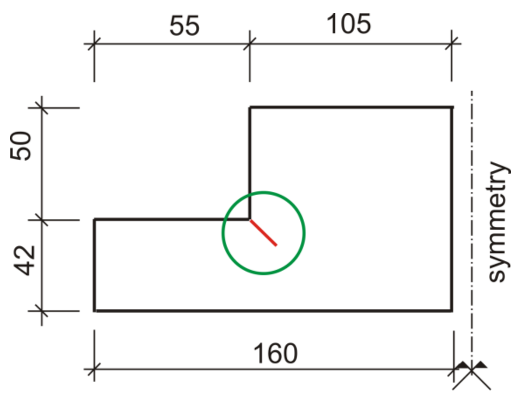	6.3 for $\sigma_{Ed}/f_y = 0{,}5$ as safe-sided assumption	fulfilled
4	anchor plate	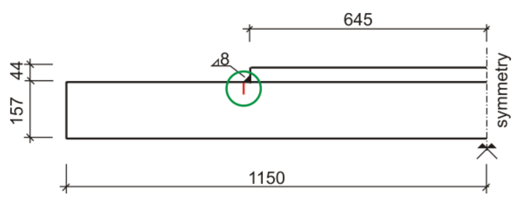 $\sigma_{Ed} = \sigma_{HS} = 31$ N/mm² (= $0{,}09 \cdot f_y$)	6.10 for $\sigma_{Ed}/f_y = 0{,}5$ as safe-sided assumption	not fulfilled*)

*) fulfilled for $\sigma_{Ed}/f_y = 0{,}25$

9.3.2 Bearings in axis 8u/C

(1) The shape and the dimensions of the steel components may be taken from Table 9-2.

Table 9-2: Steel components of bearings in axis 8u/C

No.	Steel component	Sketch	Table	Result
1	top component	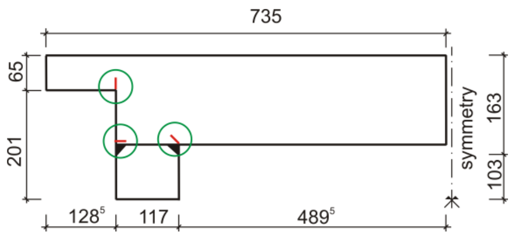 $\sigma_{Ed} = \sigma_{HS} = 77$ N/mm² (= 0,22·f_y)	6.3 for $\sigma_{Ed}/f_y = 0,5$ as safe-sided assumption	fulfilled
2	bottom component	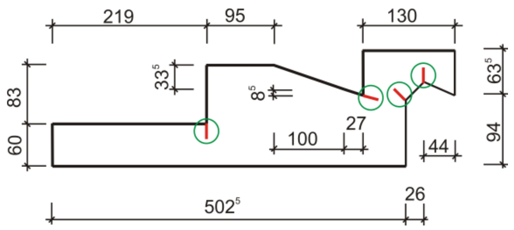 $\sigma_{Ed} = \sigma_{HS} = 103$ N/mm² (= 0,29·f_y)	6.3 for $\sigma_{Ed}/f_y = 0,5$ as safe-sided assumption	fulfilled
3	calotte	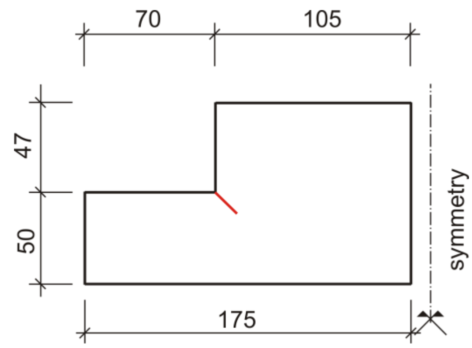	6.3 for $\sigma_{Ed}/f_y = 0,5$ as safe-sided assumption	fulfilled
4	anchor plate	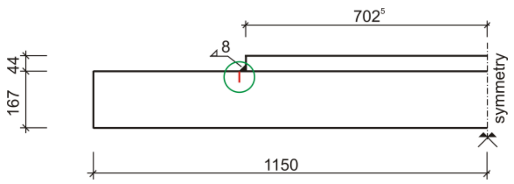 $\sigma_{Ed} = \sigma_{HS} = 30$ N/mm² (= 0,09·f_y)	6.10 for $\sigma_{Ed}/f_y = 0,5$ as safe-sided assumption	not fulfilled*)

*) fulfilled for $\sigma_{Ed}/f_y = 0,25$

9.3.3 Bearings in axis 10/B

(1) The shape and the dimensions of the steel components may be taken from Table 9-3.

Table 9-3: Steel components of bearings in axis 10/B

No.	Steel component	Sketch	Table	Result
1	calotte (compression)	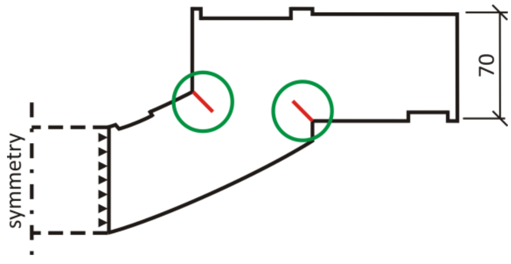 $\sigma_{Ed} = \sigma_{HS} = 58{,}2$ N/mm² (= $0{,}16 \cdot f_y$)	6.3 for $\sigma_{Ed}/f_y = 0{,}75$ as safe-sided assumption	fulfilled
2	calotte (tension)	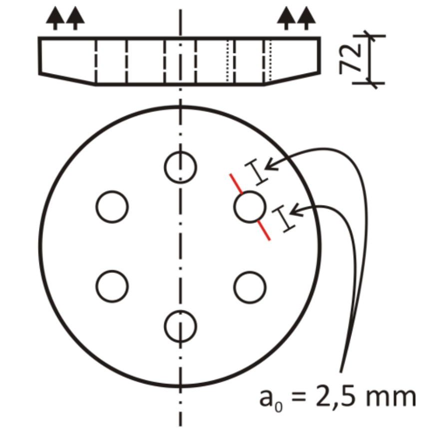 $\sigma_{Ed} = \sigma_{HS} = 104{,}6$ N/mm² (= $0{,}29 \cdot f_y$)	6.9 for $\sigma_{Ed}/f_y = 0{,}75$ as safe-sided assumption	fulfilled
3	lateral guiderail	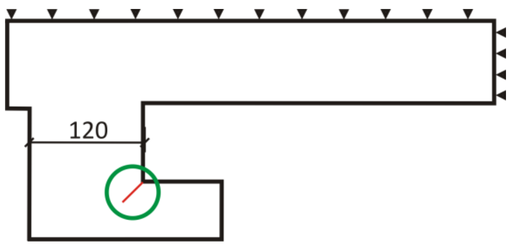 $\sigma_{Ed} = \sigma_{HS} = 43{,}4$ N/mm² (= $0{,}13 \cdot f_y$)	6.10 for $\sigma_{Ed}/f_y = 0{,}75$ as safe-sided assumption	Not fulfilled*)
4	anchor plate (connection)	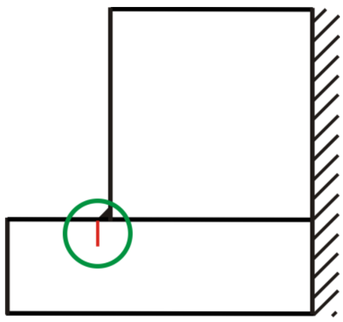 $\sigma_{Ed} = \sigma_{HS} = 17{,}6$ N/mm² (= $0{,}05 \cdot f_y$)	6.5 for $\sigma_{Ed}/f_y = 0{,}75$ as safe-sided assumption	fulfilled

*) fulfilled for $\sigma_{Ed}/f_y = 0{,}13$

9.4 Alternative procedure: Full fracture mechanics assessment

9.4.1 General

(1) As an alternative to the simplified procedure specified in this report that is applied to the three selected bearings in section 9.3 of this report, this section 9.4 gives the full fracture mechanics procedure to verify that

$T_{Ed} \geq T_{Rd}$

see (2-3).

(2) The calculations are based on the following assumptions

- minimum temperature $T_{md} + \Delta T_R = -30$ °C
- $\sigma_{tot} = \sigma_P + \sigma_S$
- where
- $\sigma_P = \sigma_{HS}$ is the Hot-Spot-stress from external frequent loads
- σ_S is a secondary residual stress = 100 MPa
- $K_1 (\sigma_P + \sigma_S)$ is the stress-intensity factor corresponding to $\sigma_{Ed} = \sigma_P + \sigma_S$

Example from calculation for bearing 10/B:

For $\sigma_P = \sigma_{HS}$ = 266 N/mm² the K_1-value from the FE-model is

K_1 = 1236 N/mm$^{3/2}$, see Table 9-5.

due to σ_S = 100 N/mm², K_1 takes the value:

$K(\sigma_P + \sigma_S)$ = 1.236·(266+100)/266 = 1.701 N/mm$^{3/2}$

The relevant value for assessment is

$$K_{appl,d} = \frac{K_{appl}}{k_{R6}-\rho} = \frac{1701}{0{,}826} = 2059\ N/mm^{3/2}.$$

This value corresponds to

$K^*_{appl,d}$ =2059 N/mm$^{3/2}$ = 65,1 MPa m$^{1/2}$, see Table 9-8.

Note: In the application of the full fracture mechanics procedure the definition

$\sigma_{tot} = \sigma_P + \sigma_S$

shall be used, whereas the use of the tables 6.2 to 6.10 for the simplified procedure is based on

$\sigma_{Ed} = \sigma_P = \sigma_{HS}$

in the same way as used for the application of table 2.1 in EN 1993-1-10.

- $f_{y,nom}$ = 355 N/mm² to be reduced for large values t (e.g. $f_{y,nom}$ = 338 N/mm² for t = 70 mm)
- $T_{27J,nom}$ = -20 °C (S 355 J2)
- ΔT_R = +7 °C is the safety element related to the use of nominal values T_{27J} and f_y according to EN 10025.

9.4.2 Design value of initial crack

(1) The initial crack sizes a_0 and the values $a_{0,d}$ used for the calculation for the various plate-thicknesses are given in Table 9-4:

Table 9-4: Design values for crack-like flaws

steel component	axis 8u/A			axis 8u/C			axis 10/B		
	t	**a_0**	**$a_{0,d}$**	**t**	**a_0**	**$a_{0,d}$**	**t**	**a_0**	**$a_{0,d}$**
top component	163	2,55	2,60	163	2,55	2,60	70	2,12	2,50
bottom component	53	1,99	2,00	70	2,12	2,50			
calotte (tension)	42	1,87	2,00	50	1,96	2,00	72	2,14	2,50
anchor plate	157	2,53	2,60	67	2,56	2,60	57	2,00	2,00
lateral guiderail							120	2,39	2,50

9.4.3 Determination of K_1-values from the FE-analysis

(1) For various values $\sigma_{Ed} = \sigma_P$ (0,25 f_y, 0,50 f_y, 0,75 f_y) Table 9-5 gives the K_1-values and K_{eff}-values obtained from Finite-Element analysis for the fracture mechanics models given in Table 9-6, Table 9-7, Table 9-8.

Table 9-5: K-values from Finite-Element-Analysis of fracture mechanics models as given in Table 9-6, Table 9-7 and Table 9-8 for various values $\sigma_{Ed}/f_y = \sigma_P/f_y$

No.	component			0,25·f_y			0,50·f_y			0,75·f_y		
				K_1	K_2	K_{eff}	K_1	K_2	K_{eff}	K_1	K_2	K_{eff}
				[N/mm$^{3/2}$]			[N/mm$^{3/2}$]			[N/mm$^{3/2}$]		
1	Oberhafen Axis 8u/A	top component	1	373	-17	364	746	-35	729	1119	-52	1093
			2	325	15	333	650	30	666	975	45	998
2		bottom component	1	443	15	451	886	30	902	1329	46	1353
			2	391	-2	390	782	-4	780	1173	-6	1170
			3	541	36	560	1083	71	1120	1624	107	1680
			4	211	76	257	422	151	515	633	227	772
3		calotte (tens.)	-	535	-4	533	1071	-9	1066	1606	-13	1600
4		anchor plate	-	1063	-306	948	2126	-612	1896	3190	-919	2844

Table 9-5: continued

No.	component			0,25·f_y			0,50·f_y			0,75·f_y		
				K_1	K_2	K_{eff}	K_1	K_2	K_{eff}	K_1	K_2	K_{eff}
				[N/mm$^{3/2}$]			[N/mm$^{3/2}$]			[N/mm$^{3/2}$]		
1	Oberhafen Axis 8u/C	top component	1	357	21	368	714	43	737	1071	64	1105
			2	236	-2	235	471	-3	469	706	-5	704
			3	585	-21	575	1170	-42	1150	1755	-63	1724
			4	366	-51	343	732	-103	686	1098	-154	1030
2		bottom component	1	354	-77	322	707	-155	644	1061	-232	966
			2	452	-113	408	904	-227	815	1357	-340	1223
			3	517	-106	473	1034	-212	946	1552	-318	1420
			4	378	-62	351	756	-123	703	1134	-185	1054
3		calotte (tens.)	-	685	-2	657	1317	-5	1314	1975	-7	1972
4		anchor plate	-	1065	-304	950	2130	-608	1901	3195	-911	2851

No.	component		0,25·f_y			0,50·f_y			0,75·f_y		
			K_1	K_2	K_{eff}	K_1	K_2	K_{eff}	K_1	K_2	K_{eff}
			[N/mm$^{3/2}$]			[N/mm$^{3/2}$]			[N/mm$^{3/2}$]		
1	Oberhafen Axis 10/B	calotte (pressure) (load case pressure”	178	-26	166	355	-53	332	533	-79	498
2		calotte (load case “tension”	376	65	412	752	130	824	1127	195	1236
3		calotte (tension)	270	20	280	540	40	560	810	60	841
4		lateral guiderail	612	-21	602	1224	-42	1203	1836	-63	1805
5		anchor plate	454	-123	407	909	-246	814	1363	-369	1221

Table 9-6: Fracture mechanics assessment for bearing in axis 8u/A for $\sigma_P = 0{,}50 \cdot f_y$

No.	Steel component	Fracture mechanics model	$K^*_{appl,d}$ [$MPa \cdot m^{1/2}$]	T_{mdr} [°C]	T_{Ed} [°C]	T_{27J} [°C]	T_{Rd} [°C]
1	Top component	Variant 1 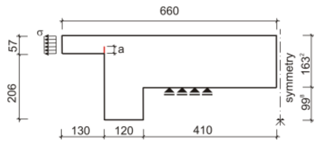	40,5	-30	97	-20	-38
		Variant 2 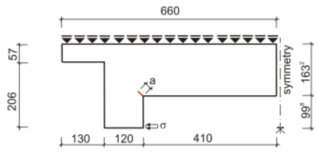	37,3	-30	97	-20	-38
2	Bottom component	Variant 1 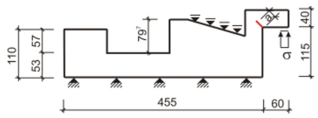	50	-30	33	-20	-12
		Variant 2 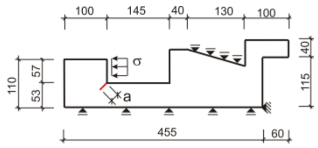	43,3	-30	47	-20	-12
		Variant 3 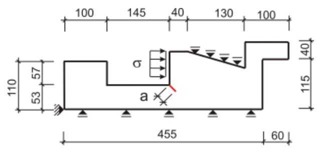	62,1	-30	5	-20	-12
		Variant 4 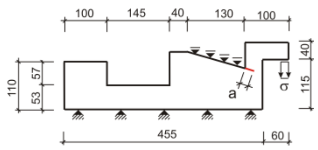	28,5	-30	97	-20	-12
3	Calotte (tension)	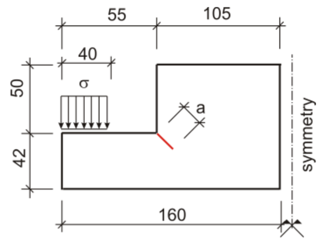	59,4	-30	13	-20	-12
4	Anchor plate	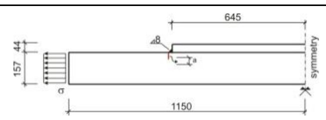	119	-30	-61*)	-20	-38*)

*) calculated for $\sigma_{Ed}/f_y = 0{,}13$

Table 9-7: Fracture mechanics assessment for bearing in axis 8u/C for $\sigma_P = 0{,}50 \cdot f_y$

No.	Steel component	Fracture mechanics model	$K^*_{appl,d}$ [$MPa \cdot m^{1/2}$]	T_{mdr} [°C]	T_{Ed} [°C]	T_{27J} [°C]	T_{Rd} [°C]
1	Top component	Variant 1 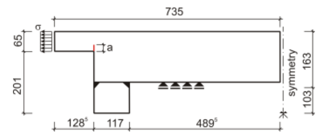	40,9	-30	52	-20	-38
		Variant 2 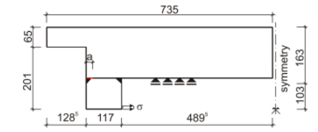	26,2	-30	97	-20	-38
		Variant 3 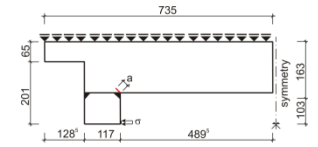	65,5	-30	-17	-20	-38
		Variant 4 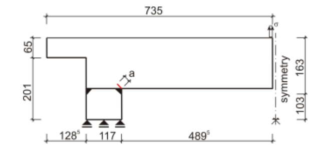	41,0	-30	34	-20	-38
2	Bottom component	Variant 1 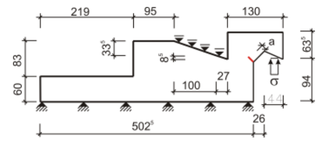	39,3	-30	57	-20	-12
		Variant 2 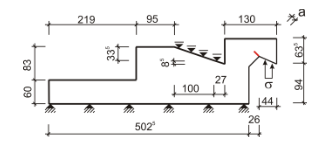	50,1	-30	31	-20	-12
		Variant 3 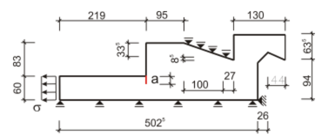	57,4	-30	11	-20	-12
		Variant 4 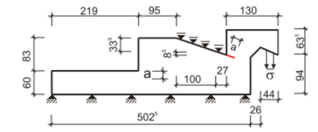	42,0	-30	50	-20	-12
3	Calotte (tension)	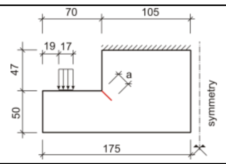	73,0	-30	-9	-20	-12
4	Anchor plate	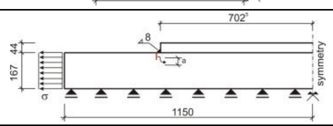	119,4	-30	63*)	-20	-38*)

*) calculated for $\sigma_{Ed}/f_y = 0{,}13$

Table 9-8: Fracture mechanics assessment for bearing in axis 10/B for $\sigma_P = 0{,}75 \cdot f_y$

No.	Steel component	Fracture mechanics model	$K^*_{appl,d}$ [$MPa \cdot m^{1/2}$]	T_{mdr} [°C]	T_{Ed} [°C]	T_{27J} [°C]	T_{Rd} [°C]
1	Calotte (compression)	**Load case 1 – Tension** 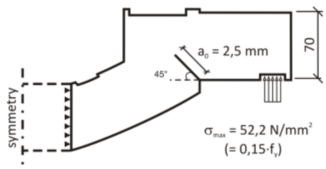	65,1	-30	-4	-20	-38
		Load case 2 – Compression 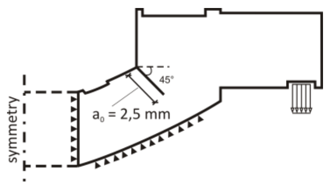	28,1	-30	97	-20	-38
2	Calotte (tension)	**Variant 1: Surface cracks located at bore holes** 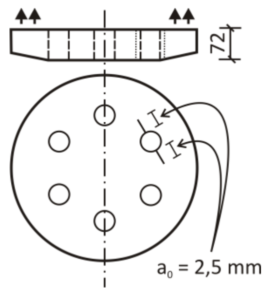	44,2	-30	38	-20	-12
3	Stegeisen	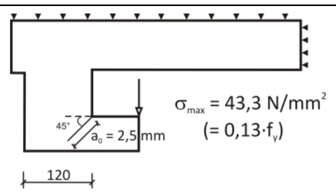	96,9	-30	-44*)	-20	-38*)
4	Anchor plate (connection)	**Variant 1: Welded connection** 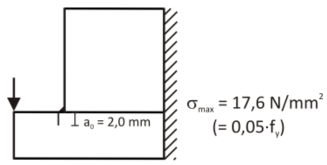	71,7	-30	-6	-20	-38

*) calculated for $\sigma_{Ed}/f_y = 0{,}13$

9.4.4 Fracture mechanics assessments

(1) In Table 9-6, Table 9-7 and Table 9-8 the fracture mechanics models used to calculate the $K(\sigma_P)$ values and the values $K^*_{appl,d}$ including residual stresses σ_S and finally T_{Ed} and T_{Rd} are given. The reference stresses are $\sigma_P = 0.50\ f_y$ in Table 9-6 and Table 9-7 and $\sigma_P = 0.75\ f_y$ in Table 9-8.

(2) The condition

$T_{Ed} \geq T_{Rd}$

is satisfied for all models except for the anchor plates in 9-6 and Table 9-7 and the lateral guiderail in Table 9-8.

(3) By choosing a more realistic reference stress σ_P = 0.25 f_y for the anchor plate and σ_P = 0.13 f_y for the lateral guiderail the improvements as given in Table 9-9 can be achieved.

Table 9-9: Modification of assessment by improving the reference stress σ_P

Bearing	σ_P	$K^*_{appl,d}$	T_{mdr}	T_{Ed}	T_{Rd}
8u/A	$0{,}25 \cdot f_y$	76,4	-30 °C	-29	-38
8u/C	$0{,}25 \cdot f_y$	76,5	-30 °C	-31	-38
10/B	$0{,}13 \cdot f_y$	38	-30 °C	52	-38

10 References

[1] DASt-Richtlinie 009: Stahlsortenauswahl für geschweißte Stahlbauten, Deutscher Ausschuss für Stahlbau. Januar 2005.

[2] EN 1993-1-10: Eurocode 3: Design of Steel Structures - Part 1-10: Material Toughness and Through Thickness Properties. 2005.

[3] JRC – Scientific and Technical Report: Commentary and Worked Examples to EN 1993-1-10 "Material Toughness and Through Thickness Properties and Other Toughness Oriented Rules in EN 1993. CRC, September 2008.

[4] JRC – Scientific and Technical Report: Choice of Steel Material to avoid Brittle Fracture for Hollow Section Structures – Addition to EN 1993-1-10. 2011.

[5] EN 1993-1-9: Eurocode 3: Design for Steel Structures - Part 1-9: Fatigue. 2005.

[6] Kühn, B.: Beitrag zur Vereinheitlichung der europäischen Regelungen zur Vermeidung von Sprödbruch. Dissertation, Lehrstuhl für Stahlbau, RWTH Aachen, 2005, Shaker Verlag Aachen, ISBN 3-8322-3901-4.

[7] EN 1337-1: Structural Bearings– Part 1: General Design Rules. 2000.

[8] DIN Fachbericht 101: Einwirkungen auf Brücken. 2009.

[9] EN 1993-2: Eurocode 3 – Design of Steel Structures – Part 2: Steel Bridges. 2006.

[10] Hobbacher, A.: Recommendations for Fatigue Design of Welded Joints and Components. IIW-documentXIII-2151-07/XV-1254-07, 2007.

[11] Marshall, P.W.: Design of Welded Tubular Connections. Basis and Use of AWS Code Provisions. Development in Civil Engineering, 37, Elsevier, 1992. pp. 412.

[12] ASME Boiler and Pressure Vessel Code: Section III, Rule for Construction of Nuclear Power Plant Components, Division 1, Subsection NB, Class 1 Componets. New York, American Society of Mechanical Engineers, 1989.

[13] Dong, P.: A Structural Stress Definition and Numerical Implementation for Fatigue Analysis of Welded Joints. International Journal of Fatigue, Vol. 23, 2001, pp. 865-876.

[14] Dong, P., Hong, J.K., de Jesus, A.M.: Analysis of recent Data using the Structural Stress Procedure in ASME Div 2 Rewrite. Proceedings ASME Pressure Vessel and Piping Conference. PVP2005-71511, New York, ASME, 2005.

Annex E to section 9 – Worked Example

Objective

(1) EN 1990 does not give a specific specification for the calculation of design values of action effects as forces, moments and movements relevant for the design of bearings.

(2) It has been left to National Annexes to EN 1990 to give such specifications in the context of the use of the Eurocodes for the design of bridges.

(3) Annex E is the National Annex from Germany. It may be used as an example for such a National Annex. It has been used as reference for preparing the worked example in section 9 - Worked examples - of the JRC-Report "Choice of steel material for bridge bearings to avoid brittle fracture – Addition to EN 1993-1-10".

Basic requirements for a National Annex to EN 1990 for preparing the technical specifications for bearings

(1) The particular specification for the calculation of design values of action effects on bearings shall take into account the following requirements:

1. It shall be consistently useable for the following cases of analysis of bridges
    1. The bridge superstructure can be separated from the substructure at the interface of the bearings and be treated by an independent analysis model.
    2. Bridge superstructure and bridge substructure interact by mechanical links provided by the bearings. As a subsequence the bridge superstructure and the bridge substructure form a unique analysis model including the bearings (e.g. for elastomeric bearings).
    3. The bridge is an integral bridge without specific bearings.
2. It shall be consistently useable for the design of transition joints.
3. Long term regional experiences with measured data of movements should be reflected by the rules.

(2) Particular features of the specification for the calculation of design values of action effect on bearings are

- correction of γ_F to be applied to thermal actions from 1.50 to 1.35 (see EN 1990-A1),
- appropriate definition of material properties e.g. for long term effects of concrete or non-metallic material in the bearings.

(3) Annex E is a proposal from the German National Annex to EN 1990-A1 and is considered to comply with these requirements.

European Commission
EUR 25390 EN– Joint Research Centre – Institute for the Protection and Security of the Citizen

Title: **Choice of steel material for bridge bearings to avoid brittle fracture**

Authors: M. Feldmann, B. Eichler, G. Sedlacek, W. Dahl, P. Langerberg, C. Butz, H. Leendertz, G. Hanswille
Editors: A. Pinto, A. Athanasopoulou , H. Amorim-Varum

Luxembourg: Publications Office of the European Union

2012 – 136 pp. – 21.0 x 29.7 cm

EUR – Scientific and Technical Research series – ISSN 1831-9424 (online), ISSN 1018-5593 (print)

ISBN 978-92-79-25439-0

doi:10.2788/33897

Abstract

Bridge bearings need verification against brittle failure at low temperatures. The design of bearings according to EN 1337 may lead to structural components with thicknesses no longer covered in the relevant technical construction regulations. Due to its specific geometry, the loading and stressing and the fabrication process the prerequisites for using the rules in EN 1993-1-10 lead to conservative restrictions or uneconomical choice of steel material. For an economical bearing design further modifications of the existing rules are necessary. This report adapts the fracture mechanical approach used in EN 1993-1-10 and gives information for a "safe-sided" choice of steel material for bearings. The main modifications refer to the hypothetical design crack scenario and the definition of the "nominal design stress" at the geometric "hot-spot". An advanced methodology using Finite Elements and a simplified method using linear bending theory are evaluated.

LB-NA-25390-EN-N

As the Commission's in-house science service, the Joint Research Centre's mission is to provide EU policies with independent, evidence-based scientific and technical support throughout the whole policy cycle.

Working in close cooperation with policy Directorates-General, the JRC addresses key societal challenges while stimulating innovation through developing new standards, methods and tools, and sharing and transferring its know-how to the Member States and international community.

Key policy areas include: environment and climate change; energy and transport; agriculture and food security; health and consumer protection; information society and digital agenda; safety and security including nuclear; all supported through a cross-cutting and multi-disciplinary approach.

ISBN 978-92-79-25439-0

Publications Office